



MEMBRANE-ASSISTED ADVANCED OXIDATION PROCESSES FOR WASTEWATER TREATMENT.

Ivonne Graciela Escalona Hernández

Dipòsit Legal: T 1832-2014

ADVERTIMENT. L'accés als continguts d'aquesta tesi doctoral i la seva utilització ha de respectar els drets de la persona autora. Pot ser utilitzada per a consulta o estudi personal, així com en activitats o materials d'investigació i docència en els termes establerts a l'art. 32 del Text Refós de la Llei de Propietat Intel·lectual (RDL 1/1996). Per altres utilitzacions es requereix l'autorització prèvia i expressa de la persona autora. En qualsevol cas, en la utilització dels seus continguts caldrà indicar de forma clara el nom i cognoms de la persona autora i el títol de la tesi doctoral. No s'autoritza la seva reproducció o altres formes d'explotació efectuades amb finalitats de lucre ni la seva comunicació pública des d'un lloc aliè al servei TDX. Tampoc s'autoritza la presentació del seu contingut en una finestra o marc aliè a TDX (framing). Aquesta reserva de drets afecta tant als continguts de la tesi com als seus resums i índexs.

ADVERTENCIA. El acceso a los contenidos de esta tesis doctoral y su utilización debe respetar los derechos de la persona autora. Puede ser utilizada para consulta o estudio personal, así como en actividades o materiales de investigación y docencia en los términos establecidos en el art. 32 del Texto Refundido de la Ley de Propiedad Intelectual (RDL 1/1996). Para otros usos se requiere la autorización previa y expresa de la persona autora. En cualquier caso, en la utilización de sus contenidos se deberá indicar de forma clara el nombre y apellidos de la persona autora y el título de la tesis doctoral. No se autoriza su reproducción u otras formas de explotación efectuadas con fines lucrativos ni su comunicación pública desde un sitio ajeno al servicio TDR. Tampoco se autoriza la presentación de su contenido en una ventana o marco ajeno a TDR (framing). Esta reserva de derechos afecta tanto al contenido de la tesis como a sus resúmenes e índices.

WARNING. Access to the contents of this doctoral thesis and its use must respect the rights of the author. It can be used for reference or private study, as well as research and learning activities or materials in the terms established by the 32nd article of the Spanish Consolidated Copyright Act (RDL 1/1996). Express and previous authorization of the author is required for any other uses. In any case, when using its content, full name of the author and title of the thesis must be clearly indicated. Reproduction or other forms of for profit use or public communication from outside TDX service is not allowed. Presentation of its content in a window or frame external to TDX (framing) is not authorized either. These rights affect both the content of the thesis and its abstracts and indexes.

Ivonne Graciela Escalona Hernández

**MEMBRANE-ASSISTED ADVANCED
OXIDATION PROCESSES FOR
WASTEWATER TREATMENT**

DOCTORAL THESIS

UNIVERSITAT ROVIRA I VIRGILI



UNIVERSITAT ROVIRA I VIRGILI

Tarragona

2014

Ivonne Graciela Escalona Hernández

**MEMBRANE-ASSISTED ADVANCED
OXIDATION PROCESSES FOR
WASTEWATER TREATMENT**

DOCTORAL THESIS

Supervised by Dr. Josep Font Capafons

**Department of Chemical Engineering
UNIVERSITAT ROVIRA I VIRGILI**



UNIVERSITAT ROVIRA I VIRGILI

Tarragona

2014



**UNIVERSITAT
ROVIRA I VIRGILI**

**Departament d'Enginyeria Química
Escola Tècnica Superior d'Enginyeria Química**

**Avinguda dels Països Catalans, 26, Campus Sescelades
43007 Tarragona, Catalunya, SPAIN
Tel: +34 977 55 96 46
Fax : +34 977 55 96 21
E-mail: jose.font@urv.cat**

I Dr Josep Font Capafons, associate professor in the Department of Chemical Engineering of the Rovira i Virgili University,

CERTIFY:

That the present study, entitled “Membrane-assisted advanced oxidation processes for wastewater treatment”, presented by Ivonne Graciela Escalona Hernández for the award of the degree of Doctor, has been carried out under my supervision at the Department of Chemical Engineering of this university, and that it fulfils all the requirements to be eligible for the European Doctorate Label.

Tarragona, 8th September 2014

*Con mucho cariño para
mi familia Escalona Hernández,
mi hijo, mi esposo y mi querida abuela Cristina*

Acknowledgements

Primeramente me gustaría agradecer por toda su colaboración y ayuda al Dr. Josep Font quien además de ser mi tutor de tesis, se ha comportado como un verdadero amigo. Muchas gracias por todas las correcciones, consejos, guías, por siempre hacer mirar hacia el lado bueno de las cosas y darme tranquilidad durante estos cinco años de trabajo. Muy especialmente por compartir conmigo sus conocimientos en oxidación avanzada y procesos de filtración con membranas, los cuales me fueron de mucha ayuda.

A la Universitat Rovira i Virgili por permitirme formar parte de esta prestigiosa institución. A la Generalitat de Catalunya, por darme el soporte financiero necesario para la culminación de este trabajo de investigación. Les estoy profundamente agradecida a ambas instituciones.

Al grupo de investigación CREPI en su totalidad, sin ellos no hubiese sido posible alcanzar esta meta. **Xavi** muchísimas gracias por introducirme en este mundo de las membranas, tus explicaciones, toda la información que me facilitaste así como todas las asesorías fueron realmente valiosas. Verdaderamente aprecio muchísimo que aún estando lejos, en los momentos que necesité de tu ayuda...siempre contestaste a mis correos. Mil gracias. **Ana...**Dios cuántas DQO hemos hecho...!!! Muchas gracias por tu compañía, risas, por saber donde están todas las cosas en los laboratorios del CREPI, manejos de equipos, papeles de la ISO, en fin no podría parar de decir...de verdad aunque ya no formes parte del CREPI, no hay mejor renglón donde ponerte que como miembro de éste, sin duda alguna si hay alguien crepiana ésta eres tu...**Torreti** ☺ muchas gracias por estar siempre dispuesta a echarme una mano con todas las cosas referente al laboratorio. **Martín y Magda** muchas gracias por lo geniales momentos vividos...incluyendo las peleitas matutinas... **Selam** muchísimas gracias por ayudarme con las redacciones en inglés y por darme tu opinión en la realización de mis presentaciones orales, diseño de experimentos, etc. Realmente eres una excelente compañera de trabajo. **Sunil** aunque no compartí mucho contigo muchas gracias por ser tan amable y regalarnos siempre una sonrisa en el aula pont. **Alberto**, te cedo el testigo! Mucha suerte en los estudios con membranas. **Judith y Yonhara**, éxitos en sus trabajos, gracias por los diferentes favores mientras estaba embarazada y por siempre estar disponible a ayudarme. **Frank** muchísimas gracias por leer mis trabajos e interesarte en los estudios por membranas que estábamos haciendo. Tus planeamientos desde otro punto de vista me fueron de gran ayuda para mejorar el enfoque de mis experimentos. **Christophe, Azael y Agustí**, gracias por compartir conmigo numerosos momentos sin los cuales estos años no hubiesen sido tan agradables, *calçotades*, cenas, comidas... Además por estar siempre dispuestos a darme sus opiniones con ideas de mejoras a mi trabajo.

I am thankful to Prof. Dr. Ir. **Kitty Nijmeijer** (Membrane Science and Technology group, University of Twente) for providing the practical support in allowing me use of their laboratories and facilities. I would like to extend my thanks to all those members of the laboratory who have contributed to make my stay research very pleasant. I am particularly thankful to Dr. Olga Kattan for their invaluable help and friendliness.

A mi amada familia Escalona Hernández, su apoyo incondicional siempre me ha dado las fuerzas necesarias para culminar mis proyectos. A mi esposo Miguel Ángel...por llenar mi vida de momentos felices, apoyarme y entenderme.

A todos mis amigos de Tarragona, realmente han llenado de lindos recuerdos estos cinco años de trabajo.

Finally, I would like to thank all the members of the Panel for accepting being examiners of this work.

Summary

Bisphenol A (BPA) and tartrazine (TAR) belong to the compounds that are potentially harmful and often present in wastewater reclamation. BPA is a typical Endocrine Disrupting Chemical (EDC) and TAR is an azo dye. A variety of industries, especially paper and textile manufacturers, produces a large volume of wastewater that is polluted with BPA and dyes. Therefore, BPA and dyes-charged effluents need to be efficiently managed in order to avoid environmental problems linked to them.

During the last decade, several methods for BPA and TAR removal of wastewater have been found to be effective and potentially applicable for subsequent scaling up. However, most of them still face cost problems, thus demanding further development. It is generally accepted that nanofiltration (NF) offers an adequate solution for the removal of BPA and dyes from the aqueous solutions due to its capacity to retain dissolved organics.

In the present thesis project, cross flow NF using thin film composite polymeric membranes was applied to reject BPA and TAR from aqueous solutions. The research was focused on typifying solute rejection and permeate flux decay as a function of two main parameters: transmembrane pressure and initial model compound concentration.

The results show that NF achieves high BPA and TAR rejection for all the studied membranes, above 80 and 95 %, respectively. The NF of BPA solutions showed that rejection is related to adsorption ability of BPA on the membrane and size exclusion mechanism. Additionally, flux decline, compared to pure water permeability, ranges from 60 to 80% and mostly correlates with concentration polarisation occurrence, while for the NF of TAR solutions the flux only declines 20-35%.

The NF of five different dyes was also studied. In this case flux decline was mostly correlated with dye molecular weight. Significant continuous fouling was observed for some dyes, which can limit the use of NF for dye concentration at acceptable operation conditions.

Later, the degradation of BPA and TAR during Fenton's process under different operation conditions, in combination with subsequent NF of low concentration effluents containing remnant BPA and TAR and compounds derived from their oxidation was investigated. The results indicate that BPA could be efficiently degraded in aqueous phase by Fenton liquor. The treatment of 300 mg/L solutions of BPA with the Fenton reagent at optimal conditions resulted in its complete removal in less than 2 min. The optimum conditions were found to be $\text{pH}_R = 3$, $\text{H}_2\text{O}_2/\text{BPA} = 0.20$ and $\text{Fe}^{2+}/\text{BPA} = 0.012$. In the NF of the effluent after Fenton oxidation, high TOC, COD, colour and Fe^{2+} (>77%) removal were achieved, although significant membrane fouling was also observed. The normalised water flux after membrane flushing with water was lower than 60% in almost all used membranes, which indicates significant non-easily removable fouling.

In the oxidation of TAR by Fenton reagent, high decolourisation was achieved although poor mineralization was found. In this case, no significant permeate flux decline was observed during the NF of the effluent after Fenton oxidation. In general the normalised permeate fluxes were higher for NF of Fenton effluents than for the NF of untreated

solutions. High rejections were obtained in the integrated treatment NF and Fenton process, allowing very high permeate quality.

The present work also describes the use of ozone to degrade BPA and TAR from aqueous solutions. The effect of initial BPA and TAR concentrations, ozone dose, ozone-air flow rate and solution pH on the degradation rate was studied. The conversion of the pollutants was found to increase with increasing inlet ozone concentration and solution pH, and to decrease with increasing initial BPA and TAR concentrations. With respect to an increasing air-ozone flow rate, the conversion reaches a maximum and then decreases again. The results show that decolourisation was remarkable under basic conditions, pH 12. In general, the pre-ozonation of model compounds was beneficial to NF process. The previous ozonation enhances the permeate fluxes observed during NF of the pre-treated solutions. These membranes underwent lower polarisation concentration and fouling in comparison with the membranes used in the NF of Fenton treated and untreated solutions. Like NF of Fenton treated effluents, high permeate quality was obtained by NF of ozonized effluent.

Finally, the application of laccase and peroxidase from horseradish (HRP) to facilitate the removal of BPA from aqueous solutions was also investigated. The effect of pH and the enzyme dose was evaluated in order to determine the optimum conditions for this alternative. The results indicate that BPA was quickly removed from aqueous solution since a BPA conversion over 95% was obtained in 180 min for both enzymes in optimal conditions; the higher the enzyme dose, the higher the removal of BPA. It was also found that the optimum pH for the enzymatic treatment of BPA was around 7 for both enzymes.

The use of a membrane-reactor integrated system with recycling of enzyme for BPA degradation is also presented. These results demonstrate the potential and limitations of using enzymatic BPA degradation, operated in a recycling mode coupled to a NF membrane. BPA removal efficiencies from several NF membranes were related to the BPA molecular weight, membrane pore sizes and membrane hydrophobicity. NF270 showed the best performance in this membrane-assisted enzymatic treatment: 89% removal of BPA for the two enzyme treatments and less than 35% flux decay.

Resumen

El bisfenol A (BPA) y la tartrazina (TAR) pertenecen al grupo de compuestos que son potencialmente dañinos para la recuperación de aguas residuales. El BPA es un disruptor del sistema hormonal o disruptor endocrino, mientras que la TAR es un colorante azoico. Una diversidad de industrias, especialmente la industria papelera y textil, producen un gran volumen de aguas residuales que están contaminadas con BPA y colorantes. Por lo tanto, los efluentes que contiene tanto BPA como colorantes deben ser gestionados de manera eficiente con la finalidad de evitar problemas ambientales vinculados a ellos.

Durante la última década, se han ensayado varios métodos para la eliminación de BPA y TAR de aguas residuales, resultando ser eficaces y potencialmente aplicables a gran escala. Sin embargo, la mayoría de ellos todavía se enfrentan a problemas de costes, lo cual exige su desarrollo. La nanofiltración (NF) ofrece una solución adecuada para la eliminación de BPA y colorantes de las soluciones acuosas debido a su capacidad para retener sustancias orgánicas disueltas.

Es por ello que en este trabajo de tesis, se utilizó la NF en flujo tangencial usando membranas poliméricas para eliminar BPA y TAR de soluciones acuosas. El estudio se centró en el rechazo y la pérdida de flujo de permeado en función de dos parámetros principales: la presión trans-membrana y la concentración inicial de los compuestos modelos.

Los resultados muestran que la NF de BPA y TAR proporcionan altos niveles de rechazo para todas las membranas estudiadas, con valores por encima del 80 y 95%, respectivamente. En la NF de soluciones con BPA, el rechazo se mostró relacionado con la capacidad de adsorción de BPA por la membrana y con la exclusión por tamaño gracias a la diferencia entre la molécula y los poros de la membrana. Además, el flujo de permeado experimentado por las distintas membranas disminuyó, en comparación con la permeabilidad del agua pura, entre 60 y 80%; este hecho se relaciona con el fenómeno de polarización de la concentración. En cuanto a la NF de TAR, el flujo de permeado solamente se redujo entre un 20 y un 35%.

También se estudió la NF de cuatro colorantes diferentes a la TAR. En este caso, la disminución del flujo se correlacionó con los diferentes pesos moleculares de los colorantes. Durante el tiempo de filtración estudiado, se observó un ensuciamiento continuo de la membrana NF270 para algunos colorantes, lo cual puede limitar el uso de esta tecnología de una forma sostenible.

Posteriormente, se ensayó la degradación de BPA y TAR por medio del proceso Fenton bajo diferentes condiciones de operación y en combinación con la posterior NF de los efluentes. De esta manera, la filtración procedió a bajas concentraciones residuales de BPA o TAR y compuestos derivados de su oxidación. Los resultados indican que el BPA puede ser degradado eficientemente en fase acuosa a través de la reacción Fenton. La eliminación completa, en menos de 2 min, de BPA de soluciones que contenían inicialmente 300 mg/L se alcanzó con el reactivo Fenton en sus condiciones óptimas. Dichas condiciones resultaron ser: $\text{pH}_R = 3$, $\text{H}_2\text{O}_2/\text{BPA} = 0.20$ y $\text{Fe}^{2+}/\text{BPA} = 0.012$.

La NF del efluente después de la oxidación Fenton de BPA resultó en elevadas retenciones de TOC, DQO, color y Fe^{2+} (> 77%), aunque las membranas sufrieron un remarcable ensuciamiento. El flujo normalizado de agua inmediatamente después del proceso de filtración fue inferior al 60% en casi todas las membranas utilizadas, lo que indica un ensuciamiento difícil de eliminar.

En lo que se refiere a la oxidación de TAR por Fenton, se alcanzó una alta decoloración, sin embargo los niveles de mineralización fueron más bien pobres. El flujo de permeado no se redujo significativamente durante la NF del efluente después de la oxidación de TAR con Fenton. En general, los flujos normalizados de permeado fueron mayores en la NF de los efluentes después de tratamiento Fenton que en la NF de soluciones no tratadas. Altos rechazos se obtuvieron en el proceso integrado NF-Fenton, lo cual resultó en una alta calidad del permeado.

Además, el presente trabajo describe el uso del ozono para la degradación de BPA y TAR presente en soluciones acuosas. Se estudió el efecto de las concentraciones iniciales de BPA y TAR, de la dosis de ozono, del caudal de aire y ozono y del pH en la degradación. Se encontró que la conversión de los contaminantes aumenta con el incremento de la concentración de ozono en la corriente aire-ozono y con el pH de la solución, pero disminuye con el aumento de las concentraciones iniciales de BPA y TAR. Por su lado, la conversión de los contaminantes aumentó con el caudal de aire-ozono hasta alcanzar un máximo para luego disminuir con un incremento adicional. Estos ensayos mostraron una notable decoloración y degradación de los compuestos estudiados en condiciones básicas de pH. En general, la pre-ozonación de los compuestos modelo fue beneficiosa para el posterior proceso de NF. La NF de las soluciones ozonadas mejoró los flujos de permeado. En este caso las membranas experimentaron una menor polarización de la concentración y ensuciamiento en comparación con las membranas utilizadas en el NF de las soluciones tratadas y no tratadas con Fenton. Al igual que en la NF de los efluentes del proceso Fenton, alta calidad del permeado fue obtenida en la NF de los efluentes ozonados.

Por último se investigó la aplicación de la lacasa y la peroxidasa (HRP) para facilitar la eliminación de BPA a partir de soluciones acuosas. Se evaluó el efecto del pH y de la dosis de enzima para determinar las condiciones óptimas de reacción. Los resultados indican que el BPA puede ser eliminado rápidamente de soluciones acuosas con esta técnica. Conversiones superiores al 95% en 180 min fueron alcanzadas para ambas enzimas en condiciones óptimas de reacción. Como mayor fue la dosis de enzima, mayor fue la conversión de BPA. Adicionalmente, se observó que el pH óptimo para la eficiente eliminación de BPA es de alrededor de 7 para ambas enzimas.

Igualmente que para los otros procesos de oxidación, en esta parte se presenta el uso de un sistema integrado membrana-reactor con reciclado de enzimas para la degradación de BPA. Estos resultados demuestran el potencial y las limitaciones del uso de la degradación enzimática acoplada con membranas de NF para la remoción de BPA. La eficiente eliminación de BPA en este caso se relacionó con el peso molecular de BPA, tamaño de poros y hidrofobicidad de las membranas usadas. La membrana NF270 mostró las mejores prestaciones en la filtración del BPA tratado enzimáticamente: 89% de rechazo de BPA, para los dos tratamientos enzimáticos, y menos del 35% en la caída de flujo de permeado.

Resum

El bisfenol A (BPA) i la tartrazina (TAR) pertanyen al grup de compostos que són potencialment nocius per a la recuperació d'aigües residuals. El BPA és un disruptor del sistema hormonal o disruptor endocrí, mentre que la TAR és un colorant azoic. Una diversitat d'indústries, especialment la indústria paperera i tèxtil, produeixen un gran volum d'aigües residuals que estan contaminades amb BPA i colorants. Per tant, els efluents que contenen tant BPA com colorants han de ser gestionats de manera eficient amb la finalitat d'evitar problemes ambientals vinculats a ells.

Durant l'última dècada, s'han assajat diversos mètodes per a l'eliminació de BPA i TAR d'aigües residuals, resultant ser eficaços i potencialment aplicables a gran escala. No obstant això, la majoria d'ells encara enfronten problemes de costos, la qual cosa exigeix el seu desenvolupament. La nanofiltració (NF) ofereix una solució adequada per a l'eliminació de BPA i colorants de les solucions aquoses, degut a la seva capacitat per retenir substàncies orgàniques dissoltes.

És per això que en aquest treball de tesi, es va utilitzar la NF en flux tangencial mitjançant membranes polimèriques per eliminar BPA i TAR de solucions aquoses. L'estudi es va centrar en el rebuig i la disminució del flux de permeat en funció de dos paràmetres principals: la pressió trans-membrana i la concentració inicial dels compostos models.

Els resultats mostren que la NF de BPA i TAR permet aconseguir un rebuig alt per a totes les membranes estudiades, obtenint valors per sobre de 80 i 95%, respectivament. A la NF de solucions amb BPA, el rebuig ha estat relacionat amb la capacitat d'adsorció de BPA per la membrana i amb l'exclusió de la molècula gràcies a la diferència de grandària entre la molècula i els porus de la membrana. A més, la pèrdua de flux de permeat experimentat per les diferents membranes, en comparació amb la permeabilitat de l'aigua pura, se situa entre el 60 i el 80%. Aquest fet es relaciona amb el fenomen de polarització de la concentració. Quant a la NF de la TAR, el flux de permeat es va reduir tan sols entre el 20 i el 35%.

A més, s'ha estudiat la NF de quatre colorants diferents a la tartrazina. En aquest cas la disminució del flux es va correlacionar amb els diferents pesos moleculars dels colorants. Durant el temps de filtració estudiat, un embrutiment continu de la membrana NF270 va ser observat per a alguns colorants, cosa que pot limitar l'ús d'aquesta tecnologia d'una forma sostenible.

D'altra banda, s'ha investigat la degradació de BPA i TAR durant el procés Fenton sota diferents condicions d'operació, i en combinació amb la posterior NF dels efluents. D'aquesta manera, es poden filtrar efluents que contenen concentracions residuals de BPA o TAR i compostos derivats de l'oxidació dels mateixos. Els resultats indiquen que el BPA es pot degradar fàcilment en fase aquosa mitjançant la reacció Fenton. Així es va aconseguir l'eliminació completa, en menys de 2 minuts, de BPA en solucions que contenien inicialment 300 mg/L, en condicions òptimes. Aquestes condicions són: $\text{pH}_R = 3$, $\text{H}_2\text{O}_2/\text{BPA} = 0.20$ i $\text{Fe}^{2+}/\text{BPA} = 0.012$. La NF de l'efluent després de l'oxidació Fenton de BPA va donar elevades retencions de TOC, DQO, color i Fe^{2+} (> 77%), puix que les membranes es van embrutar significativament. El flux normalitzat d'aigua,

immediatament després del procés de filtració, va ser inferior al 60% en gairebé totes les membranes utilitzades, el que indica un embrutiment no fàcilment eliminable.

Pel que fa a l'oxidació de TAR per Fenton, també es va assolir una alta decoloració, però amb baixos nivells de mineralització. El flux de permeat no es va reduir remarcablement durant la NF de l'efluent després de l'oxidació Fenton del TAR. En general, els fluxos normalitzats de permeat van ser majors en la NF dels efluent després del tractament Fenton que per a la NF de solucions no tractades. Alts rebutjos es van obtenir en el procés integrat NF-Fenton, la qual cosa va resultar en una elevada qualitat del permeat.

Adicionalment, el present treball descriu l'ús de l'ozó per a la degradació de BPA i TAR present en solucions aquoses. S'ha estudiat l'efecte de les concentracions inicials de BPA i TAR, de la dosi d'ozó, del cabal d'aire i ozó i del pH en la degradació. Es va trobar que la conversió dels contaminants creix amb l'increment de la concentració d'ozó en el corrent aire-ozó i amb el pH de la solució, però disminueix amb l'augment de les concentracions inicials de BPA i TAR. Altrament, la conversió dels contaminants augmenta amb el cabal d'aire-ozó fins a assolir un màxim per després disminuir amb un increment addicional. Aquests assaigs van mostrar una notable decoloració i degradació dels compostos estudiats a condicions bàsiques de pH, 12. La pre-ozonació dels compostos model va beneficiar la posterior NF. Així, en la NF de les solucions tractades amb ozó, es van millorar els fluxos de permeat. En aquest cas, les membranes van experimentar una menor polarització de la concentració i embrutiment en comparació amb les membranes utilitzades en la NF de les solucions tractades i no tractades amb Fenton. Igual que en la NF dels efluent del procés Fenton, Alta qualitat del permeat va ser obtinguda a la NF dels efluent ozonats.

Finalment es va investigar l'aplicació de la lacasa i la peroxidasa (HRP) per facilitar l'eliminació de BPA a partir de solucions aquoses. Es va avaluar l'efecte del pH i de la dosi d'enzim per determinar les condicions òptimes de reacció. Els resultats indiquen que el BPA pot ser eliminat ràpidament de solucions aquoses. Es van aconseguir conversions superiors al 95% en 180 min per a ambdós enzims en les condicions òptimes de reacció. Com més gran va ser la dosi d'enzim, més gran va ser la conversió de BPA. A més, es va observar que el pH òptim per a la eficient eliminació de BPA se situa prop de 7 per a ambdós enzims.

Igual que per als altres processos d'oxidació, en aquests part es presenta la utilització d'un sistema integrat membrana-reactor amb recirculació d'enzims per a la degradació de BPA. Els resultats mostren el potencial i les limitacions en l'ús de la degradació enzimàtica acoblada amb membranes de NF per a l'eliminació de BPA. L'eficient retenció de BPA en aquest cas es va relacionar amb el seu pes molecular, la mida de porus i la hidrofobicitat de les membranes usades. La membrana NF270 va mostrar els millors rendiments en la filtració del BPA tractat enzimàticament: el 89% de retenció de BPA, per als dos tractaments enzimàtics, i menys del 35% en la caiguda de flux de permeat.

Contents

Chapter 1. Introduction **1**

1.1 Description and relevance of the topic	3
1.2 Bisphenol A	8
1.2.1 Environmental and human exposure, source and effects	9
1.2.2 Treatments	10
1.3 Tartrazine	11
1.3.1 Exposure, source and effects	12
1.3.2 Treatments	13
1.4 Wastewater treatment	15
1.5 Advanced oxidation processes	20
1.6 Membrane filtration processes	22
1.6.1 Nanofiltration	27
1.6.1.1 Membrane rejection mechanisms	28
1.6.1.2 Transport model for NF membranes	33
1.6.1.3 Factors affecting NF permeate flux	34
1.6.1.4 Factors controlling permeate flux and flux decline	36

Chapter 2. Hypothesis and objectives **39**

2.1 Previous considerations	41
2.2 Hypothesis	42
2.3 Objectives	43

Chapter 3 Methodology **45**

3.1 Materials	46
3.1.1 Model pollutants	46
3.2 Treatments	48
3.2.1 Nanofiltration	48
3.2.1.1 Membranes	48
3.2.1.2 Filtration test	49
3.2.2 Fenton process	52
3.2.2.1 Materials	52
3.2.2.2 Fenton oxidation procedure	52
3.2.3 Ozonation	54
3.2.3.1 Materials	54
3.2.3.2 Ozonation procedure	54
3.2.4 Enzymatic oxidation	56
3.2.4.1 Materials	56
3.2.4.2 Enzymatic BPA oxidation procedure	57
3.2.4.3 NF protocol for enzymatic BPA oxidation effluent	57
3.3 Analytical procedures	58
3.3.1 Determination of BPA and TAR concentration by high performance liquid chromatography	58
3.3.2 Colour by spectrophotometry	59

3.3.3 Determination of iron concentration	60
3.3.4 Total Organic Carbon	60
3.3.5 Chemical Oxygen Demand	61
3.3.6 Measurement of ozone in the gas phase	61
3.3.5 Membrane characterization by microscopy	62
3.3.5.1 Membrane topography and roughness determination by atomic force microscopy	62
3.3.5.2 Characterisations by microscopy	64

Chapter 4 Removal of BPA and Tartrazine from aqueous solutions by nanofiltration **67**

4.1 Introduction	69
4.2 Nanofiltration applied for the removal of model compounds	69
4.2.1. Removal of BPA by nanofiltration	69
4.2.2. Removal of Tartrazine by nanofiltration	70
4.3 Nanofiltration of model compounds	71
4.3.1 Nanofiltration of BPA	71
4.3.2 Nanofiltration of Tartrazine	79
4.4 Conclusions	86

Chapter 5 Fenton coupled with nanofiltration for elimination of BPA and tartrazine **87**

5.1 Introduction	89
5.2 Fenton process	90
5.2.1. Operating parameters	92
5.2.2. Advantages and disadvantages	93
5.2.3 Fenton applied for elimination of model compounds	94
5.2.3.1. Fenton for elimination of BPA	94
5.2.3.2. Fenton for elimination of tartrazine	97
5.2.4. Fenton process assisted by nanofiltration	98
5.3 Fenton degradation of model compounds	99
5.3.1 Fenton degradation of BPA	99
5.3.2 Fenton degradation of tartrazine	106
5.4 Removal of BPA effluent after Fenton oxidation by nanofiltration membrane	111
5.5 Removal of tartrazine effluent after Fenton oxidation by nanofiltration membrane	116
5.7 Conclusions	120

Chapter 6 Ozonation coupled with nanofiltration for elimination of BPA and tartrazine **123**

6.1 Introduction	124
6.2 Ozonation	126
6.2.1 Operating conditions	129
6.2.2 Advantages and disadvantages	130
6.2.3 Ozonation applied for elimination of model compound	131
6.2.3.1 Ozonation for elimination of BPA	131

6.2.3.2 Ozonation for elimination of tartrazine	134
6.2.4 Ozonation process assisted by nanofiltration	135
6.3 Ozonation of model compounds	137
6.3.1 Ozonation of BPA	137
6.3.2 Ozonation of tartrazine	143
6.4. Ozonation membrane assisted process	148
6.4.1 Nanofiltration of ozonated BPA effluent	148
6.4.2 Nanofiltration of ozonated tartrazine effluent	151
6.5 Conclusions	154

Chapter 7. Removal of BPA by enzyme polymerization using nanofiltration membranes

7.1 Introduction	159
7.2 Enzymes	160
7.2.1 Horseradish Peroxidase (HRP)	161
7.2.2 Laccase	161
7.2.3 Enzymatic membrane system	162
7.3 Enzymatic BPA degradation	163
7.3.1 HRP enzymatic treatment	163
7.3.2 Laccase enzymatic treatment	166
7.3.3 BPA removal using HRP and laccase in a membrane nanofiltration system	167
7.4 Conclusions	175

Chapter 8. Conclusions and future work

References

About the author

List of Figures

Figure 1.1	Suitability of water treatment technologies according to COD contents.	18
Figure 1.2	Application options for membranes in municipal wastewater treatment.	19
Figure 1.3	General membrane separation process.	23
Figure 1.4	Membrane filtration modes.	25
Figure 1.5	Characteristics of pressure-driven membrane processes.	26
Figure 1.6	Mechanisms contributing to the total resistance towards mass transport.	37
Figure 3.1	Filtration experimental set-up.	50
Figure 3.2	Nanofiltration test protocol.	51
Figure 3.3	Fenton oxidation set-up.	52
Figure 3.4	Calibration curve of the ozone generator as a function of power applied and air flow rate.	55
Figure 3.5	Ozonation set-up.	56
Figure 3.6	Calibration curves for dye concentrations determination.	60
Figure 3.7	Surface topography image of virgin polymeric membranes.	63
Figure 3.8	Surface ESEM images for virgin polymeric membranes.	65
Figure 3.9	Cross section ESEM images for the virgin polymeric membranes.	66
Figure 4.1	Nanofiltration of BPA. Normalised permeate flux and BPA rejection as a function of nanofiltration time for the different membranes tested.	72
Figure 4.2	Nanofiltration of BPA. Normalised permeate flux before, at 200 min of NF (end), and after water flushing, and BPA final rejection for the different membranes tested.	73
Figure 4.3	Nanofiltration of BPA. Normalised permeate flux as a function of filtration time for the different BPA feed concentrations.	75
Figure 4.4	Nanofiltration of BPA. Normalised permeate flux before, at 200 min of NF (end), and after water flushing, and BPA final rejection for several BPA concentrations.	76
Figure 4.5	Nanofiltration of BPA. Normalised permeate flux as a function of filtration time for semi recirculation mode.	78
Figure 4.6	Nanofiltration of TAR. Normalised permeate flux and TAR rejection as a function of filtration time for the different membranes.	80
Figure 4.7	Nanofiltration of TAR. Normalised permeate flux before, at 200 min of NF (end), and after water flushing, and final TAR rejection for the several membranes tested.	80
Figure 4.8	Nanofiltration of TAR. Normalised permeate flux as a function of filtration time for several TAR feed concentrations.	81

Figure 4.9	Nanofiltration of TAR. Normalised permeate flux before, at 200 min of NF (end), and after water flushing, and final TAR rejection for several TAR concentrations.	82
Figure 4.10	Nanofiltration of several dyes. Normalised permeate flux and rejection as a function of filtration time.	83
Figure 4.11	Nanofiltration of several dyes. Normalised permeate flux before, at 200 min of NF (end), and after water flushing.	85
Figure 4.12	Used NF270 membranes after nanofiltration of several dyes.	85
Figure 5.1	Treatment flowsheet for Fenton oxidation.	92
Figure 5.2	Intermediates with one or two aromatic rings formed during oxidative degradation of BPA by sub-stoichiometric Fenton.	96
Figure 5.3	Intermediates with more than three aromatic rings formed during oxidative degradation of BPA by sub-stoichiometric Fenton.	97
Figure 5.4	Possible pathway to the fragments of the tartrazine.	98
Figure 5.5	Fenton treatment over BPA. BPA conversion as a function of reaction time for several initial BPA concentrations.	102
Figure 5.6	Fenton treatment over BPA. BPA conversion as a function of reaction time for several H ₂ O ₂ /BPA stoichiometric molar ratios.	103
Figure 5.7	Fenton treatment over BPA. BPA conversion as a function of reaction time for several Fe ⁺² /H ₂ O ₂ molar ratios.	104
Figure 5.8	Fenton treatment over TAR. TAR conversion as a function of reaction time for several TAR initial concentrations.	108
Figure 5.9	Fenton treatment over TAR. TAR conversion as a function of reaction time for several H ₂ O ₂ /TAR stoichiometric molar ratios.	109
Figure 5.10	Fenton treatment over TAR. TAR conversion as a function of reaction time for several Fe ⁺² /H ₂ O ₂ molar ratios.	110
Figure 5.11	Nanofiltration of BPA-Fenton effluent. Normalised permeate flux as a function of time for the several membranes tested.	112
Figure 5.12	Nanofiltration of BPA-Fenton effluent. Normalised permeate flux before, at the end, and after filtration, for the several membranes tested.	113
Figure 5.13	Nanofiltration of BPA-Fenton effluent. Normalised permeate flux as a function of time for several transmembrane pressures.	116
Figure 5.14	Nanofiltration of TAR-Fenton effluent. Normalised permeate flux as a function of time for the several membranes tested.	117
Figure 5.15	Nanofiltration of TAR-Fenton effluent. Normalised permeate flux before, at the end, and after water flushing for the several membranes tested.	118
Figure 6.1	Proposed reaction pathways for the formation of products in the ozonation of BPA.	133
Figure 6.2	Ozonation of BPA. BPA conversion as a function of reaction time for several ozone influent concentrations at 100 NL/h of ozone-air flow rate; and for several ozone-air flow rates.	137
Figure 6.3	Ozonation of BPA. BPA conversion as a function of reaction time for several pH ₀ at 30 °C, and for several reaction temperatures at pH ₀ 6.	139

Figure 6.4	Ozonation of BPA. BPA conversion as a function of reaction time for several BPA initial concentrations.	140
Figure 6.5	Ozonation of TAR. TAR conversion as a function of reaction time for several ozone inlet concentrations at 100 NL/h of ozone-air flow rate, and for several ozone-air flow rates.	144
Figure 6.6	Ozonation of TAR. TAR conversion as a function of reaction time for several pH_0 at 30 °C, and for several reaction temperatures at pH_0 6.	144
Figure 6.7	Ozonation of TAR. TAR conversion as a function of reaction time for several TAR initial concentrations.	145
Figure 6.8	Nanofiltration of BPA-ozone effluent. Normalised permeate flux as a function of time for several membranes.	149
Figure 6.9	Nanofiltration of BPA-ozone effluent. Normalised permeate flux before, at the end and after filtration for several membranes tested.	150
Figure 6.10	Nanofiltration of TAR-ozone effluent. Normalised permeate flux as a function of time for several membranes.	152
Figure 6.11	Nanofiltration of TAR-ozone effluent. Normalised permeate flux before, at the end and after filtration for several membranes tested.	153
Figure 7.1	Effect of H_2O_2 concentration on HRP catalyzed BPA removal.	164
Figure 7.2	Effect of HRP initial concentration on HRP catalyzed BPA removal.	165
Figure 7.3	Effect of pH on HRP catalyzed BPA removal.	166
Figure 7.4	Effect of laccase dose on laccase catalyzed BPA removal.	167
Figure 7.5	Effect of pH on laccase catalyzed BPA removal.	167
Figure 7.6	Nanofiltration of treated BPA effluent by laccase, HRP and Fenton at 6 bar, room temperature using a NF270 membrane.	168
Figure 7.7	Micrographies of virgin and NF270 membranes applied for the enzymatic degradation of BPA using laccase and HRP.	170
Figure 7.8	Permeate and feed concentration of BPA as a function of filtration time for different degradation process using NF270 membrane.	171
Figure 7.9	Nanofiltration of treated BPA effluent by Laccase and HRP at 6 bar, room temperature and NF90 membrane.	174
Figure 7.10	Permeate and feed concentration of BPA as a function of filtration time for different enzyme process using NF90 membrane.	175

List of Tables

Table 1.1	Advantages and limitations of various decolourization methods for industrial effluents.	14
Table 1.2	Wastewater treatment processes.	16
Table 1.3	Standard reduction potentials of some oxidants in acidic media.	21
Table 1.4	Formation of hydroxyl radicals by several AOPs.	22
Table 1.5	Membrane filtration processes classification as function of the driving force.	23
Table 3.1	Model compounds referenced in this study.	47
Table 3.2	Chemical characteristics of the dyes selected.	48
Table 3.3	Properties of the polymeric membranes tested.	49
Table 4.1	Nanofiltration of BPA. Final normalised permeate flux rejection for the several transmembrane pressures applied.	77
Table 4.2	Nanofiltration of TAR. Final normalised permeate flux rejection for the several transmembrane pressure applied.	82
Table 5.1	Fenton's oxidation reactions and their rate constants.	91
Table 5.2	Fenton treatment over BPA. Effect of BPA initial concentration, H_2O_2/BPA and Fe^{2+}/H_2O_2 initial molar ratio on the conversion and colour formation.	101
Table 5.3	Fenton treatment over TAR. Effect of TAR initial concentration, H_2O_2/BPA and Fe^{2+}/H_2O_2 initial molar ratio on the conversion and colour formation.	107
Table 5.4	Elemental composition of virgin and used membrane for NF of BPA Fenton effluent at 6 bar and 30 °C.	114
Table 5.5	Nanofiltration of BPA-Fenton effluent. Rejection of COD, TOC, colour and Fe^{2+} for the several membranes tested.	115
Table 5.6	Elemental composition of virgin and used membrane for NF of TAR-Fenton effluent at 6 bar and 30 °C.	119
Table 5.7	Nanofiltration of TAR-Fenton effluent. Rejection of COD, TOC, colour and Fe^{2+} for the several membranes tested.	120
Table 6.1	Ozone reactions and its rate constants.	128
Table 6.2	Ozonation of BPA. Effect of BPA initial concentration, influent ozone gas concentration, ozone-air flow rate, pH_0 and reaction temperature on the COD and TOC conversion, and colour formation after 80 min of ozonation.	141
Table 6.3	Ozonation of TAR. Effect of TAR initial concentration, influent ozone gas concentration, ozone-air flow rate, pH_0 and reaction temperature on the COD and TOC conversion, and colour formation after 80 min of ozonation.	147
Table 6.4	Nanofiltration of BPA-ozone effluent. Flux decline, fouling and rejections for several membranes after 250 min of operation.	150

Table 6.5	Nanofiltration of TAR-ozone effluent. Flux decline, fouling and rejections for several membranes after 250 min of operation.	154
Table 7.1	Elemental composition of virgin and used NF270 membrane after of BPA nanofiltration experiments at 6 bar and room temperature for enzymatic degradation process.	170
Table 7.2	Normalised permeate flow before, at the end and after of BPA nanofiltration experiments at 6 bar and room temperature for several degradation process using NF270 membrane.	173
Table 7.3	Normalised permeate flux before, at the end and after of BPA nanofiltration at 6 bar and room temperature for several degradation processes using NF90 membrane.	175

Nomenclature and abbreviations

A_m	Membrane area	(m ²)
COD	Chemical Oxygen Demand	(mgO ₂ /L)
C_b	Concentration in the bulk solution	(mg/L)
C_F	Concentration of the given compound in the feed solution	(mg/L)
C_m	Concentration at the membrane surface	(mg/L)
C_p	Concentration of the given compound in the permeate	(mg/L)
C_t	Concentration at time t	(mg/L)
C_0	Initial concentration of the model compound	(mg/L)
$F_{ozono-air}$	Ozone-air gas flow rates	(NL/h)
IP	Percentage of sample identification	(%)
J_p	Instantaneous permeate fluxes during filtration	(L/h.m ²)
J_{pf}	Final permeate flux	(L/h.m ²)
J_{w0}	Pure water permeate flux of clean membrane	(L/h.m ²)
J_{wf}	Pure water permeate flux of fouled membrane	(L/h.m ²)
K_{ow}	Octanol-water partition coefficient	(-)
m	Total collected mass of the permeate	(kg)
MW	Molecular weight	(g/mol)
MWCO	Molecular weight cut-off	(Da)
pH_0	Initial solution pH	(-)
pH_R	Reaction solution pH	(-)
pH_F	Filtration solution pH	(-)
pK_a	Acid dissociation constant	(pH)
PWP	Pure water permeability	(L/m ² .h.bar)
Q_F	Feed flow rate	(L/h)
Q_p	Permeate flow	(L/h)
R	Retention coefficient or rejection coefficient	(%)
RT	Retention time	(min)
RBPA	Rejection of BPA	(%)
RTAR	Rejection of tartrazine	(%)
R_A	Resistance due to adsorption	(1/m)
R_C	Resistance due to external deposition or cake formation	(1/m)
R_{CP}	Resistance due to concentration polarisation	(1/m)
R_f BPA	Final rejection of BPA compound	(%)
R_f TAR	Final rejection of tartrazine	(%)
R_G	Resistance due to gel formation	(1/m)
R_M	Membrane resistance	(1/m)
R_P	Internal pore fouling resistance	(1/m)
R_{TOT}	Total resistance over membrane	(1/m)
TDI	Tolerable Daily Intake	(µg/kg body weight/day)
TMP	Transmembrane pressure	(bar)
T_F	Filtration temperature	(°C)
t_F	Nanofiltration time	(min)
T_R	Reaction temperature	(°C)
t_R	Reaction time	(min)
X	Conversion of model compounds	(%)

X_{BPA}	Conversion of BPA	(%)
[BPA]	Concentration of BPA	(mg/L)
[BPA] _{Fe}	Concentration of BPA in the feed tank	(mg/L)
[BPA] ₀	Initial concentration of BPA	(mg/L)

Greek symbols

γ	Yield or recovery	(%)
η_T	Dynamic viscosity	(Pa.s)
λ_{max}	Maximum absorbance wavelength	(nm)
v	Cross-flow velocity	(cm/s)
ΔC	Gradient of concentration	(mg/L)
ΔE	Gradient of electrical potential	(V)
ΔP	Gradient of pressure	(bar)
ΔT	Gradient of temperature	(°C)

Abbreviations

ACN	Acetonitrile
AFM	Atomic Force Microscope
ANVISA	The Brazilian Sanitary Surveillance Agency
AOP	Advanced Oxidation Processes
BOD	Biological Oxygen Demand
BPA	Bisphenol A
CEC	Commission of the European Communities
CP	Concentration polarisation
EC SCF	European Commission's Scientific Committee on Food
EDC	Endocrine Disrupting Compounds
EDS	Energy Dispersive Spectroscopy
EFSA	European Food Safety Authority
EPA	US Environmental Protection Agency
ESEM	Environmental Scanning Electron Microscopy
HPLC	High Performance Liquid Chromatography
MF	Microfiltration
NHE	Normal Standard Hydrogen Electrode
NF	Nanofiltration
PSCF	Preferential sorption-capillary flow model
R	Reacting organic compound
RO	Reverse Osmosis
SD	Solution-diffusion model
TAR	Tartrazine
TFC	Thin Film Composite
UF	Ultrafiltration
US FDA	U.S. Food and Drug Administration
WWF	World Wide Fund for Nature
WWTP	Wastewater Treatment Plant

Chapter 1

Introduction

1.1 Description and relevance of the topic

In the last 100 years, humans have introduced thousands of new synthetic compounds into the environment (Schummer 1997). Many of these compounds are known, and even were specifically developed to influence microbial, plant, and animal physiological functions. Nevertheless, some have had unintended physiological consequences on non-targeted species. How these compounds ultimately influence physiology and fitness of individual organisms, dynamics of populations, and ultimately functioning of ecosystems, is not well understood yet.

Many human-introduced compounds influence the endocrine system of animals and have been termed "endocrine disrupting compounds" (EDCs). EDCs are known as a class of chemicals having xenobiotic and exogenous origins while mimicking or inhibiting the natural action of the endocrine substances in animals and human, such as synthesis, secretion, transport, and binding, although they maintain the homeostasis, reproduction, metabolism, development, and/or behaviour of living species (Chang et al. 2009a).

A wide range of chemical compounds have been found to be capable of disrupting the endocrine systems. EDCs differ in origin, size, potency, chemical life cycle, amount, and effects. Many are chemicals produced for specific purposes and they are used in pesticides, plastics, cosmetics, electrical transformers and other products. Other substances are generated as a by-product during manufacturing or are breakdown products of some other chemical. Some, like diethylstilbestrol and ethinylestradiol, are synthetic drugs, while others are natural plant compounds called phytoestrogens. A more complete list with approximately 560 substances can be found in the Annex 1 of the CEC report of the Commission of the European Communities (CEC 2001).

The effects associated with the presence of EDC in the environment are very diverse: reduction in the breakage of eggs of birds, fishes and turtles; feminization of male fish; some problems in the reproductive system in fishes, reptiles, birds and mammals; and changes in the immunologic system of marine mammals. In some cases, these effects can lead to decline in populations. The effects of EDCs in humans reported so far have been

reduction of the amount of sperm; increase of the incidence of breast; testicle and prostate cancers; and the endometriosis (Esplugas et al. 2007).

The potential effects of these “emergent” contaminants in water are still uncertain and they require further investigation. The fact that many known and suspected EDCs are being found at environmentally significant concentrations in the effluent of wastewater treatment plants (WWTPs) is receiving increasing attention in public and regulatory areas. The society is concerned about the safety of consuming trace amounts of EDCs in drinking water, though the only confirmed negative effects from EDCs exposure have involved wildlife health.

Depending on the target compound, different destructive methods allowing the efficient elimination of the pollutant from an aqueous form can be chosen. EDCs removal methods fall into three categories: physical removal such as adsorption by activated carbon (Matsui et al. 2002) and rejection by membranes (Van der Bruggen et al. 1998); biodegradation for instance with activated sludge processes (Andersen et al. 2003); and advanced oxidation processes (AOPs) (Jiang et al. 2005). The selection of any of them will depend on the concentration, the properties of the compounds, the volume flow rates of the effluent to be treated, and the cost of the process, among others.

Other important class of contaminants is the dyes. Dyes and pigments represent one of the more problematic groups of pollutants. They are emitted into wastewaters from various industrial branches, mainly from the dye manufacturing and textile finishing. Many dyes are particularly difficult to remove by conventional waste treatment methods since they are stable to light and oxidizing agents -in fact, they have been designed to- and are resistant to aerobic digestion. The removal of dyes in an economic manner remains an important problem although recently a number of successful systems have been developed using new techniques.

Dye molecules comprise of two key components: the chromophores, responsible for producing the colour, and the auxochromes, which can not only supplement the chromophore but also render the molecule to be soluble in water and give enhanced affinity (to attach) toward the fibers. Dyes exhibit considerable structural diversity and are

classified in several ways. These can be classified (Hunger 2003) both by their chemical structure and their application to the fiber type.

Dyes are considered an objectionable type of pollutant because they are toxic, generally due to oral ingestion and inhalation, leading to problems like skin and eye irritation, skin sensitization, and also due to carcinogenicity. They impart colour to water that is visible to human eye, and therefore, highly objectionable on aesthetic grounds. In addition, they also interfere with the transmission of light and upset the biological metabolism processes which cause the destruction of aquatic communities present in ecosystem. As a consequence, it is important to treat coloured effluents for the removal of dyes.

A wide range of methods has been developed for the removal of dyes from waters and wastewaters in order to decrease their impact on the environment. The technologies involve adsorption on inorganic or organic matrices, decolourization by photocatalysis, and/or by oxidation processes, microbiological or enzymatic decomposition, etc. (Hao et al. 2000).

In this work, Bisphenol A (BPA) and tartrazine are taking as the target molecule to study the removal of EDCs and dyes from aqueous solution.

BPA belongs to the numerous anthropogenic compounds considered as endocrine disruptors and it is produced when 2 mol of phenol react with 1 mol of acetone in the presence of a catalyst. BPA is used primarily in the production of epoxy resins and polycarbonate products (Staples et al. 1998). The polycarbonates have many applications in the manufacturing of many consumer products, such as food and drink packaging, compact disks, automotive lenses, medical devices, motorcycle helmets, and safety glasses. Epoxy resins are used as protective coating for food and beverage cans, PVC pipes, aerospace applications, car coatings, and anti-corrosion coatings for floors (Kang et al. 2006).

Since 1993, when Krishnan documented that BPA was released from polycarbonate flasks during autoclaving and had estrogenic activity, the effects of BPA on health have become a controversial issue (Krishnan et al. 1993). It is reported that BPA exhibited estrogenic activity, which increases the rate of proliferation of breast and prostate cancer cells and

induces acute toxicity to freshwater and marine species (Samuelsen et al. 2001). BPA can be degraded by microorganisms; however it is hard to be completely eliminated by conventional biological treatment methods, which inevitably leads to the existence of low-concentration BPA in aqueous solution. BPA has been found to be widely distributed in the environment. Therefore, the development of treatment techniques for the decomposition, detoxification and removal of BPA in water is urgently required.

Tartrazine is an azo dye usually present in many drugs, food products and cosmetics. Due to its wide applicability in various industrial processes and its hydrophilic nature, its presence can be noticed as a yellow menace in effluents. The contact of the dye is reported to result in various types of health problems like hypersensitivity (Lockey 1977), mutagenic and carcinogenic effects (Chung 1983), allergy and asthma (Pohl et al. 1987), skin eczema (Devlin and David 1992) and immunosuppressive effects (Koutsoqorqopoulou et al. 1998).

Several treatment processes for BPA and tartrazine in water have been examined, using chemical, biological, photochemical, as well as electrochemical procedures. Concerning the elimination of BPA, there are very few studies on its removal from water sources, except those concerning an electrochemical process (Kuramitz et al. 2004), photo-oxidation (Zhou et al. 2004, Rongchang et al. 2009) or sorption (Ying et al. 2003, Guifang et al. 2009). Non-conventional treatment techniques have been examined for the degradation of BPA, including Fenton process (Sajikia and Yonekubo 2004), sonochemical reaction (Inoue et al. 2008, Guo and Feng 2009), enzymatic degradation (Ispas et al. 2010), ozonation (Irmak et al. 2005), and retention of BPA by NF/RO membranes (Kimura et al. 2004, Agenson et al. 2003), among others.

There are very few studies in the literature concerning tartrazine degradation. Salem and Gemeay (2000) examined oxidation kinetics of tartrazine with peroxydisulfate in the presence and absence of Ag(I) and Fe(III) catalysts and observed higher conversion in alkaline medium. Fragoso et al. (2009) investigated the degradation of tartrazine by oxidation with hydrogen peroxide in alkaline solution. Mittal et al. (2007) studied the removal of tartrazine using waste material-hen feathers as adsorbent. Patel and Suresh (2006) studied decolourization of azo dyes using magnesium–palladium system. Gupta et al. (2011) and Tanaka et al. (2000) removed the tartrazine by photodegradation on titanium

dioxide surface. And Oancea et al. (2013) investigated the photo-Fenton process for the degradation of tartrazine in aqueous medium.

BPA and tartrazine are difficult to be degraded under natural conditions. They can be decomposed through anaerobic-aerobic biological process only when microorganisms are domesticated for a long period (Voordeckers et al. 2002). Thus, AOPs have been proposed as attractive alternative methods for treatment of polluted water. Because of their simplicity and high oxidizing power the ozonation and Fenton's process are AOPs widely used for oxidation and degradation of organic substances (Neyens and Baeyens 2003).

In the past, ozonation has shown to be effective for the oxidation of phenol (Wu et al. 2000), p-chlorophenol (Andreozzi and Marotta 1999), phthalate (Legube et al. 1983) and other organic contaminants including BPA and synthetic dyes (Deborde et al. 2008, Turhan and Turgut 2009a). Meanwhile the degradation rate of BPA and tartrazine in aqueous solution was investigated by Fenton's process (Ioan et al. 2007, Arslan et al. 2008, Arroyave et al. 2009); however limited data are available in the literature on the removal of BPA and tartrazine from contaminated water using this process.

The application of membrane processes like nanofiltration (NF) and reverse osmosis (RO) in water treatment plants are effective for removal of organic micropollutants. Studies on the removal of EDCs such as BPA during water treatment have been limited due to the low concentration of these components in water sources and the associated difficulties in analysis. Experimental results of BPA removal from wastewater using membrane bioreactor and nanofiltration technology have shown the general ability of membrane processes to contribute significantly to the removal of EDCs in wastewater treatment (Wintgens et al. 2002).

The membrane technologies are effective wastewater treatment processes developed in recent decades, and are a potential technique for wastewater reclamation. Although the effluent qualities of membrane technologies are generally better than that of conventional treatment processes, it is unknown whether it is effective enough to remove EDCs and synthetic dyes (van der Bruggen and Vandecasteele 2003). Thus, it is necessary to investigate the performance of the membrane technologies in removal of EDCs and dyes. In any case, membrane processes are non-destructive methods and must be complemented

with other technologies. Therefore, the use of membrane in combination with a chemical or biological treatment process is attractive for wastewater treatment. It answers the demand for more efficient, compact and discreet treatment units suitable for densely populated areas where both the land cost and sensitivities are high (Heng et al. 2007).

Thus, considering the widespread detection of BPA and tartrazine in the environment and the limited data available in the literature on the treatment of BPA and tartrazine contaminated water, the main objective of this study is to investigate the degradation of BPA and tartrazine during Fenton's process and ozonation under different operational conditions, additionally, to combine these processes with retention of low concentrations of BPA, tartrazine and intermediates of oxidation in a NF system. In this sense, also goals are to evaluate the removal efficiency of BPA and tartrazine by the membrane and to investigate the factors influencing retention, such as trans-membrane pressure, feed composition and membranes properties.

1.2 Bisphenol A

Bisphenol A (BPA) is a high priority organic compound for assessment of human health risk as it is considered to present the greatest potential for human exposure and has been classified on the basis of its reproductive toxicity. BPA has been identified as Endocrine Disruptor Compound (EDC) by the US Environmental Protection Agency (EPA), World Wide Fund for Nature (WWF) (Zhao et al. 2003) and is becoming a social issue of increasing interest (Bautista-Toledo et al. 2005). An EDC is defined as "an exogenous agent that interferes with the production, release, transport, metabolism, binding, action, or elimination of natural hormones in the body responsible for the maintenance of homeostasis and the regulation of developmental processes" (Wetherill et al. 2007). This definition is not limited to endocrine disrupting effects exclusive of the estrogenic system. Rather, endocrine disruption encompasses effects on other endocrine systems including those mediated by androgens, thyroid hormone, prolactin, and insulin, among others.

BPA is the commonly used name for 2,2-(4,4-dihydroxydiphenyl) propane. BPA is manufactured by two different methods. The first one condenses phenol with acetone under low pH and high temperature conditions in the presence of catalysts and catalyst

promoters. Crude BPA is then purified using distillation. The molten purified product is filtered and dried. The second is similar, but uses different catalysts and purification technology generating fewer wastes (Staples et al. 1998). Many countries throughout the world have large BPA production capacities, especially Germany, the Netherlands, the USA, and Japan. Major producers include Dow, Bayer, Shell, GE Plastics, Aristech, Mitsubishi, Mitsui, and Shin Nihon.

BPA is a chemical used primarily in the manufacture of polycarbonate plastic, epoxy resins and as a non-polymer additive to other plastics. About 65% of the BPA produced is used to make polycarbonate, and approximately 25% is used in epoxy resin production. The remaining 10% is used in other products such as special resins and in the manufacture of flame retardants, such as tetrabromobisphenol A. Final products include adhesives, protective coatings, powder paints, automotive lenses, protective window glazing, building materials, compact disks, optical lenses, thermal paper, paper coatings, and for encapsulation of electrical and electronic parts.

1.2.1 Environmental and human exposure, source and effects

Environmental and human exposure can arise from a number of sources. There are several potential routes of BPA entry into the environment. At manufacturing and processing facilities, low levels of BPA are directly released to surface waters and the atmosphere via permitted discharges. Various types of fugitive emissions to air may occur while processing and handling BPA during its manufacture or use. Additionally, BPA theoretically could be released from various products that contain small amounts of unreacted BPA or that are converted to BPA under specific conditions. Human exposure particularly comes from the direct contact of food with BPA containing plastics. BPA leaching from the plastic material used to line food and drink cans has received particular attention. Other human exposure routes that are a focus of attention include BPA leaching from babies' feeding bottles, and BPA and related compounds leaching from dental fillings and sealants. The European Commission's Scientific Committee on Food (EC SCF) estimated BPA exposure to be 0.48–1.6 µg/kg body weight/day from food sources. Alternatively, using literature from contamination in the environment (water, air, soil) and food contamination (can surfaces, plastic containers); the daily human intake of BPA has been estimated at less than 1 µg/kg body weight/day (Vandenberg et al. 2007). On 23rd

July 2008, the European Food Safety Authority (EFSA) published an updated opinion on the use of BPA based food contact materials. EFSA concluded that the permanent Tolerable Daily Intake (TDI) of 50 µg/kg body weight/day (Erickson 2008) provided a sufficient margin of safety for the protection of consumer, including sensitive subgroups, such as foetuses and infants.

BPA had been detected in all kinds of environmental water, not only found in industrial wastewater, but also can be encountered in raw water. The maximum concentrations reached up to 17,2 mg/L in hazardous waste landfill leached (Yamamoto et al. 2001), 12 µg/L in stream water (Kolpin et al. 2002) and 0,1 µg/L in drinking water (Ministry of Health, Labour and Welfare of Japan 2000). BPA is also used as a reactive agent in the production of temperature-sensitive paper with colour developing layers. Therefore, paper mill effluents (either paper making or recycling) and recycling paper products, such as toilet paper (contributing significantly to wastewater) must also be considered as a major source for BPA in wastewater and wastewater sludge (Rigol et al. 2002). BPA was also found in ground waters from agricultural and industrial wells due to leaching of this compound (Latorre et al. 2002).

Diverse biological effects have been attributed to low-dose environmental BPA exposure (level below 50 µg/kg body weight/day) in a variety of tissues. Very low doses of BPA were reported to cause proliferation of human prostate cancer cells, cardiovascular disease, type 2 diabetes, and liver-enzyme abnormalities in a representative sample of the adult US population (Wetherill et al. 2002). The primary endocrine disrupting activities of BPA extend beyond its ability to mimic, enhance or inhibit the activity of endogenous estrogens and/or disrupt estrogen nuclear hormone receptor action, and include the following: effects upon the androgen systems (Roy et al. 2004); disruption of thyroid hormone function (Ghisari and Bonfeld-Jorgensen 2005); diverse influences on development, differentiation and function of the central nervous system (Ishido et al. 2004); and influences on the immune system (Alizadeh et al. 2006).

1.2.2 Treatments

BPA can indeed be degraded by microorganisms. However, it is hard to be completely eliminated by conventional biological treatment method, which inevitably leads to the

existence of low-concentration BPA in the exited aqueous effluents. Conventional separation techniques, such as coagulation, flocculation and precipitation processes, are not effective in removing BPA (Westerhoff et al. 2005). Advanced separation processes, such as adsorption, membrane filtration, and ion exchange, normally show superior removal efficiencies (up to 99%); depending on the physicochemical properties of both BPA and separation medium. The adsorption by activated carbon is generally considered to be one of the most efficient methods to control organic contaminants in water. Several studies have reported the adsorption efficiency of BPA onto selected activated carbons. According to these reports, the high specific area and low surface polarity of activated carbon was considered the main factor to produce a high adsorption amount of BPA (Liu et al. 2009a).

It has been reported that NF/RO membrane filtration processes are capable of removing BPA (Yüksel et al. 2013). Compared to conventional processes, membrane filtration processes has a remarkable advantage because of the high quality of its effluent, including extremely low organic concentration, and removal of microbes and viruses without chemical disinfection. Other methods have been developed to remove BPA from water, such as biological methods (Staples et al. 1998, Kang and Kondo 2002, Xuan et al. 2002), chemical oxidation (Xuan et al. 2002), electrochemical oxidation (Kuramitz et al. 2004), and photocatalytic methods (Wang et al. 2009, Fukahori et al. 2003). Due to the role of highly reactive free radicals, Advanced Oxidation Processes (AOPs) have shown the ability to destructively oxidize BPA from sewage and water. Recent studies on chemical oxidation by ozone (Garoma and Matsumoto 2009), UV photolysis (Chen and Pignatello 1997), UV/H₂O₂ (Rosenfeldt and Linden 2004), photo-Fenton process (Katsumata et al. 2004) and TiO₂ photocatalysis (Wang et al. 2009) have shown the usefulness of AOPs for removing BPA.

1.3 Tartrazine

Food additives are commonly used in processed foodstuffs to improve appearance, flavour, taste, colour, texture, nutritive value and conservation (Alves et al. 2008). Synthetic colorants, as compared to natural dyestuffs, have been extensively used in food industries in the past six decades because of their higher brightness, more stability, cheapness and the wider range of shades (Ashkenazi et al. 1991). Tartrazine, also known as FD&C Yellow

No. 5, C.I. Acid Yellow 23, Food Yellow 4 (FY4), E 102, CAS 1934-21-0, is a food colouring substance.

Tartrazine essentially consists of 3-carboxy-5-hydroxy-1-(4'-sulphophenyl)-4-(4'-sulphophenylazo) pyrazole trisodium salt and subsidiary colouring matters together with sodium chloride and/or sodium sulphate as the principal uncoloured components. Tartrazine is described as the sodium salt but the calcium and the potassium salts are also permitted (EC 2008). Tartrazine is prepared from 4-amino benzenesulphonic acid, which is diazotized using hydrochloric acid and sodium nitrite. The diazo compound is then coupled with 4,5-dihydro-5-oxo-1-(4'-sulphophenyl)-1Hpyrazole-3-carboxylic acid or with the methyl ester, the ethyl ester, or a salt of the carboxylic acid. The resulting dye is purified and isolated as the sodium salt.

Tartrazine is a dye widely used in certain brands of fruit squash, fruit cordial, coloured fizzy drinks, instant puddings, cake mixes, custard powder, soups, sauces, ice cream, ice lollies, sweets, chewing gum, marzipan, jam, jelly, marmalade, mustard, sodas, yoghurt and many convenience foods together with glycerine, lemon and honey products. It is cheaper than beta carotene and therefore used as an alternative to this for achieving similar colour. Thanks to the water-solubility, tartrazine is used in drugs especially shells of medicinal capsules, syrups and cosmetics. It belongs to azo dyes, which are the largest class of synthetic dyes used in food industries. They are characterized by the presence of one or more azo bonds ($-N=N-$) in association with one or more aromatic systems, which may also carry sulfonic acid groups.

1.3.1 Exposure, source and effects

Tartrazine is a synthetic food colour authorised in the EU with maximum permitted use levels of 50 to 500 mg/kg food for various foodstuffs. It is also allowed in alcoholic beverages at levels up to 200 mg/L and non-alcoholic beverages at levels up to 100 mg/L (EC 1994). Because of its wide use in industry and water-soluble nature, tartrazine is found as contaminant in industrial effluents. Specially, food, cosmetic and pharmaceutical industries consume large quantities of water and are therefore a source of considerable tartrazine pollution. The acceptable daily intake (ADI) of human for tartrazine is 0 to 7.5 mg/kg body weight/day (Walton et al. 1999).

Tartrazine has been implicated as the food additive most often responsible for allergic reactions, having thus been targeted by the scientific community. Tartrazine is known to provoke asthma attacks and urticaria in children (U.S. Food and Drug Administration (US FDA) estimates 1/10000). In addition, it is linked to thyroid tumours, chromosomal damage and hyperactivity. Moreover, increasing evidence suggests the potential toxicological risk of tartrazine (Kamel and El-Iethy 2011). Tartrazine sensitivity is also linked to aspirin sensitivity used to colour drinks, sweets, jams, cereals, snack foods, packaged soups (Ramakrishnan et al. 2011). Some countries such as Sweden, Switzerland and Norway have included tartrazine on the groups of its anaphylactic potential (Wüthrich 1993). The Brazilian Sanitary Surveillance Agency (ANVISA), based on the severe, albeit rare, side effects of tartrazine demanded a label warning for tartrazine-dyed drugs with effect as of 2002: This product contains the yellow dye tartrazine (FD&C Yellow N°5), which may cause allergic reactions such as bronchial asthma and urticaria in susceptible people.

1.3.2 Treatments

In general, dyes are difficult to be decolourized due to their complex structure, synthetic origin and recalcitrant nature, which makes it obligatory to remove them from industrial effluents before being disposed into hydrological systems (Brown 1987). The colour of water, polluted with organic colorants, reduces when the cleavage of the $-C=C-$ bonds, the $-N=N-$ bonds and heterocyclic and aromatic rings occurs. The absorption of light by the associated molecules shifts from the visible to the ultraviolet or infrared region of the electromagnetic spectrum (Strickland and Perkins 1995). There are about 12 classes of chromogenic groups, the most common being the azo type, which is present in the molecular structure of tartrazine. Traditional wastewater treatment technologies have proven to be markedly ineffective for handling wastewater of synthetic textile dyes. A wide range of methods has been developed for the removal of synthetic dyes from waters and wastewaters to decrease their impact on the environment. Being tartrazine a synthetic dye, these methods are also applied for its removal. These technologies involve physical, chemical and biological wastewater treatment or combinations of these methods. The advantages and limitations of several of these treatment methodologies besides emerging technologies are presented in Table 1.1.

Table 1.1. Advantages and limitations of various decolourization methods for industrial effluents (adapted from Anjaneyulu et al. 2005).

Method	Advantages	Limitations
<u>Physical methods:</u>		
Adsorption (activated carbon, bagasse, peat, wood chips)	Economically attractive. Good removal efficiency.	Cost intensive regeneration process.
Irradiation	Effective removal for a wide range of colorants.	Dissolved oxygen requirement is high. Ineffective for light resistant colorants.
Ion-exchange	Regeneration with low loss of adsorbents.	Specific application.
<u>Chemical methods:</u>		
Oxidation (Fenton's reagent, ozonation, sodium hypochlorite, electrochemical oxidation)	Effective for both soluble and insoluble colorants. Low temperature requirement. Effective for azo dye removal	Problem with sludge disposal. High cost.
Coagulation and precipitation	Short detention time and low costs. Good removal efficiencies.	High cost of chemicals for pH adjustment. Dewatering and sludge handling problems.
Cucurbituril	Complete decolourization for all class of dyes.	Expensive.
<u>Biological methods:</u>		
Aerobic process	Colour removal is facilitated along with COD removal.	Longer hydraulic times and substrate specific removal. Less resistant to recalcitrant compounds.
Anaerobic process	Resistant to wide variety of complex colorants. Bio gas produced is used for steam generation.	Longer acclimatization phase.
Single cell (Fungal, Algal & Bacterial)	Good removal efficiency for low volumes and concentrations. Very effective for specific colorant removal.	Culture maintenance is costly. Cannot cope up with large volumes of coloured effluents.
<u>Emerging technologies:</u>		
Advanced oxidation Processes	Complete mineralization ensured. Effective pre-treatment methodology in integrated systems and enhanced biodegradability.	Cost intensive process.

Table 1.1 Continued.

Membrane Filtration	Recovery and reuse of chemicals and water. Wider application for complex wastes.	Dissolved solids are not separated in this process. High running cost.
Photocatalysis	Process carried out at ambient conditions. Complete mineralization with shorter reaction times.	Effective for small amount of colorants. Expensive process.
Sonication	Simplicity in use. Very effective in integrated systems.	Relatively new method and awaiting full scale application.
Enzymatic treatment	Effective for specifically selected compounds. Unaffected by shock loadings and shorter contact times required.	Relatively new method and awaiting full scale application
Redox mediators	Easily available and enhances the process by increasing electron transfer efficiency.	Concentration of mediator may give antagonistic effect. Also depends on biological activity of the system.
Engineered Wetland Systems	Cost effective technology and can be operated with huge volumes of wastewater.	High initial installation cost. Requires expertise and managing during heavy rain becomes difficult.

1.4 Wastewater treatment

Water is one of the abundantly available resources in nature and is essential for animal and plant life. Around 1850, citizens became aware of the hygienic aspects of wastewater and initiated the collection and also the treatment of the wastewater. After World War II; pollution of water bodies is steadily increasing due to industrial proliferation and urbanization. In many countries the treatment of wastewater became compulsory by law around 1970. Initially, the treatment of the wastewater was focused on the removal of oxygen consuming pollutants, i.e. ammonia and biological oxygen demand (BOD) and was later followed by removal of nutrients to decrease eutrophication of receiving water bodies. Nowadays, the worldwide production and use of chemical compounds have tremendously increased, which find their way into the environment and many of these compounds are biologically non-degradable. Therefore, the major concern is to treat the wastewater before it is discharged into the environment. In most western countries the large part of the

wastewater is treated in order to protect the water quality of the receiving rivers and lakes. In the near future the driving force may even shift towards the shortage of fresh water resources.

Untreated wastewater generally contains high levels of suspended solids, biodegradable organics, pathogenic organisms, priority pollutants, refractory organics, heavy metals, and dissolved inorganic constituents (Metcalf and Eddy 2003). Priority pollutants represent organic and inorganic compounds that are highly toxic, carcinogenic, mutagenic or teratogenic. Refractory organics compounds are those that tend to resist conventional wastewater treatment include surfactants, phenols and agricultural pesticides, among many others. Physical, chemical and biological methods are used to remove contaminants from wastewater. In order to achieve different levels of contaminant removal, individual wastewater treatment procedures are combined into a variety of systems, classified as primary, secondary, and tertiary wastewater treatment. Preliminary treatment process is also used to render an effluent suitable for further treatment.

Primary treatment involves the physical separation of suspended solids from the wastewater influent using screening and sedimentation tanks. This separation reduces total suspended solids as well as the BOD levels. Pre-aeration or mechanical flocculation with chemical additions can be used to enhance primary treatment. Secondary treatment has the objective of removing soluble and colloidal organics and suspended solids that have escaped the primary treatment and reduce BOD and chemical oxygen demand (COD) through biological process. In this biological treatment processes, microorganisms convert the colloidal and dissolved carbonaceous organic matter into various gases and into cell tissue leading to reduction of BOD and COD. This is typically done through processes, namely by activated sludge process, trickling filtration, oxidation ditch and oxidation ponds. In tertiary treatment, stubborn contaminants that secondary treatment was not able to clean up are removed. Tertiary treatment may include processes such as: membrane filtration, dechlorination and disinfection systems, reverse osmosis systems, ion exchange, activated carbon adsorption and still other physical/chemical treatments.

As above mentioned, wastewater treatment methods are also classified into physical, chemical and biological processes. Table 1.2 lists the unit operations included within each category.

Table 1.2. Wastewater treatment processes (adapted from Zhou and Smith 2002).

Process	Treatment
Physical	Screening, comminution, clow equalization, sedimentation, flotation, granular-medium filtration
Chemical	Chemical precipitation, adsorption, disinfection, dechlorination, other chemical applications
Biological	Activated sludge process, aerated lagoon, trickling filters, rotating biological contactors, pond stabilization, anaerobic digestion, biological nutrient removal

As technology changes take place in manufacturing, changes also occur in the compounds discharged and the resulting wastewater characteristics. Numerous compounds generated from industrial processes are difficult and costly to treat by conventional wastewater treatment processes. Therefore, effective industrial pre-treatment becomes an essential part of an overall water quality management program. Enforcement of an industrial pre-treatment program is a daunting task, and some of the regulated pollutants still escape to the municipal wastewater collection and must be treated.

Wastewater treatment effectiveness has become limited and ever more critical over the last two decades because of three new challenges: diminishing water resources, increasing wastewater disposal costs, and stricter discharge regulations that have lowered permissible contaminant levels in waste streams (Mallevalle et al. 1996). To resolve these new challenges and better use economical resources, various advanced treatment technologies have been proposed, tested, and applied to meet both current and anticipated treatment requirements. Advanced treatment technologies have been demonstrated to remove various potentially harmful compounds that could not be effectively removed by conventional treatment processes. Among them, AOPs and membrane filtration have been proven to successfully remove a wide range of challenging contaminants and hold great promise in water and wastewater treatment (Zhou and Smith 2002).

AOPs can potentially be used in wastewater treatment for overall organic content reduction (COD), specific pollutant destruction, sludge treatment, increasing bioavailability of recalcitrant organics, and colour and odour reduction (Bergendahl and O'Shaughnessy 2004). Advanced oxidation is the chemical oxidation with oxygen radicals, which are very reactive, short-lived oxidants. Hydroxyl radicals ($\text{HO}\cdot$) are extraordinarily reactive species, they attack the most part of organic molecules with rate constants usually in the order of $10^6\text{--}10^9 \text{ M}^{-1} \text{ s}^{-1}$ (Hoigné and Bader 1983). They could be produced in systems using: Fenton's reagent (ferrous iron and hydrogen peroxide), titanium dioxide/ultraviolet radiation, ozone/hydrogen peroxide, ultraviolet radiation/ozone, ultraviolet radiation/hydrogen peroxide, and through other means.

In the latter case, the usage of AOPs for partial oxidation of trace organic contaminants might not be an appropriate approach in the cases where other organic matter is predominantly present, since the oxidant requirement can be exceedingly high in order to achieve effective degradation of trace organics. Figure 1.1 shows the suitability of water treatment technologies according to COD contents. Only wastes with relatively small COD ($\leq 5 \text{ g/L}$) contents can be suitably treated by means of these techniques since higher COD contents would require the consumption of too large amounts of expensive reactants.

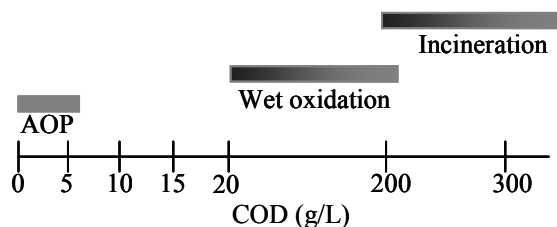


Figure 1.1. Suitability of water treatment technologies according to COD contents (Andreozzi et al. 1999).

A suitable application of AOPs to wastewater treatments must consider that they make use of expensive reactants as H_2O_2 , and/or O_3 and therefore it is obvious that their application should not replace, whenever possible, the more economic treatments as the biological degradation (Malato et al. 2002). AOPs can be installed either as tertiary treatment after the biological (secondary) treatment of wastewater, or as pre-treatment stage in order to enhance the biodegradability of trace organic contaminants.

As commercial membranes are available over a wide range of pore sizes, membrane filtration technologies can effectively remove various contaminants. Membrane filtration has become a popular water and wastewater treatment method for large volumes, because of its ability to remove minute particles such as fats, protein and pathogens, and its competitive cost in comparison with traditional treatment methods (Cheryan and Rajagopalan 1998, Abboah-Afari and Kiepper 2011). Membrane filtration has been used in the treatment of municipal water, paper machine white water (Nuortila-Jokinen et al. 1998), paper mill effluents (Ahn et al. 1998, Zhang et al. 2009), pulp mill effluents, oil and grease wastes (Reed et al. 1997), textile wastewater (Fersi et al. 2005, Wu et al. 1998), brewery wastewater (Brindle and Stephenson 1996) and many other aqueous effluents.

Applications of membrane filtration can be divided into solid–liquid separation, organic and inorganic contaminants removal. Membrane filtration are mostly applied as effluent polishing stages of municipal wastewater treatment plants, taking a secondary or tertiary effluent as feed with rather low suspended solids content, and organic matter (see Figure 1.2). Those employed in tertiary wastewater treatment are dedicated to remove suspended solids, organic matter, and for disinfection, thus recovering a high quality final effluent with various possible uses. The main purpose of membranes in water reuse schemes is therefore the retention of microorganisms. Most membrane filtration processes provide a relatively effective barrier for all microorganisms, including viruses (Wintgens et al. 2005).

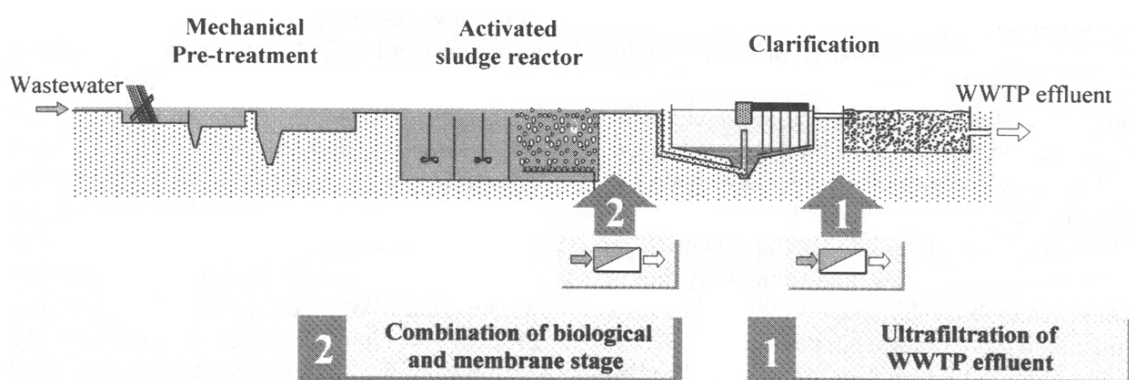


Figure 1.2. Application options for membranes in municipal wastewater treatment (Wintgens et al. 2005).

1.5 Advanced oxidation processes

In the past two decades, AOPs have been used for the treatment of wastewater containing recalcitrant organic compounds such as pesticides, surfactants, colouring matters, pharmaceuticals and endocrine disrupting chemicals. Moreover, they have been successfully used as pre-treatment methods in order to reduce the concentrations of toxic organic compounds that inhibit biological wastewater treatment processes (Legrini et al. 1993).

AOPs are defined as near ambient temperature and pressure water treatment processes, which are based on the generation of hydroxyl radicals to initiate oxidative destruction of organics. AOPs involve the two stages of oxidation: the formation of strong oxidants (e.g., hydroxyl radicals) and the reaction of these oxidants with organic contaminants in water (Azbar et al. 2004). The term AOPs refers specifically to processes in which oxidation of organic contaminants occurs primarily through reactions with hydroxyl radicals (Glaze et al. 1987). Depending on the nature of the organic species, the hydroxyl radicals can attack organic chemicals by radical addition (eq. 1.1), hydrogen abstraction (eq. 1.2) and electron transfer (eq. 1.3) (Buxton et al. 1988, Legrini et al. 1993, Pignatello et al. 2006). In the reactions represented by eq. 1.1 to 1.3, R is used to describe the reacting organic compound.



AOPs make new oxidized intermediates with lower molecular weight (MW) or carbon dioxide and water in case of complete mineralization. Thanks to its high standard reduction potential of 2.8 V vs. NHE (Normal Standard Hydrogen Electrode) in acidic media (see Table 1.3); these radicals would be able to oxidize almost any organic compound to carbon dioxide and water. Although hydroxyl radical is the second strongest oxidant, some of the simplest organic compounds, such as acetic, maleic and oxalic acids, acetone or simple chloride derivatives as chloroform have shown to be non-attackable by hydroxyl radicals (Bigda 1996). These compounds are typical remnant oxidation products from larger

molecules after fragmentation and they take part in energetic cycles of most living organisms.

Table 1.3. Standard reduction potentials of some oxidants in acidic media (Hunsberger 1977).

Oxidant	Standard reduction potential (V vs. NHE)
Fluorine (F ₂)	3.03
Hydroxyl radical (HO [•])	2.80
Atomic oxygen	2.42
Ozone (O ₃)	2.07
Hydrogen peroxide (H ₂ O ₂)	1.77
Potassium permanganate (KMnO ₄)	1.67
Hypobromous acid (HBrO)	1.59
Chlorine dioxide (ClO ₂)	1.50
Hypochlorous acid (HClO)	1.49
Chlorine (Cl ₂)	1.36
Bromine (Br ₂)	1.09

AOPs involve a wide variety of methods of activation as well as oxidant generation and can potentially utilize a number of different mechanisms for organic destruction. These generally involve generation and use of powerful but relatively non-selective transient oxidizing species. A partial list of these processes is included in Table 1.4.

The major drawback of AOPs is their high operating cost compared to other conventional physicochemical or biological treatments. Therefore, AOPs cannot achieve complete mineralization due to this restriction. One of the most reasonable solutions to this problem is coupling AOPs with other treatment methods.

Table 1.4. Formation of hydroxyl radicals by several AOPs.

	Advance Oxidation Processes	Hydroxyl radical formation	
Non-photochemical	Ozone	$3O_3 + H_2O \rightarrow 2OH\cdot + 4O_2$	(eq. 1-4)
	Hydrogen peroxide /Ozone	$H_2O_2 + 2O_3 \rightarrow 2OH\cdot + 3O_2$	(eq. 1-5)
	Fenton's reactions	$Fe^{2+} + H_2O_2 \rightarrow Fe^{3+} + OH^- + OH\cdot$	(eq. 1-6)
Photochemical	UV light	$H_2O + hv (< 190 \text{ nm}) \rightarrow H\cdot + HO\cdot$	(eq. 1-7)
		$H_2O + hv (< 190 \text{ nm}) \rightarrow H^+ + e^- + HO\cdot$	(eq. 1-8)
	Hydrogen peroxide/UV	$H_2O_2 + hv \rightarrow 2HO\cdot$	(eq. 1-9)
	Ozone/UV	$O_3 + hv + H_2O \rightarrow H_2O_2 + O_2$	(eq. 1-10)
		$H_2O_2 + hv \rightarrow 2OH\cdot$	(eq. 1-11)
		$2O_3 + H_2O_2 \rightarrow 2OH\cdot + 3O_2$	(eq. 1-12)
	Ozone/UV/Hydrogen peroxide	$2O_3 + H_2O_2 + hv \rightarrow 2HO\cdot + 3O_2$	(eq. 1-13)
	Photo-Fenton process	$Fe(OH)^{2+} + hv \rightarrow Fe^{3+} + HO\cdot$	(eq. 1-14)
	Titanium dioxide/UV	$TiO_2 + hv \rightarrow e^-_{CB} + h^+_{VB}$	(eq. 1-15)
		$H_2O + h^+_{VB} \rightarrow OH\cdot + H^+$	(eq. 1-16)
	$O_2 + e^-_{CB} \rightarrow O_2\cdot^-$	(eq. 1-17)	
	$O_2\cdot^- + H_2O \rightarrow OH\cdot + OH^- + O_2 + HO_2^-$	(eq. 1-18)	

1.6 Membrane filtration processes

A membrane filtration process can be defined as a separation process where a feed stream (liquid or gas) is separated into two product streams, the retentate (or concentrate) stream and the permeate (or filtrate) stream (Figure 1.3) by means of some physical barrier (Mulder 1997). Thus, the membrane acts as a selective barrier that allows the passage of certain components and the retention of others, implying the concentration of one or more components either in the permeate (i.e., effluent passing through the membrane) or in the retentate (i.e., the concentrated stream that does not pass through the membrane). It depends on the membrane separation properties whether certain components pass the membrane or not. The actual driving force for membrane separation is a chemical potential

difference between each side of the membrane, which results in a transport of species. The origin of the driving force is often used to classify membrane processes. As driving forces, gradients in pressure (ΔP), concentration (ΔC), temperature (ΔT) and electrical potential (ΔE) are encountered. Table 1.5 summarizes the different membrane processes in connection with their driving force.

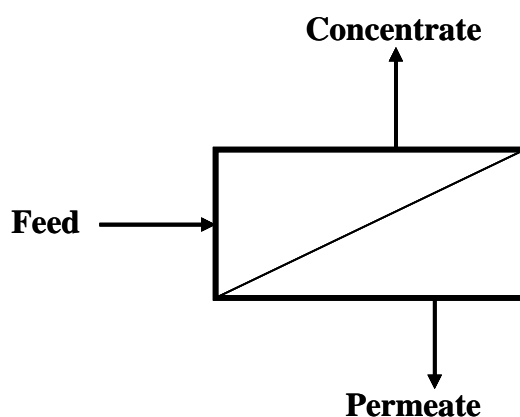


Figure 1.3. General membrane separation process.

Table 1.5. Membrane filtration processes classification as a function of the driving force (Mulder 1997).

Driving force			
ΔP	ΔC	ΔE	ΔT
Microfiltration	Gas separation	Electrodialysis	Thermo-osmosis
Ultrafiltration	Dialysis	Electro-osmosis	Membrane distillation
Nanofiltration	Pervaporation		
Reverse Osmosis	Liquid membrane		

Three main parameters characterize the performance of a given membrane process: the permeate flux, the selectivity or rejection and the yield or recovery (Braeken 2005). Permeate flux, J_p , is the term used to describe how fast permeate passes through a membrane. Permeate flux generally depends upon the individual membrane characteristics (i.e., membrane pore size, membrane surface charge, etc), the characteristics of the feed stream (i.e., viscosity, solute particle size, etc), and operating parameters (i.e., transmembrane pressure, feed temperature, etc). The permeate flux per unit of pressure is defined as the permeability. A high permeate flux is preferable for an economic operation of the filtration process. The permeate flux is given by:

$$J_p = \frac{1}{A_m} \frac{dm}{dt} \quad (\text{eq. 1.19})$$

Here, m is the total collected mass of permeate at a time t and A_m the membrane area.

The rejection is a measure of the membrane ability to retain a certain solute and is expressed as a rejection (or retention) coefficient, R . A rejection of 100% refers to total exclusion, whereas a rejection of 0% means that no solute has been retained, so no separation has been done. The rejection of a solute can be calculated by Equation 1.20, where C_p and C_F are the concentration of a given compound in the permeate and in the feed solution, respectively.

$$R(\%) = \left(1 - \frac{C_p}{C_F}\right) \cdot 100 \quad (\text{eq. 1.20})$$

The last parameter is the yield or recovery, γ , which is a useful parameter for the design of an industrial application rather than a membrane characteristic. The recovery indicates the overall production of the system. It is the relationship between the permeate flowrate, Q_p , and the feed flow rate, Q_F (eq. 1.21).

$$\gamma(\%) = \frac{Q_p}{Q_F} \cdot 100 \quad (\text{eq. 1.21})$$

Most membrane separation systems used in industrial applications are operated in a cross-flow feed configuration as opposed to dead-end mode. In the cross-flow configuration, concentrate passes tangential (parallel) to the membrane surface as opposed to perpendicular flow which is used in dead-end filtration. It is generally accepted that cross-flow configuration is advantageous over dead-end operation. In dead-end configuration, all the feed permeates through the membrane, leaving, thus accumulating, all the retained species in the feed compartment; in turn, limited accumulation of the retained compounds occurs over the membrane surface due to the continuous flow circulation in the feed compartment in cross-flow operation. Therefore, the limited solute accumulation over the

membrane surface reduces the subsequent loss of permeate flux due to the lower hydrodynamic resistance at the membrane surface.

Membrane separation systems are typically operated in one of three main filtration modes (Masciola 1999): recycle, semi-batch (“modified batch”), or batch (Figure 1.4). In recycle mode, the feed is pumped from its tank into the membrane module; then, both permeate and retentate are returned to the feed tank. Thus, the concentration of the solution in the feed tank remains constant over time. This configuration is only used for membrane performance characterization at lab- or bench-scale. In semi-batch mode, fresh feed solution is added to the feed tank at the same rate that permeate is produced whilst the retentate is recycled back, so the tank solution is concentrated over time. And in batch mode, fresh solution is not added to the feed tank while the permeate is removed and the retentate recycled back. Thus, the feed volume is reduced and the feed solution is concentrated.

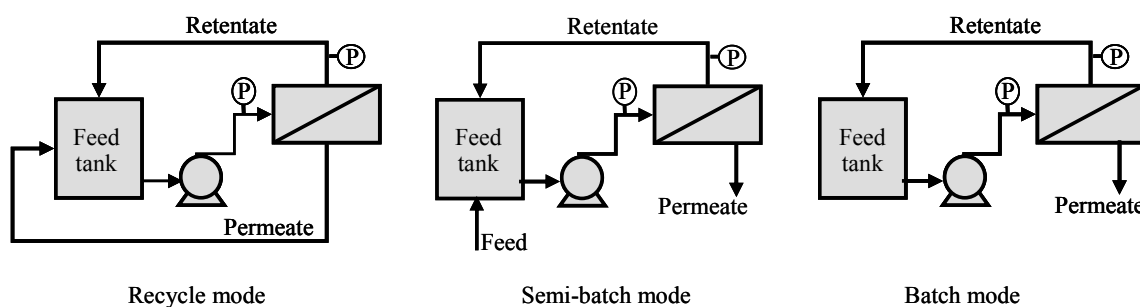


Figure 1.4. Membrane filtration modes.

Based on pressure as the driving force, four different membrane processes can be distinguished: microfiltration (MF), ultrafiltration (UF), nanofiltration (NF) and reverse osmosis (RO). Although these separation techniques are related to each other, each of them has its specific characteristics. The main features of the four pressure-driven processes are summarized in Figure 1.5. The pressure difference between both sides of a membrane is called the trans-membrane pressure (TMP) so it is the difference between the pressure at the feed side and the pressure at the permeate side. The relationship between flux, J_p , and TMP is defined by a modified form of the Darcy’s law and is given in Equation 1.22, where ΔP is the pressure difference, TMP , η_T is the dynamic viscosity and R_{TOT} is total resistance over the membrane.

$$J_p = \frac{\Delta P}{\eta_T \cdot R_{TOT}} = \frac{TMP}{\eta_T \cdot R_{TOT}} \quad (\text{eq. 1.22})$$

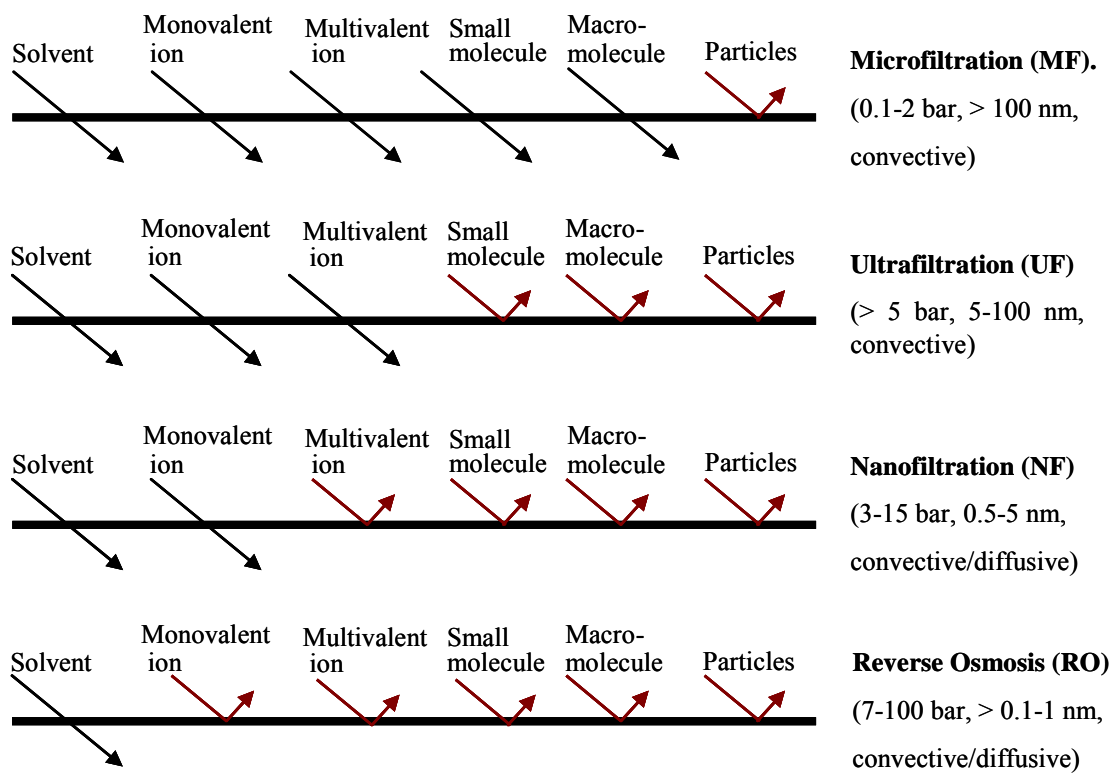


Figure 1.5. Characteristics of the pressure-driven membrane processes (Mulder 1997). In parenthesis are emphasized the applied pressure range, membrane pore size range and type of transport.

MF membranes have the largest pore size and typically reject large particles and many microorganisms. MF is a pressure-driven membrane process based on a “sieving mechanism” in which particles are separated from solution based on size. It is applied to separate particles in the size range from 0.1 to 10 μm . It is frequently used as a pre-treatment step for NF or reverse osmosis. Similarly to MF, UF is used to separate material in the 0.001-1 μm size range, i.e., from 2000 to 500000 of Molecular Weight Cut-Off (MWCO), by sieving. The MWCO is defined as the molecular weight (MW) of standard solutes that are 90% rejected by the membrane. This definition, however, strongly depends on the process circumstances, therefore is only a qualitative characterization parameter (Koops 1995). Components with a MW above the MWCO have a high retention whereas molecules with a MW below the MWCO are barely retained. The typical unit of MWCO is Dalton (Da), being equivalent to one gram per mol. UF membranes have smaller pores

than MF membranes and, therefore, in addition to large particles and microorganisms, they can easily reject bacteria and soluble macromolecules such as proteins (Élysée-Collen and Lencki 1997). There is no a clear distinct border between MF and UF processes. TMPs ranging from 0.1 to 5 bar are common in UF and MF applications.

RO is a membrane separation technique used to separate materials with molecular diameters from $\sim 10^{-4}$ to 10^{-3} μm (less than ~ 200 Da in MWCO). RO is generally used to remove salts and ions from solutions. Its major application is as both brackish and seawater desalination technology. The transport mechanism in RO is based on the sorption-diffusion concept. The typical TMP range from 7 to 100 bar. NF membranes are relatively new and are sometimes called “loose” RO membranes. NF membranes were born from the modification of RO membranes. They are porous membranes, but since the pores are on the order of 1 nm or less, they exhibit performance between that of RO and UF membranes. Its MWCO is typically found to be between 200 and 1000 Da; and TMP ranging from 3 to 15 bar are common in NF applications. NF is generally used to remove species nearly in the range from 10^{-3} to 10^{-2} μm . NF is often used to dewater low MW organic species such as pesticide and herbicide solutions (Perry and Green 1997). Additionally, NF membranes are able to efficiently retain organic micropollutants and multivalent ions from water and wastewater (Ahn et al. 1999, Kimura et al. 2003).

1.6.1 Nanofiltration

NF is a recently introduced term in membrane filtration processes. NF was developed in the 1970s and 1980s through modification of reverse osmosis membranes (Braeken 2005). Eriksson (1988) was one of the first authors using the word NF explicitly, some years before FilmTec started to use this term for their NF50 membrane which was supposed to be a very loose RO membrane or a very tight UF membrane (Conlon 1985). UF can provide higher flux at lower operating pressure and can remove macromolecules. However, it can not remove salts, acids, sugars etc. RO has lower flux at higher operating pressure and is used for demineralization of total dissolved solids. NF appears as a process falling between RO and UF, where it combines some attributes of RO and UF with the ability to reject macromolecules and multivalent ions effectively at moderate operating pressure (Amy et al. 1990). Using NF, effective removal of salts (multivalent), heavy metals, colour, all viruses, bacteria and parasites from water and wastewater is possible

(Cluff 1992). Thus NF is nowadays considered the most promising technique if a high water quality has to be obtained, but extreme demineralization is not required.

Since its introduction, the application range of NF has extended tremendously. New possibilities were discovered for drinking water production, providing answers to new challenges such as arsenic removal (Brandhuber and Amy 1998, Kosutic et al. 2005, Shih 2005), removal of pesticides, endocrine disruptors and chemicals (Yoon et al. 2007, Xu et al. 2005, Nghiem et al. 2004), and partial desalination (Hassan et al. 1998, Hassan et al. 2000, Al-Sofi et al. 1998). NF membranes can be divided into two categories concerning their structures, i.e. porous and dense membranes. The porous and dense membranes have the same separation performance, although their mechanism is different. Solutes will be separated by sieving mechanism in case of porous membranes; whereas in dense membranes a solution-diffusion type of mechanism will determine the transport (Peeters 1997).

At this moment, several polymeric NF membranes are commercially available. Typical polymers are polyvinylalcohol (PVA), polyethersulfone (PES), cellulose acetate (CA), polyamide (PA) and polypiperazineamide (PPA). Except those based on cellulose acetate, which are symmetric membranes, all these membranes are thin film composite membranes (TFC), i.e., membranes having a thin dense top layer (tens to hundreds of nanometres) deposited on a more porous support. For solvent applications, the stability of polymeric membranes is lower than in aqueous solution applications and low fluxes combined with relatively low retentions are obtained (Schaepe 1999). Ceramic NF membranes are being developed to solve this problem.

As aforementioned, the separation performance (such as rejection, R , and permeation flux, J) of a NF membrane generally depends on the characteristics of the feed stream, the individual membrane characteristics, and the operating parameters.

1.6.1.1. Membrane rejection mechanisms

Depending on the physicochemical characteristics of the solute and the membrane, separation can be achieved by one or several mechanisms. Physicochemical characteristics imply that separation can be due to physical selectivity (charge repulsion, size exclusion or

steric hindrance) or chemical selectivity (solvation energy or solute adsorption). This section will provide a brief overview of these mechanisms.

Size exclusion

Transport of charged and uncharged solutes through a membrane pore will be susceptible to steric hindrance/size exclusion effects. Steric hindrance is mainly determined by the size of the solute, relative to the size of the membranes pores. Solute larger than the membrane pores (or with a molar mass above the MWCO) are well rejected; solutes smaller than the membrane pores (or with a molar mass lower than the MWCO) can permeate through the membrane more easily. The ratio of molecular size and membrane pore size plays an important role in the transport through the membrane, not only because it has a large influence on the rejection of the compound, but since it may also influence the water flux when pores become blocked (Van der Bruggen and Vandecasteele 2001). As it was already mentioned, the MWCO of a membrane is a parameter that indicates the relative size of membranes pores.

Steric hindrance is comparable to a sieving phenomenon except that in membrane filtration, pores neither have a uniform pore size nor are the solutes of a uniform shape. Solute of varying structures are not easily represented by equivalent spheres. However, several researchers consider size exclusion as sieving phenomena since they have an identical retention mechanism (Nghiem 2005). Several studies have shown that steric hindrance represented by MW and/or molecular width is one of the main factors affecting removal of uncharged organic solutes (Kiso et al. 2000, Kiso et al. 2001a, Ozaki and Li 2002, Kimura et al. 2003).

Anyway, MW is the most used parameter reflecting molecular size, although it is not a direct measure of size. The MW is the molecular mass of a compound. MW can be used for the rejection prediction of non-charged and non-polar compounds in low pressure applications (Ozaki and Li 2002). Other possible parameters that can represent the molecular size are the effective diameter (Van der Bruggen et al. 2000), the molecular width (Kiso et al. 1992), the molecular volume, the Stokes radius (Van der Bruggen et al. 1999), and equivalent molar diameter (Davidson and Deen 1988).

Charge exclusion

Electrostatic repulsion is known to be an important mechanism to separate charged solutes from membranes. Most studies on electrostatic interactions have reported an increase in rejection of negatively charged organic solutes due to electrostatic repulsion between the negatively charged membrane surface and the negatively charged organic solute (Yoon et al. 2006, Nghiem et al. 2006, Reed et al. 1997). This high rejection, however, depends on feed water pH, since both membrane surface charge and organic solute charge change with varying pH (Bellona and Drewes 2005).

Most NF/RO membranes carry fixed charged groups and the membrane surface or pore wall can be considered as a charged surface (Nghiem 2005). Membrane surface charge is usually quantified by zeta potential measurements. Membrane surface materials like cellulose acetates or polyamides give a negative charge to most commercial NF membranes (Thorsen 1999).

The effect of the membrane charge on the transport of charged components has already been described by Donnan in the beginning of the last century (Donnan 1911). The well-known Donnan exclusion mechanism is often used to give a qualitative explanation for the retention of ions, frequently mentioned in the desalting and softening processes using NF/RO membranes. Because of the presence of this fixed membrane charge, the concentrations of the ionic species in the membrane surface are not equal to those in the solution. The counter-ion (opposite sign of charge to the fixed charge in the membrane) concentration is higher in the membrane phase than in the bulk solution, while the co-ion (same sign of charge as the fixed membrane charge) concentration is lower in the membrane phase. An electrical potential difference at the interface, called the Donnan potential, is created to counteract the transport of counter-ions to the solution phase and of co-ions to the membrane phase. When a pressure gradient across the membrane is applied, water is transported through the membrane. The effect of the Donnan potential is then repelling the co-ion from the membrane (Schaep et al. 1998). Several numerical models have been suggested to explain the electrostatic effects on the rejection of charged solutes and inorganic ions (Schaep et al. 2001, Vezzani and Bandini 2002). These models always account for the Donnan exclusion.

The organic solute charge is a function of the solute acid dissociation constant, pK_a . The acid dissociation constant, K_a , is an equilibrium constant that measures the ability of a Brønsted acid to donate a proton to a specific reference base, the greater the value of K_a , the stronger the acid. In dilute aqueous solutions, water is the reference base. The acidity constant, pK_a , is defined as $-\log K_a$. The pK_a of a compound is a measure of its acid strength, and practically tells the pH above which the compound is mostly charged (acids) or neutral (bases). The charge of a compound at a given pH depends for compounds containing acidic or basic groups. In combination with the pH of the solution, pK_a influences the rejection because charge interactions are different at different pH values. Hence, depending on its charge, the compound will be attracted to the membrane or repelled. Attraction of molecules to the membrane surface may enhance flux decline.

The moment dipole can also be a measure for electrostatic interactions between the molecule and the membrane. A molecule has an electric dipole moment when it has a net separation of centres of positive and negative charge. If the separation is characteristic of the molecule without the application of an electric field, the molecule is said to have a permanent electric dipole moment. The dipole moment is usually expressed in Debye units, equal to 10^{-8} esu-cm. The permanent dipole moment reflects the charge distribution within a molecule in solution. Thus, the dipole is directed towards the membrane charge in such a way that the side of the dipole with the opposite charge is closer to the membrane. This direction is not static, but must be seen as a statistical tendency of the fast moving molecules to have this preferential orientation. The dipole is thus directed towards the pore and enters more easily into the membrane structure. Once the molecule is in a non dead-end pore, it will permeate. Thus this could possibly be connected with an enhanced flux decline for compounds with high dipole moments (Van der Bruggen et al. 1999).

Adsorption

The adsorption of compounds onto membranes may be an important factor in the rejection of organic solutes during membrane applications. Molecules can get attached to the membrane pores or to the membrane surface by adsorption. This can be physical or chemical in nature or both. Physical adsorption arises from dispersive and electrostatic interaction and chemical adsorption is a result of chemical bonding. By adsorption, pores could become narrower making thinner the free path for the water flow, which decrease the

net pore opening and lead to flux decline. When adsorption has a strong effect, it could even lead to pore blocking when the whole cross section of the pore is filled. When the top surface of the membrane is in contact with the solution, solute molecules adsorb onto the membrane surface due to physico-chemical interactions, e.g. hydrophobic interactions (dispersion forces), polar interactions (dipole-dipole and dipole-induced dipole forces) and charge transfer (hydrogen bonding).

Kiso et al. (2001b) showed over 99% compound rejection by NF membranes of more hydrophobic alkyl phthalates in their study. Researches have shown that hydrophobic solutes can also adsorb onto hydrophobic membranes and into the membrane pores by hydrophobic interactions (Agenson et al. 2003, Kiso et al. 2001b, Nghiem and Schäfer 2002). Hydrophobicity of organic molecules is usually expressed as the logarithm of the octanol-water partition coefficient, $\log K_{ow}$. The octanol-water partition coefficient, K_{ow} , describes equilibrium partitioning of a chemical between octanol and water phases. A chemical that resides preferentially in the water phase is called hydrophilic; a chemical that resides preferentially in the octanol phase is called hydrophobic or lipophilic, and has a large value of K_{ow} (probably 10^3 , 10^4 or even greater). Since measured values range from 10^{-4} to 10^8 , the logarithm of the octanol-water partition coefficient ($\log K_{ow}$ or $\log P$) is commonly used as a measure for the hydrophobicity of a compound. $\log K_{ow}$ is defined only for neutral species, the partition coefficient for partially ionised mixtures or the effective partition coefficient for dissociative systems need the correct description of the complex partitioning equilibrium (Sangster 1997).

Compounds with $\log K_{ow} \geq 2$ are referred to as hydrophobic, and those with $\log K_{ow} \leq 2$ are hydrophilic (Connell 1990). Partitioning of trace organics to the membrane substrate and organic matter in the feed water can be understood and predicted to some extent based on the $\log K_{ow}$. It has been reported that trace organics, which can adsorb to polymeric membranes, usually have high $\log K_{ow}$ and are sparsely soluble in water (Kiso et al. 2001b). Adsorption of trace organics to the membrane can implicate the accumulation of them, which can lead to several deteriorative problems. Additionally, concentration gradient built-up as a result of adsorption followed by diffusion can partly reduce the membrane effectiveness (Nghiem 2005).

Furthermore, the solubility of a given compound in water reflects its affinity for water. Thus, the component tends to remain in the aqueous solution as more high its water solubility is, so less adsorption on the membrane surface is expected. Therefore, water solubility might be a first indication of the effect of a compound on the water flux.

In turn, the hydrophobicity of the membrane surface is measured by the contact angle water-membrane. In this method, a drop of liquid (i.e. water) is placed upon a flat surface (membrane) and the contact angle is measured (Shaw 1992). More hydrophobic membranes are less wettable by a drop of water; the contact angle will consequently have a value greater than 90° . If this is the case, they often exhibit lower water flux. Meanwhile, for membranes with high water affinity, more hydrophilic, the contact angle will be less than 90° . Adsorption of organic compounds has been related to a change in hydrophobicity/hydrophilicity of the membrane surface. Thus, the change of the contact angle may be a tool to measure adsorption (Van der Bruggen et al. 2000). Some results have shown that membranes with larger contact angles can adsorb more mass of organic compounds per unit area than membranes with smaller contact angles, and hydrophobic molecules are more easily adsorbed than hydrophilic molecules (Kimura et al. 2003).

1.6.1.2 Transport model for NF membranes

The mechanism of transport and rejection characteristics of NF membrane are quite complex. Mass transport in UF is due to pure convection, whereas diffusion determines the transport in RO. Because NF is an intermediate process between UF and RO (considering pressure, pore size, etc, both convection and diffusion contribute to the solute transport. In addition, NF membranes carry a charge due to dissociation of acidic and basic groups on the polymer chains. Charge interactions can thus influence the solute transport, too. Many models have been developed to identify the effect of different parameters on the transport mechanism and to predict the NF membrane performance. The two major theories are Souriraja's sorption surface-capillary flow approach and the solution-diffusion theory.

The preferential sorption-capillary flow (PSCF) model proposed by Sourirajan (1970), assumes that the mechanism of separation is determined by both surface phenomena and fluid transport through pores in the RO/NF membranes. In this model the membrane is assumed to be microporous. The model states that the membrane barrier layer has chemical

properties such that it has a preferential sorption for the solvent or preferential repulsion for the solutes of the feed solution. As a result, a layer of almost pure solvent is preferentially adsorbed on the surface and in the pores of the membrane. Solvent transport occurs as solvent from this layer is forced through the capillary membrane pores under pressure. Charged solutes are excluded, even smaller than the membrane pores, by Donnan effect.

The solution-diffusion (SD) model was proposed by Lonsdale et al. (1965); as its name implies, this model is based on diffusion of the solute and solvent through the membrane. The model assumes that the RO/NF membrane has a homogeneous, nonporous surface layer; both the solute and solvent dissolve in this layer and then each diffuses across it; the solute and solvent diffusion is uncoupled and due to its own chemical potential gradient across the membrane; and these gradients are the result of concentration and pressure differences across the membrane.

1.6.1.3 Factors affecting NF permeate flux

Different factors affect the flux through the membrane. These are briefly discussed in the following blocs:

Temperature

The increase of the process temperature enhances the NF membrane flux due to viscosity reduction. However, deviations occur in practice because the total resistance also changes with temperature. When adsorption is the dominant mechanism of flux decline, the adsorption equilibrium is influenced by temperature. The effect of viscosity can thus be partly counterbalanced by mechanisms of flux decline. The rejection of NF membranes is usually not dependent on the process temperature.

Pressure

Generally, the pure water flux through a porous membrane in pressure driven processes is directly proportional to the applied hydrostatic pressure. However, when solutes are added to the water the behaviour observed is completely different. When the pressure is increased

the flux increases, but beyond a finite (minimum) pressure has been attained, the flux does not increase further on increasing the pressure. This maximum flux is called the limiting flux (Mulder 1997). Cheryan (1998) defined this behaviour in two regions. The pressure-controlled region where the increase in the pressure result in an increase in the permeate flux and the mass transfer-controlled region where the limiting flux is reached. The solute rejection used to be greater at higher filtration pressure. Physically, that occurs because an increase in transmembrane pressure causes higher water flux whereas the solute flux is electrically (Donnan exclusion) and sterically hindered and, therefore, does not change as much (Labbez et al. 2003).

Feed concentration

The increase of the feed concentration during NF generally results in a decrease in the permeate flux as the higher the bulk solute concentration, the higher the osmotic pressure and the lower the permeate flux obtained (García et al. 2006). Osmosis is the flow of solvent (usually water) through a semi-permeable membrane from a region of low chemical potential to a region of higher chemical potential. When the concentration increases, an osmotic pressure will result. The reason for this is that when dissolved components cannot permeate the (NF) membrane, a concentration difference between feed and permeate side of the membrane arises.

pH

The pH affects the performance of NF membranes in more than one way. The charged sites on the NF membrane surface can be modified depending on the feed solution pH. It is well know that the rejection of NF membranes could vary at different pH. Since different membrane manufacturers use different chemistries to produce their thin film composite layer, the pH dependency of the membrane should be determined for each membrane type.

Cross-flow velocity

The increase of cross-flow velocity improves the mass transfer of the system as the degree of mixing near the membrane surface is better. This could reduce the fouling on the membrane surface and thus increases the permeate flux.

1.6.1.4 Factors controlling permeate flux and flux decline

The decline in flux is caused by an increase in resistance against mass transfer. The total resistance presented in Equation 1.22 is the sum of all individual resistances. The resistances R_{CP} , R_A , R_G , R_P and R_C denote the additional resistances which result from the exposure of the membrane to a solution containing foulants, and R_M is the membrane resistance. Specifically, R_{CP} is the resistance due to concentration polarisation, R_A the resistance due to adsorption, R_G the resistance due to gel formation, R_P the internal pore fouling resistance, and R_C the resistance due to external deposition or cake formation. It should be noted here that the selection of resistances varies in literature and is somewhat ambiguous (Schäfer et al. 2004). The term “fouling” is used to represent all the different additional resistance with exception of R_{CP} . The different resistances are shown in Figure 1.6 and their contribution in the permeate flux is represented in Equation 1.23.

$$J = \frac{\Delta P}{\eta_T \cdot (R_{CP} + R_A + R_G + R_P + R_C + R_M)} \quad (\text{eq. 1.23})$$

Concentration polarization

The build-up of solute at the membrane surface is known as “concentration polarization”, (CP), and is largely responsible for the deviation of the permeate flux from the linear flux-pressure model. The CP is the process of accumulation of retained solutes in the membrane boundary layer and was first documented by Sherwood (Sherwood et al. 1965). It creates a high solute concentration at the membrane surface, C_m , compared to the bulk solution, C_b , Figure 1.6. The retained solutes are brought into the boundary layer by convection and removed by a generally slower back diffusion. This back diffusion of solute from the membrane is assumed to reach an steady state with the convective transport. The extent of the CP will be determined by the transport mechanisms in the boundary layer and in the membrane. For both sections, a concentration profile can be obtained.

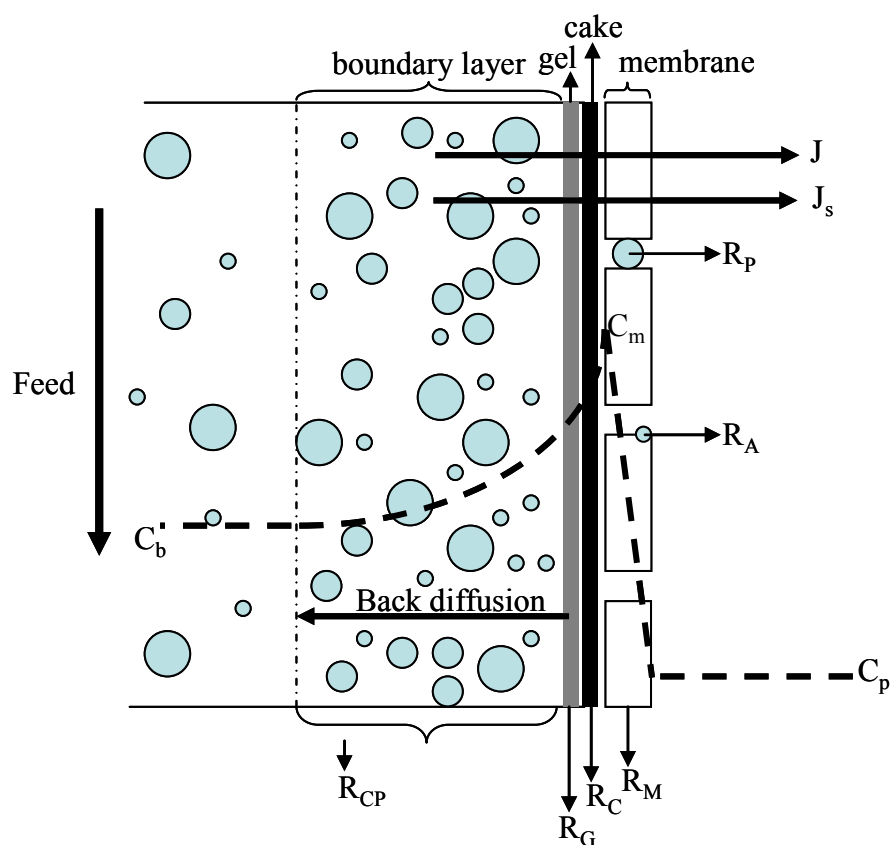


Figure 1.6. Mechanisms contributing to the total resistance towards mass transport (adapted from Mulder 1997).

The CP is a reversible process and will disappear when the driving force ceases. The occurrence of CP results in a fast reduction in flux through the membrane and eventually in adsorption, precipitation or gel formation of the solutes on the membrane surface. To avoid CP, the thickness of the boundary layer can be decreased by increasing the tangential velocity, which corresponds to a change from laminar to turbulent flow. When a turbulent flow pattern is obtained, the CP will have only a marginal effect, due to the constant velocity profile.

Fouling

Fouling is one of the main problems in any membrane separation, but for NF it might be even somewhat more complex because the interactions leading to fouling take place at nanoscale, and are therefore difficult to discern (Jarusutthirak et al. 2007, Her et al. 2007). Fouling is a term used to describe the loss of throughput of a membrane device as it becomes chemically or physically changed by a process fluid. Fouling is different from CP. Both phenomena result in a reduced membrane system output and the resulting

resistances due to both phenomena are additive, however, while CP disappears after stopping the flux, fouling remains unaltered unless some cleaning is performed.

The feed water constituents retained on or in the membrane surface are called foulants. With the increase of the foulants, the resistance of the membrane increases and with a constant TMP, the flux decreases. Membrane fouling can be classified into inorganic or mineral fouling, organic fouling, particles and biofouling, depending on the nature of the involved foulants (Flemming 1995). The fouling mechanisms occurring in a membrane are adsorption inside the membrane pores, gel formation, blocking of the membrane pores, and deposition on the membrane surface even forming a cake layer. During filtration, the fouling mechanisms may occur simultaneously.

Adsorption may occur on the membrane surface or inside the pores, essentially at any point of contact between the solute and the membrane. Details about this mechanism were already presented in the section 2.5.1.1. Gel formation is considered as the precipitation of organic solutes on the membrane surface. This process usually occurs when the wall concentration due to concentration polarisation exceeds the solubility of the organic (or inorganic) species (Schäfer et al. 2004). The resistance against mass transport that is exerted by the gel layer is very high. However, the gel layer formation occurs usually when solutions containing macromolecules are filtered. In the case of pore blocking, solute molecules or other minor constituents of the feed stream are forced into the membrane pores resulting in a loss of permeate flow channels and thus a decrease in permeate flux. If the membrane pores are bigger than the solute diameter, complete and partial pore blocking can occur. Also an internal fouling of the pores is possible, leading to pore narrowing. If the pores are very small in comparison to the solute diameter, the formation of a so-called cake layer is favourable. The cake layer is affected by a lot of parameters, such as pH, ionic strength, TMP, hydrodynamic conditions and still others (Cornelissen 1997).

Chapter 2

Hypothesis and objectives

2.1 Previous considerations

It has been evidenced that BPA and tartrazine cannot be completely eliminated by conventional treatment in drinking water supplies and in some cases, can drive to by-products with higher environmental and health problems (Korshin et al. 2006). Due to the role of powerful free radicals, AOPs have shown the ability to destructively oxidize several pollutants up to 80% from municipal sewage and water (Nakada et al. 2007).

An AOP is defined as the oxidation process, which generates hydroxyl radicals in sufficient quantity to carry out water treatment. For instance, AOPs could use Fenton's and ozone reagent to achieve high performance (Weinberg and Glaze 1997). Hydroxyl radicals possess very high oxidizing power, next only to fluorine, and are able to degrade the organic hazardous compounds to CO_2 and H_2O .

Fenton reactions and ozone oxidation are still the most basic and yet practical AOPs for the treatment of industrial effluents (Banerjee et al. 2007). The ozonation method is known to be effective for degrading organic chemicals containing carbon-carbon double bonds, olefinic double bonds, acetylenic triple bonds, aromatic compounds, phenols, polycyclic aromatics, heterocyclics, carbon-nitrogen double bonds, carbon-hydrogen bonds, silicon-hydrogen and carbon-metal bonds (Gould and Groff 1987). On the other hand, Fenton process is considered as one of the most promising AOPs for leachate treatment (Lopez et al. 2004). However, the removal of BPA and tartrazine from water and wastewater with ozonation and Fenton process has scarcely been researched. Similarly, since the nanofiltration was introduced, its application range has extended tremendously. New possibilities were discovered for drinking water production, providing answers to new challenges such as arsenic removal (Brandhuber and Amy 1998), removal of pesticides, EDCs and chemicals (Xu et al. 2005), and water softening and partial desalination (Hassan et al. 1998).

It should be noted that Fenton and ozonation have some disadvantages. Since Fenton process requires iron salts for the oxidation reaction to take place, the environmentally hazardous iron sludge formed after the reaction has to be removed before discharging. Additionally, the tight acidic pH range in which the Fenton reaction proceeds forces the

effluent neutralization after treatment, because the pH of most waters is not within the optimal reaction range. Meanwhile, the major limitation of the ozonation process is the relatively high cost of ozone generation process coupled with very short half-life period of ozone. Thus, ozone needs to be generated always in site.

There have been numerous attempts to enhance oxidation with additional process steps. In this sense, membrane separation is becoming a very attractive alternative because of its purely physical nature of separation as well as the modular design of membrane processes (Rautenbach and Mellis 1995). Separation without phase change, less energy consumption, operability at ambient temperature, etc., have given an edge to membrane processes over the conventional processes.

Independently, membrane and oxidation processes are well known processes in the field of wastewater treatments by their capacity to eliminate pollutants from water. The combination of these two processes appears to be of special interest due to the different properties that these techniques present. Thus, some compounds produced in the oxidation can be later separated by membrane filtration, or a concentration step by membrane filtration can subsequently allow working at higher oxidation rate.

Most of integrated processes suffer from a lack of information on how to combine pre-treatment and downstream processes. Detailed studies concerning the chemical step are desirable for the design of an efficient integrated process, allowing a systematic approach to decide the necessary degree of chemical oxidation severity in the pre-treatment step. This work is to describe a process in which a nanofiltration membrane is used to retain molecules derived from Fenton and ozonation process over BPA and tartrazine.

2.2 Hypothesis

The coupled integration of AOPs with NF will allow saving cost whilst retain the inherent advantages of both isolated processes, assuming zero harmful pollutant discharges in the treated wastewater.

2.3 Objectives

The overall objective of the present work was the degradation of BPA and tartrazine and their removal by the combination of AOPs and NF. In AOPs, BPA and tartrazine degradation will be faster if the concentrations of them are high, but the processes become extremely slow at trace concentrations. Moreover, an AOP introduces other chemicals into the system. On the other hand, NF yields higher permeate flux when the concentration of pollutant is low. Thus, the purpose of this work was to conduct experimental studies of the combined Fenton's and ozonation oxidation with membrane process to find out the right combination. The combined treatment process would offer considerable advantages non encountered by each of them individually. So, combination of these methods into a single process could offer an attractive alternative to remedy the inherent disadvantages of Fenton oxidation, ozonation and membrane filtration, separately.

The following specific tasks were formulated in order to meet the main objective:

- To optimize the performance of home-made cross flow laboratory membrane cell, in terms of net fluxes and applied trans-membrane pressures in the NF of BPA and tartrazine. To select the nanofiltration membrane and the operating conditions to achieve the best permeate quality and the highest permeate flux. To discuss the filtration mechanisms. To investigate the effect of transmembrane pressure (TMP); initial concentration and membrane properties on permeate flux decrease. Additionally, to compare the performance of NF of tartrazine with the NF of synthetic dyes used in different industries (**Chapter 4**).
- To study the classical Fenton process (hydrogen peroxide oxidation with ferrous salt as catalyst) of target solutions in a batch reaction system. To determine the dependence of BPA and tartrazine degradation on H_2O_2 , Fe^{2+} catalyst, pH and initial concentration. To select the Fenton's process conditions to achieve the best degradation rates (**Chapter 5**).

- To test the ozonation of target solutions in a batch reaction system. To study the pH effect, ozone dosage, reaction time, initial concentration and ozone/air flow rate on the BPA and tartrazine ozone oxidation. To select the ozonation conditions to achieve the best degradations rate (**Chapter 6**).
- To examine the applicability of the nanofiltration technique in the recovery of low BPA and tartrazine concentration solutions resulting from Fenton and ozonation degradation and in their oxidation intermediates (**Chapter 5 and 6**, respectively). To study the effect of membrane properties, trans-membrane pressure on permeate flux decline, BPA and tartrazine rejection and membrane fouling. To demonstrate that, by means of a combination of an oxidation and a separation step, a higher permeate quality of the overall process toward partial oxidation can be achieved.
- To compare the effectiveness of Fenton process against an emerging oxidation process, specifically, the enzymatic oxidation using peroxidase and laccase was selected (**Chapter 7**).

Chapter 3

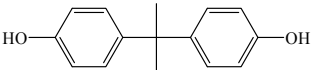
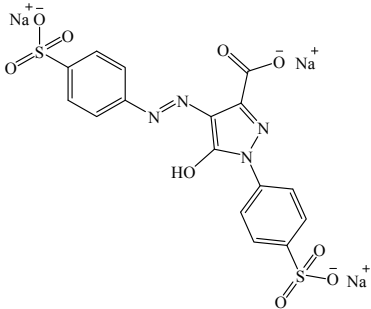
Methodology

3.1 Materials

3.1.1 Model pollutants

All chemicals and reagents in the research were obtained in analytical grade. Model pollutants were Bisphenol A (BPA) and tartrazine (TAR), purchased from Sigma-Aldrich. Some properties of these compounds are shown in Table 3.1. Deionised water was used to prepare all the solutions.

Table 3.1. Model compounds referenced in this study.

Properties	Bisphenol A	Tartrazine
Chemical name	2,2-(4,4-dihydroxydiphenyl) propane	Trinatrium-3-carboxy-5-hydroxy-1-p-sulfophenyl-4-p-sulfophenylazo-pyrazol
Formula	C ₁₅ H ₁₆ O ₂	C ₁₆ H ₉ N ₄ Na ₃ O ₉ S ₂
Molecular weight	228.28	534.3
Specific gravity at 25 °C, (g/cm ³)	1.06	---
Octanol-water partition coefficient	3.32	-1.76
pK _a	9.6 to 10.2	pK _{a1} = 1.8 ; pK _{a2} = 8.3 ; pK _{a3} = 10.8
Water solubility at 20 °C, (mg/L)	120-300	Soluble in water
Molecular size (nm)	Molecular width X: 0.383; Molecular width Y: 0.587; Molecular width Z: 1.068	
Supplier	Sigma-Aldrich	Sigma-Aldrich
Purity	99%	85%
Molecular structure		

In Chapter 4, four synthetic dyes, which have a wide industrial application, were selected, namely; rhodamine 6G, reactive orange 16, reactive black 5 and procion red (from Sigma–Aldrich) to investigate the effect of dyes molecular weight on permeate flux and dye rejection in NF experiments. Dye solutions at 1000 mg/L were prepared by dissolving accurately weighed amounts of dyes in deionised water. Table 3.2 summarises the principal chemical and solution properties for these commercial dyes.

Table 3.2. Chemical characteristics of the dyes selected.

Dye	Molecular formule	MW (g/mol)	$\lambda_{\max}^{(a)}$ (nm)	pH ^(b)
Rhodamine 6G	C ₂₈ H ₃₁ N ₂ O ₃ Cl	479.01	524	4.94
Reactive black 5	C ₂₆ H ₂₁ N ₅ Na ₄ O ₁₉ S ₆	991.82	597	5.41
Reactive Orange 16	C ₂₀ H ₁₇ N ₃ Na ₂ O ₁₁ S ₃	617.54	380	5.74
Procion Red	C ₁₉ H ₁₀ Cl ₂ N ₆ Na ₂ O ₇ S ₂	615.33	530	6.04

^(a) The maximum absorbance, λ_{\max} , was experimentally measured, see section 3.3.2.

^(b) The pH of the solution containing dye at 1000 mg/L was experimentally measured.

3.2 Treatments

3.2.1 Nanofiltration

3.2.1.1 Membranes

Because of its commercial availability and successful application on different cases, five standard polymeric NF membranes, i.e., NFD, NF90, NF270 (Dow Filmtec), ESNA1-LF2 (Hydranautics) and CK (GE Osmonics), were used for studying the potential of NF over model compounds and oxidation product solutions. These names correspond to the commercial designations with the exception of NFD. NFD is commercially designated as NF but, for avoiding confusions with the universally accepted acronym for nanofiltration (NF), this membrane is named NFD throughout the text. Table 3.3 gives the most important properties of the selected membranes.

Table 3.3. Properties of the polymeric membranes tested.

Membrane name	NFD	NF90	NF270	CK	ESNA1-LF2
Supplier	Dow-filmtec	Dow-filmtec	Dow-filmtec	GeOsmonics	Hydranautics
Isoelectric point, (pH)	5.1 ^(c)	4.0 ^(d)	3.5 ^(d)	-	4.9 ^(c)
Pore radius, (nm)	-	0.34 ^(d)	0.42 ^(d)	-	-
MWCO, (Da)	≤200 ^(e)	200	300 ^(f)	150-300 ^(g)	100-300 ^(c)
PWP ^(a) , (L/m ² .h.bar)	8.17 ± 0.46	10.97 ± 0.37	14.44 ± 0.80	1.56 ± 0.02	9.69 ± 1.09
Support	Polysulphone	Polysulphone	Polysulphone Rnwf	-	Polysulphone Rnwf
Active layer	semi-aromatic piperazine-based polyamide TFC	Polyamide TFC	semi-aromatic piperazine-based polyamide TFC	Cellulose Acetate	meta-phenylene diamine-based polyamide
Roughness ^(b) , (nm)	0.16	57.23	4.47	8.36	60.68
Contact angle, (°)	42 ^(d)	30 ^(d)	54 ^(g)	-	60 ^(h)
Salt rejection, (%)	98.0 (MgSO ₄)	85-95 (NaCl) & > 97 (MgSO ₄)	40-60 (CaCl ₂) & < 92 (MgSO ₄)	92 (Na ₂ SO ₄) & < 97 (MgSO ₄)	86 (CaCl ₂)
Maximum Operating Temperature ⁽ⁱ⁾ , (°C)	45	45	45	30	45
Maximum Operating Pressure ⁽ⁱ⁾ , (°C)	41	41	41	31	41
pH range ⁽ⁱ⁾	3-10	3-10	2-11	5.0-6.5	2-10
thickness ^(j) , (µm)	139 ± 10	132 ± 5	128 ± 24	142 ± 14	125 ± 3

^(a) Pure Water Permeability, PWP, as experimentally measured; see section 3.2.1.1.

^(b) Roughness as determinate from AFM images using WSxM v5.0 Develop 6.2 software; see section 3.3.7.1

^(c) From Tanninen et al 2006, ^(d) Nghiem 2005, ^(e) Balannec et al. 2005, ^(f) Liikanen 2006,

^(g) Benitez et al 2009, ^(h) Negaresha et al. 2012.

⁽ⁱ⁾ Values supply by the manufacturer.

^(j) Membrane thickness as measured by microscopy image, see section 3.3.7.2.

3.2.1.2 Filtration tests

Model compound solutions and effluents, after Fenton and ozonation degradation at selected optimal oxidation conditions, were filtered in a NF system. The equipment was a home-made cross flow laboratory unit. It includes a cross flow cell (CF042 Sterlitech Corporation), a feed pump (ProMinent), an 1 L reservoir tank, a pressure dampener and

several pressure gauges to control pressure along the experiment. Recycle mode was used during all the experiments, where both the retentate and the permeate were returned to the feed tank in order to maintain constant feed concentration at room temperature ($T_F=30 \pm 1$ °C). The permeate side was open at atmospheric pressure. The effective membrane surface was 42 cm² and the cross flow velocity and Reynolds used were adjusted in 5.3 cm/s and 290, respectively; corresponding to 20 L/h in the feed flow rate, Q_F . Figure 3.1 depicts a scheme of the system. Temperature and pH of the feed solution were monitored using a Metter Toledo pHmeter. To control the feed temperature, the glass reservoir tank was water-jacketed.

Membrane preconditioning is essential for the experiments. Prior to use, every membrane was immersed in deionised water for 24 h to ensure the complete removal of any impurity and to preserve the solution in the membrane. Later, the membrane was compacted for at least 1 hour using deionised water at 8 bar. Pure permeate water flux of the clean membrane, J_{w0} , was determined at the end of the compaction process. A typical NF test started by filling up the feed tank with 1 L of given solution and then putting the system at specified operational conditions. Permeate flux in the NF of model solution, J_p , was followed for approximately 250 min. Permeate and feed samples were collected for analysis at specified intervals during NF. Once finished a filtration run, the pure water flux, J_{wf} , was again measured using deionised water in order to know the permeate flux decrease due to membrane fouling after filtration. The effect of initial concentration, membrane type and transmembrane pressure on permeate flux were studied. A schematic diagram of the NF test protocol is presented in Figure 3.2.

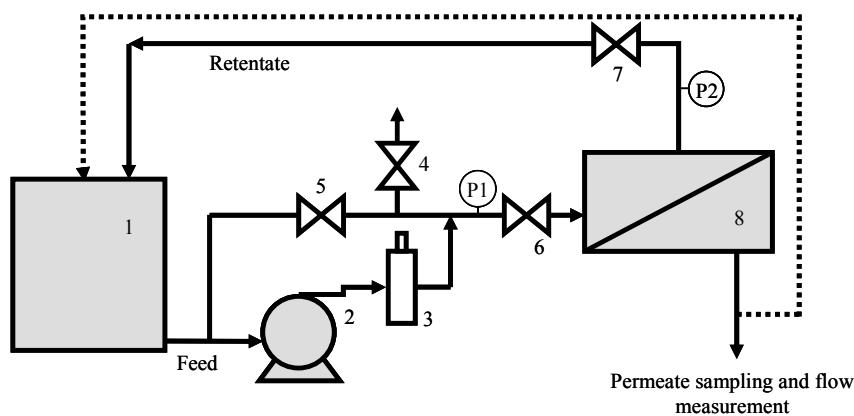


Figure 3.1. Filtration experimental set-up. (1) Feed tank, (2) pump, (3) pulse dampener, (4) relief valve, (5) bypass valve, (6) and (7) backpressure valves, (8) membrane cell, (P1) and (P2) pressure gauges.

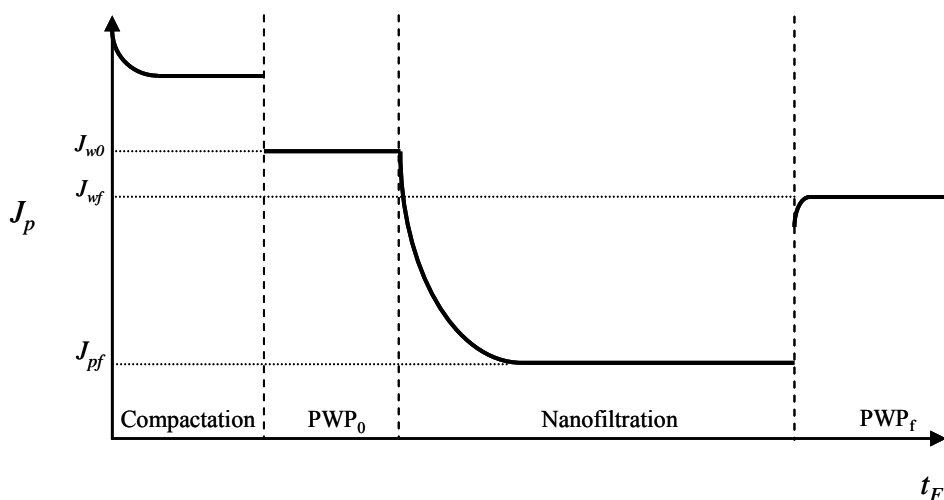


Figure 3.2. Nanofiltration test protocol.

Membrane performance was assessed using the normalised permeate flux, i.e., the ratio between permeate flux, J_p , and pure permeate water flux of the clean membrane, J_{w0} , which is a measure of the flux decline and the rejection, R . Samples from de feed and permeate solution were characterised in terms of total organic carbon (TOC), chemical oxygen demand (COD), and colour. In the NF of Fenton effluents the Fe^{2+} concentration in the feed and the permeate was also measured.

To evaluate the repeatability in the NF experiments, an arithmetic mean was calculated from three well-reproduced repetitions in each series of NF experiments. For instance, in the NF of BPA at 300 mg/L, 6 bar and 30 °C using NF90 membrane, the difference between each value and its corresponding arithmetic mean was less than 5 and 13% for normalised flux and BPA rejection, respectively, which is typical and usually accepted.

As abovementioned, the pure water flux (J_{w0}) was always measured before starting a filtration run. The permeate flux of water is proportional to the transmembrane pressure (TMP) and the water flux per unit of pressure is defined as water permeability. Table 3.3 shows the pure water permeabilities of the selected membranes. They were calculated as the average of pure water permeabilities determined for each new membrane at 30 °C.

3.2.2 Fenton process

3.2.2.1 Materials

Hydrogen peroxide (H_2O_2) and iron (II) sulphate heptahydrate ($\text{FeSO}_4 \cdot 7\text{H}_2\text{O}$) were used as Fenton oxidant and catalyst sources, respectively. Hydrogen peroxide was received and employed as 30% w/v solution and ferrous sulphate heptahydrate as 99.0% purity solid. Both reagents were manufactured by Panreac.

3.2.2.2 Fenton oxidation procedure

Appropriate amounts of model solution and ferrous iron were added to a beaker and diluted with deionised water to 1 L. The Fenton reaction was done in a water-jacketed glass reactor. The experimental set-up used in the Fenton oxidation experiments is depicted in Figure 3.3. The reactor was filled with 1 L of BPA and ferrous ion solution at selected model compound concentrations and $\text{Fe}^{2+}/\text{H}_2\text{O}_2$ molar ratio. Iron hydrolysis was found to affect Fenton process efficiency (Pignatello et al. 2006). In order to avoid it, the model compound and ferrous ion solution were immediately used after their preparation. Then, the initial pH was measured and in some cases adjusted at 3 using HCl 2 M. According to literature (Guedes et al. 2003), the optimum pH is 3 to promote the generation of hydroxyl radicals in a Fenton process. The reaction time started when hydrogen peroxide was added. The actual H_2O_2 to stoichiometric H_2O_2 molar ratio was tested in the range from 0.05 to 1.00 and from 0.17 to 1.40 in the Fenton oxidation of BPA and TAR, respectively.

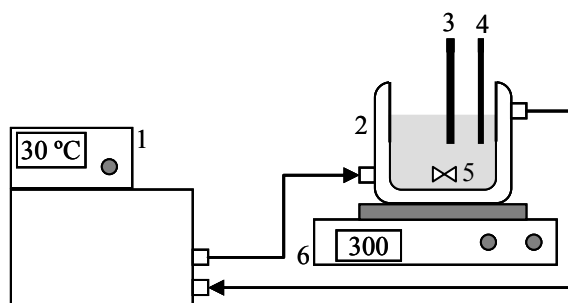
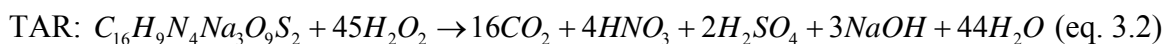
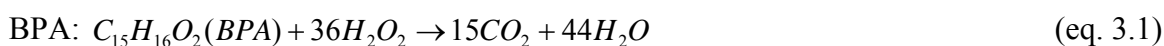


Figure 3.3. Fenton oxidation set-up. (1) Thermostatic bath, (2) reactor, (3) pH probe, (4) temperature sensor, (5) magnetic stirrer and (6) magnet.

Samples (5 mL) were periodically withdrawn for analysis and placed in the refrigerator at 4 ± 1 °C or basified at pH 11-12 with NaOH 2 M to stop the reaction. When the reaction solution was prepared with the aim of testing the efficiency of the subsequent membrane treatment, basification was not used because the nature of the solution would change, affecting the filtration efficiency and thus the reliability of the filtration results. Basification was only applied in samples for Chemical Oxygen Demand (COD) measurements because residual H_2O_2 was found to affect COD determinations (Kang et al.1999).

The effect of different system variables, namely Fe^{2+}/H_2O_2 molar ratio, H_2O_2 /model compound, and initial model compound concentration, was studied. All experiments were conducted at room temperature ($T_R = 30 \pm 1$ °C) and at a stirring rate of 300 rpm for a reaction time, t_R , of 120 min. Stoichiometric mineralization of BPA and TAR would be give by eq. 3.1 and 3.2, respectively. This equation was used to normalise the oxidant to BPA and TAR molar ratio; it means, for instance, that H_2O_2 /BPA stoichiometric molar ratio equal to 1 represents the addition of stoichiometric amounts of the reagents (1 mol of BPA and 36 mol of H_2O_2).



The disappearance of organic compounds or removal efficiency was measured as conversion of model compound, X . It was calculated as

$$X(\%) = \frac{(C_0 - C_t)}{C_0} \times 100 \quad (\text{eq. 3.3})$$

where C_0 is the initial concentration of the model compound, and C_t is the concentration at time t .

3.2.3 Ozonation

3.2.3.1 Materials

Ozonation experiments were carried out by using a Laboratory Ozonizer 301.19 ozone generator (Erwin Sander Elektroapparatebau GmbH, Germany) combined with synthetic air (78% nitrogen and 21% oxygen). The flow rate of air was adjusted with a needle valve, built into the flow meter settled on the ozonizer control panel. The ozone-air gas flow rates, $F_{\text{ozono-air}}$, and concentration of used ozone gas varied from 50 to 200 NL/h and 11 to 33 mg/L, respectively.

3.2.3.2 Ozonation procedure

The purpose of this study was to optimize the operating parameters, which were further used as the optimized conditions in the NF of ozonation effluents. To find out the characteristics of the ozone generated, the ozone generator was initially calibrated. The calibration was made as the concentration of the ozone generated as function of the fed air flow rate and voltage applied for the generator. Since the ozone generator consists of a silent electric discharge between two electrodes converting the oxygen to ozone, different dosage of ozone can be achieved by adjusting the voltage of ozone generator. To determine the ozone generated, its concentration in the gas phase was determined by iodometric method, explained in section 3.3.6. Figure 3.4 shows the calibration curve underwent by the ozone generator.

The experimental set-up for the ozonation treatment is presented in Figure 3.5. Air is led through the ozone generator in which oxygen is partly converted to ozone. The ozone enriched air then flowed into the reactor. All experiments were conducted in a semi-batch mode where ozone was continuously fed to the reactor containing the model compound solution. All experiments were carried out with 1 L model solution in a 1 L glass reactor. The reactor was equipped with openings for ozone-air gas inlet and outlet, pH and temperature probes and sampling collection. One glass diffuser was used to sparge ozone gas into the solution. The air flow rate was controlled by a needle valve and measured by air flow meters. The temperature was fixed at $T_R=30.0 \pm 0.1$ °C during all the experiments. It was controlled by thermostatic bath. The pH of the model solutions was adjusted to the

desired value with NaOH 2 M and HCl 2 M. The reaction solution was stirred continuously using a magnetic stirrer at 300 rpm. The remnant ozone was taken out of the bubble reactor through a Teflon tubing, and bubbled into 40 mg/L KI solution in washing bottles. The ozone concentration both in the inlet gas and outlet effluent was measured. Samples (5 mL) were periodically withdrawn for analysis and placed in the refrigerator at 4 ± 1 °C.

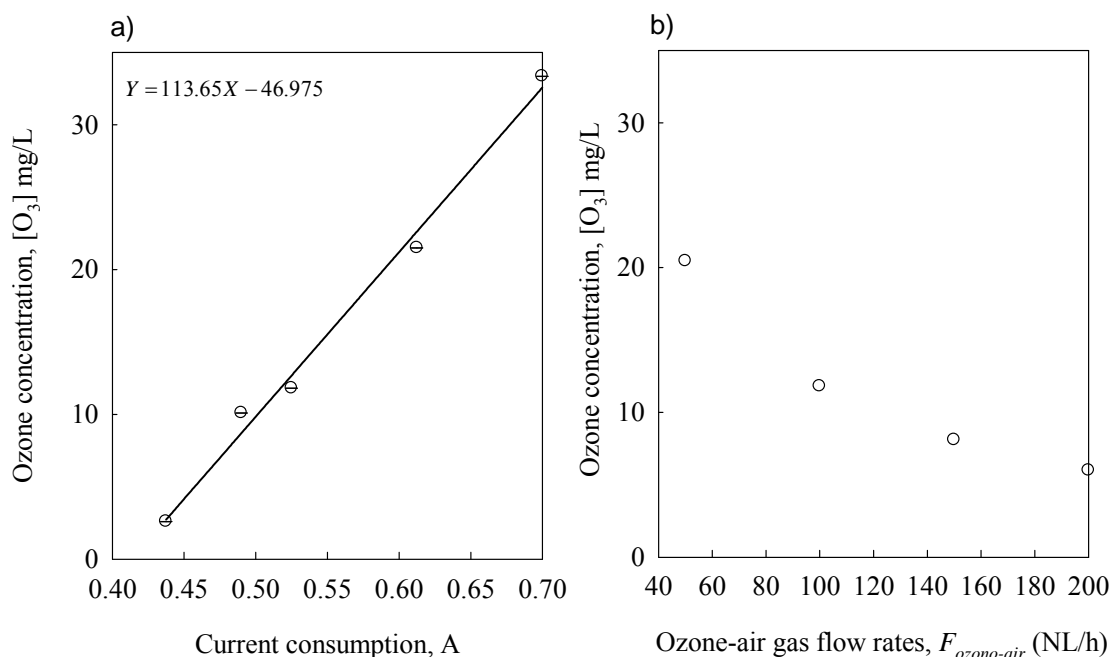


Figure 3.4. Calibration curve of the ozone generator as a function of a) power applied and b) air flow rate.

The degradation of model compound during ozonation was investigated under different experimental conditions by varying initial compound concentration, influent ozone gas concentration, ozone-air flow rate, pH and temperature.

The consumed ozone by the reaction was determined by using the equation below:

$$O_{3\text{consumed}} = O_{3\text{feed}} - (O_{3\text{trap}} + O_{3\text{residual}} + O_{3\text{headspace}}) \quad (\text{eq. 3.4})$$

where $O_{3\text{consumed}}$ is the amount of ozone interacted with model compound molecules, $O_{3\text{feed}}$ is the total ozone generated during an experiment and $O_{3\text{trap}}$ is the ozone captured by the trap. The $O_{3\text{residual}}$ and $O_{3\text{headspace}}$ is the residual dissolved ozone and the amount of ozone collected in the head space above the reaction mixture. $O_{3\text{residual}}$ and $O_{3\text{headspace}}$ are very

small when compared with O_3 trap, therefore, they can be neglected. The conversion of the studied organic compounds by ozonation was determined using the eq. 3.3.

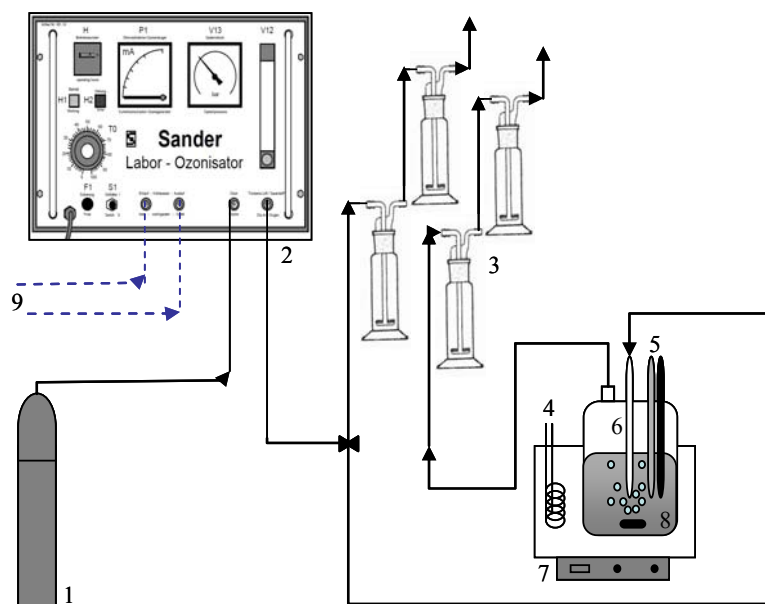


Figure 3.5. Ozonation set-up. (1) synthetic air gas cylinder, (2) ozone generator, (3) washing bottles, (4) heater, (5) pH probe and temperature sensor, (6) reactor, (7) magnetic stirrer and (8) magnet.

3.2.4 Enzymatic oxidation

Enzymatic oxidation experiments were carried out during a research stay at the Faculty of Science and Technology at University of Twente (Enschede, The Netherlands) in the Membrane Technology Group. The enzymatic treatment was only applied for BPA removal.

3.2.4.1 Materials

MilliQ water was used to prepare all the solutions in the enzymatic oxidation. Phosphate buffer, Na_2HPO_4 , was obtained from Acrös Organics and hydrogen peroxide, H_2O_2 , 50% wt. was purchased from Sigma-Aldrich. Horseradish peroxidase, HRP, was kindly provided by X-Flow (The Netherlands) and was used without further purification. Laccase 10 U/mg produced from *Trametes versicolor* was purchased from Sigma-Aldrich.

3.2.4.2 Enzymatic BPA oxidation procedure

HRP and laccase performance was tested in a wide range of reaction conditions. HRP treatment experiments were performed by varying the aqueous phase pH (from 3 to 12), H_2O_2 initial concentration (from 0 to 40 mg/L) and HRP doses (from 0 to 7.5% v/v). Experiments were conducted batchwise in a 50 mL glass reactor. In each test, the reactor contained 20 mL of 20 mg/L of BPA in 300 mg/L of phosphate buffer Na_2HPO_4 (pH 8.7), as well as predetermined amounts of HRP and H_2O_2 . The reaction solution was prepared following a fixed protocol. BPA was first added to phosphate buffer solution, followed by addition of HRP. Then, the pH of the buffer, BPA and HRP solutions was adjusted using 0.01 M H_3PO_4 and 0.01 M NaOH. H_2O_2 was added to the reactor as the final reagent to initiate the reaction. The reaction mixture was continuously mixed with a magnetic stirrer at 120 rpm during the reaction at a temperature of 30 °C. Triplicate experiments were conducted for each reaction condition. After 180 min, 1 mL samples were taken and filtered with a 0.22 μm filter for analysis. To stop the reaction, 50 μL of 37% v/v HCl was added to each sample.

The laccase treatment was performed in the same manner as the HRP treatment except that laccase was added, instead of H_2O_2 as the final reagent in order to initiate the reaction. In these assays, before the reaction was initiated, BPA and oxygen were dissolved in the reaction solution by vigorous shaking. The pH of the reaction medium was varied from 3 to 11 and laccase initial concentration from 0 to 0.4 U/mL. The enzymatic BPA removal efficiency was measured as BPA conversion, X_{BPA} . For both enzymatic treatments, it was calculated according to equation 3.3.

3.2.4.3. Nanofiltration protocol for enzymatic BPA oxidation effluent

In order to evaluate the enzymatic BPA removal when operated in a recycle mode and coupled to a NF membrane, experiments were conducted by employing optimized parameters selected from HRP and laccase BPA degradation experiments. Optimal conditions represent those where over 95% in the BPA removal was achieved. The combination of enzyme degradation and NF allows recycling of the soluble enzyme to the reaction vessel for reuse in subsequent batch BPA degradation.

The NF equipment was a home-made cross flow lab scale filtration system. It includes the same components than the NF system used for the filtration of model compound solutions and effluents after Fenton and ozonation degradation, Figure 3.1. In this case it had a 5 L feed tank, also performing as reactor, which did not allow temperature control. Full recycling mode was used during the experiments. All experiments were consequently performed at room temperature. The effective membrane area was 40 cm² and the cross flow velocity and Reynolds number used were adjusted to 10.9 cm/s and 777, respectively; and to 70 L/h in the feed flow rate, Q_F .

NF procedure was carried out in the same manner as the NF of model compounds, section 3.2.1.1. However, in this case the reaction and NF were conducted simultaneously. A typical test started by filling up the feed tank (or reactor) with 2 L of enzymatic reaction solution and adjusting the NF system at the selected transmembrane pressure, TMP, of 6 bar and initial T_F of 30 °C. Permeate and feed samples were periodically withdrawn for analysis. Permeate and feed conductivities were also measured using a WTW COND 3210 conductimeter.

3.3 Analytical procedures

3.3.1 Determination of BPA and TAR concentration by high performance liquid chromatography

Liquid samples from Fenton's process, ozonation, enzymatic treatment and NF experiments were analyzed by means of high liquid performance chromatography (HPLC) in an Agilent Serie 1100 chromatograph using a C18 reverse phase column (Tracer Extrasil ODS-2, 5 µm, 25 x 0.4 cm). To properly separate compounds from the partial oxidation products, the mobile phase was a mixture of methanol (99.9 %, Sigma-Aldrich) and Milli-Q water, slightly acidified. The HPLC analysis will let the identification and quantification of BPA and TAR and their main oxidation intermediates.

As stated, a methanol/water mixture (55/45 v/v) was used as the mobile phase with a flow-rate of 1 mL/min to determine BPA aqueous concentration. For each sample, the injected volume was 200 µL. Column effluent was monitored using a UV-visible spectrometer at

270 nm (at a retention time (RT) = 7.77 min). The column temperature was maintained at 28 °C. TAR and sulfanilic acid, its main intermediate, concentrations were measured applying a gradient of methanol-water mobile phase with a flow rate of 1 mL/min. At the start, methanol was kept at 0% for three minutes; then it was linearly increased up to 70% during the next 5 min, kept constant for the next 4 min, and finally linearly decreased back to 0% in 3 min. TAR was determined at 427 nm (at a RT = 13.99 min) and sulfanilic acid was determined at 252 nm (RT = 2.18 min).

In the experiments carried out in Twente University, BPA concentrations were determined by ultra HPLC (Dionex Ultimate 3000 RS) using an Acclaim RSLC 120 C18 Phase column (2.2 μm , 2.1 x 100 mm). The mobile phase was prepared using HPLC grade acetonitrile (ACN) and an aqueous Na_2HPO_4 (20 mmol/L) buffer solution. Two mobile phase solutions were prepared and designated as Eluent A (5% ACN/95% buffer solution) and Eluent B (95% ACN/5% water). The injection volume was 50 μL and separation of analytes was achieved using a flow rate of 1 mL/min and a specially designed gradient method. At the start, eluent B was kept at 0% for a minute; then the percentage of B was linearly increased up to 95% during the next 3 min, kept constant for the next 1 min, and finally linearly decreased back to 0% in 0.5 min. The column temperature was maintained at 65 °C. Column effluent was monitored with a Dionex Ultimate 3000 RS Variable Wavelength Detector at 225 nm.

3.3.2 Colour by spectrophotometry

Colour in oxidised and filtered Fenton and ozonation effluents was measured by absorbance in the visible range using an UV-VIS spectrophotometer (Dinko, model 8500). A wavelength scan was first carried out and the wavelength corresponding to the maximal absorbance was selected for assessing the colour of the samples.

Additionally, the compound concentration of the dyes used in section 4.3.2 was also determined by finding out the absorbance characteristic wavelength using the same UV-spectrophotometer. Standard dilute solutions of the dyes were taken and the absorbances were determined at different wavelengths to obtain a plot of absorbance versus wavelength. The wavelength corresponding to maximum absorbance (λ_{max}) was determined from this plot. Calibration curves were plotted between absorbance and

concentrations of the dye solutions (Figure 3.6). These curves helped in making a quantitative evaluation of the performance of decolourization by the NF process.

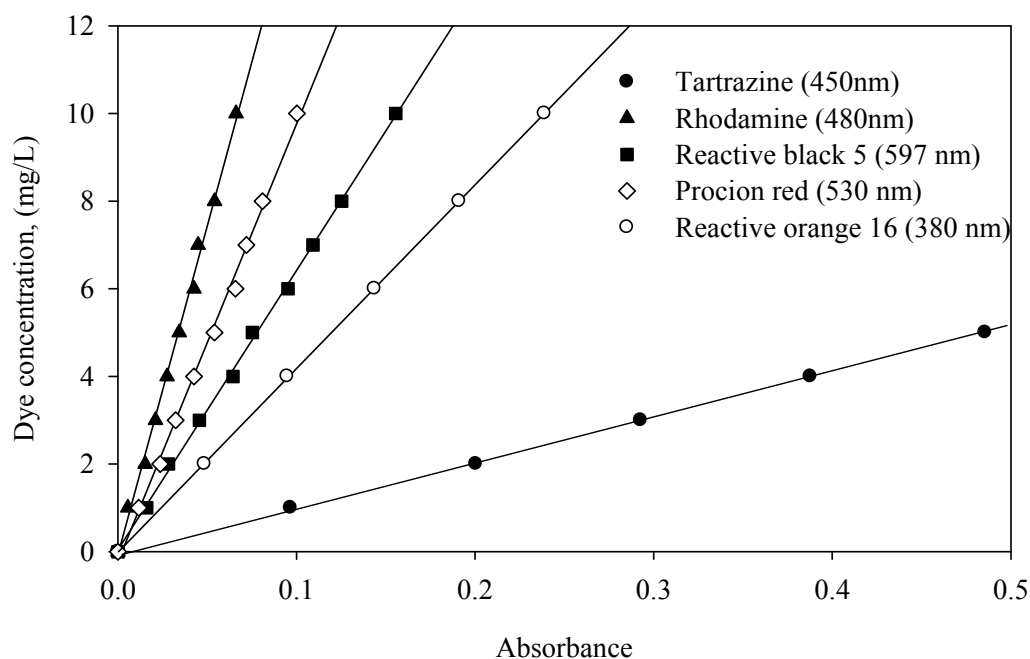


Figure 3.6. Calibration curves for dye concentrations determination.

3.3.3 Determination of iron concentration

Atomic absorption spectrometry was used to analyze the concentration of Fe^{2+} in Fenton reaction solutions and Fenton-NF experiments. Iron was quantified in a Perkin Elmer (model 3110) atomic absorption spectrometer. The iron concentration was determined by absorbance at its characteristic wavelength and at specific analytical conditions. 1% wt./vol. HCl was used to dilute the samples prior to metal analysis thus preventing hydrolysis inside the sample vials. Iron was analysed in an oxidant acetylene-air flame and absorbance was read at 248.8 nm. Previously, a calibration curve was completed in the range of better sensibility.

3.3.4 Total Organic Carbon

The parameter most commonly used to describe the performance of any oxidation process is the reduction of Total Organic Carbon (TOC), which is directly related to the concentration of organics in solution. For TOC analysis, an Analytic Jena TOC Analyzer

(model multi N/C 2100) was used. As previously mentioned, TOC values are of major importance in view of the fact that they show the level of mineralization (i.e. conversion to CO_2 and H_2O) of the samples, which is a way to measure the efficiency of the process.

Besides to the determination of TOC in aqueous samples, this general parameter has also been used to inform the percentage of sample identification (%IP). Sample identification can be defined as the ratio of calculated TOC estimated from the concentration of organic compounds (analysed by HPLC) to the analysed TOC. The difference accounts for the compounds that are neither identified nor measured by HPLC.

3.3.5 Chemical Oxygen Demand

The Chemical Oxygen Demand (COD) is the amount of oxygen consumed to completely oxidise the organic water constituents in inorganic end products. COD is commonly used to indirectly measure the amount of organic compounds in water, being a useful measure of its quality. Remaining COD in the oxidation samples was analysed by the Closed Reflux Colorimetric Standard Method 5220D (American Water Association 1999, Clesceri et al. 1989), which consists of digesting a sample for two hours in an acidic medium in the presence of a strong oxidant as potassium dichromate ($\text{K}_2\text{Cr}_2\text{O}_7$) and a silver sulphate catalyst. Mercury sulphate is usually added to eliminate possible interferences from chloride ions. During the test, organic compounds are oxidised and the orange coloured dichromate ($\text{Cr}_2\text{O}_7^{2+}$) is reduced to green coloured chromium ion (Cr^{3+}), which is then detected colourimetrically. The relation between Cr^{3+} absorbance and COD concentration is established by calibration with a standard solution of hydrogen phthalate, in the range of COD values between 25 and 500 mg/L.

3.3.6 Measurement of ozone in the gas phase

Feed and trap ozone amounts in the gas phase were determined by iodometric method titration with sodium thiosulphate, (Clesceri et al. 1989). The amount of ozone produced was transferred to react with 40 mg/L KI directly. In the titration process, KI is used as iodide ion source, ammonium molybdate as catalyst, starch as indicator and sulphuric acid as protons' source. The titration endpoint is marked by a colour change from blue to colourless. For each flow rate of synthetic air with variation of ozone contact time and

supply voltage, the ozone consumed per unit of time was calculated by potassium iodide (KI) method and equation 3.4.

3.3.5 Membrane characterization by microscopy

Membranes were characterised in terms of permeability, flux and rejection. However, in particular applications, a more intensive characterisation was performed. Advanced methods, such as atomic force microscope, AFM, and other characterisations by microscopy were employed when it was necessary. In this section, the methods used are explained.

3.3.5.1 Membrane topography and roughness determination by atomic force microscopy

The AFM is an excellent tool to study the topography of the membrane skin layer. Surface morphology of the membranes was characterised using an Agilent Molecular Imaging model Pico SPM II (Pico+) microscopy (model 5500). The AFM was handled in a contact mode with standard contact mode tips. Images were scanned at a rate of 1 Hz. Ambient conditions were maintained at approximately 20 °C and 30% relative humidity. AFM images of virgin polymeric membranes used in this study are shown in Figure 3.7. Membrane roughness was determined from AFM images using WSxM v5.0 Develop 6.2

software.

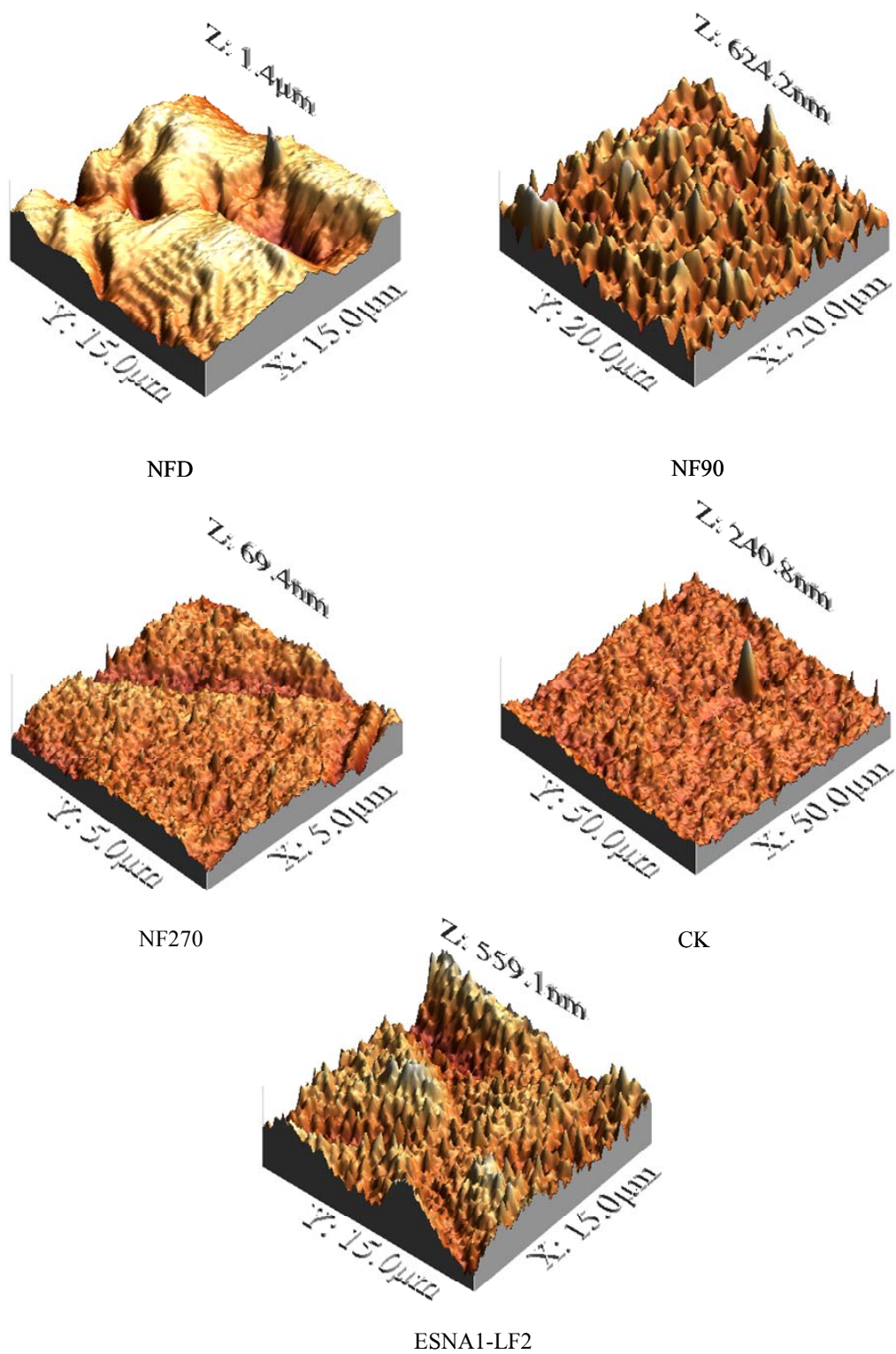
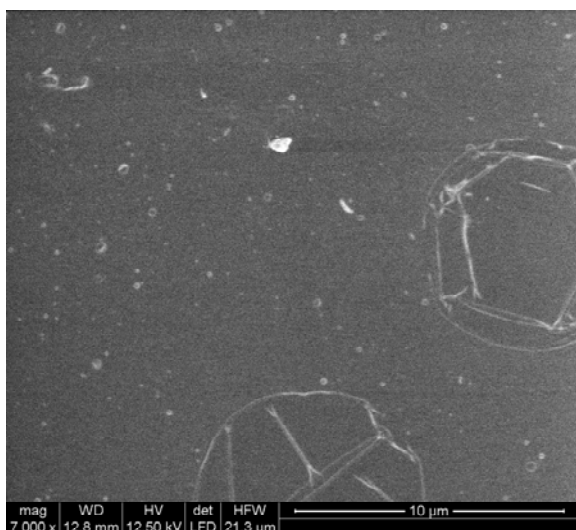


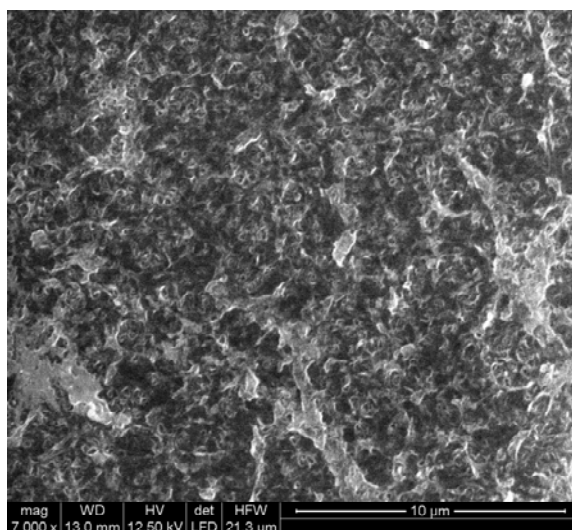
Figure 3.7. Surface topography image of virgin polymeric membranes.

3.3.5.2 Characterisations by microscopy

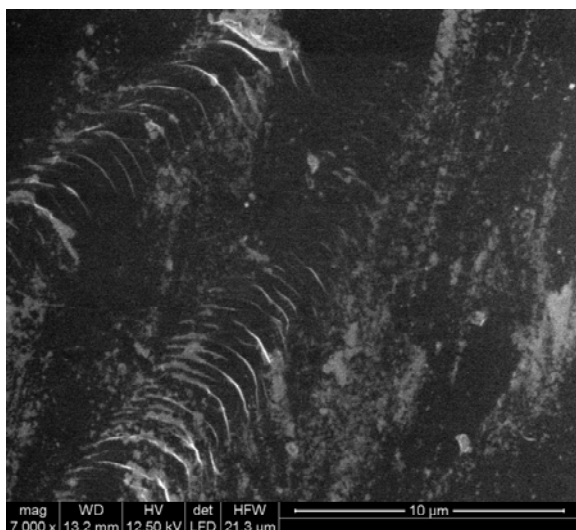
Microscopic characterisation of membranes allows determining their morphological properties. A large list of membrane separation studies have used these tools to understand membrane properties as well as fouling and cleaning processes (Bowen et al. 1997, Al-Almoudi and Lovitt 2007, Chakrabarty et al. 2008, Kim et al. 2008). Environmental Scanning Electron Microscopy (ESEM) allows membrane surface and transversal morphological characterisation by throwing electrons to the surface of the sample to be characterised. This causes interactions between the beam and the material, which give information on the membrane surface or transversal cut. When Energy Dispersive Spectroscopy (EDS) is coupled to ESEM (ESEM-EDS), semiquantitative elemental composition of membrane surface can be obtained. ESEM-EDS was used in this study for characterising virgin polymeric NF membranes and after use, too. A FEI instrument (model Quanta 600) was used for this purpose. ESEM images are presented in Figures 3.8 and 3.9 for virgin polymeric membranes.



NFD



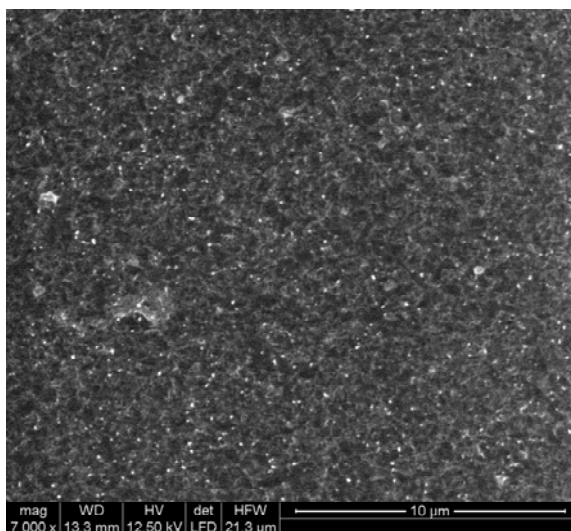
NF90



NF270

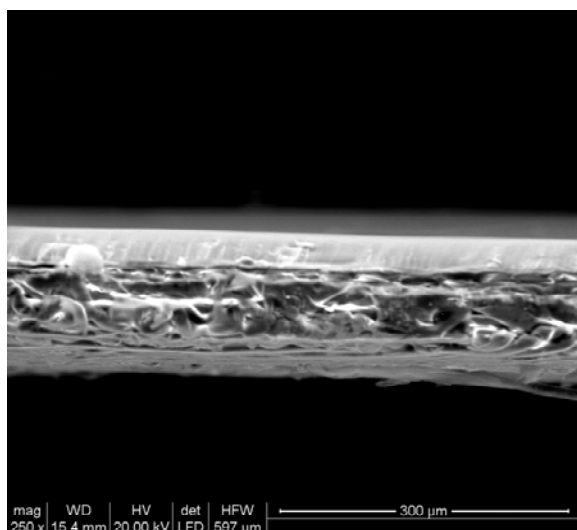


CK

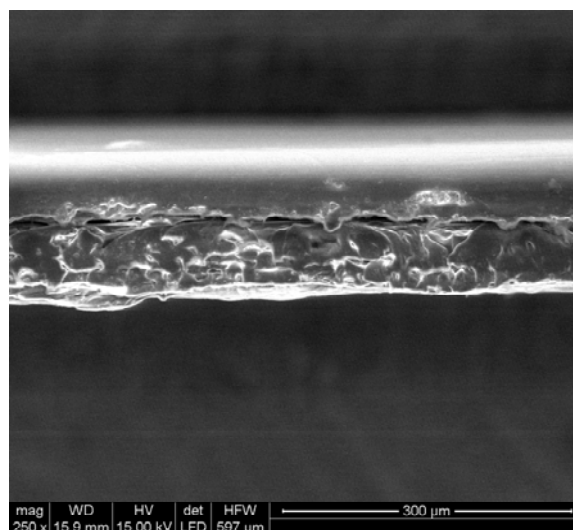


ESNA1-LF2

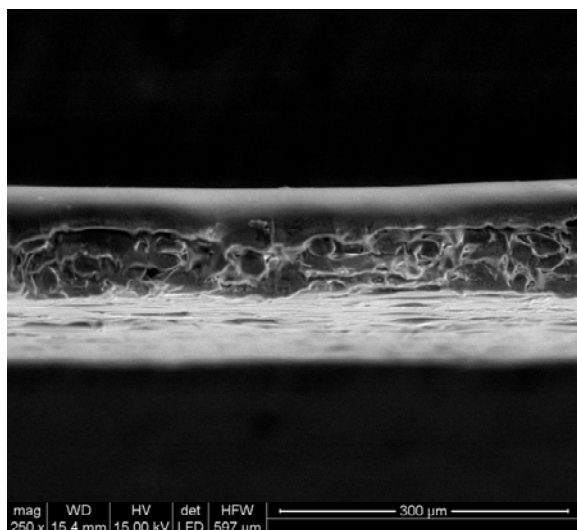
Figure 3.8. Surface ESEM images for virgin polymeric membranes.



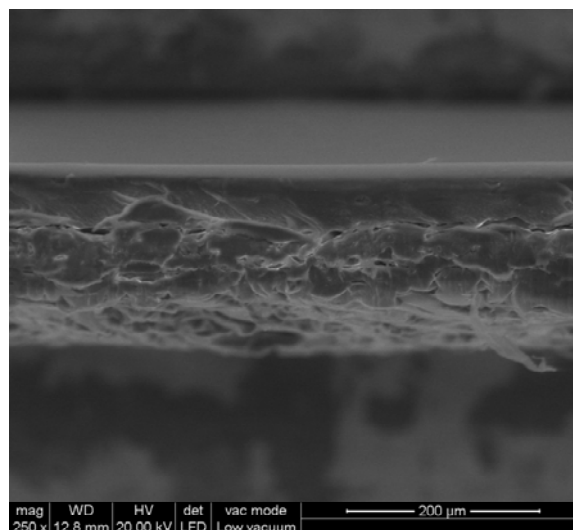
NFD



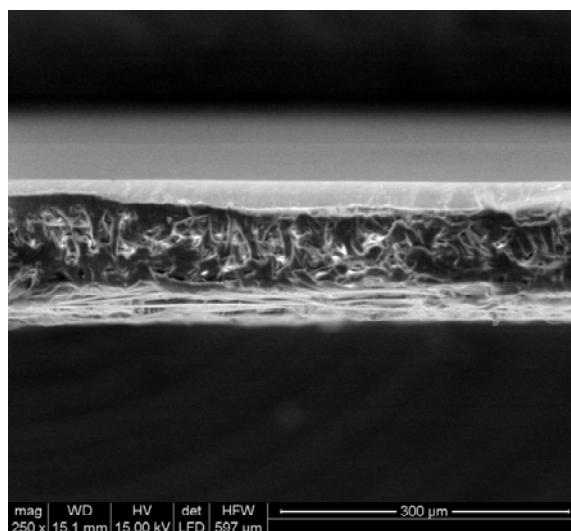
NF90



NF270



CK



ESNA1-LF2

Figure 3.9. Cross section ESEM images for the virgin polymeric membranes.

Chapter 4

Removal of BPA and tartrazine from aqueous solutions by nanofiltration

4.1 Introduction

Various potential physico-chemical treatment methods have been investigated for their ability to remove BPA and tartrazine as it has been presented in Chapter 2. However, membrane separation technologies have already demonstrated to be a practical and competitive alternative for the removal of a large variety of dyes as well as BPA from aqueous solutions due to their easiness of construction, process control, and feasible recovery of these pollutants (Fersi et al. 2005, Yüksel et al. 2013). Lower cost and improved materials are making membrane processes, such as nanofiltration (NF), more and more attractive for water and wastewater treatment in general. Indeed, this process is now an important part of reclaimed water production and close-loop water recycle schemes used in many industries (Alcaina et al. 2009).

There are many factors affecting the membrane performance: membrane characteristics such as molecular weight cut off (MWCO), porosity, surface charge and membrane hydrophobicity; solute characteristics and chemistry such as molecular weight (MW), molecular size and shape, charge and polarity; background composition and solution chemistry such as pH, ionic strength, hardness, and organic matter presence; or operation conditions such as transmembrane pressure (*TMP*), temperature, cross-flow velocity and recovery (Capar et al. 2006). In this chapter, NF was tested to treat BPA and one azo dye (tartrazine). The effect of individual components was investigated with regard to the permeate flux and rejection. The final goal of this part was to concentrate the effluent in order to reduce volume handling, which could additionally be subjected to destructive treatments, and obtain a permeate quality that could be safely and efficiently re-used in the industry with minimal subsequent treatment.

4.2 Nanofiltration applied for the removal of model compounds

4.2.1. Removal of BPA by nanofiltration

Application of membrane technologies as treatment for wastewater has grown in recent years. When applying membrane technology as wastewater treatment, a typical configuration involves combined systems of microfiltration (MF), ultrafiltration (UF),

nanofiltration (NF) and reverse osmosis (RO) (Côté et al. 2004). This allows flexibility and means that the quality of the water produced can be adjusted to suit the different purposes. Indeed, it has been reported that MF, UF, NF and RO processes are capable of removing BPA at different extent.

Schäfer et al. (2006) studied the performance of submerged and direct UF of synthetic greywater, regarding the retention of a model trace organic contaminant, BPA, and fouling. Their results indicated that UF can only remove 30-45% of BPA. Gómez et al. (2007) determined the retention capacity of membrane technologies for high concentrations of non-charged organic molecules such as BPA, which are frequent in industrial wastewater and landfill leachate. Two modes of treatment were tested, the first consisting of a MF module and an UF module working in parallel, and the second consisting of a RO module. Although, MF and UF membranes demonstrated certain effectiveness at retaining BPA (retention values of 50-60%), RO membranes achieved much better results. The removal of BPA from drinking water by UF membrane using dead-end model was investigated by Bing-zhi et al. (2008). UF with 2000–10000 molecular weight cut-off (MWCO) removed BPA by over 92%, starting from an initial concentration of BPA ranging from 100 to 600 µg/L.

NF of BPA was investigated by Nghiem et al. (2005) and Zhang et al. (2006). They concluded that adsorption of BPA onto the membrane was the dominant removal mechanism at the initial stage of filtration. At later stages, adsorption and subsequent diffusion of BPA in the membrane resulted in lower rejection where size exclusion was the dominant mechanism. Various NF and RO membranes were compared for their BPA rejections from a model solution of 50 mg/L at 10 bar of applied pressure (Yüksel et al. 2013). The polyamide based membranes exhibited much better performance than cellulose acetate membranes for BPA removal.

4.2.2. Removal of tartrazine by nanofiltration

Although, many studies have found that NF is a suitable process for the effective removal of dyes from coloured wastewater, few researches have been carried out to separate and purify tartrazine from aqueous solution. Kaya et al. (2009) treated a model solution of liquid dishwasher detergent wastewater by using a two-step NF process. This wastewater

contained an anionic surfactant, a non-ionic surfactant, tartrazine, and sodium chloride. In the first step, a loose NF membrane was used for recovery of surfactants and dye. In the second step, the quality of the permeate obtained from the loose NF membrane was improved using a tight NF membrane. Results showed that concentration of tartrazine was achieved (over 99%) for re-using in the production of liquid dishwasher detergent. Aydiner et al. (2010) evaluated the membrane fouling and flux decline related with mass transport in NF of a tartrazine solution. The feed solution pH seemed to be an important operational parameter affecting the process performance rather than feed-dye concentration and transmembrane pressure. Permeate flux and rejection increase as feed solution pH increases. They also showed that the process could be employed to give a rejection rate of almost 100%.

4.3 Nanofiltration of model compounds

4.3.1 Nanofiltration of BPA

The evolution of the normalised fluxes, expressed as the ratio between the instantaneous permeate flux, J_p , and the pure water permeate flux, J_{w0} , (measured with a fresh membrane and deionised water) and BPA rejection for several NF membranes are presented in Figure 4.1. These results were measured using a feed solution containing 300 mg/L BPA, whereas NF was operated at 6 bar and 30 °C. As expected, it is evident that normalised permeate flux is always lower than that corresponding to pure water flow. Of course, the decrease must be assigned to the accumulation of BPA species close to the membrane surface, thus affecting the membrane permeability, namely polarisation concentration (CP) (Van der Bruggen and Vandecasteele 2001), although other phenomena as solute adsorption or fouling on the membrane polymeric material (Gomes et al. 2005) can take place.

In fact, all the membranes depicted a typical permeate flux profile where the membrane is organically fouled. The normalised fluxes dropped between 47 and 77% within the first minutes after starting the filtration; afterwards, the normalised fluxes remained almost constant in a mostly steady state permeate flux. The normalised flux for the ESNA1-LF2 membrane presented the slowest decline, followed by NF90, NFD, NF270 and CK

membranes. Therefore, the decline of the normalised flux during operation can mainly be ascribed to CP or fouling; this latter can be reversible or irreversible. Irreversible fouling, which cannot be removed by mechanical or chemical cleaning, can result from the irreversible binding of substances -foulants- onto the membrane surface or even inside the pores, which could ultimately determine the membrane lifetime.

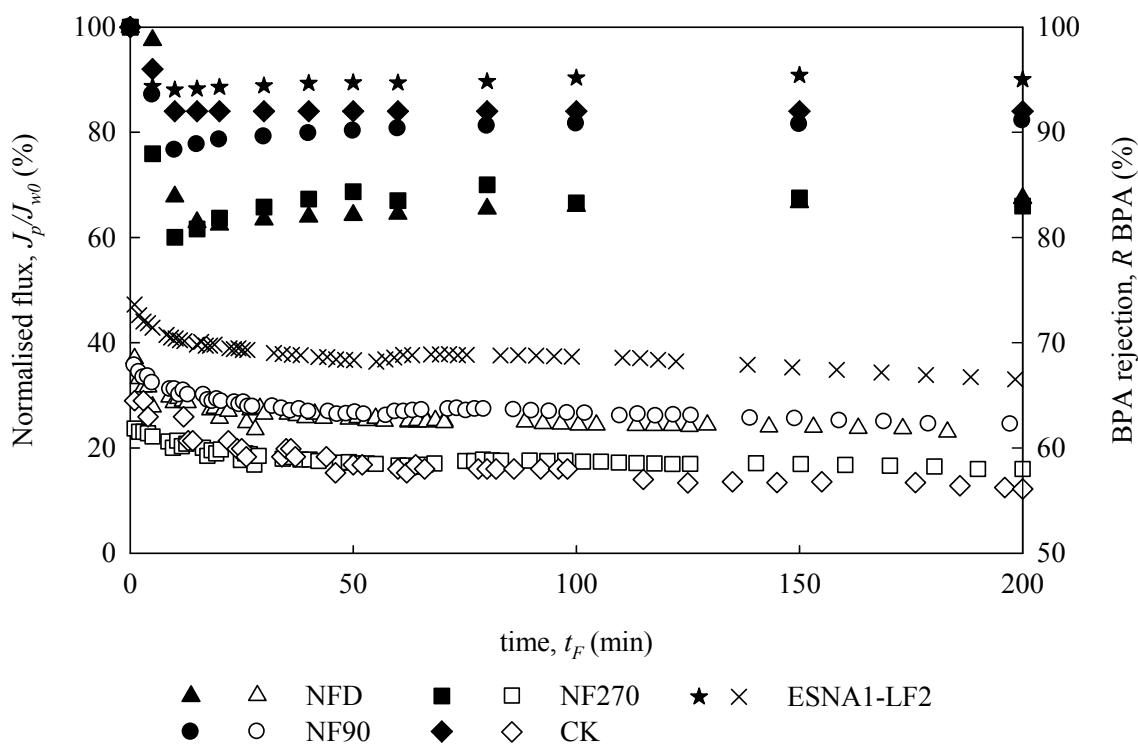


Figure 4.1. Nanofiltration of BPA. Normalised permeate flux and BPA rejection as a function of filtration time for the different membranes tested. Experimental filtration conditions:

$[BPA]_{\text{feed}} = 300 \text{ mg/L}$, $TMP = 6 \text{ bar}$, $v = 5.3 \text{ cm/s}$, $pH_F \approx 6$, and $T_F = 30 \text{ }^\circ\text{C}$.

Open symbols represent normalised fluxes and full symbols BPA rejections.

The NF protocol consisted of three main steps: (1) the clean water flux, J_{w0} , was measured just after compaction of the membrane; (2) then the BPA permeate flux, J_p , was followed for 250 min; finally, (3) the membrane was flushed with water and its clean water flux, J_{wf} , was measured again. Normalised fluxes using the steady state values and final BPA rejection are depicted in Figure 4.2. The flux recovery after flushing the membranes with water is an indicator of the CP and fouling. The portion of the flux not recovered represents the irreversible flux decline (caused by fouling) and the reversible flux decline represents CP and/or reversible adsorption phenomena. Since the reversible adsorption phenomena is a slower process than the immediately elimination of CP by the water

flushing, the normalised permeate flux measured after water flushing could be a qualitative measure of CP. Thus, Figure 4.2 corroborates that both CP and fouling occurred in all the membranes during the NF of BPA. CP is represented by the portion of normalised flux recovered by water flushing, while the fouling is assumed to be the portion lost.

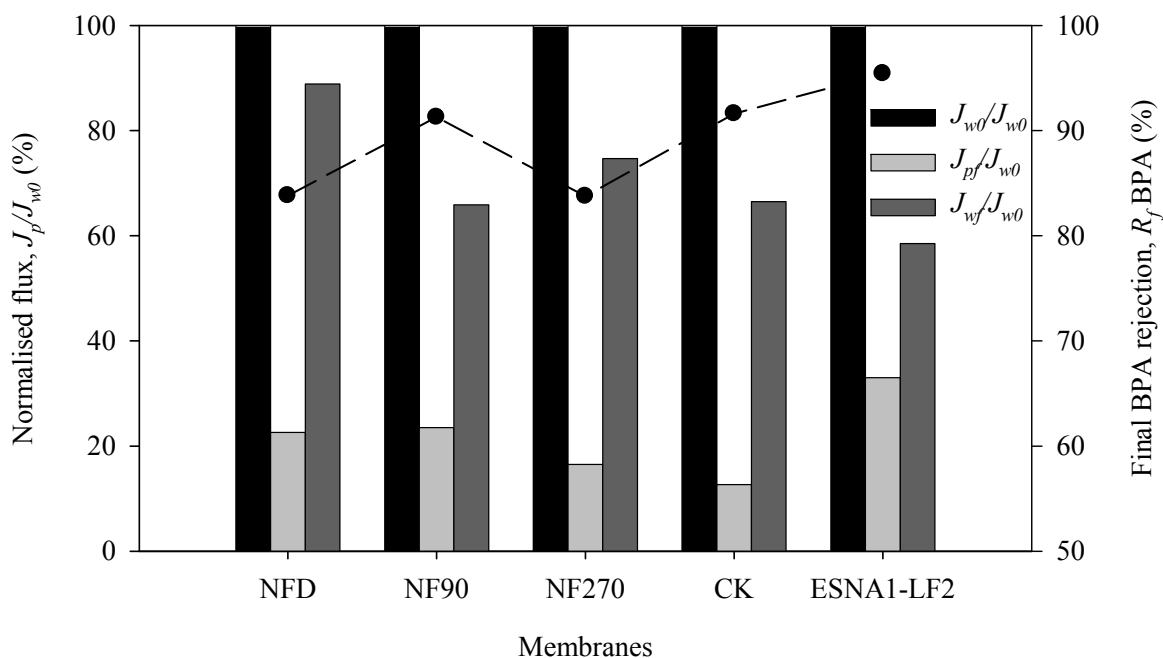


Figure 4.2. Nanofiltration of BPA. Normalised permeate flux before, J_{w0}/J_{w0} , at 200 min of NF (end), J_{pf}/J_{w0} , and after water flushing, J_{wf}/J_{w0} , and BPA final rejection (symbols) for the different membranes tested. Experimental filtration conditions: $[BPA]_{\text{feed}} = 300 \text{ mg/L}$, $TMP = 6 \text{ bar}$, $v = 5.3 \text{ cm/s}$, $pH_F \approx 6$, and $T_F = 30 \text{ }^\circ\text{C}$.

As it can be seen, CP was the main responsible of the normalised flux decline for all the studied membranes. The amounts of normalised fluxes lost by CP were much higher than the loss by fouling. Membrane fouling showed to increase in the following order: NFD < NF270 < CK < NF90 < ESNA1-LF2. The increased concentration of solutes at the surface of the membrane increases the overall resistance to permeate flow. BPA has similar size to the membrane pores, which suggests a fouling mechanism by pore blocking (Schäfer et al. 2004). However, in the evaluation of the performance of membranes for the rejection of hydrophobic compounds, as BPA, the adsorption of the compound on the membrane has to be taken into account. Hydrophobic compounds tend to strongly bind to hydrophobic materials. Hence, adsorption of organic compounds may be related to the hydrophobicity of the membrane surface, and may be a tool to predict the fouling. By inspecting Figure 4.2 and Table 3.3 at once, it can be deduced that the fouling increased as long as water contact angle did. Hence, the fouling mechanism is, besides pore blocking, probably due to

adsorption of BPA by hydrophobic-hydrophobic solute-membrane interactions, too. In fact, both mechanisms are related as adsorption can occur inside the pores and, consequently, totally or partially, hinder the pass of water. Similar rapid flux decline as a result of initial pore restriction and compound adsorption on the membrane surface has also been reported in previous studies (Van der Bruggen and Vandecasteele 2001, Nghiem and Hawkes 2007, Xu et al 2005).

Furthermore, BPA rejection follows the same trend than membrane fouling. An increase on membrane fouling could even enhance the rejection. Rejection of organic compounds by NF membranes can be attributed to several mechanisms. The most common mechanisms are size and charge exclusion. Since BPA is essentially hydrophobic and a non-charged compound over almost the entire pH range, ionic (charge) interactions between BPA and the membrane are assumed to be practically absent and size exclusion effect is expected to dominate. The fact that results have shown a clear relationship between fouling and the increase in BPA rejection suggests that an increase in BPA rejection might result from stronger membrane fouling. Thus, adsorption of BPA onto the membrane might contribute to BPA rejection, besides steric hindrance.

In fact, previous studies have reported that membrane fouling can either increase or decrease solute rejection, depending on the solute, membrane, and foulant (Bellona et al 2010, Comerton et al. 2008, Nghiem and Hawkes 2007). The rejection of trace organics is often explained by the solution diffusion model. According to this model, solute transport across the membrane is a two-step process. First, the solute is dissolved in the membrane; and, second, it migrates through the membrane by diffusion. This would mean that an increase in the BPA adsorption, i.e., higher BPA concentration over the membrane surface, could facilitate transport by diffusion, resulting in a decrease of its rejection. Hypothetically, when the adsorption does not reach the equilibrium or saturation state, the membrane accumulates the solute and the rejection is overestimated. The overestimation in the BPA rejection before reaching equilibrium state was also recorded by Xu et al. (2005), who found that the bromoform, which is more hydrophobic than chloroform, had a higher initial removal. However, after approximately five hours of operation, its rejection decreased significantly and levelled off to 20 to 35% for chloroform and 35 to 45% for bromoform, respectively. This behaviour can slightly modify the interpretation of the actual BPA rejections.

The performance of NF90 membrane at different feed concentrations is shown in Figure 4.3. Although ESNA1-LF2 membrane showed the lowest flow decay and highest BPA rejection, NF90 membrane was selected as the best membrane for BPA removal by NF, since NF90 membrane fouling was lower than ESNA1-LF2. Additionally, ESNA1-LF2 membrane showed a BPA precipitation or scaling phenomenon, which was corroborated by the presence of white precipitate on the membrane after filtration. Thus, the examination of the effect of feed concentration was done using NF90. It can be clearly seen that the feed concentration globally had a negative effect on BPA nanofiltration. Normalised flux after 200 min of filtration decreased from 58.3 to 23.5% when the BPA feed concentration increased from 25 to 300 mg/L. As it was expected, the progressive decline in the normalised flux results from the creation of the CP and fouling layer, leading to a loss in membrane performance. In Figure 4.4, it can be observed how these resistances increased as a function of the feed concentration, considering as aforementioned the CP as the portion of normalised flux recovered by water flushing, and the fouling as the portion lost. The increase in the feed concentration enhances the accumulation of solutes retained by the membrane thus increasing the CP.

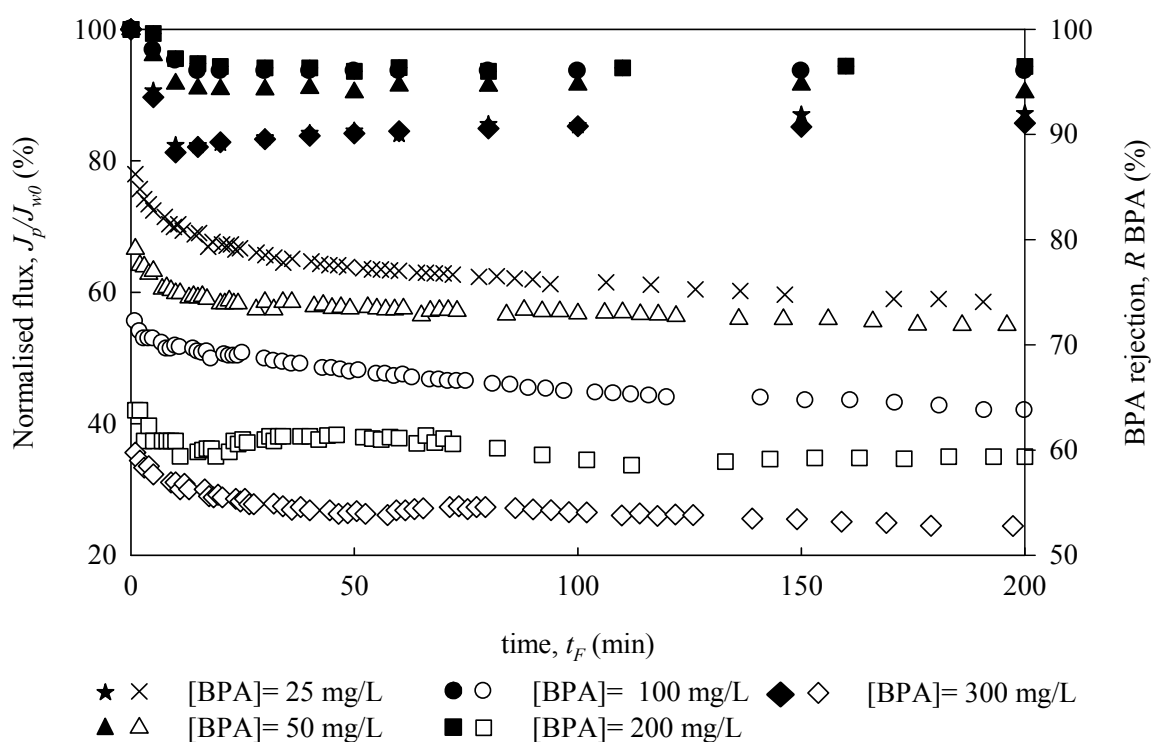


Figure 4.3. Nanofiltration of BPA. Normalised permeate flux as a function of filtration time for the different BPA feed concentrations. Experimental filtration conditions: Membrane = NF90, $TMP = 6$ bar, $v = 5.3$ cm/s, $pH_F \approx 6$, and $T_F = 30$ °C. Open symbols represent normalised fluxes and full symbols BPA rejection.

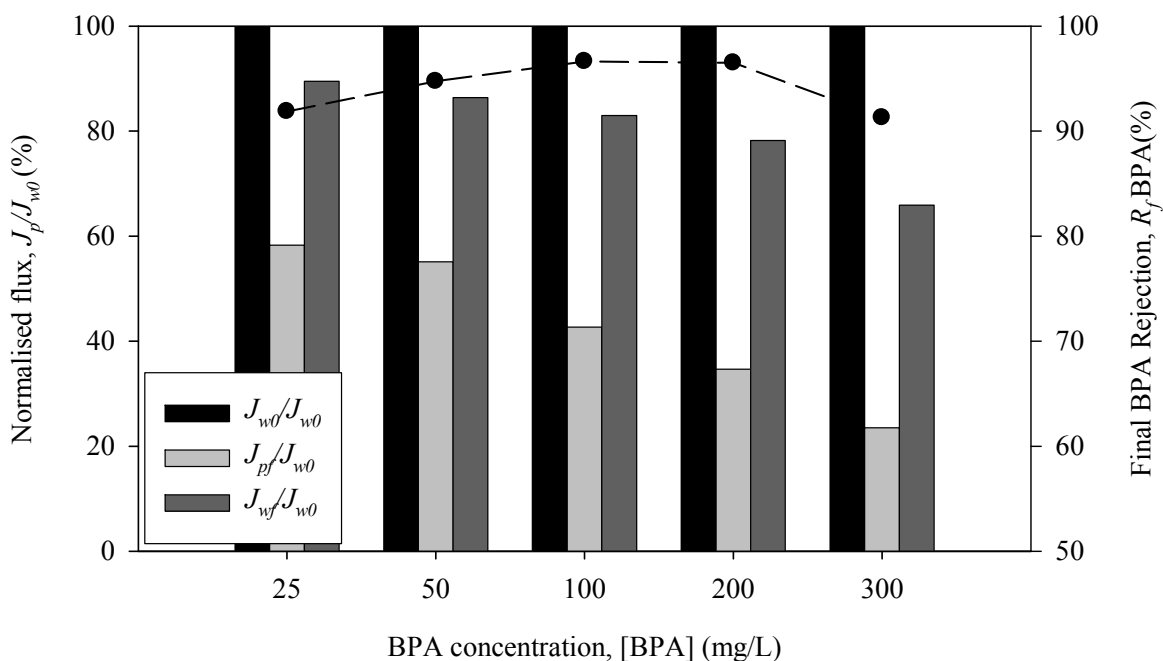


Figure 4.4. Nanofiltration of BPA. Normalised permeate flux before, J_{w0}/J_{w0} , at 200 min of NF (end), J_{pf}/J_{w0} , and after water flushing, J_{wf}/J_{w0} , and BPA final rejection (symbols) for several BPA concentrations. Experimental filtration conditions: Membrane = NF90, $TMP = 6$ bar, $v = 5.3$ cm/s, $pH_F \approx 6$, and $T_F = 30$ °C.

Figure 4.4 also depicts the final BPA rejection, after 200 min of filtration, for the different feed concentration tested. BPA rejection seems to have a maximum value at 100 mg/L of BPA. This removal behaviour by NF90 membrane shows the effect of adsorption mechanism on BPA rejections. Below 100 mg/L of BPA, many available sites for adsorption allowed membrane adsorbing more BPA, apparently resulting in higher BPA removal. With the increase of BPA concentration, the membrane became close to saturation, resulting in reduced BPA removal.

The fact that the BPA rejection depends on feed concentration obtained in this study is somewhat inconsistent with previous studies (Su-Hua et al. 2010, Zhang et al. 2006), where the BPA rejection decreased following the increase of feed concentration. This may own to the high concentration of BPA used here or other different solution and/or membrane characteristics. In contrast, similar results have also been reported by Bing-zhi et al. (2010) for the removal of BPA by a hollow fiber microfiltration membrane.

Table 4.1 shows the effect of the TMP on the permeate flux decline. TMP is an important operation parameter in pressure-driven membrane processes as it determines plant

productivity. In this study, constant-pressure filtration experiments were conducted (i.e. applied pressure was kept constant along the filtration time) for *TMP* of 2, 4, 6 and 8 bar. As expected, it was observed that the permeate flux tended to increase as the applied pressure was larger. Final permeate fluxes, at steady state, increased from 6.6 to 20.1 L/h m² as the *TMP* increased from 2 to 8 bar. This agrees with the fact that *TMP* is the driving force of the filtration and, consequently, the higher the *TMP*, the higher the amount of solvent able to permeate through the membrane per unit of time. Cheryan (1998) defined two regions in the filtration processes: a pressure-controlled region and a mass transfer-controlled region. At low pressure, still in the first region, the permeate flux increases mostly linearly along with the operating pressure. However, in the mass transfer-controlled region, the permeate flux is no longer proportional to the applied pressure, because any increase in pressure only results in a build-up of the solute layer over the membrane and an additional resistance. As the linear tendency of permeate flux with *TMP* was appreciated (Table 4.1), the filtration system is probably inside the pressure controlled region. As Table 4.1 shows, a slight decrease on % J_{pf}/J_{w0} was observed when *TMP* increased. This was a consequence of the growing membrane fouling as long as the filtration proceeded, because of the compaction of the fouling layer at high pressure. Additionally, the higher the flux through the membrane at high pressure, the greater the chance of membrane fouling.

Table 4.1. Nanofiltration of BPA. Final normalised permeate flux rejection for the several transmembrane pressures applied. Experimental filtration conditions: Membrane = NF90, $v = 5.3$ cm/s, $\text{pH}_f \approx 6$, $T_f = 30$ °C, and $t_f = 200$ min.

<i>TMP</i> (bar)	Final flux (± 0.8 L/h m ²)	Final J_{pf}/J_{w0} ($\pm 5\%$)	Flux decline (%)	\approx CP (%)	\approx Fouling (%)	R_{fBPA}
			$100 - J_{pf}/J_{w0}$	$J_{w0}/J_{w0} - J_{pf}/J_{w0}$	$100 - J_{w0}/J_{w0}$	
2	6.6	26	74	49	25	88.9 ± 0.1
4	13.3	28	72	48	24	93.9 ± 0.4
6	15.9	23	77	51	26	93.5 ± 0.8
8	20.1	21	79	44	35	94.4 ± 0.2

The potential of using NF membranes to concentrate BPA was later investigated. In this assay the system was running at a batch mode (only the retentate was recycling back to the feed reservoir). In this case, 5 L of a 25 mg/L BPA solution was concentrated at 30 °C at

20 L/h of feed flowrate and at 6 bar using the NF90 membrane. NF90 membrane was selected to evaluate the concentration of BPA due to its better performance in the membrane screening experiments (Figures 4.1 and 4.2). The information on maximum concentration is valuable for further process design, especially for those processes favouring concentration instead of permeate purity. From Figure 4.5 showing the behaviour of this BPA concentration test, NF90 gave a low normalised permeate flux at the beginning and, as expected, it underwent further decrease over the filtration time. As it can be seen, the normalised permeate flux decreases as concentration in retentate (concentration in the feed tank, too) increases.

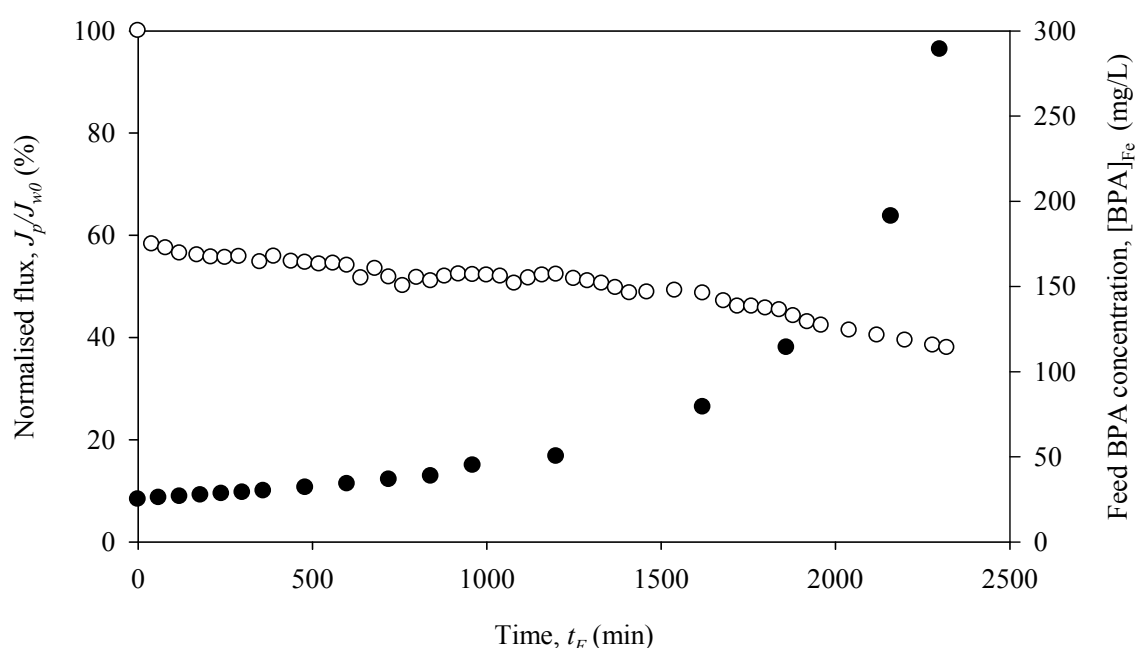


Figure 4.5. Nanofiltration of BPA. Normalised permeate flux as a function of filtration time for semi recirculation mode. Experimental filtration conditions: $[BPA]_0 = 25$ mg/L, membrane = NF90, $TMP = 6$ bar, $v = 5.3$ cm/s, $pH_F \approx 6$, and $T_F = 30$ °C. Open symbols represent normalised flux and full symbols BPA concentration in the feed tank.

The high flux decline was expected due to the derived enlargement of CP and fouling by the increase in the BPA concentration in the bulk retentate side. The maximum BPA concentration reached was 289 mg/L at 2300 min, when the experiment was stopped. This means that BPA initial solution was concentrated by a factor of near 12. After the membrane flushing with water, the NF90 membrane recovered 33% of the total normalised flux loss during the filtration, which indicates that the flux decline was mainly due to recalcitrant fouling rather than CP. Additionally, rejections of BPA over 98% were

underwent during all the concentration experiment. Thus, in spite of the high flux decay, due to its high concentration efficiency, this proves that NF can be used as a separation-concentration process for BPA removal.

4.3.2 Nanofiltration of tartrazine

The normalised flux performance for tartrazine NF using three different membranes (NFD, NF90, and NF270) under a constant applied pressure of 6 bar is shown in Figure 4.6. Normalised permeate fluxes decreased slowly over time, but relatively stable permeate fluxes were achieved above 150 min in all cases (<36% flux reduction). The more permeable membranes (NF270 and NF90) experienced greater flux reduction. As evidenced in Figure 4.7, where the normalised fluxes corresponding to the virgin membrane, after 200 min of filtration of TAR, and after flushing with water are depicted, the major contribution to flux reduction owned to CP for membranes with higher initial water permeabilities. For instance, the relative flux reduction for the membrane NF270 was almost totally recovered when this was flushed with deionised water, indicating that most of the additional resistance under operation was due to CP. In Figure 4.7 is also represented the final TAR rejection for the NF membranes used. As observed, the TAR rejection was very similar for all the membranes and very high (> 99%). This high TAR rejection can be explained by size exclusion mechanism because the dye molecular size is markedly higher than the NF membranes mean pore sizes. Therefore, the greater flux reduction by CP was probably due to the increased hydrodynamic permeate drag at higher initial flux, which facilitates the concentration of solute near to the membrane surface.

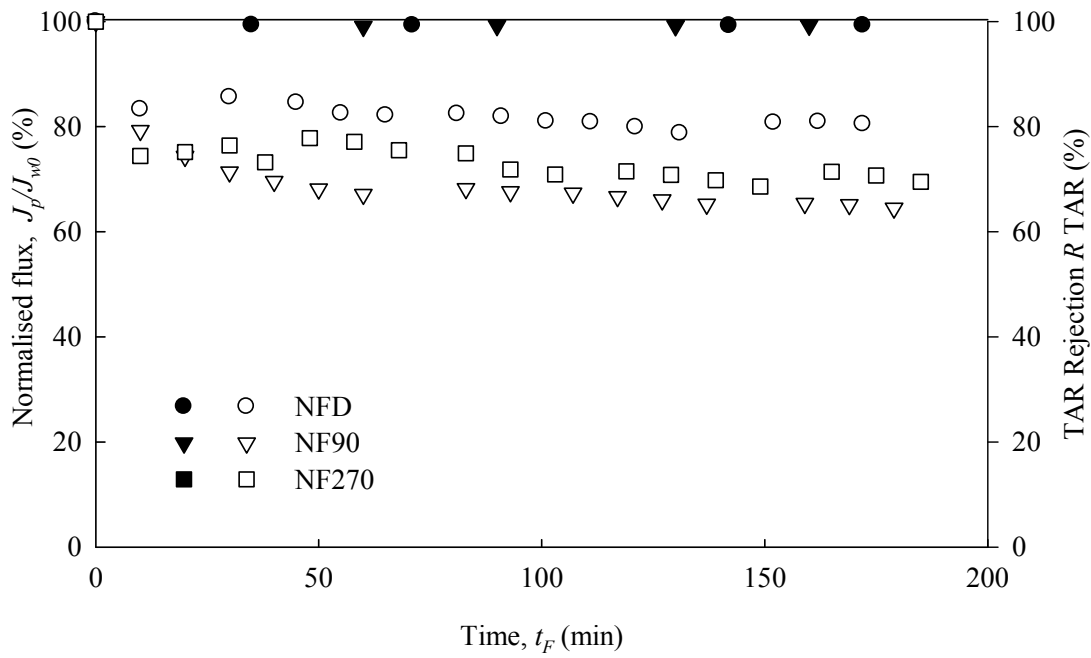


Figure 4.6. Nanofiltration of TAR. Normalised permeate flux and TAR rejection as a function of filtration time for the different membranes. Experimental filtration conditions: $[TAR]_{\text{feed}} = 1000 \text{ mg/L}$, $TMP = 6 \text{ bar}$, $v = 5.3 \text{ cm/s}$, $pH_F \approx 6$, and $T_F = 30 \text{ }^\circ\text{C}$. Open symbols represent normalised fluxes and full symbols TAR rejections.

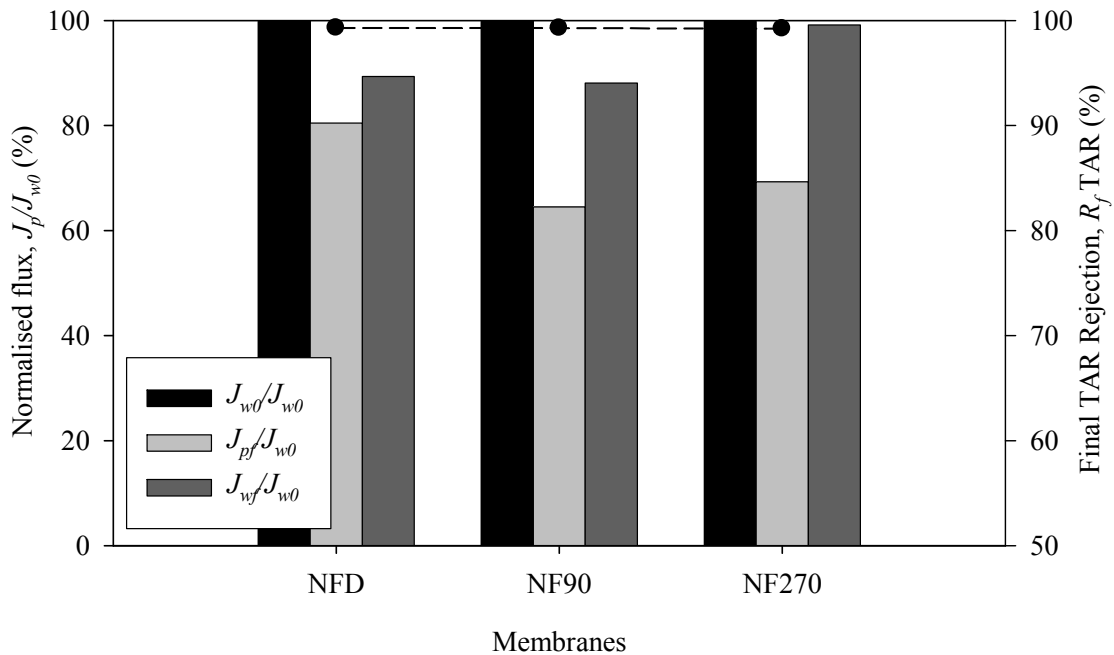


Figure 4.7. Nanofiltration of TAR. Normalised permeate flux before, J_{w0}/J_{w0} , at 200 min of NF (end), J_{pp}/J_{w0} , and after water flushing, J_{wf}/J_{w0} , and final TAR rejection (symbols) for the several membranes tested. The feed solution contained 1000 mg/L of TAR in deionised water. Experimental filtration conditions: $TMP = 6 \text{ bar}$, $v = 5.3 \text{ cm/s}$, $pH_F \approx 6$, and $T_F = 30 \text{ }^\circ\text{C}$.

To study the influence of the inlet concentration, feed solutions containing 100, 400, 800 and 1000 mg/L of tartrazine were nanofiltered using the NF270 membrane at 35 °C and 6 bar of TMP . The evolution of the normalised fluxes during the filtration is shown in Figure 4.8. A maximum decline of the NF270 permeate flux of around 26% was observed after 10 min of filtration for the highest feed concentration, 1000 mg/L of TAR. Regarding the effect of the initial dye concentration, it is expected that the permeate flux decreases when increasing the dye concentration, due to the enlarged CP. In fact, Figure 4.9 evidenced this expectation since the permeate flux at 200 min of NF decreases when dye concentration in the feed solution is higher. Permeate flux values were found to vary over 21.9% between maximum and minimum dye concentration. On the other hand, a slight but continuous decline of the permeate flux along the time is observed irrespective of the initial concentration selected, which points out some kind of fouling in addition to CP. In turn, dye rejection was found to be almost over 96% and practically constant regardless of the inlet dye concentration used.

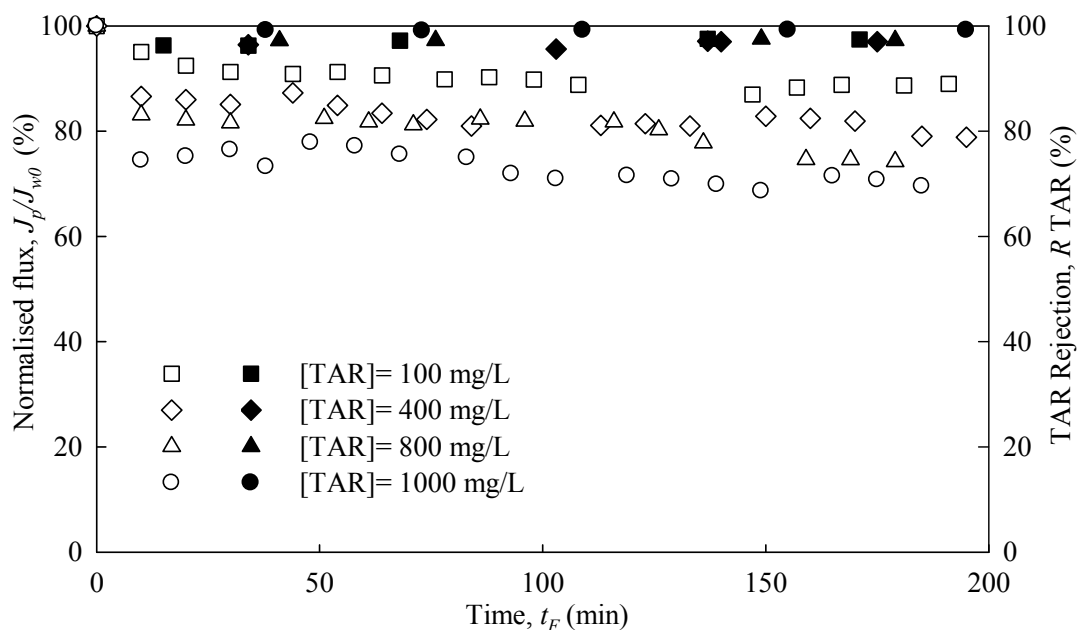


Figure 4.8. Nanofiltration of TAR. Normalised permeate flux as a function of filtration time for several TAR feed concentrations. Experimental filtration conditions: Membrane = NF270, $TMP = 6$ bar, $v = 5.3$ cm/s, $pH_F \approx 6$, and $T_F = 30$ °C. Open symbols represent normalised fluxes and full symbols TAR rejections.

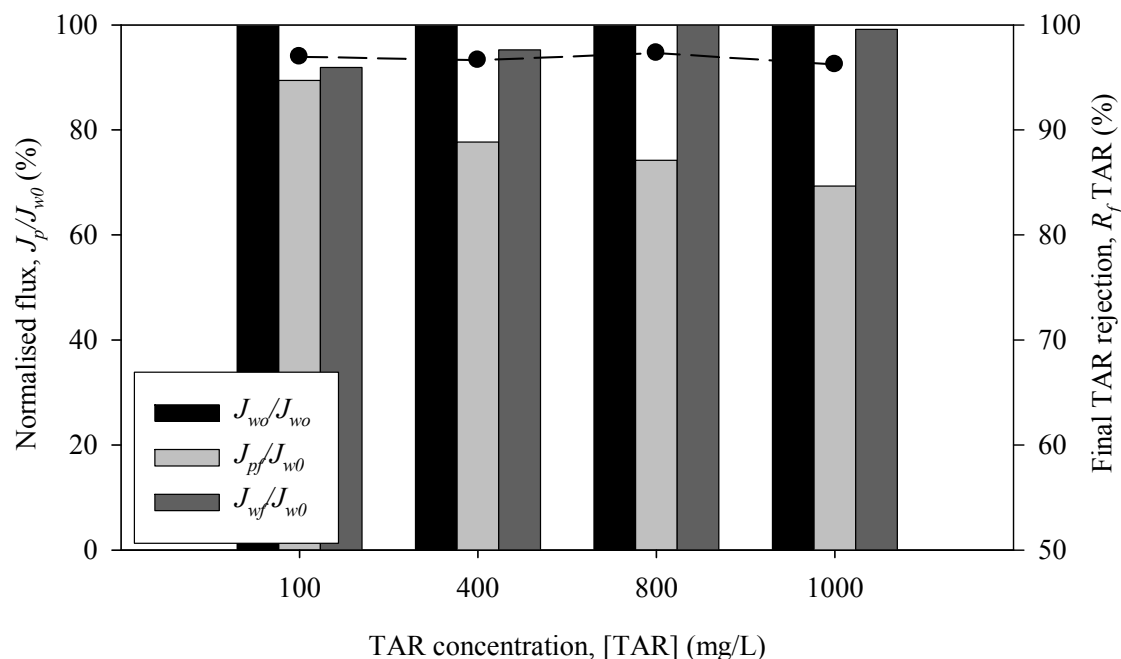


Figure 4.9. Nanofiltration of TAR. Normalised permeate flux before, J_{w0}/J_{w0} , at 200 min of NF (end), J_{pf}/J_{w0} , and after water flushing, J_{wf}/J_{w0} , and final TAR rejection (symbols) for several TAR concentrations. Experimental filtration conditions: Membrane = NF270, $TMP = 6$ bar, $v = 5.3$ cm/s, $pH_F \approx 6$, and $T_F = 30$ °C.

The effect of transmembrane pressure on the permeate flux behaviour is presented in Table 4.2. As expected, these results show that the final permeate flux (at 200 min of filtration) increased with increasing transmembrane pressure. As already observed during the NF of BPA at several TMP s (Table 4.1), a relatively good agreement is observed between experimental results and theoretical predictions. Thus, an increase in the transmembrane pressure results in an increase in the permeate flux as predicted by Darcy's law in the pressure-controlled region.

Table 4.2. Nanofiltration of TAR. Final normalised permeate flux rejection for the several transmembrane pressure applied. Experimental filtration conditions: Membrane = NF270, $v = 5.3$ cm/s, $pH_f \approx 6$, $T_f = 30$ °C and $t_f = 200$ min.

TMP (bar)	Final flux (± 0.8 L/h.m ²)	Final J_{pf}/J_{w0} ($\pm 5\%$)	Flux decline (%)	$\approx CP$ (%)	$\approx Fouling$ (%)	R_f TAR (%)
			$100 - J_{pf}/J_{w0}$	$J_{wf}/J_{w0} - J_{pf}/J_{w0}$	$100 - J_{wf}/J_{w0}$	
2	23.5	69	31	28	3	98.1 ± 0.6
4	49.0	74	26	18	9	97.9 ± 0.7
6	70.7	69	31	30	1	99.1 ± 0.5
8	86.9	75	25	25	0	98.1 ± 0.5

The effect of dye molecular weight over permeate flux decline and dye retention was also investigated. Figure 4.10 shows the NF results obtained with the five dyes tested at 6 bar and 35 °C using the NF270 membrane. These experiments aim at evaluating the effect of molecular size in the decrease of the permeate flux. The molecular weight (MW) of the dyes can play a crucial role in the dye transport through the membrane, not only because it has a large influence on the rejection of the compound, but it may also influence the permeate flux when pores become (partially) blocked (Van der Bruggen et al. 2001).

In almost all the cases, it is noted that a higher MW produces higher permeate flux decline. This is clearly related to the fact that high MW dyes are more easily deposited onto the membrane surface increasing cake layer resistance. It must be noted that procion red and rhodamine 6G do not follow this general trend. The permeate flux can be mostly correlated with the MW for tartrazine, reactive orange 16 and reactive black 5 dyes. For procion red and rhodamine 6G the lower the MW, the lower the permeate flux, which suggests that for these two dyes the permeate flux can be mostly assigned to a different fouling mechanism.

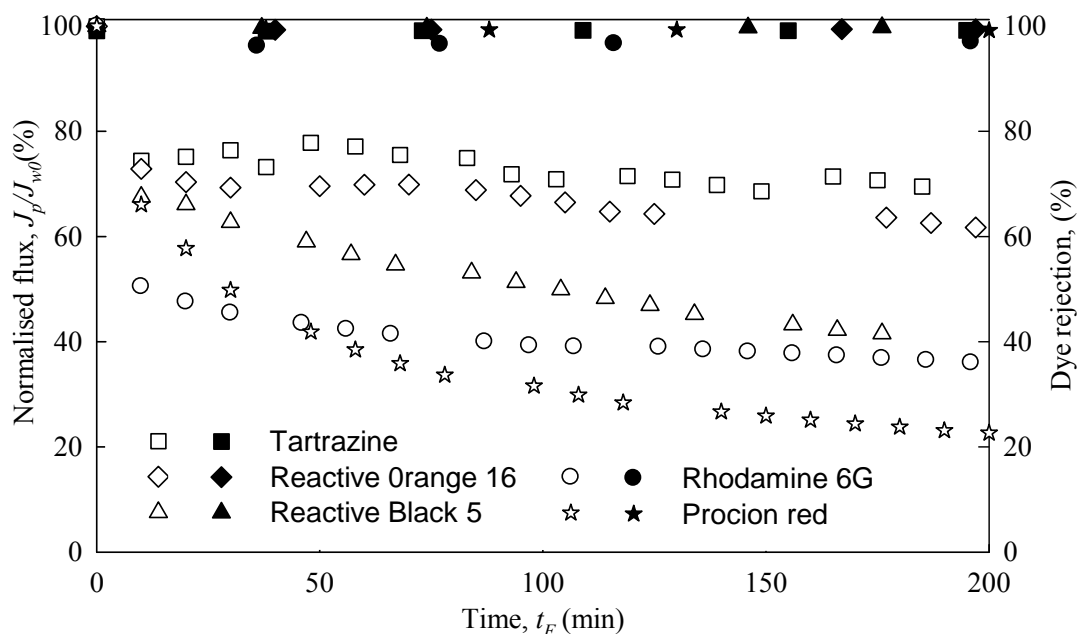


Figure 4.10. Nanofiltration of several dyes. Normalised permeate flux and rejection as a function of filtration time. Experimental filtration conditions: [dyes] = 1000 mg/L, membrane = NF270, $TMP = 6$ bar, $v = 5.3$ cm/s, $pH_F \approx 6$, and $T_F = 30$ °C. Open symbols represent normalised fluxes and full symbols dye rejections.

In fact, when stable conditions were attained for tartrazine and reactive orange 16 runs, almost no further decrease on the permeate flux was observed, so the flux became practically constant as a function of time. This behaviour is a typical example of CP phenomenon where flux decline is completely reversible and no significant fouling occurs. In turn, for reactive black 5, rhodamine 6G and procion red experiments, a continuous flux decline was noted along the time. This behaviour could be the result of the membrane fouling, which may be defined as the irreversible (reversible only after cleaning) deposition of retained species onto the membrane surface or into the membrane pores. This includes adsorption, pore blocking, and cake formation as potential mechanisms.

Figure 4.11 shows normalised water flux before and after filtration of the different dyes using the same membrane in order to corroborate if fouling actually occurs. For each experimental sequence, three procedures were performed. Excepting for tartrazine, it was found that the initial water flux was not completely recovered after the filtration runs in any case. This means that probably there was some permanent fouling on or within the membrane in all the cases, but especially for procion red and rhodamine 6G, which led to the lower values in normalised water flux after use. Tartrazine filtration experiments suggest that its fouling can be easily removed by cross flow or relaxation operations, while for the other dyes used the permanent lost flux can be caused by strong dye adsorption on the membrane surface. This possibility is supported by the presence of colour on the membrane after filtration (Figure 4.12), and is in accordance with findings from other studies (Van der Bruggen et al. 2001).

As shown in Figures 4.8 and 10 and Table 4.2, feed dye concentration, *TMP* or dye molecule type do not exhibit any significant effect on dye rejection given and its evolution along the filtration time. The retention was always higher than 95% independently of the operation parameters or dye. This behaviour can be related to the molecular size exclusion mechanism and the electrostatic interactions between the membrane and dyes, which are very effective leading to high rejection. The isoelectric point of the clean NF270 membrane is around pH 3.3 (Tanninen et al. 2006) and, according to the zeta potential data reported, the membrane surface was negatively charged during NF experiments because the pH of the dye solutions was always higher than the isoelectric point as Table 3.3 shows. These azo dyes, which have an anionic behaviour, can experiment an electrostatic repulsion with the membrane material when the pH is higher than its isoelectric point.

Therefore, this phenomenon can contribute to the good rejection of dye molecules by NF270, coexisting with sieving effects.

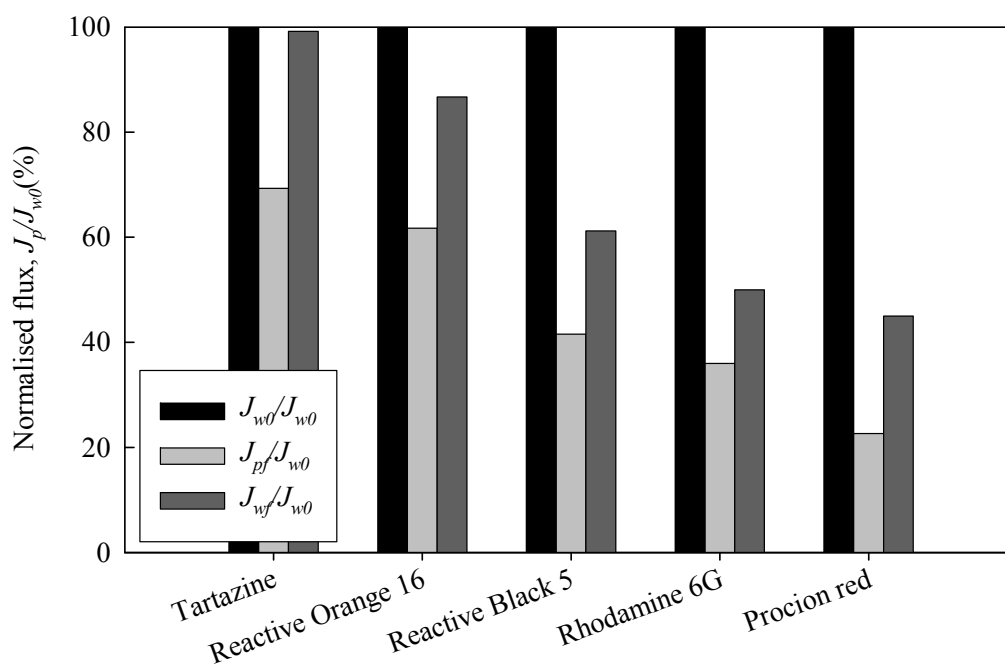


Figure 4.11. Nanofiltration of several dyes. Normalised permeate flux before, J_{w0}/J_{w0} , at 200 min of NF (end), J_p/J_{w0} , and after water flushing, J_{wf}/J_{w0} . Experimental filtration conditions:

[dyes] = 1000 mg/L, membrane = NF270, $TMP = 6$ bar, $v = 5.3$ cm/s, $pH_F \approx 6$, and $T_F = 30$ °C.

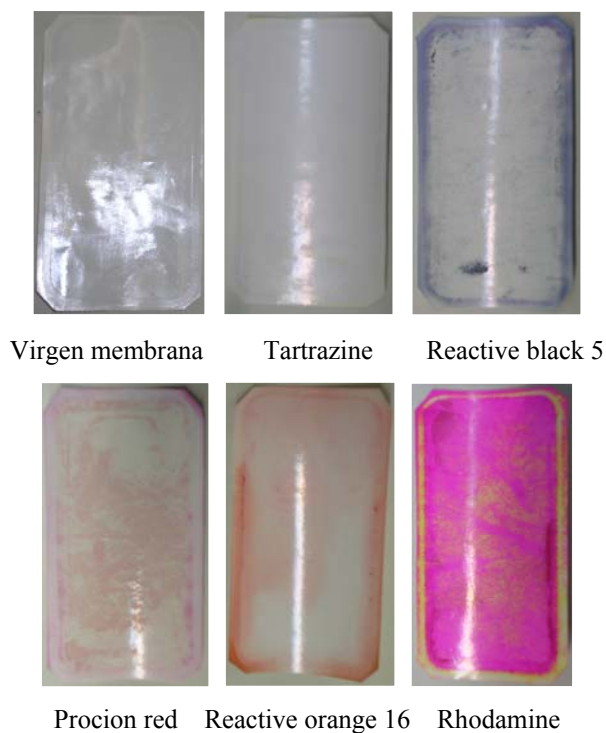


Figure 4.12. Used NF270 membranes after nanofiltration of several dyes.

4.4 Conclusions

The NF of BPA showed the general ability of membrane processes to contribute significantly to the removal of this contaminant in wastewater treatment. The BPA removal was attributed to sieving as well as adsorption of BPA on membrane; this latter related with the membrane hydrophobicity. This study suggests that an accurate evaluation of NF polymeric membranes in terms of the rejection of BPA could need the previous saturation of the membrane with BPA. Normalised flux decline in the NF of BPA was strongly influenced by concentration polarisation. Since concentration polarisation is a phenomenon that can be easily reduced by changes in the process hydrodynamics, this behaviour does not limit the use of NF for removing BPA. NF90 was the membrane showing the best performance to the NF of BPA; it gives a relative high BPA retention, over 90% and one of the lowest permeate flux decay. Thus, NF90 membrane demonstrates the potential use of NF membrane to concentrate BPA since it was able to concentrate near 12 times an initially 25 mg/L BPA solution.

On the other hand, high retention and flux was found for tartrazine NF regardless of the NF membranes, TMP and feed dye concentration applied. NF270 was the membrane providing the best performance since this membrane gave the highest permeate flux with relatively low flux decay. The removal of commercial dyes from aqueous solution by NF has thus shown to be an efficient option for coloured wastewater purification, achieving retentions above 95% for all the dyes tested (tartrazine, reactive black 5, reactive orange 16, procion red and rhodamine 6G). Most of the flux decline occurs during the first minutes of the filtration and almost steady permeate flux is only achieved after three hours of operation and for certain dyes (tartrazine and reactive orange 16). Although permeate flux was found mostly related to the dye MW, ranging from 50 to 75% of the original water permeability, indeed clear dye behaviour differences are noted when compared along the operation time. For instance, reactive black 5, procion red and rhodamine 6G showed continuous flow decline suggesting significant fouling due to specific interaction with the membrane surface. This fact could limit the feasibility of dye concentration to satisfactory ratios.

Chapter 5

Fenton coupled with nanofiltration for elimination of BPA and tartrazine

5.1 Introduction

The Fenton, as an AOP, can be an effective way to treat wastewater and remove pollutants such as BPA and tartrazine (TAR). Fenton's reagent is particularly attractive because of the low cost, the lack of toxicity of the reagents (i.e., Fe^{2+} and H_2O_2), the absence of mass transfer limitation due to its homogeneous catalytic nature and the simplicity of the technology required (Walling 1975). In contrast, other AOPs have high demand of electrical energy for devices such as ozonators, UV lamps, ultrasounds, etc., and this makes them economically disadvantageous. However, since Fenton process requires ferrous salt for the oxidation reaction to take place; then, the iron sludge, formed after neutralization of the treated effluent, has to be removed before discharging.

The application of nanofiltration (NF), as mature membrane technology, can effectively confine the iron cations in the reaction side, thus allowing recycling the catalyst and could also be an alternative method for retaining and concentrating low molecular weight organic pollutants derived from oxidant so they can subsequently be deeply oxidised. There have been numerous attempts to enhance oxidation with additional process steps. In this case, membrane separation is becoming a very attractive alternative because of its intrinsic characteristics. Therefore, NF has a potential applicability in Fenton process as catalyst remover, in order to reduce the iron concentration in wastewater before discharge and the subsequent formation of iron hydroxide sludge. Additionally, the combination of Fenton process and NF allows recycling of the soluble iron to the reaction tank for reuse during continuous process of BPA degradation, which also reduces the constant addition of catalyst as well as decreases treatment cost.

Thus, considering the widespread detection in the environment, extensive use and the limited data available in the literature on the treatment of BPA and tartrazine; the main objective of this chapter was to investigate the degradation of BPA and tartrazine by means of Fenton's process under different operational conditions, in addition to combine these processes with rejection of low concentration of pollutant residues, and intermediates derived from oxidation in a membrane system.

5.2 Fenton process

Fenton's liquor, consisting of hydrogen peroxide (H_2O_2) and ferrous salts, commonly requires a relatively short reaction time compared with other AOPs (Zazo et al. 2005). Historically, Fenton's reagent was discovered about 100 years ago by H.J.H. Fenton (Fenton 1894), but its application as an oxidation process for destroying toxic organics was not applied until the late 1960s (Huang et al. 1993). Among AOPs, oxidation using Fenton's reagent has been employed for the treatment of both organic and inorganic substances under laboratory conditions as well as real effluents from different processes (Bigda 1996, Nesheiwat and Swanson 2000). Fenton's reagent has been used to reduce the organic load or toxicity of many different contaminated waters and wastewaters. This includes residual water from a variety of industries, for instance, textile (Shyh-Fang et al. 2002, Karthikeyan et al. 2011), dyes (Kuo 1992, Núñez et al. 2007), pharmaceutical (Tekin et al. 2006, Sirtori et al. 2009), olive oil (Martínez et al. 2011, Zorpas and Costa 2010) and so on. Fenton process and related methods can be divided into: homogeneous processes, such as $\text{Fe}^{2+}/\text{H}_2\text{O}_2$, $\text{Fe}^{3+}/\text{H}_2\text{O}_2$, $\text{Fe}^{2+}/\text{H}_2\text{O}_2/\text{light}$, $\text{Fe}^{3+}\text{-ligand}/\text{H}_2\text{O}_2/\text{light}$, $\text{Fe}^{3+}\text{-ligand}/\text{light}$; and heterogeneous processes, such as $\text{Fe(III) oxide}/\text{H}_2\text{O}_2$; supported iron catalysts, electrochemical Fenton processes and still other options. The Fenton system exploits the reactivity of the hydroxyl radicals produced in acidic solution by the catalytic decomposition of H_2O_2 . The production of hydroxyl radicals with these reagents triggers a series of reactions shown in Table 5.1. Reaction (eq. 5.1) corresponds to the chain initiation reaction whereby the reactive $\bullet\text{OH}$ is formed and is formally recognized as the Fenton reaction. If both $\bullet\text{OH}$ and Fe^{2+} ions are in excess, reaction (eq.5.3) will terminate the chain reaction.

The newly formed ferric ions may also catalyse, with excess hydrogen peroxide, causing its decomposition as shown (eq. 5.2) and forming back ferrous ions and new radicals. This reaction is called Fenton-like reaction and is slower than the Fenton one. Equations 5.1 and 5.2 show that the Fenton process follows a cyclic mechanism in terms of iron species with continuous consumption of hydrogen peroxide. Thus, iron can be considered a catalyst in the Fenton reaction whilst hydrogen peroxide is a reagent. Production of hydroperoxyl radicals ($\text{HOO}\bullet$) in reactions (eq. 5.2 and 5.7) plays a critical role in the regeneration of Fe^{2+} ions (eq. 5.5) as well as in the attack of organic contaminants. However, they are less

powerful than hydroxyl radicals. Because equations 5.2 and 5.5 are responsible for the regeneration of ferrous ions, they represent the rate-limiting step in the Fenton chemistry. Radical-radical reactions or hydrogen peroxide-radical reactions can also take place during the Fenton process (eqs. 5.6 to 5.9). As seen in equation 5.7, hydrogen peroxide itself can act as •OH scavenger as well as initiator (eq.5.1).

Table 5.1 Fenton's oxidation reactions and their rate constants.

Reaction equation		Rate constants (M ⁻¹ s ⁻¹)	Reference
Fe ²⁺ + H ₂ O ₂ → Fe ³⁺ + •OH + OH ⁻	(eq. 5.1)	40-80	(Rigg et al. 1954)
Fe ³⁺ + H ₂ O ₂ → Fe ²⁺ + HO ₂ • + H ⁺	(eq. 5.2)	0.01	(Chen and Pignatello 1997)
Fe ²⁺ + •OH → Fe ³⁺ + OH ⁻	(eq. 5.3)	3·10 ⁸	(Walling 1975)
Fe ²⁺ + HO ₂ • → Fe ³⁺ + HO ₂ ⁻	(eq. 5.4)	3.3·10 ⁵	
Fe ³⁺ + HO ₂ • → Fe ²⁺ + O ₂ + H ⁺	(eq. 5.5)	3.3·10 ⁵	(Pontes et al. 2010)
•OH + •OH → H ₂ O ₂	(eq. 5.6)	5.2·10 ⁹	(Pontes et al. 2010)
•OH + H ₂ O ₂ → H ₂ O + HO ₂ •	(eq. 5.7)	3.3·10 ⁷	
HO ₂ • → O ₂ • ⁻ + H ⁺	(eq. 5.8)	1.6·10 ⁵	(Kang et al. 2002)
HO ₂ • + •OH → O ₂ + H ₂ O ₂	(eq. 5.9)	1.0·10 ¹⁰	(Sun et al. 2007)

Hydroxyl radicals oxidize organics (RH) by abstraction of protons and producing organic radicals (R•) as shown in eq. 5.10, which are highly reactive and can be further oxidized in the following equations (Walling and Kato 1971):



The organic free radicals produced in eq. 5.10 may be oxidized by Fe³⁺, reduced by Fe²⁺, or dimerised according to the following reactions (Tang and Tassos 1997, Neyens and Baeyens 2003):



Figure 5.1 shows a typical reactor system used for Fenton oxidation. It consists of a batch reactor non-pressurized and stirred, with metering pumps for the addition of acid, base, a ferrous sulphate catalyst solution and industrial strength hydrogen peroxide. It is recommended that the reactor vessel to be coated with an acid-resistant material, because the Fenton reagent is very aggressive and corrosion is easily produced.

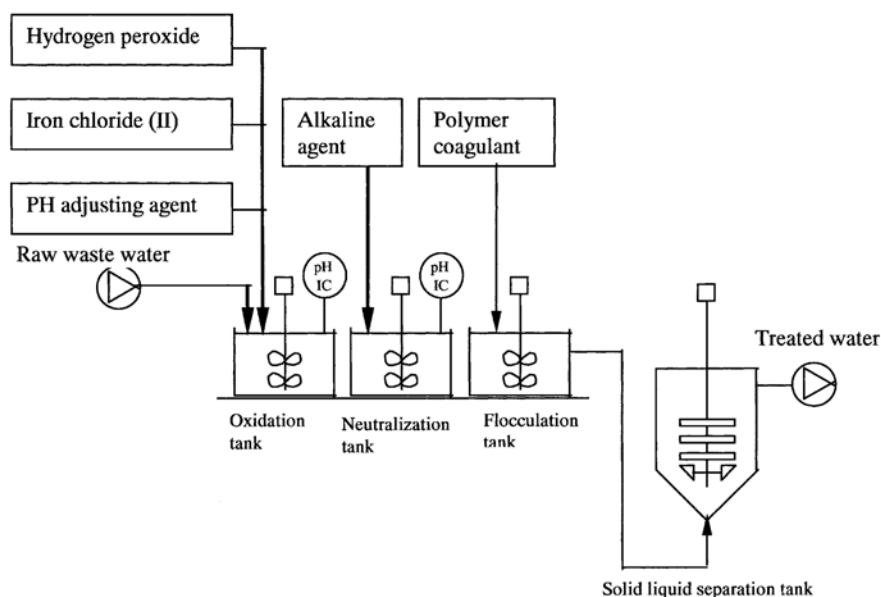


Figure 5.1. Treatment flowsheet for Fenton oxidation (Gogate and Pandit 2004).

5.2.1. Operating parameters

Major parameters controlling the efficiency of the Fenton process are initial pH, dosage of hydrogen peroxide and ferrous ion, temperature, and the initial concentration of the pollutant. For many chemicals, ideal pH for the Fenton reaction is between 3 and 4 (Venkatadri and Peters 1993, Tang and Huang 1997, Ma et al. 2000, Rivas et al. 2001). At very low pH, less than 2, the reaction is slower due to the formation of complex iron species $[\text{Fe}(\text{II})(\text{H}_2\text{O})^{2+}]$ reacting more slowly with hydrogen peroxide and, therefore, producing less amount of effective hydroxyl radicals, thereby reducing the degradation efficiency. As well, the formation of oxonium ion $[\text{H}_3\text{O}_2]^+$, which makes hydrogen peroxide more stable and presumably reduces its reactivity with ferrous ions (Kwon et al. 1999). At higher pH values, the generation of hydroxyl radical is slower due to the presence of relatively inactive iron oxohydroxides or even iron (III) hydroxide precipitate (Parsons

2004). Additionally, at $\text{pH} > 8$ H_2O_2 is also unstable and may decompose to directly give oxygen and water, losing its oxidation ability.

Usually the rate of degradation increases with an increase in the concentration of hydrogen peroxide and ferrous ions (Lin and Peng 1995, Lin and Lo 1997, Benitez et al 2001). However, care should be taken while selecting the operating oxidant and ferrous dosage. For instance, the loading of hydrogen peroxide should be adjusted in such a way that the entire amount is utilized and avoid the decrease in degradation efficiency where Fenton oxidation is used as a pre-treatment to biological oxidation.

Not many studies are available dealing with the effect of temperature on the degradation rates since ambient conditions can safely be used with good enough efficiency. An increase in the reaction temperature will increase the reaction rate. However, once the temperature reaches a certain point, some chemical species may be altered and, consequently, the reaction could slow down or even stop (Kavitha and Palanivelu 2005, Guedes et al. 2003). Lin and Lo (1997) have reported an optimum temperature of $30\text{ }^\circ\text{C}$ whereas Rivas et al. (2001) reported that the degradation efficiency is unaffected even when the temperature is increased from 10 to $40\text{ }^\circ\text{C}$. Fenton oxidation of organic compounds is inhibited by phosphate, sulphate, fluoride, bromide and chloride ions. Inhibition by these species may be due to precipitation of iron, scavenging of $\text{HO}\cdot$ or coordination to dissolved Fe(III) to form a less reactive complex (Pignatello et al. 2006).

5.2.2. Advantages and disadvantages

While other AOPs have high demand of electrical energy for devices such as ozonators, UV lamps, ultrasounds, etc., and this makes them economically disadvantageous; Fenton's reagent is particularly attractive due to the facts that: iron is a highly abundant and non toxic element, hydrogen peroxide is easy to handle and environmentally benign, and the absence of mass transfer limitation due to its homogeneous catalytic nature and the simplicity of the technology required (Walling 1975). Additionally, no energy input is necessary to activate hydrogen peroxide. Therefore, this method offers a cost-effective source of hydroxyl radicals, using easy-to-handle reagents (Bautista et al. 2007).

However, Fenton has some disadvantages. Since Fenton process requires ferrous salt for the oxidation reaction to take place, the environmentally hazardous iron sludge formed after the reaction has to be removed before discharging. Continuous injection of catalyst (due to its loss in the reactor effluent) is thus needed, which increases treatment costs. The radical scavenger character of the hydrogen peroxide itself, driving to autodecomposition into water and inactive molecular oxygen, makes necessary the use of excess amounts of H_2O_2 and the consequent waste of bulk oxidant. Likewise, residual oxidant in the effluent from the Fenton process can damage microorganisms into a subsequent biological degradation, what forces its destruction before driving to any biological treatment. Moreover, the tight acidic range, in which the reaction proceeds, first requires the acidification because the pH of most waste water is not within the optimal reaction range and later forces its neutralization after treatment, to precipitate the iron hydroxide and adjust to pH for a subsequent biological treatment or just disposal. Finally, the Fenton deactivation by some ion-complexing agents like phosphate anions can prevent the completion of the oxidation.

5.2.3 Fenton applied for elimination of model compounds

5.2.3.1. Fenton for elimination of BPA

Several studies have investigated BPA degradation using a modified Fenton reaction such as photo-Fenton (Katsumata et al. 2004), Fenton in combination with a glide arc discharge (Abdelmalek et al. 2006), and Fenton with ultrasound (Ioan et al. 2007); however there is a limited number of studies on its degradation using the conventional Fenton reagent alone. Sajiki and Yonekubo (2004) studied the degradation rate of BPA in seawater by Fenton oxidation. Although the BPA response to Fenton in seawater was poorer than in deionised water, they concluded that BPA leaching to seawater from plastic debris could be degraded to oxidative metabolites such as BPA-o-quinone in presence of hydroxyl radicals. Furthermore, substantial BPA removal was obtained by He et al. (2009) from municipal solid waste landfill leachates by a Fenton process.

The BPA degradation using four AOPs, i.e., Fenton reagent, UV/ H_2O_2 , UV and ultrasound, was presented by Young et al. (2013). Fenton reagent showed to be the most effective process, resulting in the complete removal of the BPA in less than 1 min. Torres et al

(2007) and Poerschmann et al (2010) reported the formation of aromatic intermediates during oxidative degradation of BPA by Fenton. It is generally accepted that an array of stable aromatic products including p-isopropylphenol, 4-isopropenylphenol and 4-hydroxyacetophenone are formed in abiotic Fenton reactions (Katsumata et al. 2004) in addition to common aliphatic-ring opening products mainly including short chain dicarboxylic acids.

Torres et al. (2007) evaluated the feature of ultrasound in the BPA sonochemical degradation and its comparison to Fenton's reaction in the cases of deionised acidic water and natural water. They identified seven main aromatic by-products that had been reported by authors in the investigation of electrochemical Fenton's process and TiO₂ photocatalysis (Fukahori et al. 2003) of BPA. These by-products, in the range of 150 and 242 g/mol are more hydrophilic than the BPA.

They also detected the occurrence of some aliphatic acids such as oxalic, formic and acetic acids. Meanwhile, Poerschmann et al. (2010) expanded the presence of aromatic by-products in the molecular weight range between 94 Da (phenol) and 470 Da, the overwhelming majority of which have not been reported by far. Figure 5.2 gives molecular structure of these aromatic intermediates identified with MW lower and similar than BPA. 4-isopropenylphenol and 4-hydroxyacetophenone were the most abundant aromatic intermediates with molecular weights lower than BPA. Likewise, ring opening products including lactic acid, as well as dicarboxylic acids could be detected. Lactic acid proved to be the most abundant ring-opened surrogate in the diethyl ether extract. In addition, they identified the occurrence of some aromatic intermediates larger than BPA, Figure 5.3. These compounds typically share either a biphenyl or a diphenylether structure. The formation of them was explained by oxidative coupling reactions of stabilized free radicals or by the addition of organoradicals (organocations) onto BPA molecules or benzenediols.

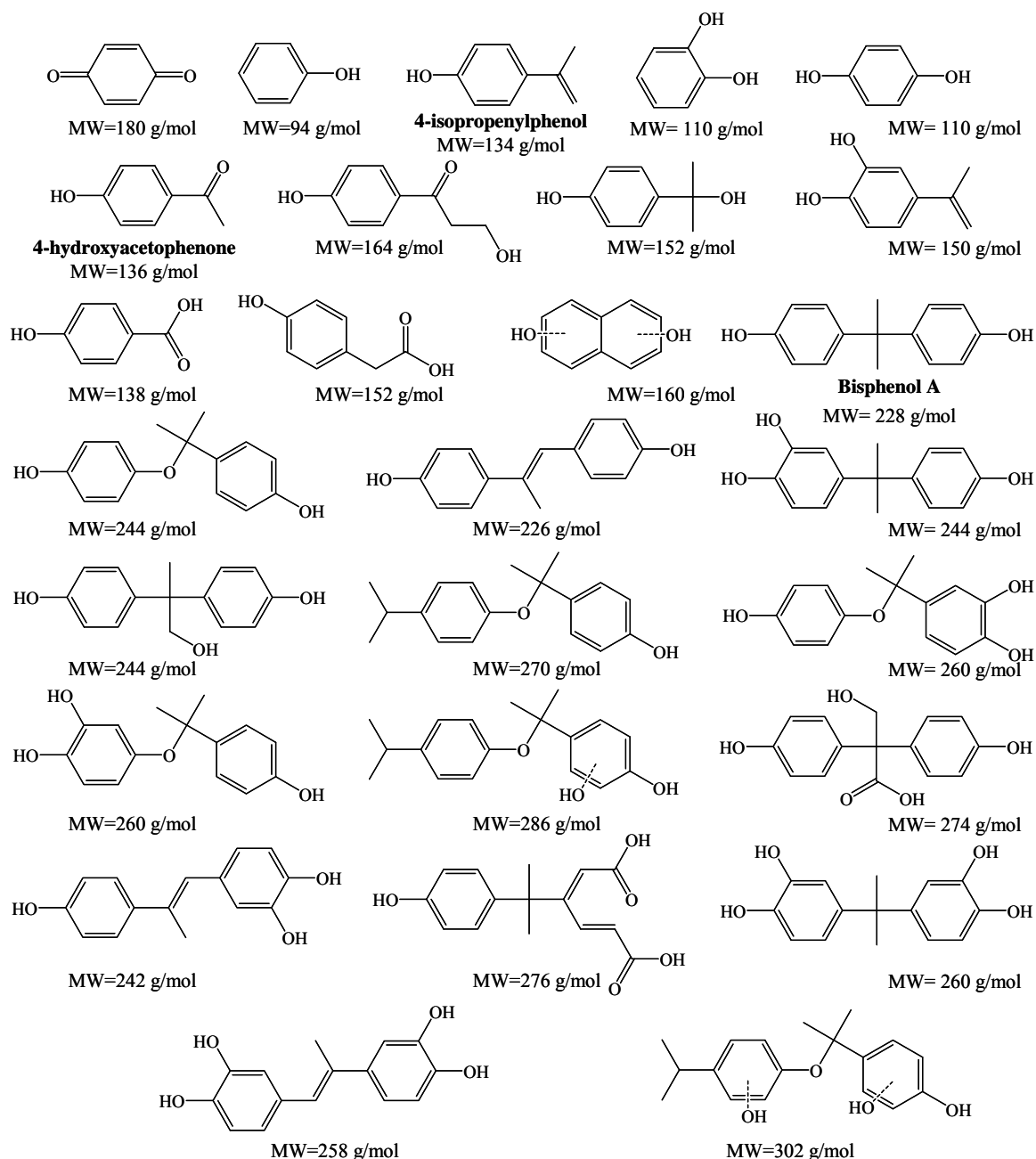


Figure 5.2. Intermediates with one or two aromatic rings formed during oxidative degradation of BPA by sub-stoichiometric Fenton (adapted from Poerschmann et al. 2010).

It is worthwhile that some intermediates of the diphenyl ether- and biphenyl-type identified by Poerschmann et al. (2010) are recalcitrant and possess a potential ecotoxicological risk, too. Therefore, further research needs to address the extent to which these reactions contribute to ecotoxicological risks.

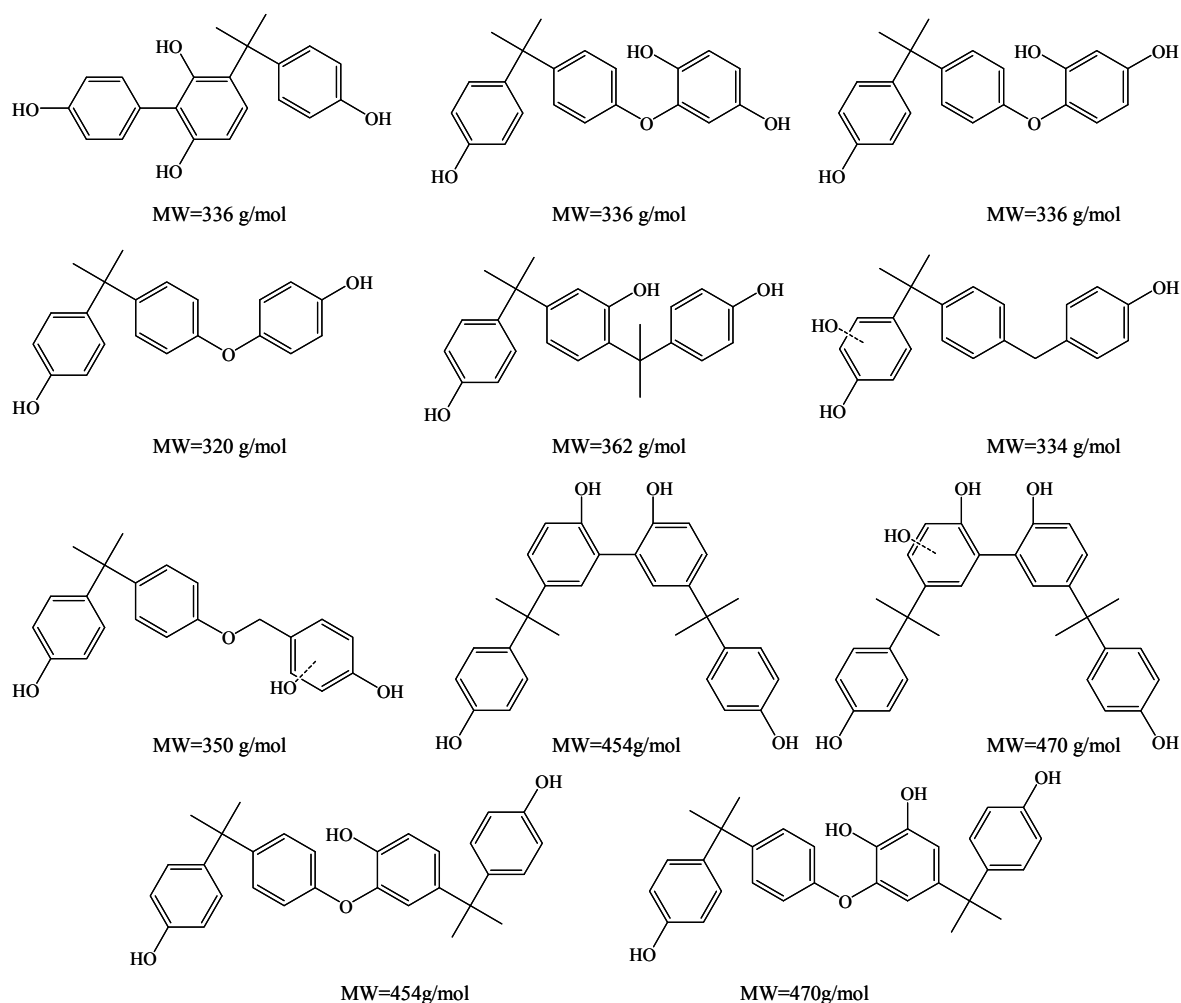


Figure 5.3. Intermediates with more than three aromatic rings formed during oxidative degradation of BPA by sub-stoichiometric Fenton (adapted from Poerschmann et al. 2010).

5.2.3.2. Fenton for elimination of tartrazine

There is still very little information in literature about removal of tartrazine using Fenton process. Behnajady et al. (2007) published the decolourization of C.I. Acid Yellow 23 (tartrazine) by Fenton process. They also included a kinetic model to predict its decolourization at different Fenton operation conditions. Their results showed the power of Fenton for decolourization of tartrazine, achieving conversions as high as 98%. The kinetics of the degradation of Food Yellow 3 and Food Yellow 4 (tartrazine) dyes by oxidation using hydrogen peroxide in alkaline solution was studied by Fragozo et al. (2009). They also concluded in the viability of the processes using hydrogen peroxide for the decolourisation of dye effluents. Moreover, they proposed a route to the fragmentation of the tartrazine, based on the structures and routes proposed by López et al. (2004) in the enzymatic degradation of the azo dye Orange II, where symmetrical azo bond cleavage and

asymmetrical azo bond cleavage coexist. Figure 5.4 shows this tartrazine degradation route.

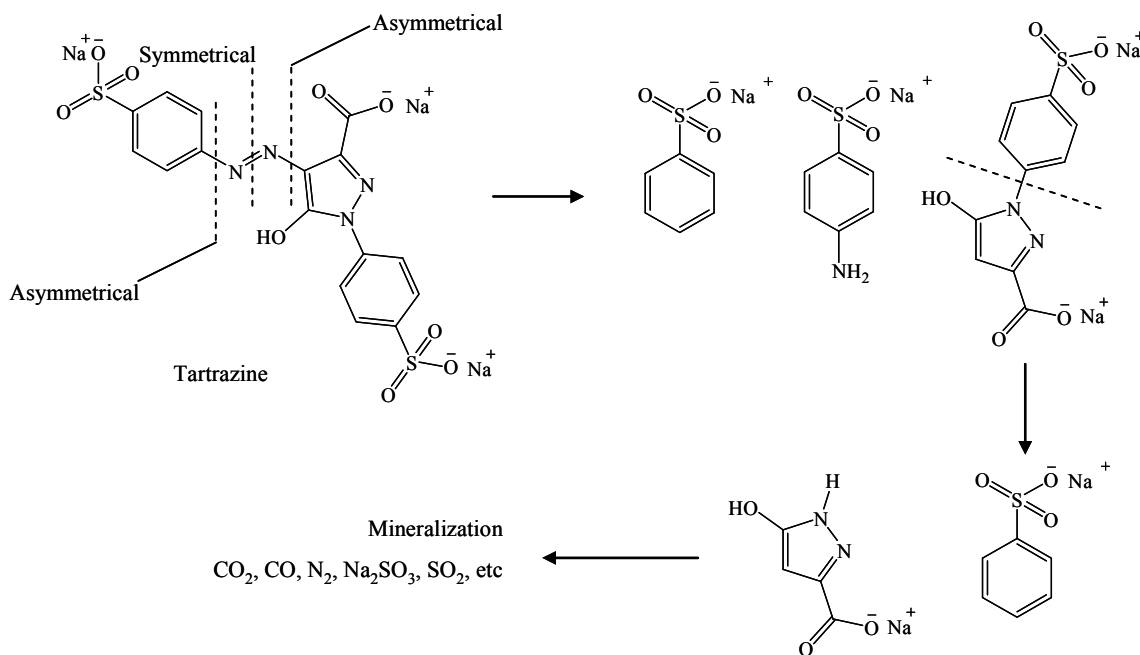


Figure 5.4. Possible pathway to the fragments of the tartrazine (adapted from Fragoso et al. 2009).

In Figure 5.4, it can be pointed out that the 4-aminobenzenesulfonate and benzenesulfonate must be some of the intermediates present in the degradation of tartrazine. Quantitative estimation of the reaction products in the Fe-TAML/hydrogen peroxide degradation of concentrated solutions of the commercial azo dye tartrazine was done by Beach et al. (2011). They identified 4-phenolsulfonic acid as a major product, which was result of asymmetric hydrolytic cleavage of the azo bond of tartrazine. Formic, maleic, fumaric, and malonic acids were also detected. They are well-known late oxidation products from phenol oxidative degradation. The presence of these compounds was linked with the action of Fe-TAML/ H_2O_2 on the intermediate 4-phenolsulfonic acid and they were terminal products of the tartrazine degradation.

5.2.4. Fenton process assisted by nanofiltration

Nanofiltration is increasingly being used for the removal of EDCs and dyes because of the high removal rate of low molecular weight organic micropollutants (Zhang et al. 2006, Gómez et al. 2007, Bellona et al. 2010, Ellouze et al. 2012). However, membrane processes by themselves are unable to destroy organics as they only transport them from

one phase to another, therefore, require the subsequent disposal of concentrated pollutants. Consequently, organic pollutants in the NF concentrated stream ultimately must be mineralized and/or transformed into harmless or less harmful chemical species.

Membrane processes can be useful in applications where subsequent solute separation is required; such is the case of Fenton process. Since iron ions end in form of environmentally hazardous sludge, the recovery of the catalyst remains a problem to be solved. Thus, membrane processes could be employed as iron recovery step after the Fenton reaction, as well as, they can use to deeply oxidize pollutants, by recirculation of the retentate back to the degradation step.

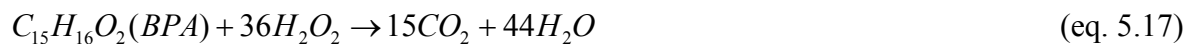
Membranes have been successfully employed in coupled processes where they are combined with hydrogen peroxide oxidation technologies. Song et al. (2004) discussed the applications of H_2O_2/UV oxidation pre-treatment with NF processes. Kim et al. (2008) developed a new hybrid system combining the advantages of NF and homogeneous catalytic oxidation. They used iron(III)–tetrasulfophthalocyanine (Fe(III)–TsPc), a homogeneous catalyst, which used hydrogen peroxide as an oxidant to degradation of BPA. In this research, the catalyst was retained in the system by the NF membrane and was used to continuously oxidize pollutants. They conclude that the combination of Fe(III)–TsPc/ H_2O_2 and NF membrane enhanced removal of BPA compared with a conventional NF-only system, BPA removal efficiency was >95%. Although membrane technology in combination with Fenton processes for removal of BPA has been studied to solve some of the Fenton process drawbacks; little has been checked out about the removal of tartrazine by Fenton process and its coupling to membrane processes.

5.3 Fenton degradation of model compounds

5.3.1 Fenton degradation of BPA

The effect of different system variables, namely Fe^{2+}/H_2O_2 and H_2O_2/BPA molar ratio, initial BPA concentration and reaction time were studied. All experiments were conducted at room temperature, $T_R = 30 \pm 1$ °C, $pH_0 = 3.00 \pm 0.01$, stirring rate at 300 rpm for a time reaction, t_R , of 120 min. Theoretical complete mineralization of BPA is given by eq. 5.17.

This equation was used to normalise the oxidant to BPA molar ratio, so a H₂O₂/BPA stoichiometric molar ratio equal to 1 represents the addition of one time the stoichiometric amount of H₂O₂ (36 mol) needed to completely oxidize 1 mol of BPA.



The oxidation experiments were carried out in the 1 L batch reactor using hydrogen peroxide as oxidizing agent and iron(II) sulphate heptahydrate as catalytic agent (Fenton reagent). Table 5.2 summarizes the operating conditions in terms of BPA initial concentration and H₂O₂/BPA as defined, and Fe²⁺/H₂O₂ initial molar ratio. Sub-stoichiometric amounts of H₂O₂ oxidant and Fe²⁺, what correspondingly does not allow complete mineralization, were used to simulate viable processes and operation under economically and ecologically feasible conditions aimed at reducing high operating costs. The purpose of the treatment is the elimination of the target compound rather than a deep mineralization since a partially oxidized waste stream could be subsequently driven to a biological process if its treatability has been sufficiently improved. The Fenton reaction has been widely studied, but the optimal ratio of Fe²⁺/H₂O₂ still differs between authors. In the present study, the optimal ratio was considered to be 0.012, far from the theoretical optimum ratio of 0.091 reported in some previous studies (Poerschmann et al. 2010, Tang and Huang 1997).

Table 5.2 illustrates the effect of BPA concentration on the final conversion of BPA (X_{BPA}) after being subjected to Fenton treatment. The increase of BPA concentration between 100 and 300 mg/L decreases the conversion in 13.7% however; the amount of BPA destroyed in a 1L of solution for 120 min increases in all the studied concentrations. Hydroxyl radical is mainly responsible for BPA degradation and its concentration is expected to remain constant for all BPA concentrations, since H₂O₂ and Fe²⁺ initial concentration used were constant in this set of tests. The increase in BPA concentration increases the number of BPA molecules but not the hydroxyl radical concentration, so the BPA disappearance rates increase. These results demonstrate that BPA is a highly reactive species, as well as the efficient use of oxidant at higher BPA concentration.

Table 5.2. Fenton treatment over BPA. Effect of BPA initial concentration, H₂O₂/BPA and Fe²⁺/H₂O₂ initial molar ratio on the conversion and colour formation. Conditions: T_R = 30 °C, t_R = 120 min, pH₀ = 3 and 300 rpm.

[BPA] (mg/L)	[H ₂ O ₂] (mg/L)	[Fe ²⁺] (mg/L)	H ₂ O ₂ /BPA (¹)	Fe ²⁺ /H ₂ O ₂	X _F BPA (%)	X _F COD (%)	X _F TOC (%)	Abs ⁽²⁾ ±0.0002	pH _f ± 0.01
13	150	3	2.23	0.012	100 ± 2.1	19.5 ± 1.0	11.4 ± 0.9	0.0201	2.94
25	150	3	1.12	0.012	100 ± 2.8	22.4 ± 2.3	14.7 ± 0.1	0.0385	2.91
50	150	3	0.56	0.012	100 ± 2.2	45.3 ± 2.1	36.9 ± 0.6	0.1200	2.84
100	150	3	0.28	0.012	100 ± 2.1	38.3 ± 0.2	16.8 ± 0.8	0.1920	2.81
200	150	3	0.14	0.012	97.5 ± 2.1	19.1 ± 1.3	7.3 ± 0.9	0.3245	2.81
300	150	3	0.09	0.012	86.3 ± 2.0	11.9 ± 0.1	3.3 ± 0.1	0.3256	2.83
300	75	1	0.05	0.012	57.5 ± 1.9	37.8 ± 0.2	16.5 ± 0.5	0.3252	2.98
300	159	3	0.10	0.012	85.5 ± 1.8	26.6 ± 0.1	13.8 ± 0.8	0.3922	2.80
300	242	5	0.15	0.012	97.9 ± 1.8	35.5 ± 1.8	16.5 ± 0.6	0.5800	2.81
300	323	6	0.20	0.012	99.7 ± 1.8	44.6 ± 2.1	26.1 ± 0.8	0.6523	2.71
300	644	13	0.40	0.012	99.8 ± 1.8	66.1 ± 2.2	29.5 ± 0.6	0.2671	2.54
300	1608	31	1.00	0.012	100 ± 1.2	78.2 ± 1.3	59.1 ± 0.6	0.1059	2.45
300	323	0	0.20	0.000	19.8 ± 1.4	6.7 ± 1.6	3.7 ± 0.6	0.0258	2.97
300	323	2	0.20	0.003	93.3 ± 1.7	24.8 ± 1.7	19.9 ± 0.6	0.6973	2.80
300	323	3	0.20	0.006	94.8 ± 1.7	25.0 ± 1.9	19.6 ± 0.6	0.6958	2.77
300	323	26	0.20	0.050	97.8 ± 1.1	23.6 ± 1.8	13.9 ± 0.3	0.7429	2.72
300	323	52	0.20	0.100	98.4 ± 1.2	23.8 ± 1.6	14.3 ± 0.7	0.7565	2.79

(¹) H₂O₂/BPA as the stoichiometric molar ratio.

(²) Measured at 400 nm.

Figure 5.5 presents the temporal evolution of BPA conversion for 100, 200 and 300 mg/L of initial BPA concentration. It must be noted that the maximum conversions were immediately reached upon initiation of the reaction. The faster degradation of BPA is believed to be due to the higher efficiency for the production of a large amount of hydroxyl radicals by the reaction of Fe²⁺ with H₂O₂ (eq. 5.1). This trend also suggests that there was little competition between formed by-products and BPA for their attack by hydroxyl

radicals, leading to the faster degradation of BPA and indicating that BPA is more reactive specie.

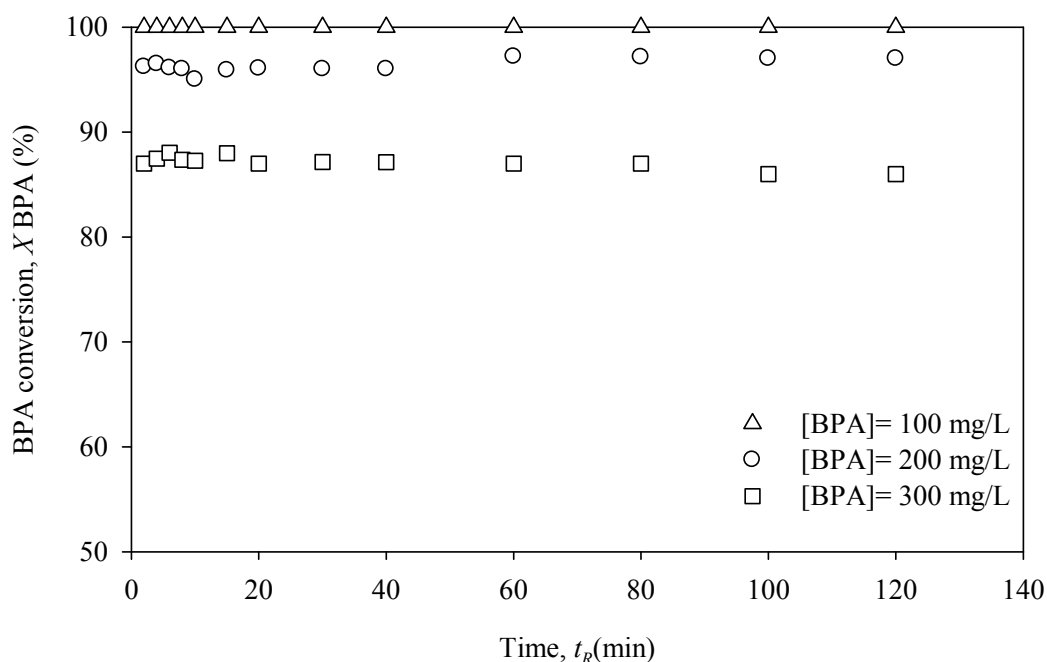


Figure 5.5. Fenton treatment over BPA. BPA conversion as a function of reaction time for several initial BPA concentrations. Conditions: $[Fe^{2+}] = 3 \text{ mg/L}$, $[H_2O_2] = 150 \text{ mg/L}$, $pH_0 = 3$, $T_R = 30^\circ\text{C}$ and 300 rpm.

The effect of H_2O_2 /BPA stoichiometric molar ratio on the Fenton process is also shown in Table 5.2 and Figure 5.6. In those experiments, a Fe^{2+}/H_2O_2 molar ratio and a BPA initial concentration of 0.012 and 300 mg/L were chosen, respectively. Altogether, an increase in the H_2O_2 /BPA stoichiometric molar ratio was positive, as expected, for the degradation of BPA in all the studied range. The mineralization efficiency was better when increasing the H_2O_2 /BPA ratio in the range from 0.20 to 1. This behaviour could be due to the improved oxidation power with increasing hydroxyl radical amounts in the solution generated from H_2O_2 concentrations. For H_2O_2 /BPA above 0.20, the BPA conversion kept constant, still very high, and $X_f\text{COD}$ and $X_f\text{TOC}$ continuously increased. $X_f\text{COD}$ increased from 44.6 to 78.2% and $X_f\text{TOC}$ from 26.1 to 59.1%. This was due to enhanced intermediate degradation due to the improved availability of radicals. Furthermore, the increase in the $X_f\text{COD}$ as a function of H_2O_2 /BPA stoichiometric molar ratio in all the studied range is related to the generation of by-products with a lower number of carbons atoms in their structures, which required fewer amounts of oxygen moles for their oxidation. It is worth mentioning that, in spite of the use of the stoichiometric amount required (H_2O_2 /BPA = 1), so complete

mineralization of BPA can hardly be achieved, as evidenced by the 59.1% in the X_T TOC at this condition, a notable mineralization was reached. In general, the maximum BPA conversions were reached before 15 min of reaction as shown in Figure 5.6.

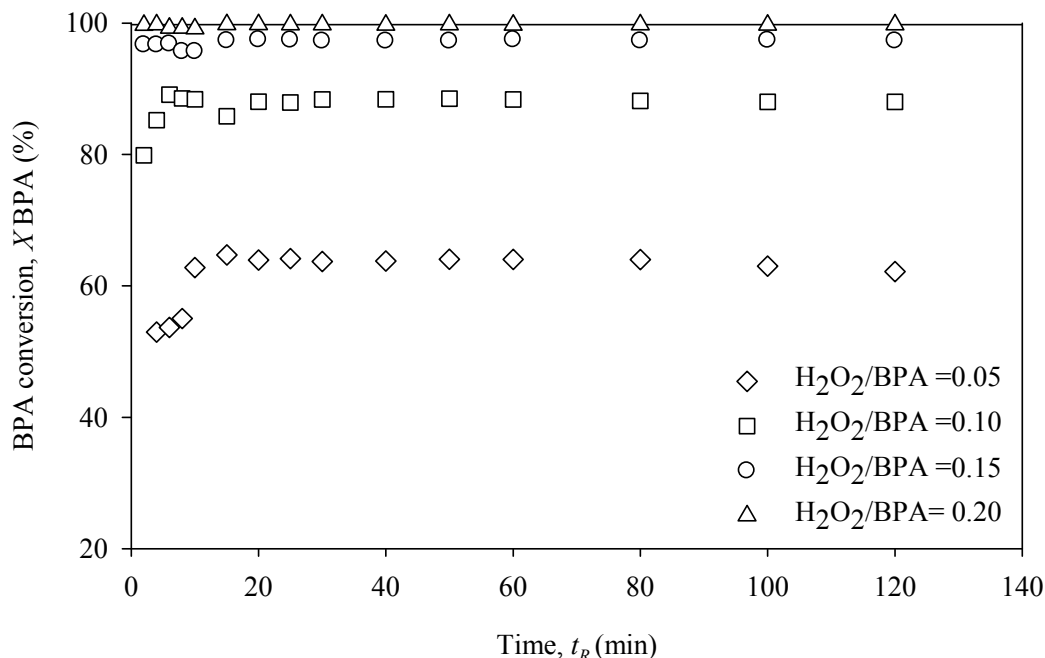


Figure 5.6. Fenton treatment over BPA. BPA conversion as a function of reaction time for several H_2O_2/BPA stoichiometric molar ratios. Conditions: $[BPA]_0 = 300$ mg/L, $Fe^{2+}/H_2O_2 = 0.012$, $pH_0 = 3$, $T_R = 30$ °C and 300 rpm.

To find out the optimal iron load, several experiments were performed by increasing the catalyst concentration from 0 to 52 mg/L. For this, the initial BPA concentration, H_2O_2/BPA stoichiometric molar ratio and reaction time were set at 300 mg/L, 0.20 and 120 min, respectively. The BPA achieved 93% degradation under most experimental conditions (Table 5.2). A Fe^{2+}/H_2O_2 ratio as low as 0.003 already yielded a BPA degradation of 93.3%. The increase on the catalyst load improves the generation rate of hydroxyl radicals, which in turn leads to a higher radical attack probability. However, an increase of the mineralization was not observed with the further increase of the catalyst concentration. Beyond $Fe^{2+}/H_2O_2 = 0.003$, the X_T COD and X_T TOC remained almost unaltered despite increasing doses of Fe^{2+} . Thus, the use of a much greater Fe^{2+} concentration could also lead to the self-scavenging of hydroxyl radicals by Fe^{2+} (eq. 5.3) so there is not further degradation of the intermediates created. Likewise, the ferric ions generated during Fenton reaction could be coordinated by the benzene rings, thus stabilized, inhibiting the cyclic mechanism of Fenton process, therefore hampering the regeneration of ferrous ions, and

stopping the formation of new radicals responsible of the degradation. It was also observed that in the absence of Fe^{2+} , there was a significant degradation, indicating that H_2O_2 can directly react with BPA without any catalyst. From the experiments in the range studied, it is possible to conclude that higher iron load has not too much impact on BPA degradation in Fenton treatment.

The BPA degradation rate as a function of the reaction time for several $\text{Fe}^{2+}/\text{H}_2\text{O}_2$ molar ratio is shown in Figure 5.7. It is noteworthy that, at this low $\text{H}_2\text{O}_2/\text{BPA}$, the BPA is rapidly consumed and the final conversion reached in minutes. Given the low $X_f\text{COD}$ and $X_f\text{TOC}$ simultaneously achieved, this again evidences that the radicals are preferentially consumed by the BPA instead of by the oxidation intermediates produced. This behaviour clearly indicates that the BPA is highly reactive and its destruction is easily completed with low doses of H_2O_2 . In contrast, in the absence of Fe^{2+} , the reaction progresses more slowly and stops at near 20% conversion. As the initial amount of H_2O_2 is in excess, if just the BPA disappearance is considered, and could reach total BPA elimination, this suggests that there occurs a self-decomposition of the H_2O_2 even in absence of catalyst.

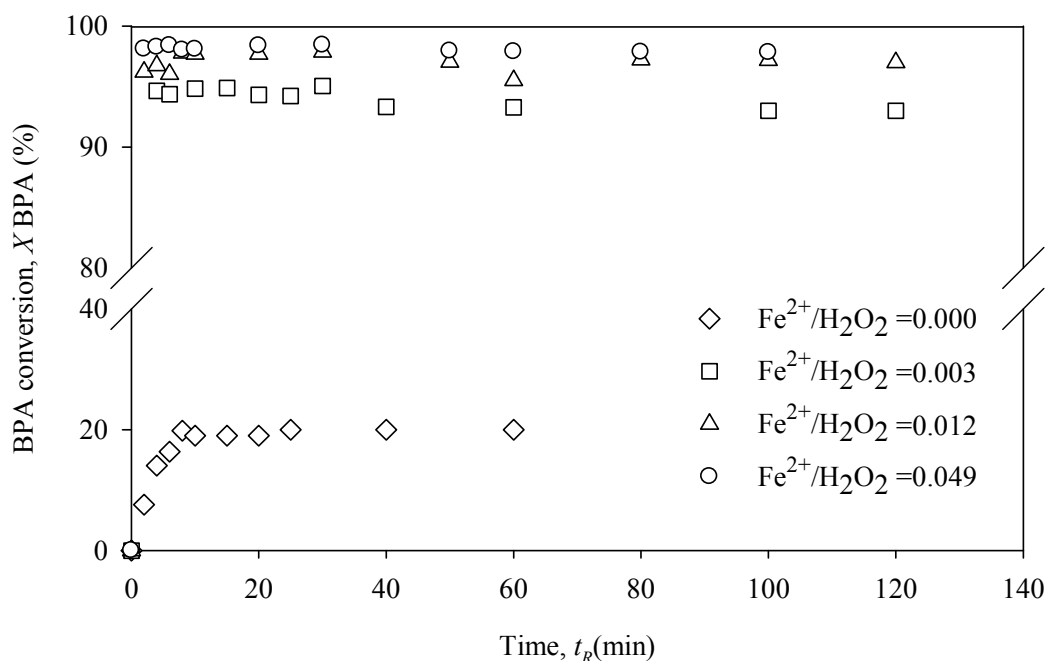


Figure 5.7. Fenton treatment over BPA. BPA conversion as a function of reaction time for several $\text{Fe}^{2+}/\text{H}_2\text{O}_2$ molar ratios. Conditions: $[\text{BPA}] = 300 \text{ ppm}$, $\text{H}_2\text{O}_2/\text{BPA} = 0.20$, $\text{pH}_0 = 3$, $T_R = 30 \text{ }^\circ\text{C}$ and 300 rpm.

In addition, Table 5.2 collects the absorbance (abs) of the pre-oxidized effluents spectrophotometrically measured at a 400 nm wavelength. The colour differences or absorbencies could be correlated with the formation of coloured aromatic intermediates. Mijangos et al. (2006) analyzed the development of dark colour observed in phenol oxidation by Fenton liquor. They related the colour generation to three main contributions: 1) phenol can be degraded to dihydroxylated rings (catechol, resorcinol, and hydroquinone), which generate higher coloured compounds such as ortho- and parabenzoquinone; 2) the dihydroxylated rings can react with their own quinones to generate charge transfer complexes (quinhydrone), compounds imparting a dark colour at low concentrations; and 3) iron reacts with hydrogen peroxide to form ferric ions that can coordinate to benzene rings producing highly coloured metal complexes.

Since BPA is formed by two phenol rings, colour generation might be related with the production of those intermediates, also expected. It was visually observed during BPA oxidation by Fenton that, in the first minutes of the reaction, the BPA solution underwent a fast colour change from colourless to dark brown in less than 5 min. Later, depending on reaction conditions, it began to slowly clear up back to a light brown. Regarding Table 5.2, the effect of the initial H_2O_2 amount on colour formation showed to have a maximum value. For $H_2O_2/BPA=0.20$ the absorbance at 400 nm was 0.6523. During the first steps of oxidation, highly coloured intermediate compounds such as p-benzoquinone (yellow) and o-benzoquinone (red) could be generated (Santos et al. 2002). Their colour comes from their quinoidal structure, which contains chromophore groups substituted in benzene rings. In addition, the mixture of single p-benzoquinone and hydroquinone (colourless) solutions fits brown colour, resulting of occasional intermolecular interactions between quinones and dihydroxylated rings. All these coloured species are very stable due to the conjugated carbonyl groups contained in their internal structure, which render difficult to their further degradation. Consequently, colour formation is also promoted by higher H_2O_2/BPA stoichiometric molar ratio up to 0.20 by speeding up the degradation of BPA to coloured compounds. When H_2O_2/BPA stoichiometric ratio is higher than 0.20 the final colour decreased back due to the significant degradation of the coloured quinones, which need high oxidant doses.

The final pH, pH_f , of the oxidized effluent is also shown in Table 5.2. The uncontrolled pH slightly decreases along the reaction in all conditions tested. The highest decrease was

observed in the evaluation of the effect of H_2O_2 /BPA stoichiometric molar ratio; the pH varied from 2.98 to 2.43 for 0.05 to 1.00 in the H_2O_2 /BPA stoichiometric molar ratio, respectively. These pHs suggest the formation of acid species in the reaction medium. As already mentioned in section 5.2.3.1, Torres et al (2007) and Poerschmann et al (2010) reported the formation of aromatic intermediates during oxidative degradation of BPA by Fenton. They detected a wide variety of aromatic products, including the occurrence of aromatic intermediates larger than BPA. However, ring opening products, such as lactic, acetic and dicarboxylic acids, were mostly detected. The decrease in the pH should be related to the presence of these acid species.

5.3.2 Fenton degradation of tartrazine

The degradation of TAR was carried out at different conditions: Fe^{2+}/H_2O_2 and H_2O_2 /BPA molar ratios and initial TAR concentration. All the assays were performed at room temperature, $T_R = 30 \pm 1$ °C, $pH_0 = 3.00 \pm 0.01$ and stirring rate of 300 rpm for a time reaction of $t_R = 120$ min. The equation 5.18 represents the theoretical complete mineralization of TAR:



The effect of TAR initial concentration on the degradation efficiency was investigated at different concentrations in the range of 100-1000 mg/L and is presented in Table 5.3 and Figure 5.8. It was observed that the X_TAR , X_{COD} , X_{TOC} and X_{Colour} decrease with increasing the initial concentration of the tartrazine. TAR destroyed, which are respectively, 99.8 mg, 274.8 mg, 391.2 mg and 236.0 in 1L of solution after 120 min of treatment for the studied concentrations, increases as initial TAR concentration did. As well as in the case of BPA degradation, while the initial concentration of the dye is increased, the H_2O_2 amount is maintained so the hydroxyl radical concentration is presumed to remain constants. Thus, the highest destruction rate was at 800 mg/L, accordingly more oxidant was used for the target compound degradation. At lower

Table 5.3. Fenton treatment over TAR. Effect of TAR initial concentration, H_2O_2/TAR and Fe^{2+}/H_2O_2 initial molar ratio on the conversion and colour formation. Conditions:
 $T_R = 30\text{ }^\circ\text{C}$, $t_R = 120\text{ min}$, $pH_0 = 3$ and 300 rpm .

[TAR] (mg/L)	$[H_2O_2]$ (mg/L)	$[Fe^{2+}]$ (mg/L)	$H_2O_2/TAR^{(1)}$	Fe^{2+}/H_2O_2	X_fTAR (%)	X_fCOD (%)	X_fTOC (%)	$X_fColour$ $\pm 0.01\%$	pH _f ± 0.01	SA $\pm 0.01\text{ mg/L}$	IP $\pm 0.01\%$
100	300	6	1.05	0.012	99.8 \pm 0.3	63.7 \pm 7.1	25.9 \pm 0.4	86.73 \pm 0.03	2.74	19.65	22.58
400	300	6	0.26	0.012	68.7 \pm 0.2	26.7 \pm 1.4	14.2 \pm 0.4	51.48 \pm 0.01	2.94	67.15	23.78
800	300	6	0.13	0.012	48.9 \pm 0.9	11.2 \pm 1.5	4.4 \pm 0.1	41.16 \pm 0.01	2.95	81.58	12.88
1000	300	6	0.10	0.012	23.6 \pm 0.6	4.36 \pm 0.01	1.3 \pm 0.6	35.63 \pm 0.01	2.83	103.60	12.66
300	1200	24	1.40	0.012	100 \pm 0.8	79.6 \pm 0.9	34.0 \pm 0.9	92.28 \pm 0.04	2.47	156.01	91.59
300	600	12	0.70	0.012	100 \pm 0.3	73.4 \pm 1.1	29.3 \pm 0.4	82.69 \pm 0.02	2.58	141.62	78.31
300	300	6	0.35	0.012	95.3 \pm 0.4	56.9 \pm 1.4	21.2 \pm 0.2	73.95 \pm 0.03	2.69	146.34	70.21
300	146	3	0.17	0.012	90.3 \pm 0.6	37.1 \pm 1.1	3.89 \pm 0.09	47.20 \pm 0.01	2.81	130.58	54.00
300	150	0	0.17	0.000	0.7 \pm 0.7	4.0 \pm 0.6	0.0 \pm 0.2	1.10 \pm 0.07	2.96	0.00	0.00
300	150	1.5	0.17	0.006	60.0 \pm 0.6	19.4 \pm 1.3	4.7 \pm 0.3	32.58 \pm 0.09	2.9	48.08	19.53
300	150	6	0.17	0.024	99.7 \pm 0.6	51.7 \pm 1.4	23.6 \pm 0.6	38.41 \pm 0.02	2.72	187.51	94.20

concentrations, the oxidant is probably used in TAR intermediates degradation and wasted in inefficient oxygen, whereas at higher concentrations (>800mg/L), the intermediates efficiently compete for the radicals leaving less for the TAR. This behaviour could be corroborated observing the decrease in the conversion of $X_f\text{COD}$, $X_f\text{TOC}$ from 63.7 to 4.36% and from 25.9 to 1.3%, respectively.

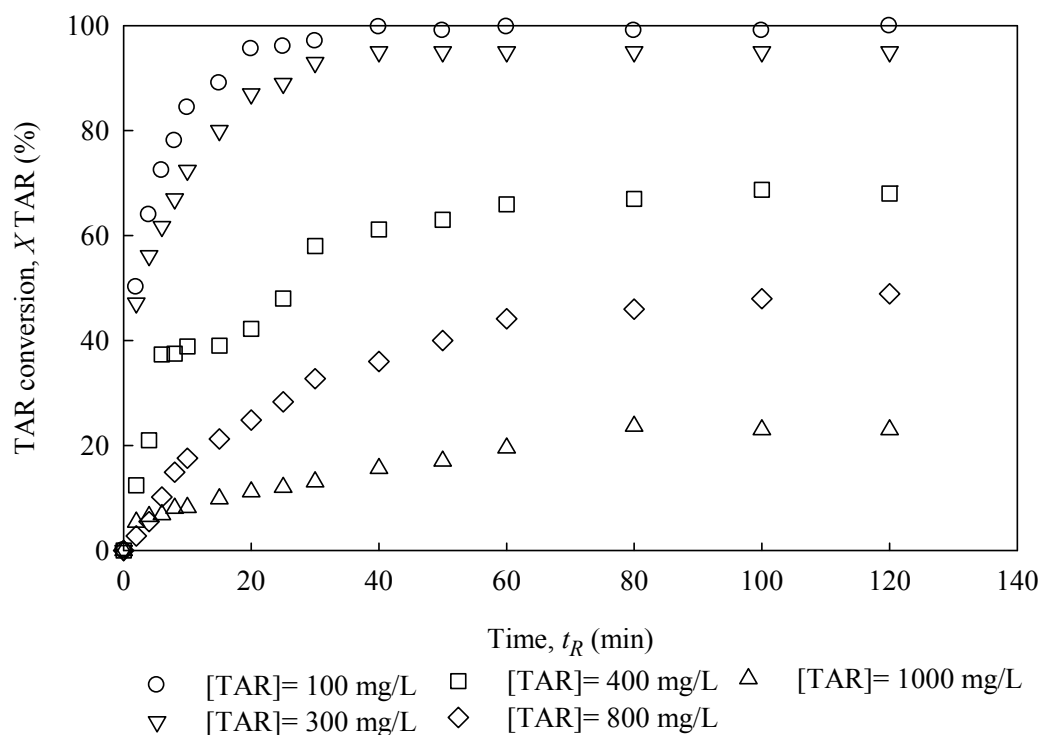


Figure 5.8. Fenton treatment over TAR. TAR conversion as a function of reaction time for several TAR initial concentrations. Conditions: $[\text{Fe}^{2+}] = 6 \text{ mg/L}$, $[\text{H}_2\text{O}_2] = 300 \text{ mg/L}$, $pH_0 = 3$, $T_R = 30 \text{ }^\circ\text{C}$ and 300 rpm.

The effect of both $\text{H}_2\text{O}_2/\text{TAR}$ and $\text{Fe}^{2+}/\text{H}_2\text{O}_2$ molar ratios was also investigated. Firstly, in order to check out the effect of hydrogen peroxide dosage on the decolourization rate, experiments were conducted at different $\text{H}_2\text{O}_2/\text{TAR}$ stoichiometric molar ratios from 0.17 to 1.40 at a fixed $\text{Fe}^{2+}/\text{H}_2\text{O}_2$ molar ratio of 0.012, as it is illustrated in Table 5.3 and Figure 5.9. The increase of $\text{H}_2\text{O}_2/\text{TAR}$ stoichiometric molar ratio from 0.17 to 1.40 increases the $X_f\text{TAR}$, $X_f\text{COD}$, $X_f\text{TOC}$ and $X_f\text{Colour}$ from 90.3 to 100%, 37.1 to 79.6%, 3.89 to 34.0 and 47.20 to 92.28% respectively. This can be explained by the effect of the additionally produced hydroxyl radicals. It is worth noting that while the $\text{H}_2\text{O}_2/\text{TAR}$ stoichiometric molar ratio increased gradually, for values higher than 0.70, the conversion values changed slightly. At high H_2O_2 dosage the decrease in TAR Fenton efficiency is

due to the greater contribution of the hydroxyl radical scavenging effect of H_2O_2 and recombination of hydroxyl radicals. The highest TOC and TAR removals were found at 1.40 of $\text{H}_2\text{O}_2/\text{TAR}$ stoichiometric molar ratio.

Later, the effect of addition of Fe^{2+} represented as $\text{Fe}^{2+}/\text{H}_2\text{O}_2$ on the decolourisation of TAR was studied. The results are shown in Table 5.3 and Figure 5.10. It can be seen that decolourization of TAR distinctly improved along increasing amounts of Fe^{2+} . The application of $\text{Fe}^{2+}/\text{H}_2\text{O}_2$ from 0.000 to 0.024 increases X_{TAR} , X_{COD} , X_{TOC} and X_{Colour} removal from 0.7 to 99.7, 4.0 to 51.7, 0.0 to 23.6 and 1.10 to 38.41, respectively, after 120 min of reaction. As eq. 5.1 shows, more hydroxyl radicals are expected after the increase in the concentration of Fe^{2+} . Thus, 0.024 of $\text{Fe}^{2+}/\text{H}_2\text{O}_2$ appears to be the optimum molar ratio for TAR decolourisation by Fenton.

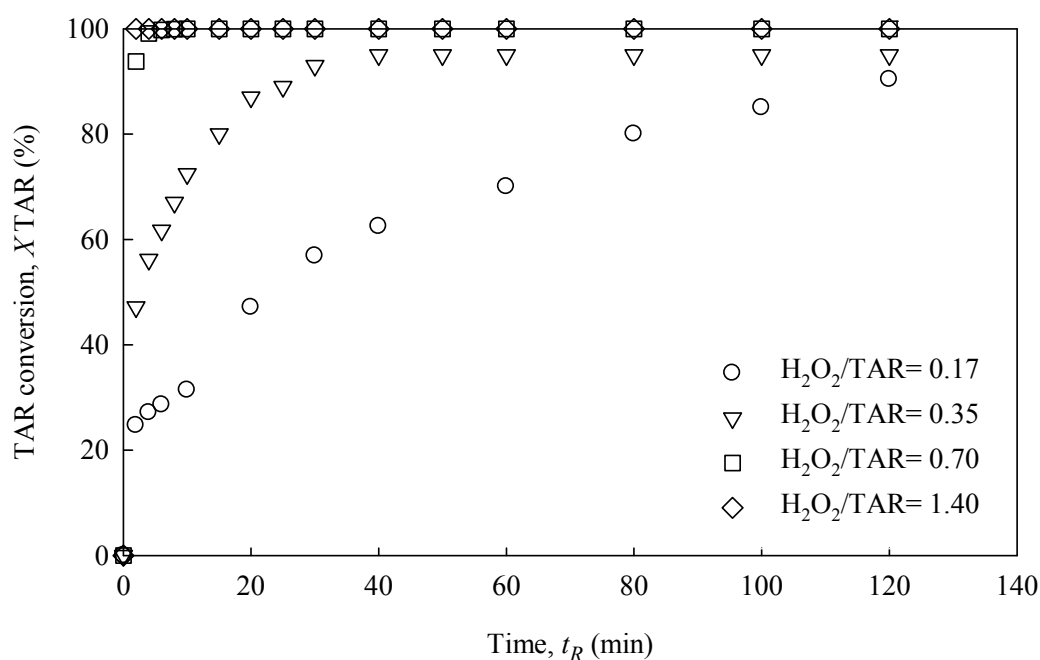


Figure 5.9. Fenton treatment over TAR. TAR conversion as a function of reaction time for several $\text{H}_2\text{O}_2/\text{TAR}$ stoichiometric molar ratios. Conditions: $[\text{TAR}]_0 = 300 \text{ mg/L}$, $\text{Fe}^{2+}/\text{H}_2\text{O}_2 = 0.012$, $\text{pH}_0 = 3$, $T_R = 30 \text{ }^\circ\text{C}$ and 300 rpm.

In general, for the degradation of TAR by Fenton, the decolourisation was faster in the early stage of the reaction than in the late stages. This trend suggests that most of the H_2O_2 was consumed in the early stage of the Fenton reaction. Since Fe^{2+} catalyses H_2O_2 to quickly form hydroxyl radical as the initiation of the reaction, more decolourisation occurs in the early stage of reaction. Thus, as expected, at low Fe^{2+} and H_2O_2 dosage, longer

treatment time was required for complete decolourisation. Instead, an immediate TAR degradation was observed at $[\text{TAR}]_0 = 300 \text{ mg/L}$, $\text{H}_2\text{O}_2/\text{TAR} = 1.40$, $\text{Fe}^{2+}/\text{H}_2\text{O}_2 = 0.012$, $\text{pH}_0 = 3$, $T_R = 30 \text{ }^\circ\text{C}$ and 300 rpm.

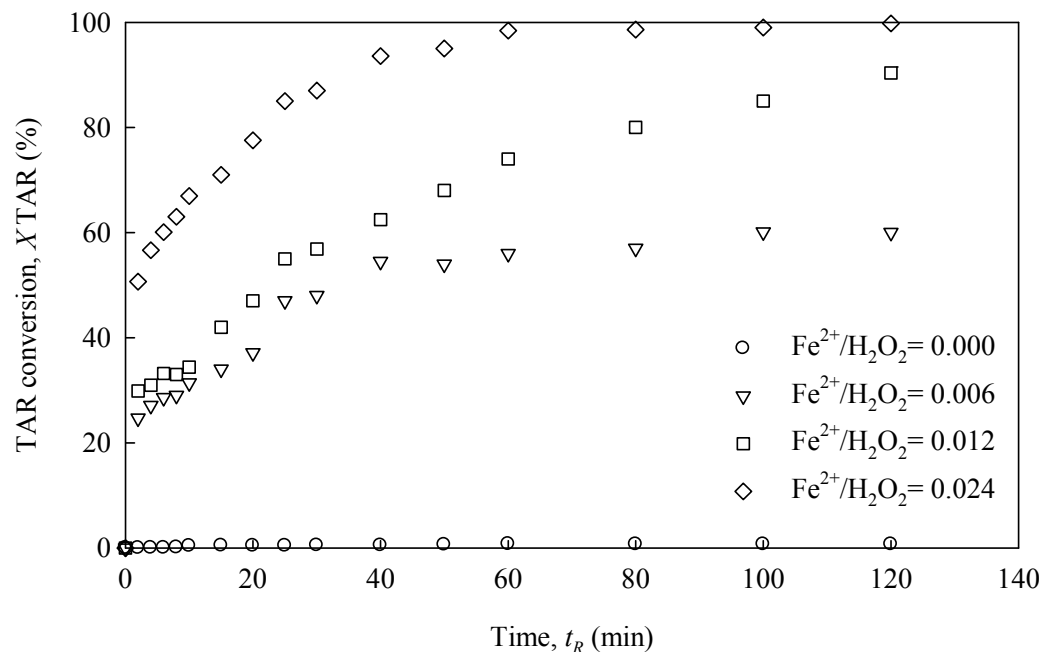


Figure 5.10. Fenton treatment over TAR. TAR conversion as a function of reaction time for several $\text{Fe}^{2+}/\text{H}_2\text{O}_2$ molar ratios. Conditions: $[\text{TAR}]_0 = 300 \text{ mg/L}$, $\text{H}_2\text{O}_2/\text{TAR} = 0.17$, $\text{pH}_0 = 3$, $T_R = 30 \text{ }^\circ\text{C}$ and 300 rpm.

Normally, hydroxyl radicals attack unsaturated dye molecules and the azo bond ($\text{N}=\text{N}$), which is the chromophore or chromogen bond, thereby decolorizing wastewater. It appears that the Fenton process is more beneficial for decolourization rather than for mineralization (TOC removal), since the maximum X_{TOC} reached was only 34.0%. Although the chromophoric structure of TAR molecules was easily destroyed by hydroxyl radicals, some colourless degradation intermediates were formed in the solution during the reaction. In most cases, the adjacent aromatic ring structure is one of the intermediates. For efficient removal of COD from dyes, one should add much more Fenton reagent than that strictly used for dye decolourization. In this case, sulphanilic acid (SA) was the only by-product identified, which has been previously reported as the product of asymmetric hydrolytic cleavage of the azo bond (Fragoso et al. 2009) in TAR structure. Noteworthy that in absence of iron no degradation was observed for Fenton treatment of TAR.

SA production increased as a function of initial concentration, $\text{H}_2\text{O}_2/\text{TAR}$ and $\text{Fe}^{2+}/\text{H}_2\text{O}_2$. Low TAR concentration at higher $\text{H}_2\text{O}_2/\text{TAR}$ might facilitate the degradation of the by-

products formed SA being one of them, due to the greater availability of hydroxyl radicals in the reaction solution. Therefore, higher $\text{H}_2\text{O}_2/\text{TAR}$ and $\text{Fe}^{2+}/\text{H}_2\text{O}_2$ molar ratios allowed higher degradation level, which help the transformation of TAR into by-products, such as SA. As explained in Chapter 3, the percentage of IP is defined as the ratio of theoretical TOC, which is estimated from the concentration of identified organic compounds calculated by HPLC, to the measured final TOC, excluding the final TOC of the parent compound. Thus, this percentage gives an idea of the product fraction which has not been directly identified. The % of IP is proportional to the increase of $\text{H}_2\text{O}_2/\text{TAR}$ and $\text{Fe}^{2+}/\text{H}_2\text{O}_2$ molar ratios or, in other words, to the production of hydroxyl radicals. This means that the SA, once produced, is hardly attacked by hydroxyl radicals, becoming one of the end products of the reaction.

These results indicate that the efficiency of Fenton oxidation of TAR is lower than that for BPA. Tartrazine needs more severe conditions to reach complete removal with lower mineralization level. Furthermore, at similar reaction conditions, BPA showed to be specie more reactive than TAR, since the reaction time to achieve the maximum conversion value was much lower.

5.4 Removal of BPA effluent after Fenton oxidation by nanofiltration membrane

The feed solution in this series of membrane NF experiments was the final solution after Fenton process of BPA (BPA-Fenton effluent) in optimal conditions selected ($[\text{BPA}]_0 = 300 \text{ mg/L}$, $\text{H}_2\text{O}_2/\text{BPA} = 0.20$ and $\text{Fe}^{2+}/\text{BPA} = 0.012$). Optimal conditions represent those where complete removal of BPA was practically achieved with the minimal addition of H_2O_2 and Fe^{2+} . The BPA-Fenton effluent contained $571 \pm 50 \text{ mg/L}$ of COD, $222 \pm 20 \text{ mg/L}$ of TOC, and showed a pH 2.71 ± 0.04 and an absorbance of 0.6523 ± 0.0002 read at 400 nm. Figure 5.11 represents the normalized permeate flux for the studied membranes as a function of time for the NF of this BPA-Fenton effluent.

In general, the flux declined strongly during the first period of filtration. For instance, the flux was 40% of the original pure water flux after 25 minutes of filtration for NF90 membrane. Afterwards, the flux declined more gradually until, in some cases, an almost

steady state value was obtained at approximately 200 minutes. The patterns of flux decline varied between the membranes in this screening study. As it can be seen from Figure 5.11, the CK membrane featured the lowest permeate flux decay at 6 bar, followed by NFD, NF270 and ESNA with close flux declines, and finally by NF90 with the highest flux fall. These trends are connected to an increase of the resistance to the pass through the membrane, which could result from either CP, adsorption of solutes on the membrane, gel formation, internal pore fouling (pore blocking) and external deposition or cake formation.

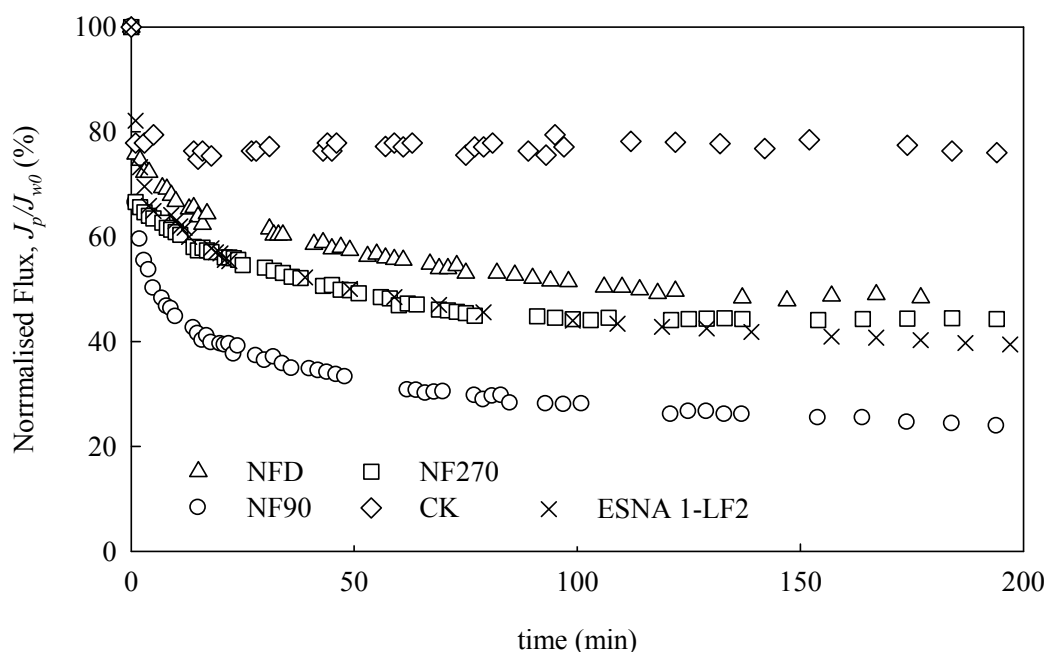


Figure 5.11. Nanofiltration of BPA-Fenton effluent. Normalised permeate flux as a function of time for the several membranes tested. Experimental filtration conditions: $TMP = 6$ bar, $v = 5.3$ cm/s, $pH_F \approx 3$, and $T_F = 30$ °C.

Figure 5.12 proved that, in the NF of BPA-Fenton effluent, membrane fouling plays a predominant role in the loss of flux. As it can be seen, after flushing the membranes with water, the normalised permeate fluxes were recovered at the best 14% of the maximum flux decay experienced by each membrane. Excluding NF270 membrane, the membrane fouling seemed to be related with the pore size, porosity and pK_a of the membrane. Based on pure water permeabilities and MWCO of the studied membranes, it could be expected that the pore size and porosity follow the same trend.

Depending on the ratio between the solute diameter and the pore diameter of the membrane, the different types of fouling can occur. If the pores are very small in

comparison to the solute diameter, the formation of a cake layer is favoured. If the pores are bigger than the solute diameter, complete and/or partial pore blocking can occur. In this study, the fouling increased with the membrane PWPs (pore size and porosity), see Table 3.3. However, which specific type of fouling was predominant could be difficult to distinguish, since it would require the detailed characterization of BPA-Fenton effluent.

The only fouling that could be confirmed was the formation of a cake layer, which was visually observed at the end of each experiment as a dark brown layer of organic materials firmly attached to the membrane. The used membranes in the filtration experiments of BPA-Fenton effluent were characterised with ESEM-EDS. The differences in the elemental composition due to the operation with respect to virgin membranes were analysed.

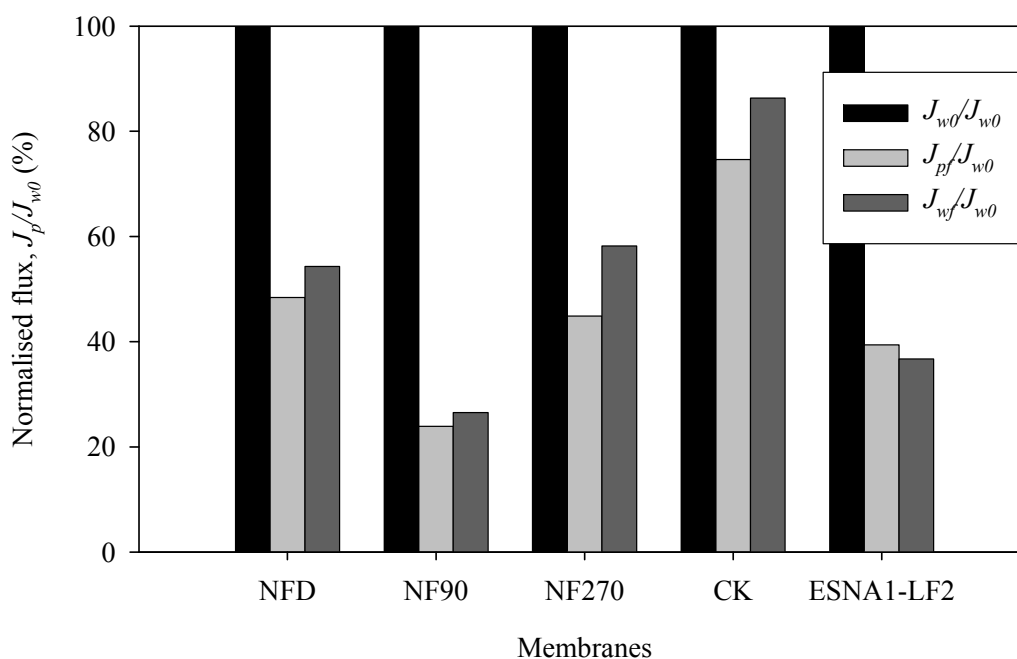


Figure 5.12. Nanofiltration of BPA-Fenton effluent. Normalised permeate flux before, at the end, and after filtration, for the several membranes tested. Experimental filtration conditions:

$TMP = 6$ bar, $v = 5.3$ cm/s, $pH_F \approx 3$, and $T_f = 30$ °C.

As Table 5.4 shows, the % wt. of C increased in 25.61, 3.05 and 5.66%, after the membrane use, for NF90, CK and ESNA1-LF2, respectively. Thus, as it could be expected, the fouling on the membrane surfaces was mainly organic, and no iron was detected in the elemental analysis performed by EDS. The changes in % wt. C for NFD and NF270 were considered to fall within the experimental error, whereby do not provide

information about the superficial fouling of these membranes. It is important to note the fact that EDS analysis was carried out just in three points and not in the whole membrane. Hence, the presence of iron or changes in % wt. of C could be different to those reported in Table 5.3, especially because the cake layer formed on these membranes was not homogeneous in the entire membrane surface.

Table 5.4. Elemental composition of virgin and used membrane for NF of BPA-Fenton effluent at 6 bar and 30 °C.

Membrane	Condition	C (% wt.)	N (% wt.)	O (% wt.)	S (% wt.)
NFD	Virgin	72.65 ± 1.28	n.d	17.48 ± 1.26	9.87 ± 1.84
	Used	69.70 ± 1.35	n.d	21.51 ± 1.16	8.79 ± 1.36
NF90	Virgin	43.89 ± 0.40	30.81 ± 1.23	18.98 ± 0.17	6.32 ± 0.42
	Used	69.50 ± 1.11	n.d	22.11 ± 1.35	8.38 ± 1.12
NF270	Virgin	70.68 ± 1.14	n.d	18.87 ± 1.22	10.45 ± 1.34
	Used	72.53 ± 1.16	n.d	18.37 ± 1.23	9.10 ± 1.21
CK	Virgin	43.78 ± 1.13	n.d	56.22 ± 1.10	n.d
	Used	46.83 ± 1.10	n.d	53.17 ± 1.03	n.d
ESNA1-LF2	Virgin	66.49 ± 0.53	n.d	22.87 ± 0.38	10.63 ± 0.07
	Used	72.13 ± 0.41	n.d	19.97 ± 0.59	7.88 ± 0.99

The sieving features of a NF membrane are important for the separation of uncharged molecules; however, in the case of charged species, both sieving features and electrostatic repulsion between the charged membrane and the solute may become important. The production of species positively charge during the Fenton oxidation at $pH_R \approx 3$ could facilitate their rejection by repulsion between the positively charged membrane and the solutes, which decreased the probability of fouling. Regarding Table 3.3 and Figure 5.12, one can observe that the fouling is less relevant for more positively charged membranes.

The normalised flux decays for NF of BPA-Fenton effluent were generally lower compared to those from NF of BPA. Although the fouling in almost all the membranes was higher than those experimented during the NF of BPA; excepting for the final normalised

flux of NF90 which was slightly higher. From Figure 5.12 and 4.2 it can be found that the final normalised permeate fluxes increased within 25,3; 28,0; 61,9 and 3,37% for NFD, NF270, CK and ESNA1-LF2, respectively.

In general, the rejection of COD, TOC, colour and Fe^{2+} in all NF of BPA-Fenton effluent were higher than 80%, Table 5.5. This behaviour can be related to the molecular size exclusion and the formation of a fouling layer. The membrane showing the best performance in term of rejections was CK membrane. Bernat (2010) tested three out of the commercial membranes used in this study: NF-D, NF90 and NF270. He proved that these membranes are adequate candidates for retaining dissolved Fe(II) from acidic synthetic solutions and Fenton treated phenol effluents. In good agreement with his study, in terms of iron rejection, NF90 and ESNA1-LF2 were the most attractive membranes for retaining the homogeneous catalyst used in Fenton treatment of BPA-containing effluents.

Considering the process as a whole, the starting solution containing 300 mg/L of BPA (757 mg/L of COD and 237 mg/L of TOC) was oxidised by Fenton and then NF with several polymeric membranes allowed obtaining permeates of <65 mg/L of COD and <27 mg/L of TOC without presence of BPA.

Table 5.5. Nanofiltration of BPA-Fenton effluent. Rejection of COD, TOC, colour and Fe^{2+} for the several membranes tested. Experimental filtration conditions: $TMP = 6$ bar, $v = 5.3$ cm/s, $\text{pH} \approx 3$, and $T_F = 30$ °C.

Membrane	R_{COD} (%)	R_{TOC} (%)	C_{colour} (%)	$R_{\text{Fe}^{2+}}$ (%)
NFD	88.3 ± 1.3	87.5 ± 0.8	93.2 ± 1.3	81.9 ± 1.9
NF90	84.0 ± 2.8	76.5 ± 0.5	97.7 ± 1.1	96.2 ± 0.3
NF270	97.7 ± 0.2	88.9 ± 0.1	95.5 ± 1.4	92.4 ± 0.2
CK	100.0 ± 2.0	91.9 ± 0.7	100.0 ± 2.7	91.10 ± 0.01
ESNA1-LF2	85.1 ± 2.1	82.2 ± 0.1	94.2 ± 0.7	97.7 ± 0.4

The flux decay behaviour at different pressures was also studied. Four transmembrane pressures (2, 4, 6 and 8 bar) were applied during the NF of BPA-Fenton effluent using NF270 membrane, Figure 5.13. The normalised flux falls more quietly when the TMP is

higher. This behaviour can be explained by the increase in particle deposition rate at greater TMPs to form an enhanced cake layer. The formation of a more densely packed cake layer can also contribute to the higher flux decline at high transmembrane pressure. If the increase in fouling is severe, the additional resistance can set off the expected increase in permeate flux due to the higher TMP applied, even the final flux can be smaller. If the high pressure additionally induces the consolidation of the particle cake layer because of the compressive forces, an increased hydraulic resistance due to the cake layer is generated and, hence, an even lower flux (Seidel and Elimelech 2002). Thus, in this study, low operating pressures showed lower membrane flux decline by decreasing the permeation drag through the membrane, and consequently the contact between fouling material and membrane.

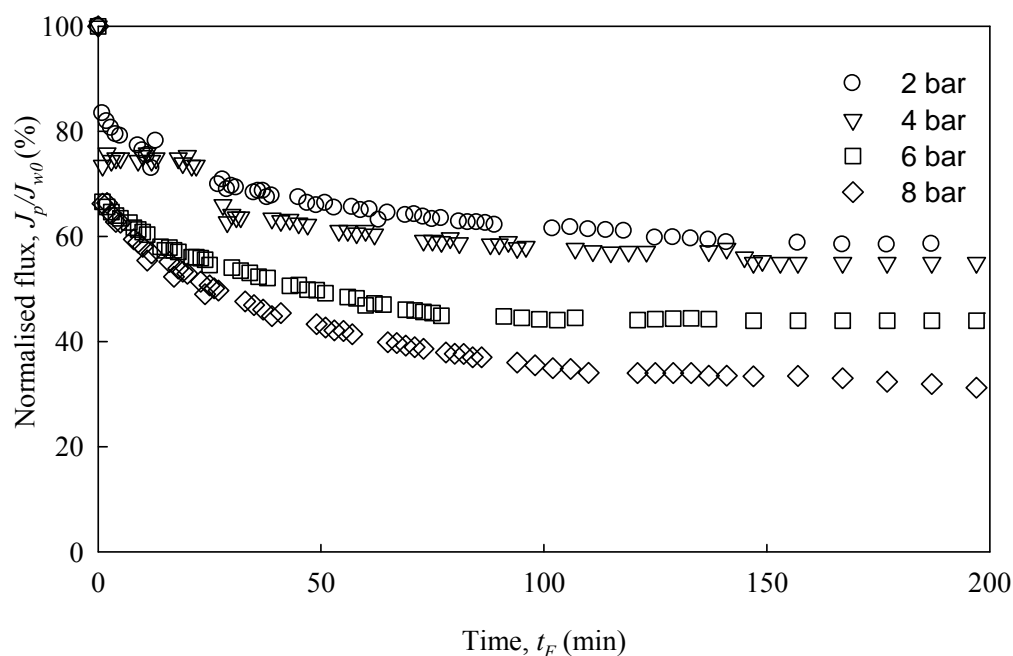


Figure 5.13. Nanofiltration of BPA-Fenton effluent. Normalised permeate flux as a function of time for several transmembrane pressures. Experimental filtration conditions: Membrane = NF270, $v = 5.3$ cm/s, $pH_F \approx 3$, and $T_F = 30$ °C.

5.5 Removal of tartrazine effluent after Fenton oxidation by nanofiltration membrane

The observed normalised flux decline as a function of time at constant TMP, which reflects fouling generation, is shown for the different tested membranes in Figure 5.14. This set of experiments uses the effluent after Fenton oxidation of tartrazine (TAR-Fenton effluent) as a feed solution. The Fenton conditions, in which this effluent was obtained, are: $[TAR]_0 =$

300 mg/L, $H_2O_2/TAR = 0.035$, $Fe^{2+}/H_2O_2 = 0.024$, $pH_0 = 3$, $T_R = 30\text{ }^\circ\text{C}$ and 300 rpm. The TAR-Fenton effluent contained 103 ± 26 mg/L of COD, 77 ± 6 mg/L of TOC, $pH\ 2.71 \pm 0.04$ and an absorbance of 0.0806 ± 0.0200 read at 427 nm. No significant permeate flux decline was observed for NFD, NF270, CK and ESNA1-LF2 membranes, whose permeate normalised fluxes at 200 min were higher than 80%. NF90 membrane showed to be the membrane that undergoes the largest drop in the normalised permeate flux, reaching 61%. ESNA1-LF2 did not reach steady permeate flux during the time filtration; it slowly decreased up to 82.5% at 200 min. No trend was clearly observed to correlate the differences in normalised flux decline and membrane properties such as isoelectric point, pore radio, MWCO, roughness and water contact angle. Excepting NF270 membrane, the flux loss appeared to decrease according to the pore size and porosity of the membrane, these latter governing the PWP of each membrane (see Table 3.3). In addition, the differences in normalised flux decline could be also related to the active layer material of the membrane and its interactions with occurring by-products after Fenton treatment. NFD and NF270 membranes showed almost the same flux decline having the same active layer. However, the presence of other organic species in the TAR-Fenton effluent did not cause a detrimental influence on the permeated flux evolution compared to that of TAR nanofiltration, Figures 4.6 and 5.14.

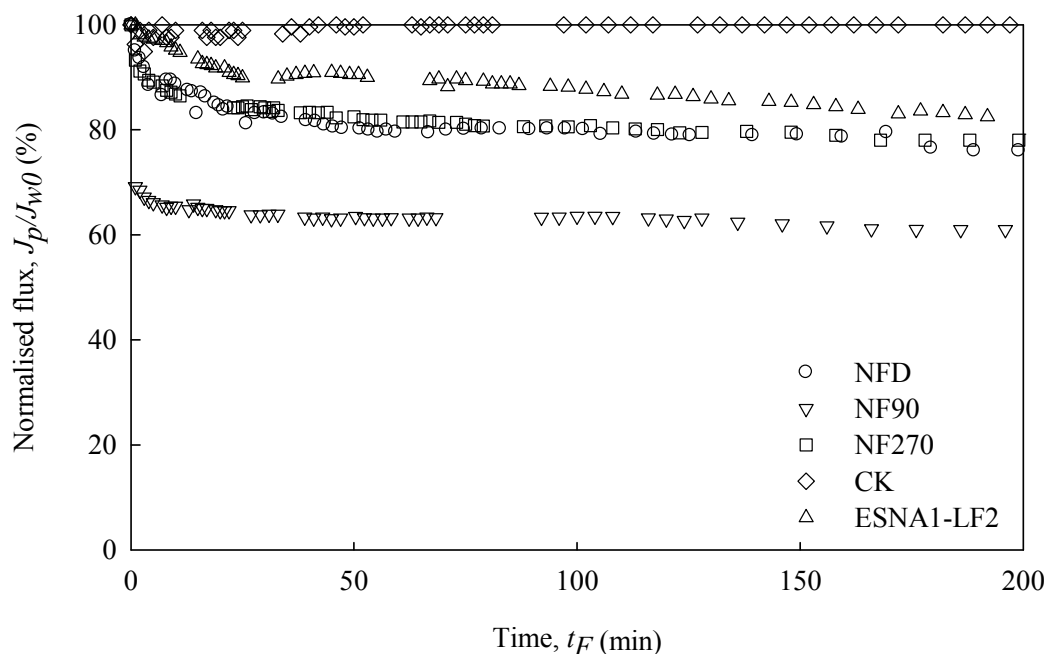


Figure 5.14. Nanofiltration of TAR-Fenton effluent. Normalised permeate flux as a function of time for the several membranes tested. Experimental filtration conditions: $TMP = 6$ bar, $v = 5.3$ cm/s, $pH_F \approx 3$, and $T_F = 30\text{ }^\circ\text{C}$.

In this case, both, CP and fouling were equally contributing to the loss of permeate flux. NF270 was the only membrane where the fouling seemed to have more relevance than CP. After the flushing of NF270 with water, the permeate flux was recovered in just 5.5%, remaining a 15.6% permanently lost (unless a chemical cleaning performed). These results are evidenced by Figure 5.15, where the normalised fluxes of virgin, after filtration, and after water flushing (indicator of the fouling) of the membranes are represented. The highest fouling was observed for NF90 membrane, which could be related to its high roughness. It can be assumed that the flux losses observed in this set of experiments are mainly due to the internal fouling of organic matter in the membrane, since there was not visual presence of colour or cake layer on the membranes after filtration. What is more, no changes were detected in the elemental analysis performed by EDS between virgin and used membranes for NF90, NF270 and CK, corroborating the absence of some cake layer deposition, see Table 5.6. The slightly increase of C for NFD and ESNA1-LF2 membranes, respectively; suggest the presence of a small fouling layer in these membranes.

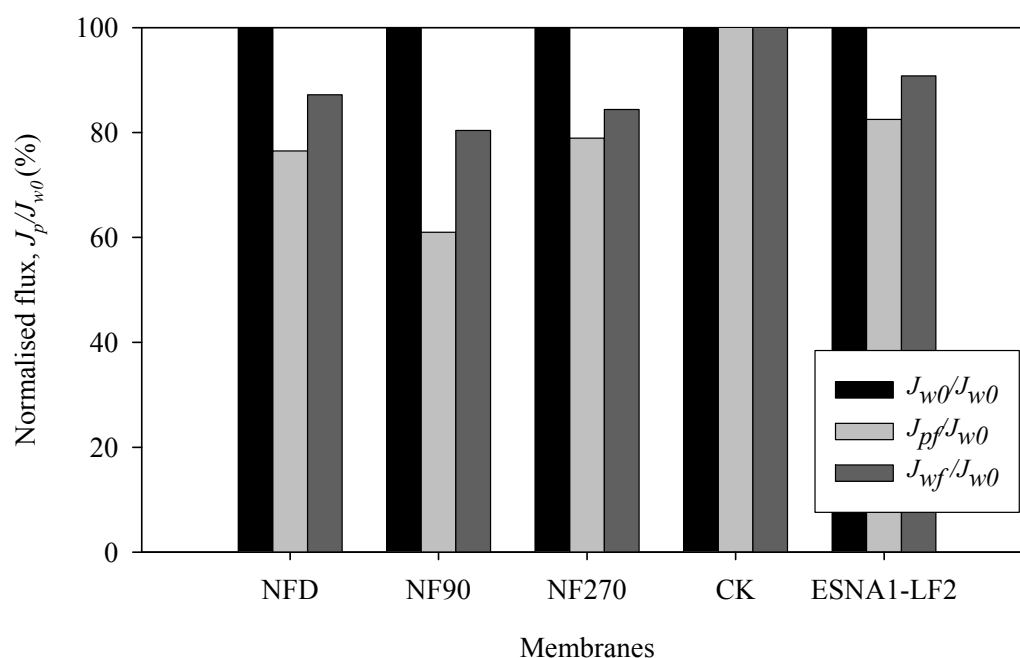


Figure 5.15. Nanofiltration of TAR-Fenton effluent. Normalised permeate flux before, at the end, and after water flushing for the several membranes tested. Experimental filtration conditions:

$TMP = 6$ bar, $v = 5,3$ cm/s, $pH_F \approx 3$, and $T_F = 30$ °C.

Table 5.6. Elemental composition of virgin and used membranes for NF of TAR-Fenton effluent at 6 bar and 30°C.

Membrane	Condition	C (% wt.)	N (% wt.)	O (% wt.)	S (% wt.)
NFD	Virgin	45.34 ± 1.56	29.58 ± 1.11	18.62 ± 1.06	6.47 ± 0.98
	Used	72.65 ± 1.28	n.d	17.48 ± 1.26	9.87 ± 1.84
NF90	Virgin	43.89 ± 1.02	30.81 ± 1.15	18.98 ± 1.56	6.32 ± 1.03
	Used	43.60 ± 1.05	32.33 ± 1.23	17.95 ± 1.26	6.12 ± 1.31
NF270	Virgin	70.68 ± 1.14	n.d	18.87 ± 1.22	10.45 ± 1.34
	Used	70.82 ± 1.26	n.d	19.72 ± 1.11	9.46 ± 1.56
CK	Virgin	43.78 ± 1.13	n.d	56.22 ± 1.10	n.d
	Used	45.40 ± 0.95	n.d	54.60 ± 0.76	n.d
ESNA1-LF2	Virgin	66.49 ± 0.53	n.d	22.87 ± 0.38	10.63 ± 0.07
	Used	72.45 ± 0.87	n.d	19.27 ± 0.56	8.23 ± 0.95

The performance of Fenton coupled with nanofiltration for removal of TAR was also evaluated as the capability of the different membranes to remove COD, TOC, colour, Fe²⁺ and SA (Table 5.7). As it can be seen, the highest COD and TOC rejections were found for NF90 membrane, whereas the highest colour, Fe²⁺ and SA rejections were obtained by ESNA1-LF2 membrane. The rejections varied with PWP of the membranes, so the rejection was greater when the porosity was larger. Membranes with low permeabilities, besides being less porous, may have pores with higher diameters allowing the easier pass of compounds and causing low rejections.

In the whole process, the starting solution containing 300 mg/L of TAR (280 mg/L of COD and 117 mg/L of TOC) was first oxidised by Fenton and then subjected to nanofiltration with several polymeric membranes obtaining permeates of <39 mg/L of COD and <28 mg/L of TOC without detectable TAR.

With an increase in pressure, flux is expected to accordingly increase. The increase in the feed pressure side improves the driving force, overcoming membrane resistance. This phenomenon where flux grows linearly with increasing pressure was experimentally

observed in this case. The permeate flux was as low as 23.1 L/h·m² at 2 bar, and it increased along with the operating pressure to finally reach 72.38 L/h·m² at 8 bar during the NF of TAR-Fenton effluent using NF270 membrane. For TAR-Fenton, unlike BPA-Fenton, the normalised flux increased from 81.1 to 95.2% at 200 min as TMP went from 2 to 8 bar. Hence, an increasing pressure probably only resulted here in some compaction of internal membrane fouling.

Table 5.7. Nanofiltration of TAR-Fenton effluent. Rejection of COD, TOC, colour and Fe²⁺ for the several membranes tested. Experimental filtration conditions: *TMP* = 6 bar, *v* = 5.3 cm/s, pH ≈ 3, and *T_f* = 30 °C.

Membrane	R _{COD} (%)	R _{TOC} (%)	C _{colour} (%)	R _{Fe²⁺} (%)	R _{SA} (%)
NFD	75.8 ± 1.7	64.6 ± 0.1	32.2 ± 1.9	77.6 ± 0.6	68.93 ± 0.03
NF90	81.9 ± 1.6	84.8 ± 0.1	65.3 ± 1.8	90.0 ± 0.9	88.8 ± 0.9
NF270	83.3 ± 1.9	69.3 ± 0.5	36.5 ± 1.4	90.4 ± 0.9	87.4 ± 0.7
CK	50.8 ± 1.5	60.7 ± 0.8	40.4 ± 1.8	81.2 ± 0.5	77.1 ± 0.3
ESNA1-LF2	79.1 ± 1.9	77.7 ± 0.1	87.2 ± 1.4	96.91 ± 0.02	96.9 ± 0.5

5.7 Conclusions

The degradation of BPA and TAR in an aqueous stream by Fenton process under various operating conditions was investigated. The experimental results indicate that both BPA and TAR could be efficiently degraded in solution by Fenton treatment. The removal of BPA, TAR, TOC and COD was hindered by excess H₂O₂, which acts as scavenger of the hydroxyl radicals usable in the process.

BPA proved to be a more reactive compound than TAR against the Fenton reagent, achieving higher levels of mineralization in softer conditions. Coupling Fenton process and NF to deal with Fenton treated effluents allows almost total BPA and TAR abatement. The NF of BPA-Fenton effluent achieved high COD, TOC, colour and Fe²⁺ rejections; however the initial high fluxes rapidly drop because severe fouling occurred. This makes necessary

the study of some way to control cake layer formation and internal fouling, and draw a cleaning protocol before future use.

Meanwhile, in NF of TAR-Fenton effluent, the observed flux decline was less significant ($J_p/J_{w0} > 80\%$). Furthermore, the high rejections observed corroborate the idea that this coupling system could give a good contribution for not only the overall elimination of TAR, but also for BPA.

Chapter 6

Ozonation coupled with nanofiltration for elimination of BPA and tartrazine

6.1 Introduction

A number of methodologies based on physical and chemical treatment processes are currently applied to the removal of EDCs and dyes (Liu et al 2009b, Forgacs et al. 2004). Advanced oxidation processes (AOPs) have been regarded as a new technology for the decomposition of several organic compounds including BPA and dyes. These processes include ozonolysis (Al-kdasi et al 2004, Umar et al. 2013), Fenton oxidation (Su et al. 2011, Young et la. 2013), photocatalysis (Reutergårdh and Iangphasuk 1997, Lu et al. 2013) and wet air oxidation methods (Zhou and He 2007, Erjavec et al. 2013). Ozonation process is a faster and cheaper process than photocatalysis or wet air oxidation and moreover no extra chemicals are required as Fenton process does. When considering the overall factors, ozonation has sometimes shown to be superior among the AOPs.

Ozonation has a particular interest in the removal of colour, since it specifically attacks the conjugated chains that impart colour to a dye molecule (Sarayu et al. 2007). Although, ozone has been demonstrated to have the ability to destroy dyestuffs, even high doses of ozone do not completely convert the organic matter to carbon dioxide and water (Sancar and Balci 2013, Soares et al. 2006, Muthukumar et al. 2004). In general, despite the fact that ozone is a very strong oxidant, complete mineralization by ozonation is usually not achievable (Ruppert et al. 1994, Jansen 2005), so the removal of the products following ozonation is required. Therefore, systematic investigation of combining ozonation with other treatment methods is quite necessary.

One process that appears to complement the needs for the treatment of ozonation products, because it could potentially reduce waste volume for further oxidation while simultaneously reduce the organic matter in its effluent stream (permeate), is membrane filtration. The use of a membrane process in combination with a chemical or biological treatment process is attractive for wastewater treatment (Sanchez and Tsotsis 2002). It answers the demand for more efficient, compact and modular treatment units suitable for densely populated areas where both the land cost and social sensitivity are exigent. The most important disadvantage of membrane filtration is the loss of permeate flux due to membrane fouling. A number of ways have been described for controlling fouling and

concentration polarisation. Among them, the pre-treatment of the feed filtration solution is where precisely the ozonation can be applied.

The ozonation as a pre-treatment, besides participating in the degradation of organic matter, can enhance the permeate flux by reducing the membrane fouling through the reduction of the organic load driven to the membrane process. Thus, the aim of this chapter is to study the factors affecting the rate of BPA degradation and tartrazine (TAR) solutions by ozone, and its effect on flux and retention over NF polymeric membranes in a combined treatment.

6.2 Ozonation

Ozone as a gas was discovered in 1839 by the Swiss chemist Schönbein. The gas was named “ozone” which is derived from the word “ozo”, Greek for smell (Jasen 2005). Later it was found that the molecule is an allotrope of oxygen, build from three oxygen atoms (O_3). Since its discovery, this oxidant has been often used for water purification, due to its strong bactericide activity. In the early period, a widespread application of ozone was only seen in a few countries in Europe, namely France, Germany and Switzerland, in water treatment for disinfection, and colour and odour removal. Nowadays, ozonation is introduced in more and more water treatment plants as a replacement of primary chlorination in order to control the formation of chlorination by-products, and it is widespreading to many countries.

Because ozone is a strong oxidant, it can be used for both water and wastewater treatment. Ozone use can be generalized into two applications: a deep disinfection and a strong oxidation to remove colour and odour. Ozone is used for the treatment of water polluted with pesticides or other anthropogenic substances. It can react with most species containing multiple bonds ($C=C$, $C=N$, $N=N$, etc.), but not with singly bonded functionalities such as $C-C$, $C-O$, $O-H$ at high rates. Therefore, although the thermodynamics for ozone-induced oxidation may be favourable (due to ozone high oxidation potential), kinetic factors will mostly dictate if ozone could oxidize a pollutant in a reasonable time frame. Albeit ozone has many advantages, it can be hazardous because the third unstable atom has a strong tendency to break away and attach itself to other

substances. Therefore, most ozone treatments usually require ozone trappers or ozone destroying systems to eliminate the residual ozone in the exhaust gas before being emitted to the atmosphere.

Ozone is thermodynamically unstable and its decomposition to oxygen is exothermic. Therefore, it is mostly found as a mixture of oxygen and ozone. It is moderately soluble in water. The solubility of ozone in pure water at 1 atm and 273 K is 1.1 g/L, which means that it is more soluble than oxygen in water. Under standard conditions, ozone is a gaseous compound with a pale blue colour. Ozone systems are typically comprised of four basic parts: ozone generator, feed gas preparation system, contactor, and off-gas disposer. After its generation from oxygen, the ozone gas is fed into the reaction medium or water. A number of devices can be used to transfer the generated ozone into water such as counter current bubble column, packed and plate columns, static mixers, jet reactors and agitated vessels (Gogate and Pandit 2004). Ozone transfer efficiency should be maximized by increasing the interfacial area of contact (reducing the bubble size by using small size ozone diffusers such as porous disks, porous glass diffusers (Ledakowicz et al. 2001), ceramic membranes (Janknecht et al. 2001) and increasing the contact time between the gas and the effluent (increase the depth in the contactor).

Basic chemistry studies (Glaze et al. 1987) have shown that ozone spontaneously decomposes during water treatment by a complex mechanism involving the generation of hydroxyl free radicals. Ozone reacts with organic compounds through a direct pathway by molecular ozone and a radical pathway by means of hydroxyl radicals. The direct oxidation with aqueous ozone is relatively slow (compared to hydroxyl free radical oxidation) but this is partially balanced by the relatively high concentration of aqueous ozone. On the contrary, the hydroxyl radical reaction is faster, but the concentration of hydroxyl radicals under normal ozonation conditions is relatively small.

The stability of ozone in water strongly depends on the water environment. Especially, the pH of the water is important because the hydroxide ions initiate the ozone decomposition, which takes place in chain reactions including initiation (eqs. 6.1 and 6.2), propagation (eqs. 6.3–6.7) and termination steps as given in Table 6.1. Termination step involves any recombination with $\bullet\text{OH}$, $\text{HO}_2\bullet$ and O_2 . Under acidic conditions and in presence of radical scavengers that inhibit the chain reactions and accelerates the decomposition of O_3 , the

direct ozonation pathway dominates. However, under basic conditions or in presence of solutes that promote the radical-type chain reaction and accelerates the transformation of ozone into •OH radicals, the hydroxyl radical reactions dominate. The ozone molecule selectively reacts with compounds containing C=C bonds, certain functional groups (e.g., OH, CH₃, OCH₃) and anions (those from N, P, O, S) (Alvares et al. 2001). Nevertheless, oxidation by •OH is non-selective. Due to the presence of several types of radical scavengers in wastewater, e.g. carbonate and bicarbonate, oxidation by molecular ozone is the dominant mechanism particularly at lower ozone dosages.

Table 6.1 Ozone reactions and their rate constants.

Reaction equation		Rate constant (M ⁻¹ s ⁻¹)
$O_3 + OH^- \rightarrow HO_2^- + O_2 \bullet^-$	(eq. 6.1)	70
$HO_2^- + O_3 \rightarrow HO_2 \bullet + O_3 \bullet^-$	(eq. 6.2)	$2.2 \cdot 10^6$
$O_3 + O_2 \bullet^- \rightarrow O_3 \bullet^- + O_2$	(eq. 6.3)	$1.6 \cdot 10^9$
$O_3 \bullet^- + H^+ \rightarrow HO_3 \bullet$	(eq. 6.4)	$5.0 \cdot 10^{10}$
$HO_3 \bullet \rightarrow \bullet OH + O_2$	(eq. 6.5)	$1.4 \cdot 10^5$
$O_3 + \bullet OH \rightarrow HO_4 \bullet$	(eq. 6.6)	$2.0 \cdot 10^9$
$HO_4 \bullet \rightarrow HO_2 \bullet + O_2$	(eq. 6.7)	$2.8 \cdot 10^4$

Typically, ozonation rarely produces complete mineralization to CO₂ and H₂O, but leads to partial oxidation products such as organic acids, aldehydes and ketones where oxygen is introduced into carbonaceous sites within the product molecules (Gerald 1994). It has been reported that the rate-limiting step in the ozonation of wastewater is the mass transfer of ozone from the gas phase to the wastewater (Kabdash et al. 2002). Other AOPs are applied when simple ozonation is not sufficient. In some cases, resulting intermediate products after ozonation may be as toxic as or even more toxic than the initial compounds. The generation of extra •OH could complete the oxidation by supplementing the reaction with it. AOPs in which •OH radicals are generated, are usually a combination of two or three of the following methods: ozone, H₂O₂ and UV radiation. Also the application of ozone in a high pH environment can be considered as AOPs by the generation of •OH.

By properly combining ozone, H_2O_2 and UV radiation, different AOP approaches have been developed thus allowing making the choice of the most appropriate for each specific problems. The O_3/UV process is more effective when the compounds of interest can be degraded through the absorption of the UV irradiation as well as through the reaction with hydroxyl radicals (Metcalf and Eddy 2003). The O_3/UV process makes use of UV photons to activate ozone molecules, thereby facilitating the formation of hydroxyl radicals (Shu and Huang 1995). While under H_2O_2/UV irradiation, H_2O_2 are photolyzed to form two hydroxyl radicals that subsequently react with organic contaminants (Al-Kdasi et al 2004). The addition of both H_2O_2 and O_3 to wastewater accelerates the decomposition of ozone and enhances the production of hydroxyl radicals.

Ozone finds its niche in any of the stages of a WWTP. During the preliminary step, ozone is used for detoxification, whilst at secondary stage it is used for sludge reduction, or during the tertiary stage ozone is more common and used for disinfection, micropollutant removal, COD reduction and decolouration. The location of ozone is dependant on the goal pursuit. In each of these cases, the use of ozone has been found to be very productive in decolourisation, deodorization, detoxification, disinfection, COD/BOD reduction, and sludge reduction. General applications of ozone in WWT are found in the oxidation of organic wastes, cyanides, ground water petrochemicals, pulp and paper effluents, textile mill effluents, textile dye and starch residues in the elimination of fate, oil and grease (FOG), pesticides, herbicides and insecticides; in the reduction of BOD of domestic wastes; and also as a secondary treatment for municipal wastewater, and mining heavy metal precipitation (Chaturapruek 2003).

6.2.1 Operating conditions

The rate of decomposition of ozone is a complex function of temperature, pH, and concentration of organic solutes and inorganic constituents (Hoigné and Bader 1976). The accelerated ozone decomposition is undesirable because the residual ozone dissipates faster and therefore reduces its efficient use, requiring a corresponding increase in the ozone applied and its associated cost. Hence, the ability to maintain a high aqueous ozone concentration is critical.

The influence of the operation temperature can result from the two simultaneous effects: the increase of the reaction rate constant, and the indirect effect derived from the variation of ozone solubility with temperature. Due to an increase in the temperature, ozone solubility decreases, thereby reducing the amount of ozone available for the reaction, which may result in poorer degradation (Beltran et al. 1994). However, some researchers have reported an increase in the degradation rate along an increase in the temperature (Meijers et al 1995, Wu and Wang 2001). Additionally, the oxidation rate has been found to be relatively independent of temperature at typical water treatment plant operating temperatures, despite the reduction in solubility and stability at higher temperatures (Kinman 1975).

Usually high pH is recommended. Ozone decomposition occurs faster in higher pH aqueous solutions, forming various types of oxidants with differing reactivities (Langlais et al. 1991). Higher organic solute concentration causes more ozone consumption, which enhances mass transfer that causes a decrease in ozone concentration in liquid phase, thus the increase of organics removal. Also, more intermediates, which consume more ozone, are generated when the organic solute concentration is high. Increased ozone concentration also enhances mass transfer; however, it is usually associated with a substantial increase in the cost of ozone generation. Consequently, any additional demand in the degradation rate must carefully be checked against the increase in the costs before the selection of the operation conditions is made. It is worth to mention that the presence of radical scavengers such as HCO_3^- ions and humic substances impairs the extent of degradation. These compounds act as inhibitors of the radical chain propagation. This is a very important point to be considered as natural waters are expected to contain large amounts of these substances.

6.2.2 Advantages and disadvantages

Ozone has unique properties, which offer advantages in wastewater treatment including (Chaturapruek 2003):

- Ozone is more effective than chlorine in destroying viruses and bacteria as it has twice potential than chlorine. This assures bactericidal and virucidal action with shorter contact times and less sensibility towards pH and temperature than for chlorine.

- Ozone reactions are very rapid. The ozonation process needs a short contact time to reach the required effluent contaminant level.
- There are no harmful residuals that need to be removed after ozonation because it leaves beneficial residual oxygen as reaction product resulting in more dissolved oxygen (DO). The increase of DO can eliminate the need for reaeration and also raises the level of DO in the receiving stream.
- Ozone is generated onsite, and thus, there are fewer safety problems associated with shipping and handling.

The major limitation of the ozonation process is the relatively high cost of ozone generation process in addition to its very short half-life period. Thus, ozone needs to be generated always onsite. Additionally, ozonation has some other disadvantages:

- Low dosage may not effectively inactivate some viruses, spores, and cysts.
- Ozonation is a more complex technology than chlorine or UV disinfection, requiring complicated equipment and efficient contacting systems.
- Ozone is very reactive and corrosive, thus requiring corrosion-resistant material, e.g., stainless steel.
- Ozonation is not economical for wastewater with high levels of suspended solids (SS), biochemical oxygen demand (BOD), chemical oxygen demand (COD), or total organic carbon (TOC).
- Ozone is extremely irritating and possibly toxic, so off-gases from the contactor must be destroyed to prevent worker exposure.

6.2.3 Ozonation applied for elimination of model compound

6.2.3.1 Ozonation for elimination of BPA

Ozone has been demonstrated to be highly effective for degrading BPA in water and wastewater at both laboratory and full scale. However, most authors studied the loss of BPA and only a limited number of studies investigated the mineralization of BPA. Complete removal of BPA (initial concentration 5–50 mg/L) was reported during the ozonation of water at 1 mg O₃/L·min (Lee et al., 2003). They studied the effect of ozonation concentration (0.4-2 mg/min), ozonation time (7-70 min) and pH (2, 7 and 12) on the removal of BPA. Unexpectedly, apparent BPA degradation apparently was almost

independent of the pH. Increasing ozone dosage enhanced BPA degradation efficiency. The conversion of BPA decomposition was not dependent on the initial concentration.

Later, Choi et al. (2006) studied the above mentioned effects on BPA removal from river water. They performed ozonation of BPA at various influent ozone concentrations (1-10 mg/L), at different initial BPA concentrations ($10-8.4 \cdot 10^{-4}$ mg/L) and pH 8.2-8.5. Unlike the results reported by Lee et al. (2003), for low concentrations of BPA, the removal of BPA was higher in the earliest minutes of reaction with ozone, but no further improvement occurred thereafter and the removal remained constant indicating the need of high ozone demand and prolonged contact time to further improve the degradation. Xu et al. (2007) also analyzed the BPA degradation under conditions of different ozone dosage, BPA initial concentration, and ozone adding time. Their results showed that ozone dosage plays a dominant role during the process of BPA degradation while no change in the overall oxidation efficiency was found at various ozonation times (7-34 min). They recorded a decrease in BPA removal efficiency with increasing initial BPA concentration. Similar results were reported by Kim et al. (2008) where a decrease in the BPA removal efficiency was observed when the initial concentration of BPA was increased from 11 to 22.8 mg/L for a similar inlet concentration of 15 mg O₃/L. Xu et al. (2007) also studied the effect of the presence of organic carbon on the degradation of BPA in water, concluding that the consumption of ozone was greater in the presence of higher TOC due to the additional ozone demand exerted by the organic compounds.

Although a significant amount of information is available about the removal of BPA by ozonation, knowledge of the formation of the by-products during ozone treatment is relatively limited. A mechanistic study of BPA ozonation has been undertaken by Deborde et al. (2008). They identified oxidation products of BPA ozonation by LC coupled with a UV diode array detector and a mass spectrometer. The formation of each degradation compound was rationalized by taking into account the knowledge concerning ozone reactivity and the structure of BPA. Due to the phenolic ring in BPA, the mechanisms and by-products similar to the reaction of ozone with phenol were expected.

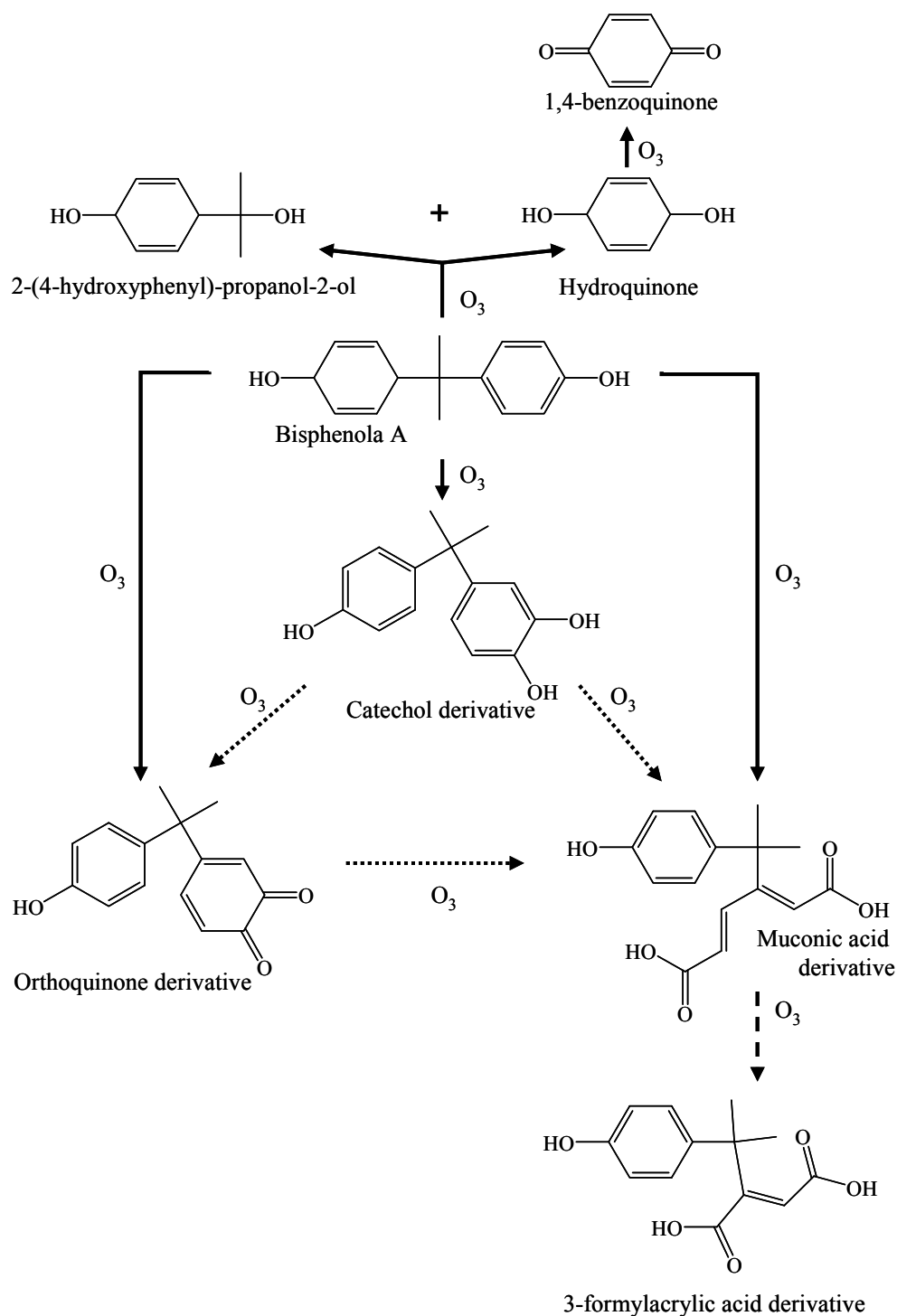


Figure 6.1 Proposed reaction pathways for the formation of products in the ozonation of BPA (adapted from Deborde et al. 2008).

The authors identified five major transformation products, namely muconic acid derivatives of BPA, benzoquinone, 2-(4-hydroxyphenyl)-propan-2-ol, orthoquinone, and catechol, in addition to several other minor transformation products. They proposed the reaction pathways depicted in Figure 6.1 to explain major transformation products with MW lower or similar to BPA. The identification of reaction intermediates during ozonation

of BPA in deionized water at pH 6 showed catechol as one of the major intermediate products. In addition, Garoma et al. (2010) identified acetone, resorcinol, formaldehyde, and the organic acids, acetic, formic, maleic and oxalic acid as additional reaction intermediates during the ozonation (influent ozone concentration, 10 mg/L) of BPA at an initial concentration of 11.6 mg/L.

6.2.3.2 Ozonation for elimination of tartrazine

There is a significant lack of information on the ozonation of tartrazine. However, AOPs provide up-to-date methods for decolorizing dye effluent and reducing the proportion of recalcitrant wastewater in industry that uses dyes. Among the various AOPs, the treatment with ozone has been particularly successful (Wu and Ng 2008). Ozone is very effective for decolourising dye wastewater because it attacks conjugated double bonds and these are often associated with colour (Sarasa et al 1998). Thus, many researchers investigated the use of ozonation to discolour dye effluents.

Results presented by some researchers revealed that ozone decolorize all dyes, except non-soluble disperse and vat dyes, which react slowly and take longer time (Marmagne and Coste, 1996; Al-kdasi et al. 2004). High colour removal could be achieved on wastewater containing high initial dye concentration. Alkaline pH and high temperature have been also found as favourable conditions for high TOC and COD removals. In spite of having high colour removal efficiency, limited COD and TOC removal efficiencies have been reported at soft conditions in the literature (Al-kdasi et al. 2004).

Sarayu et al. (2007) investigated the degradation of eight commercial reactive azo dyes with different structures containing different substituted groups in a semi-batch reactor by ozonation, both individually and in mixture. Their results demonstrated that ozonation proved to be a viable technique for the treatment of highly recalcitrant azo dyes in wastewater. A pH of 10 was effective for colour and COD removal of these dyes. Reactive Yellow 145 (RY145) azo dyes and synthetic textile dye-bath effluents were treated by Gül and Özcan-Yildirim (2009) with O₃ and H₂O₂/UV processes. It was found that the fastest colour and the highest TOC removal were obtained by ozonation at pH 11. Factors affecting the rate of COD of a synthetic waste solution containing water soluble direct dyes (Sirius Red F3B and Sirius Blue SBRR) by ozone gas were studied by Turhan and Turgut

(2009b). They used a batch bubble column. Recently, Sancar and Balci (2013) used the ozonation process to decolorize a wastewater containing nine commercial reactive dyes containing different chromophore groups. The colour removal efficiency showed differences according to the chromophore group of the reactive dye and dye amount in the effluent. With increasing dye amount in the effluent, the removal of colour became harder.

6.2.4 Ozonation process assisted by nanofiltration

Although ozonation and membrane processes are extensively studied in literature, only a few researchers have investigated the process where ozonation and membrane processes are somehow combined. Investigations of ozonation combined with membrane process are divided in three main uses: 1) ozonation as a pre-treatment to reduce membrane fouling, and to prolong the life-expectancy of the membrane as well as to enhance the water quality; 2) the application of a membrane filtration system before the ozonation process in order to remove organic compounds and ions which could act as inhibitors in the oxidation, reducing the overall removal; and 3) as an ozone membrane reactor where membranes are used for ozone distribution, as a reaction contactor and for product separation.

Park (2002) conducted experimental studies of ozonation and Fenton's oxidation before MF membrane process. They treated raw chemical wastewater obtained from a large dyeing and finishing plant in the Gyungkido-South Korea area. They obtained that their combination offered considerable advantages compared with each isolated treatment. The permeate flux rate increased as the input amount of ozone increased, however ozonation did not show a significant role to prevent membrane fouling. Chang et al (2009b) proposed a process where digital textile printing wastewater was ozone oxidized first, and then was filtrated by UF and RO consecutively. The proposed process showed that could be satisfactorily used. The fouling calculated after ozonation was lower than that without ozonation, thus pre-ozonation was beneficial to enhance flux and to obtain good permeate quality. Reduction of the total fouling rate of 70% was achieved by Stüber et al. (2013) when applied ozonation as a pre-treatment step in the MF of secondary effluent of Ruhleben-Germany WWTP, confirming the high potential of combining those processes. The positive impact of ozonation on the membrane process performance is usually attributed to the reduction, transformation, and change of organic matter characteristics of

the filtering solution due to ozonation, which results in an improvement in the membrane fouling. The membrane performance has also been highly correlated with the residual aqueous O_3 concentration in the permeate. A higher membrane flux is obtained if the aqueous O_3 concentration at the membrane surface increases (Schlichter et al. 2004, Karnik et al. 2005).

Because the literature on membrane fouling is generally focused on MF and UF, and O_3 resistant membrane materials are usually available for those membrane processes, there are few studies reporting O_3 oxidation combined with NF or reverse osmosis. Van Geluwe et al. (2010) investigated if membrane fouling can be reduced by decomposition of humic acids in the concentrate stream by means of O_3 oxidation using a NF membrane process. Like UF and MF membrane processes, the membrane permeability of the ozonated solution across NF membranes was higher than the permeability of the untreated solution.

Membrane processes, used as pre-treatment method in the removal of atrazine from surface water by ozonation process, were applied by Luis et al. (2011). Membrane process was aimed to remove organic compounds and ions prior to the oxidation. They could state that the coupling of a membrane filtration with a subsequent ozone treatment can be beneficial for an enhanced removal of atrazine from surface waters, since the removal of carbonate/bicarbonate ions present in the surface water and inhibitors of the $\bullet OH$ radicals production by RO increased the atrazine elimination.

A novel membrane reactor was designed by Heng et al (2007) for the ozonolysis of refractory organic pollutants in water. The reactor was equipped with a porous alumina membrane as ozone contactor and a ZSM-5 zeolite membrane for selective water pervaporation. The uniform, microscopic ozone bubbles produced by the membrane contactor ensured rapid ozone dissolution and transport, while the selective water removal by membrane pervaporation concentrated the organic pollutants in the reaction zone. A 30 times higher TOC reduction was observed when a porous alumina capillary membrane was used to produce a fine cascade of ozone bubbles instead of the traditional frit glass sparging in the ozonolysis of phthalate in water. The zeolite membrane pervaporation unit produced clean water with 99.7% of TOC rejection. Ho et al. (2012) designed an advanced ozone membrane reactor using a mathematical model to guide the optimization and scale-up the process for treatment of organic endocrine disrupting pollutants in water. The

membrane reactor increased mineralization rate of phthalate, improved ozone utilization, reduced membrane fouling and enhanced clean water production.

6.3 Ozonation of model compounds

6.3.1 Ozonation of BPA

Determination of the required ozone dose in the treatment of effluents is essential for the economical evaluation of the process. It is evident that the treatment cost directly relates with the applied ozone dose, which can be adjusted by two ways: influent ozone gas concentration and ozone-air flow rate. To evaluate the effect of this parameter, influent ozone gas concentration and ozone-air flow rate were investigated, and the results are compiled in Figure 6.2a,b.

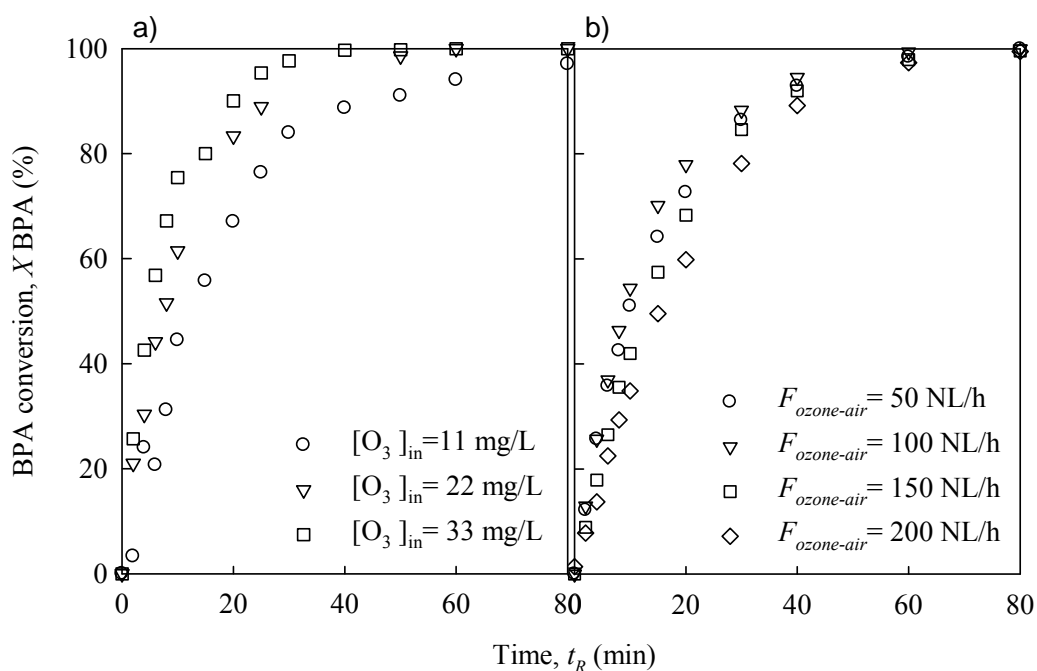


Figure 6.2. Ozonation of BPA. BPA conversion as a function of reaction time for a) several ozone influent concentrations at 100 NL/h of ozone-air flow rate; and for b) several ozone-air flow rates at 11 mg/L in ozone influent concentration. Conditions: $[BPA]_0 = 300$ mg/L, $pH_0 = 6$ and $T_R = 30^\circ C$.

The effect of the influent ozone gas concentration, $[O_3]_{in}$, on the removal of BPA from aqueous solution was investigated using influent ozone gas concentrations of 11, 22, and 33 mg/L. Other operation parameters, including initial BPA concentration, pH_0 ,

temperature, and ozone-air flow rate were kept constant at 300 mg/L, 6, 30 °C and 100 NL/h, respectively. The experimental results are presented in Figure 6.2a. These results revealed that, as the influent ozone gas concentration increased, the removal rate of BPA also increased. Complete BPA removal was achieved at 40, 60 and 80 min for experiments conducted with influent ozone gas concentrations of 11, 22, and 33 mg/L, respectively. These results were consistent with the theory of mass transfer. According to this theory, as the ozone concentration increases in the air bubbles (carrier of ozone), the driving force for ozone transport into the aqueous solution grows, also resulting in an increase of the oxidation rate. It must be noted that the gas-phase resistance to mass transfer is assumed to be negligible since ozone is only slightly soluble in water and the amount of ozone reacted with organics is limited by the dissolved ozone in the liquid reaction environment.

The effect of ozone-air flow rate, $F_{\text{ozone-air}}$, on BPA removal was also investigated using 300 mg/L of BPA initial concentration at pH_0 6 and 30 °C. The ozone-air flow rate affects fluid dynamic conditions of the reaction medium. The increase of the ozone-air flow rate results in the increase of the gas holdup and the turbulence of the system. Hence, the gas-liquid mass-transfer limitation lowers along an increasing gas volumetric flow rate. Therefore, in the improved volumetric mass transfer coefficient, and thus ozone mass transfer, correspondingly allows increasing the O_3 concentration in the liquid phase. On the other hand, it was experimentally observed during the performance of the ozonator that the ozone capacity (grams of O_3 produced per liter of air fed) increased in the inlet reactor gas as a result of the increase of air flow rate to the ozonator, while the ozone concentration decreased. An increase in the ozone production capacity favours an increase of removal efficiency. Although both of these factors suggest the continuous increase of the BPA removal as a function of ozone-air flow rate, the BPA removal efficiency actually showed to peak at 100 NL/h in the range studied (Figure 6.2b) and then slowly decline beyond this value. This behaviour could be related with the efficient use of the ozone; note that with a higher ozone-air flow rate is also associated to a lower residence time of the ozone in the reactor, which can offset the improved ozone transport conditions.

The effect of pH on the reaction between ozone and substrate is well known. As it was above mentioned (section 6.2.1), the reaction of organics with ozone is directed in two ways by pH. One of them is direct attack or electrophilic attack (at acidic pH) and the other

mainly goes through free radical attack (at basic pH). Figure 6.3a presents the effect of pH on the removal of BPA during ozonation. Initial BPA concentration, inlet ozone gas concentration, ozone-air flow rate and reaction temperature were maintained constant at 300 mg/L, 11 mg/L, 100 NL/h and 30 °C, respectively.

BPA conversion improved as the pH_0 increased from 3 to 12. As stated, at basic pH, $\bullet\text{OH}$ radical attack predominates and these radicals are much more reactive than molecular ozone in aqueous phase. However, during the ozonation, an extreme foaming occurred in the experiments carried out at higher pH_0 (9 and 12), making difficult the sampling. This can be a serious drawback for its large scale application.

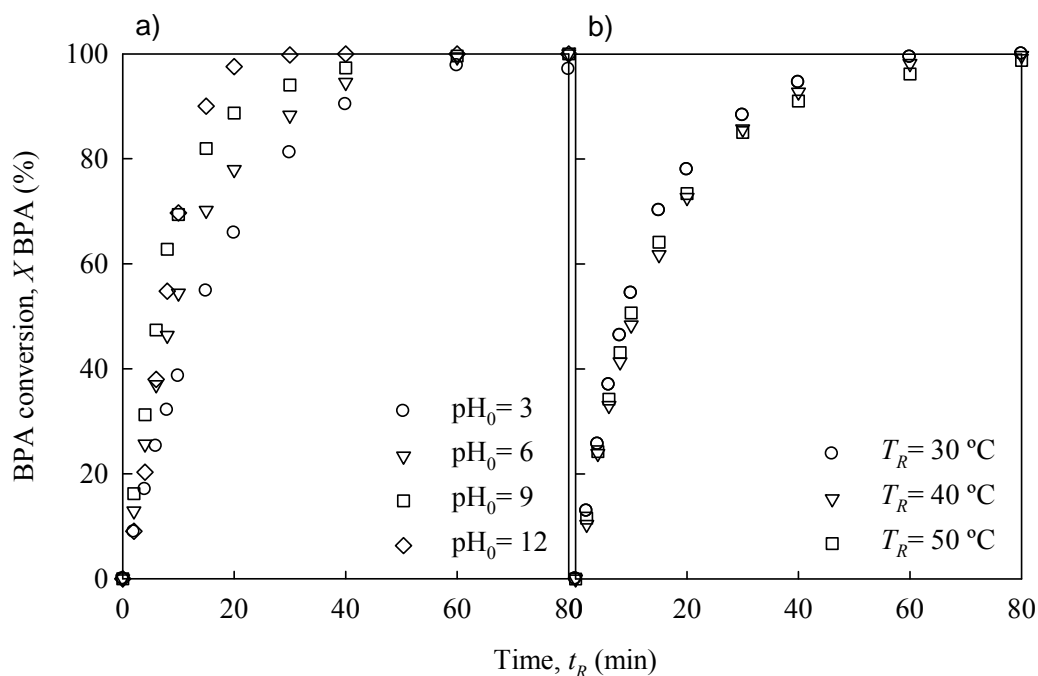


Figure 6.3. Ozonation of BPA. BPA conversion as a function of reaction time for a) several pH_0 at 30 °C, and for b) several reaction temperatures at pH_0 6. Conditions: $[\text{BPA}]_0 = 300$ mg/L, $[\text{O}_3]_{\text{in}} = 11$ mg/L, $F_{\text{ozone-air}} = 100$ NL/h.

The effect of reaction temperature on the BPA ozonation was investigated between 30 and 50 °C (Figure 6.3b). These assays used 300 mg/L of BPA initial concentration, 11 mg/L of inlet ozone gas concentration, 100 NL/h of ozone-air flow rate, at pH_0 6. The reaction temperature may influence ozonation processes in two aspects. First, the Henry's law coefficient for the ozone increases at higher temperature (25–65 °C), so a progressive decreased solubility is expected at high temperature, which can seriously affect the degradation efficiency (Phattaranawik et al. 2005). Second, a higher temperature may

enhance both the instability of the ozone itself, as well as the activation of the reactive species leading to an enhancement of the degradation rate (Zhao et al., 2009). However, no clear effect over the BPA removal as a function of the temperature is seen in Figure 6.3b within the studied range. Thus, it could not be discriminated which of these effects was the dominant in the present conditions.

Figure 6.4 shows the effect of the initial BPA concentration on the BPA removal using 11 mg/L of inlet ozone gas concentration, 100 NL/h of ozone-air flow rate, at pH₀ 6 and 30 °C. As the initial concentration of BPA increased, BPA conversion evolution significantly slows down for this constant inlet ozone gas concentration. Obviously, this is because, as the BPA initial concentration increases, the molar ratio of ozone to BPA is lower, so the high BPA conversion is achieved later. Anyway, even at the lower ozone to BPA ratio, practically full conversion is reached at acceptable time reaction, around 10 min for 25 mg/L and near 60 min for 300 mg/L. In term of O₃/BPA stoichiometric molar ratio, the ozone was overfed. The addition of 19, 12, 6, 3 and 2 times the stoichiometric amount of O₃ (12 mol to completely mineralization of 1 mol of BPA) were fed in the assays with initial BPA concentrations of 25, 50, 100, 200 and 300 mg/L, respectively.

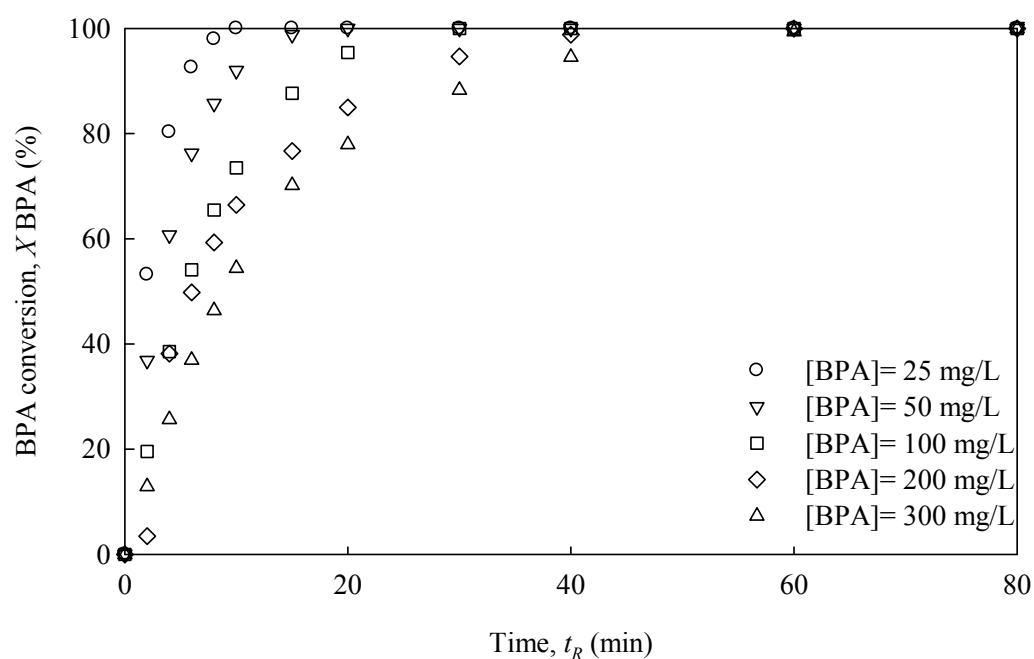


Figure 6.4. Ozonation of BPA. BPA conversion as a function of reaction time for several BPA initial concentrations. Conditions: $[O_3]_{in} = 11 \text{ mg/L}$, $F_{ozone-air} = 100 \text{ NL/h}$, $T_R = 30 \text{ }^\circ\text{C}$ and $\text{pH}_0 = 6$.

The deepness of the BPA oxidation is illustrated using TOC and COD changes during ozonation treatment. Table 6.2 presents X_f TOC as well as X_f COD at the end of ozonation for the different experimental conditions. After 80 min of ozonation, X_f TOC reduced a maximum of 34.9%, while initial BPA concentration was completely depleted at the end for all experimental conditions. This maximum value was obtained using 300 mg/L of BPA initial concentration, 11 mg/L of influent ozone gas concentration, 100 NL/h of ozone-air flow rate at pH_0 12 and 30 °C.

Table 6.2. Ozonation of BPA. Effect of BPA initial concentration, inlet ozone gas concentration ($[\text{O}_3]_{\text{in}}$), ozone-air flow rate ($F_{\text{ozone-air}}$), pH_0 and reaction temperature (T_R) on the COD and TOC conversions, and colour formation after 80 min of ozonation.

[BPA] (mg/L)	$[\text{O}_3]_{\text{in}}$ (mg/L)	$F_{\text{ozone-air}}$ (NL/h)	pH_0	T_R (°C)	X_f BPA ($\pm 1.8\%$)	X_f COD (%)	X_f TOC (%)	abs(400nm) ± 0.0002	pH_f ± 0.01	$X_f\text{O}_3$ (%)
25	11	100	6	30	100.0	88.3 \pm 0.8	30.2 \pm 0.2	0.0462	3.24	31.7 \pm 0.5
50	11	100	6	30	100.0	81.1 \pm 0.8	28.6 \pm 0.5	0.0583	3.23	38.4 \pm 0.1
100	11	100	6	30	100.0	71.2 \pm 1.6	29.3 \pm 0.6	0.0635	3.19	35.3 \pm 0.4
200	11	100	6	30	100.0	49.4 \pm 0.9	29.4 \pm 0.1	0.0809	3.19	35.1 \pm 0.2
300	11	100	6	30	100.0	36.9 \pm 1.2	14.1 \pm 0.7	0.1374	3.03	42.0 \pm 0.2
300	22	100	6	30	100.0	45.2 \pm 1.4	11.4 \pm 0.1	0.0880	2.96	51.1 \pm 0.2
300	33	100	6	30	100.0	40.9 \pm 1.5	33.1 \pm 0.1	0.0749	2.67	47.2 \pm 0.1
300	20	50	6	30	100.0	21.8 \pm 0.8	11.0 \pm 0.3	0.1404	2.95	35.9 \pm 0.1
300	8	150	6	30	99.6	30.3 \pm 1.4	9.4 \pm 0.7	0.1463	3.06	49.5 \pm 0.1
300	6	200	6	30	99.5	28.5 \pm 0.5	8.6 \pm 0.4	0.1492	3.10	52.1 \pm 0.2
300	11	100	3	30	97.2	26.2 \pm 1.1	9.3 \pm 0.5	0.1306	2.81	40.8 \pm 0.2
300	11	100	9	30	100.0	37.8 \pm 1.9	15.4 \pm 0.7	0.1643	3.01	69.6 \pm 0.1
300	11	100	12	30	100.0	55.2 \pm 1.1	34.9 \pm 0.7	0.1513	9.90	96.0 \pm 0.2
300	11	100	6	40	99.7	29.6 \pm 1.3	8.2 \pm 0.8	0.1216	2.90	37.5 \pm 0.1
300	11	100	6	50	98.8	38.7 \pm 1.7	10.5 \pm 0.6	0.1229	2.77	37.0 \pm 0.1

As it can be seen, the mineralization of BPA by ozonation was relatively low. The rate of TOC removal increased when greater inlet ozone gas concentration and pH_0 was applied, this relates with the enhanced availability of oxidant in the aqueous medium and the

derived generation of $\bullet\text{OH}$ radicals. This behaviour again demonstrates that the BPA is preferentially attacked by the oxidant species, so it is readily degraded. Meanwhile, as expected, COD removal was positively influenced by ozone-air flow rate and pH_0 , and negatively by BPA initial concentration. However, ozone possesses higher capacity to abate COD than TOC. This means that ozone is capable to easily oxidize BPA and the earlier intermediates but the later partially oxidized compounds are hardly mineralized into carbon dioxide and water. As aforementioned in section 6.2, ozone reacts weakly with singly bonded compound, which usually appear as later reaction intermediates, for instance, organic acids such as acetic, formic or oxalic acid.

BPA initial concentration and pH were the variables that more strongly impacted the X_{COD} . As previously stated, variations in pH bring changes in the reaction mechanism. In acidic conditions ($\text{pH}_0 = 3$), the COD conversion is just 26.2%, in turn, in basic medium ($\text{pH}_0 = 12$), the COD conversion is twofold. The fact that COD removal drops as a function of increasing BPA initial concentration is an indicator of the superior reactivity of BPA with ozone, so the ozone is consumed by BPA rather than used in the degradation of by-products.

During the ozonation of BPA, colour generation was observed. The reaction solution passed from uncoloured BPA solution to dark green liquor. The ozonated BPA solution showed a maximum in the absorbance spectrum at 400 nm of wavelength. Table 6.2 displays the absorbance (abs) at 400 nm at 80 min of ozonation for the different conditions studied. As it can be seen, the colour generation is strongly influenced by the pH_0 , reaching the maximum value at pH_0 9. Table 6.2 also reports the pH after ozonation treatment of BPA. The final pH of the reaction solution dropped around 3 units for the experiments conducted at initial pH of 6, and in 6 and 2 units for those made at pH_0 9 and 12, respectively. The pH of the reaction medium immediately dropped after starting the ozone addition. This is an indication of the formation of acidic groups during the ozonation process. These groups are split from BPA molecules as a result of the oxidation. As it was above mentioned (section 6.2.3.1), the oxidation of BPA leads to the formation of catechol and hydroquinone, these in turn to o- and p-benzoquinone. Further oxidation leads to the formation of aliphatic diacids as well as muconic acid which can reduce pH in the reaction solution.

The ozone consumption, X_jO_3 , demonstrates that ozone was added in excess and was not used efficiently. For most experimental conditions, only between one third and one half of the ozone added was consumed during the process. Ozone consumption showed to vary as a function of ozone-air flow rate and mainly of pH. Thus, a pH_0 of 12 yields an ozone consumption of 90.0%.

6.3.2 Ozonation of tartrazine

Figure 6.5a,b shows the effect of ozone dose on tartrazine (TAR) ozonation in terms of inlet ozone gas concentration and ozone-air flow rate. In particular, Figure 6.5a draws the experiments carried out at different influent ozone gas concentrations (11, 22 and 33 mg/L) at 300 mg/L of initial TAR concentration, pH_0 6, 30 °C and 100 NL/h of ozone-air flow rate. As expected, it can be noticed that an increase in the inlet ozone gas concentration speeded up the TAR oxidation. A higher inlet ozone gas concentration results in a greater aqueous ozone concentration, which either directly reacts with TAR or decomposes to produce $\bullet OH$ that in turn reacts with TAR. The time required to achieve 100% TAR removal decreased from 80 to 30 min if the inlet ozone gas concentration goes from 11 to 33 mg/L. Although larger values of TAR removal should be in principle presumed at higher ozone-air flow rate, Figure 6.5b showed a decreasing TAR conversion as ozone-air flow rate increases. Like in the BPA ozonation, this behaviour could be related with the efficient ozone use, which gets worsen because of the residence time drops when ozone-air flow rate is higher.

The effect of pH of the initial solution on removal efficiency of tartrazine by ozonation is shown in Figure 6.6a. These assays were done at 300 mg/L of initial TAR concentration, 11 mg/L of inlet ozone gas concentration, 100 NL/h of ozone-air flow rate and 30 °C. It can be seen that the maximum TAR removal, essentially complete conversion, could be achieved for pH_0 values of 3, 6, 9 and 12 at 80, 60, 40 and 15 min, respectively. In acidic pH, the ozone is available as molecular ozone while, in alkaline medium, it decomposes into secondary oxidants such as $\bullet OH$, $HO_2\bullet$, $HO_3\bullet$ and $HO_4\bullet$. Therefore, it could be assumed that the increase of TAR removal following the increase of pH owns to the self-decomposition of ozone to generate oxygen free radicals that can oxidize the organic compounds more efficiently. It can be noticed from Figure 6.6b that an increase in reaction temperature from 30 to 50 did not result in substantial change of the removal efficiency for

TAR. This suggests that the process is actually mass transfer controlled, although it can be also speculated that the two opposed influences of temperature, i.e., the positive effect of Arrhenius dependence on reaction rate and the negative drop of ozone solubility, balances one each other.

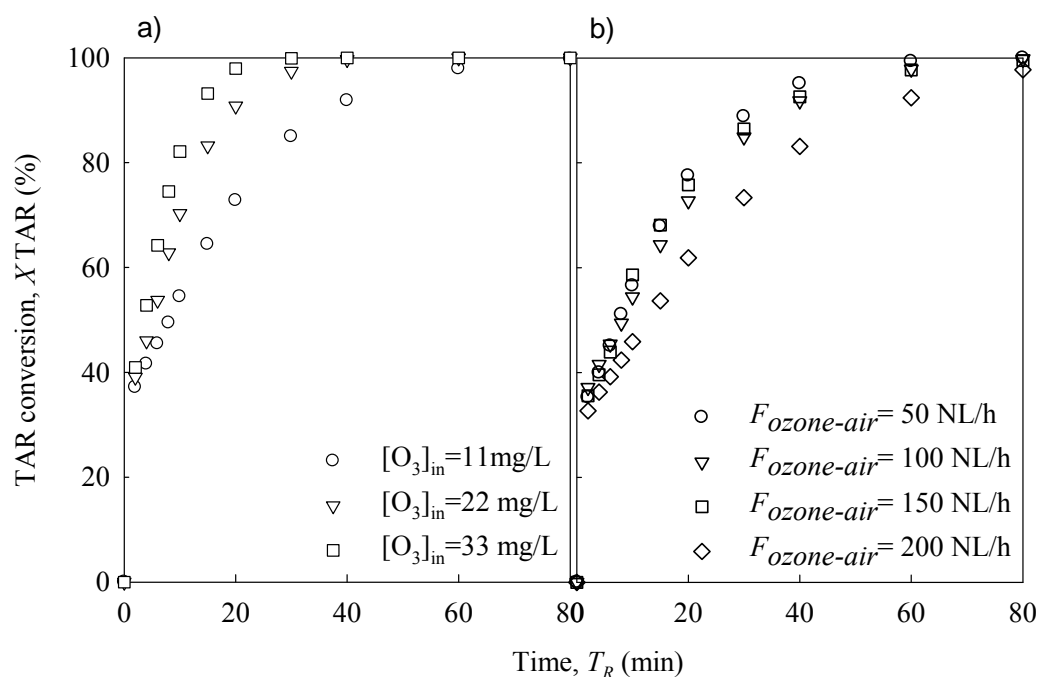


Figure 6.5. Ozonation of TAR. TAR conversion as a function of reaction time for a) several ozone inlet concentrations at 100 NL/h of ozone-air flow rate, and for b) several ozone-air flow rates. Conditions: $[TAR]_0 = 300$ mg/L, $pH_0 = 6$ and $T_R = 30^\circ C$.

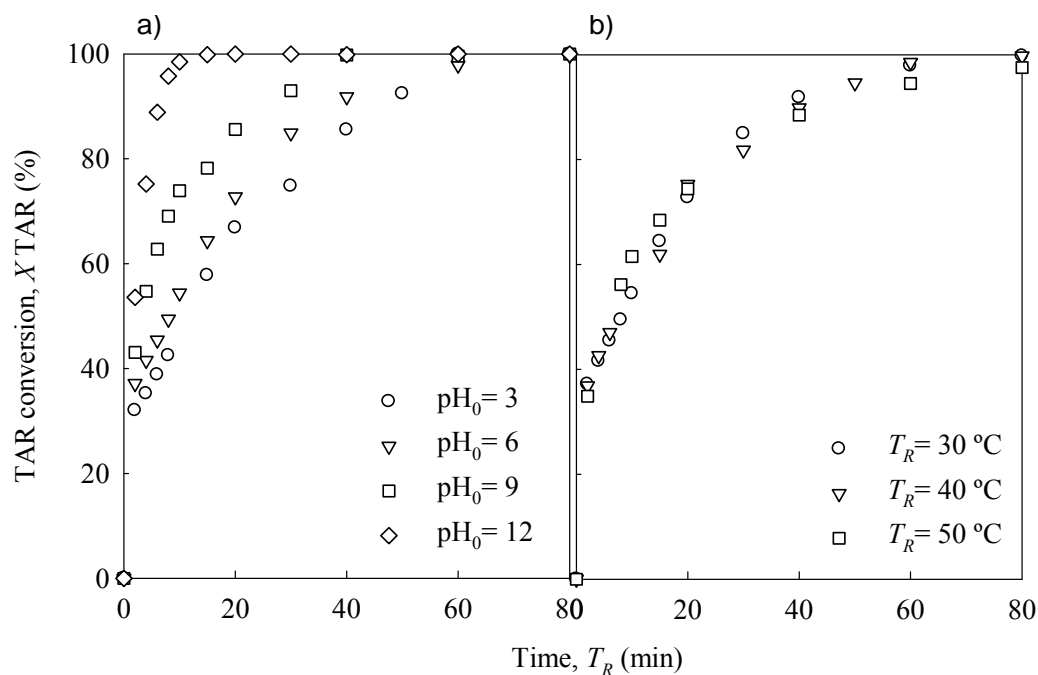


Figure 6.6. Ozonation of TAR. TAR conversion as a function of reaction time for a) several pH_0 at $30^\circ C$, and for b) several reaction temperatures at $pH_0 = 6$. Conditions: $[TAR]_0 = 300$ mg/L, $[O_3]_{in} = 11$ mg/L, $F_{ozone-air} = 100$ NL/h.

In order to inspect the effect of the initial dye concentration on the TAR removal, five different initial TAR concentrations (100, 300, 400, 800 and 1000 mg/L) were fed (Figure 6.7). The data evidence that dye degradation varied considerably with dye concentration. At the large dye concentration, the reaction rate is at such extent that the ozone is no longer present in excess, resulting in reduced conversion.

The effect of several parameters (inlet dye concentration, ozone dose fed, pH and temperature) in COD, TOC and colour removal of a TAR solution was also investigated and summarized in Table 6.3. A maximum COD and TOC removal of 92.0 and 68.0%, respectively, were obtained at 33 mg/L of inlet ozone gas concentration, 100 NL/h of ozone-air flow rate, pH₀ 6 and 30 °C for a TAR solution of 300 mg/L after 80 min of ozonation. Overall, higher values of X_{fCOD} and X_{fTOC} were observed for higher inlet ozone gas concentration and low values for high TAR initial concentrations. Of course, COD and TOC removal increased because the applied ozone dose per volume of dye solution was also greater. Meanwhile, the reduction of available ozone at high dye concentration favours the incomplete oxidation of the dye, limiting the oxidation of intermediate compounds and hence the reduction of COD and TOC.

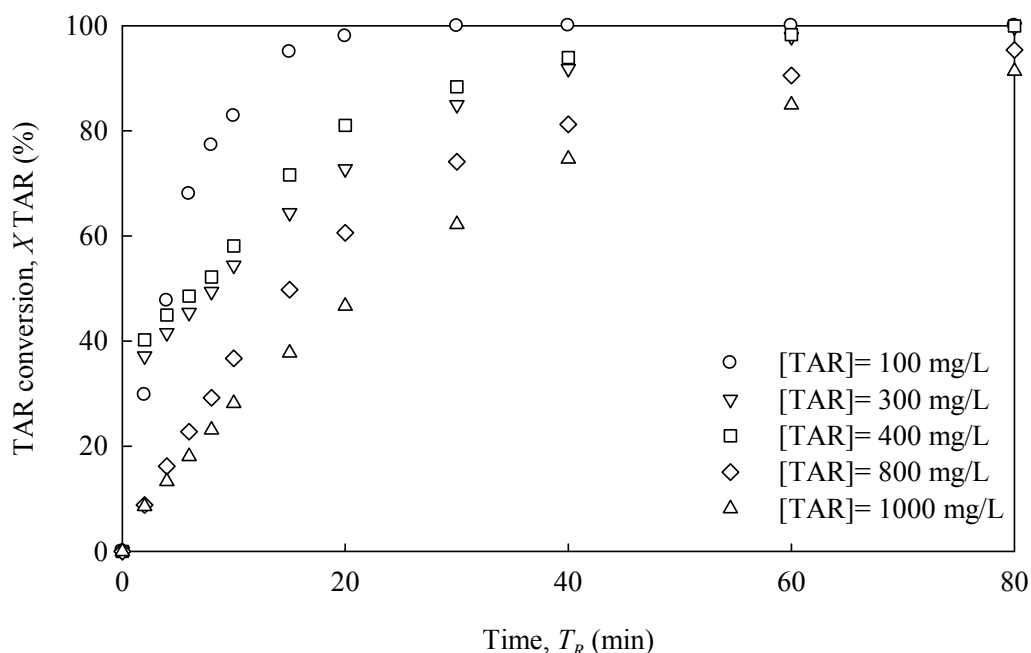


Figure 6.7. Ozonation of TAR. TAR conversion as a function of reaction time for several TAR initial concentrations. Conditions: $[O_3]_{in} = 11$ mg/L, $F_{ozone-air} = 100$ NL/h, $T_R = 30$ °C and $pH_0 = 6$.

Although, the mineralization is relatively low, very high values of colour removal were observed for the different ozone doses and pH_0 (values always beyond 65% and frequently over 90%). Although, hydroxyl radicals have superior oxidation potential than ozone, its selectivity is poor to preferentially break up the double bond usually present in a dye. Hence, as seen in Table 6.3, the colour slightly decreased as pH_0 increased.

On the other hand, the COD and TOC removal slightly dropped from 65.41 to 47.22% and from 24.54 to 13.67%, respectively, when temperature varied from 30 to 50 °C. The amount of ozone dissolved in the water phase is expected to be smaller at higher temperature by the increase of Henry's law coefficient, i.e., lower solubility, which in practice results in a reduction of COD and TOC removal capacity. It was found that the final pH values of the reaction solution decreased throughout the ozonation time, which points out the generation of by-products of acid nature as a result of the oxidation by ozone. The pH decreased in average 3.3 ± 0.2 units for those experiments conducted at pH_0 of 6. At extreme acid and alkaline conditions (pH 3 and 12) no significant changes were observed. The consumption of ozone was very similar in almost all studied conditions. Only pH_0 seems to somewhat influence the ozone consumption. At low pH, 3, an ozone consumption of 35.87% was observed in 80 min whereas at pH 12 the ozone consumption was of 51.8%, probably because the ozone decomposition is favoured in basic conditions.

Tabla 6.3. Ozonation of TAR. Effect of TAR initial concentration, influent ozone gas concentration ($[O_{3in}]$), ozone-air flow rate ($F_{ozone-air}$), pH₀ and reaction temperature (T_R) on the COD, TOC and colour conversion after 80 min of ozonation.

[BPA] (mg/L)	$[O_{3in}]$ (mg/L)	$F_{ozone-air}$ (NL/h)	pH ₀	T_R (°C)	X_fTAR (±1.8%)	X_fCOD (%)	X_fTOC (%)	$X_fColour$ (%)	pH _f ±0.01	X_fO_3 (%)	SA ±0.01 mg/L	IP ±0.01%
100	11	100	6	30	100	100	56.2 ± 0.2	95.09 ± 0.05	2.78	38.9 ± 0.2	10.77	23.53
300	11	100	6	30	99.74	65.4 ± 1.1	24.5 ± 0.4	92.56 ± 0.03	2.68	41.1 ± 0.2	89.66	50.90
400	11	100	6	30	99.91	60.1 ± 1.7	23.6 ± 0.7	94.07 ± 0.02	2.54	38.1 ± 0.2	129.01	47.74
800	11	100	6	30	99.2	43.3 ± 1.4	6.3 ± 0.4	63.60 ± 0.07	2.63	39.2 ± 0.5	278.01	49.03
1000	11	100	6	30	98.39	30.5 ± 1.6	12.4 ± 0.4	39.93 ± 0.06	2.64	44.2 ± 0.2	327.31	51.80
300	22	100	6	30	100	81.7 ± 1.5	36.3 ± 0.8	95.39 ± 0.07	2.73	40.2 ± 0.6	30.79	21.40
300	33	100	6	30	100	92.0 ± 0.9	68.0 ± 0.2	97.88 ± 0.01	2.20	34.7 ± 0.7	25.90	34.64
300	20	50	6	30	99.97	61.6 ± 1.1	24.3 ± 0.6	91.43 ± 0.01	2.72	38.2 ± 0.4	71.02	40.40
300	8	150	6	30	99.52	45.7 ± 1.6	19.2 ± 0.3	73.40 ± 0.07	2.73	41.0 ± 0.3	88.26	46.44
300	6	200	6	30	97.75	44.8 ± 0.9	15.6 ± 0.4	65.31 ± 0.01	2.75	35.6 ± 0.7	103.63	50.50
300	11	100	3	30	99.96	60.4 ± 0.9	14.1 ± 0.5	97.23 ± 0.01	2.53	35.81 ± 0.06	73.03	45.60
300	11	100	9	30	100	69.4 ± 0.8	10.91 ± 0.07	91.63 ± 0.02	2.73	46.89 ± 0.07	63.94	37.03
300	11	100	12	30	100	87.4 ± 1.4	12.5 ± 0.2	77.22 ± 0.04	11.53	51.8 ± 0.5	24.27	17.36
300	11	100	6	40	99.76	57.9 ± 1.4	19.9 ± 0.5	95.61 ± 0.05	2.66	32.4 ± 0.5	84.44	46.52
300	11	100	6	50	97.56	47.2 ± 1.2	13.6 ± 0.7	100.00 ± 0.05	2.85	35.2 ± 0.5	94.97	49.62

6.4. Ozonation membrane assisted process

6.4.1 Nanofiltration of ozonated BPA effluent

Figure 6.8 shows the normalised flux decline in front of time for the filtration of the final BPA effluent after ozonation (BPA-ozone effluent) using several NF membranes. Ozonation was carried out in the optimal selected conditions: $[BPA]_0 = 300$ mg/L, 33 mg/L of inlet ozone gas concentration, 100 NL/h of ozone-air flow rate, pH_0 6 and 30 °C. Optimal conditions represent those where complete removal of BPA was achieved within the lower ozone exposure time. The BPA-ozone effluent contained 324 ± 13 mg/L of COD, 134 ± 12 mg/L of TOC, at pH 2.67 ± 0.04 and with an absorbance of 0.0749 ± 0.0002 read at 400 nm. In general, the fluxes decreased rapidly for all the studied membranes at the beginning of filtration process. After 50 min of filtration, all membranes had already reached a closely steady state. Decline in normalised flux followed the order: ESNA1-LF2 < NFD < NF270 < CK < NF90.

The contributions of the concentration polarisation and fouling to the flux decline in NF90 and NF270 were comparables. These results can be seen in Figure 6.9, where the normalised fluxes measured with the virgin membrane (before), after 250 min of filtration (end) and after flushing the membranes (after) are represented. As pointed out, the flux recovery after flushing the membranes with water is an indicator of the concentration polarisation and fouling. The portion of flux not recovered represents the irreversible flux decline (caused by permanent fouling) and the reversible flux decline represents concentration polarisation and/or easily reversible adsorption phenomena. As it can be seen, the losses of flux by concentration polarisation were 44 and 56% of the total flux decline for NF90 and NF270, respectively. This fact indicates that both phenomena were equally dominants. These trends are clearly evidenced in Table 6.4 summarizing the flux decline after 250 min of operation for all the studied membranes. NFD and CK were the membranes showing a contribution of the concentration polarisation greater than those provided by fouling. NFD and CK are the membranes with the lowest PWP, probably because they are less porous with smaller pore diameter. These properties facilitate the rejection of the organic compounds present in the BPA-ozone effluent at the beginning of

the filtration, when the concentration polarisation layer forms. For ESNA1-LF2 membrane, the fouling showed to be the main responsible for the flux decline.

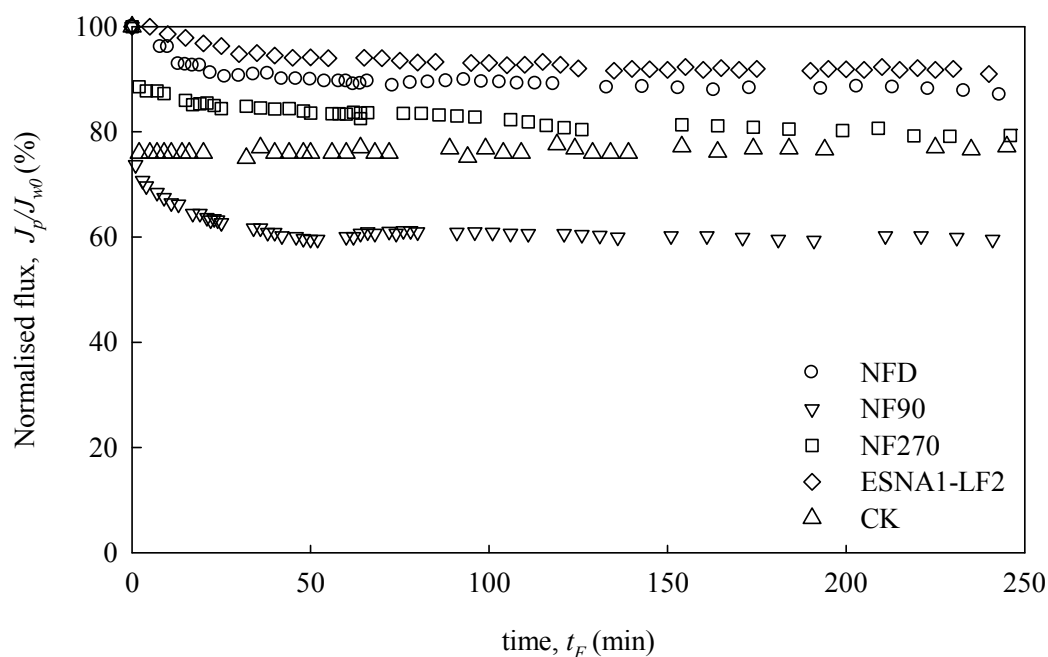


Figure 6.8. Nanofiltration of BPA-ozone effluent. Normalised permeate flux as a function of time for several membranes. Experimental filtration conditions: $TMP = 6$ bar, $v = 5.3$ cm/s, $pH_F \approx 3$ and $T_F = 30$ °C.

The absolute values of the concentration polarisation and fouling contributions underwent by the studied membranes give the following order: $NFD < CK$, $ESNA1-LF2 < NF270 < NF90$ and $ESNA < NFD < NF270 < CK, NF90$, respectively. It is difficult to relate the order of these contributions with the membrane properties reported in Table 3.3 since no clearly tendency is observed. In this sense, it is worthwhile that the adsorption could play an important role in the fouling of NF membranes by organic compounds. This could alter the membrane surface characteristics and thus the solute-membrane interactions, leading to unexpected flux variations. This behaviour has been reported in previous studies (Schäfer et al. 2004).

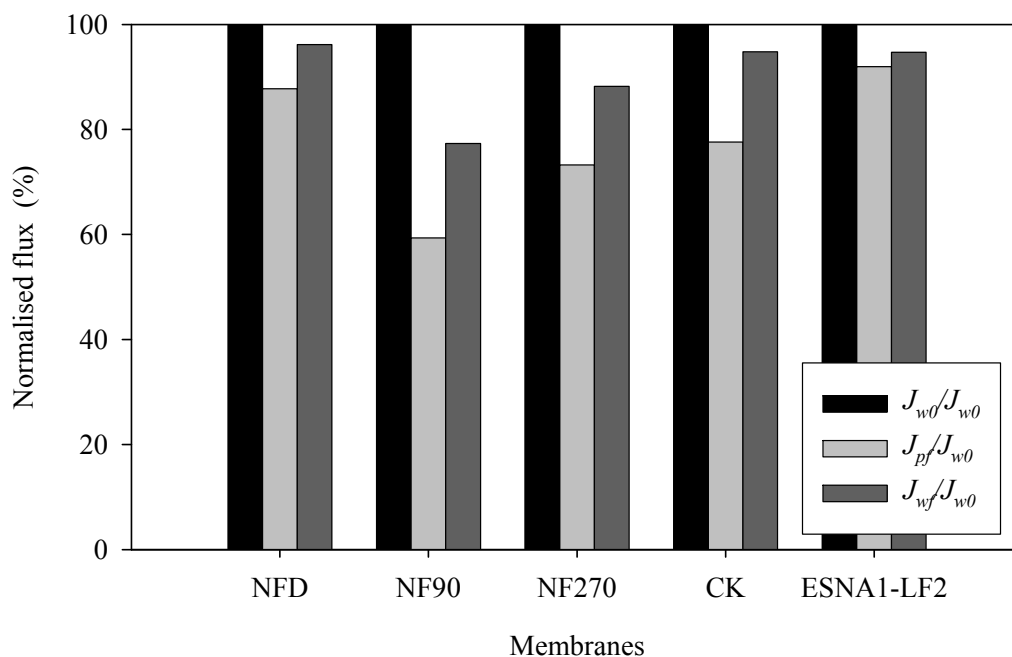


Figure 6.9. Nanofiltration of BPA-ozone effluent. Normalised permeate flux before, J_{w0}/J_{w0} , at the end, J_{pf}/J_{w0} and after filtration, J_{wf}/J_{w0} , for several membranes tested. Experimental filtration conditions: $TMP = 6$ bar, $v = 5.3$ cm/s, $pH_F \approx 3$ and $T_F = 30$ °C.

Table 6.4. Nanofiltration of BPA-ozone effluent. Flux decline, fouling and rejections for several membranes after 250 min of operation. Experimental filtration conditions: $TMP = 6$ bar, $v = 5.3$ cm/s, $pH_F \approx 3$ and $T_F = 30$ °C.

Membrane	Final J_p/J_{w0} ($\pm 5\%$)	Flux decline	CP	Fouling	R_f COD (%)	R_f TOC (%)
		(%)	(%)	(%)		
		$100 - J_p/J_{w0}$	$J_{wf}/J_{w0} - J_p/J_{w0}$	$100 - J_{wf}/J_{w0}$		
NFD	88	12 ± 1	8 ± 2	4 ± 1	67.2 ± 1.7	46.6 ± 0.8
NF90	59	41 ± 4	18 ± 4	23 ± 4	87.2 ± 1.3	76.2 ± 0.5
NF270	73	27 ± 1	15 ± 2	12 ± 1	72.9 ± 0.8	56.4 ± 0.2
CK	78	22 ± 3	17 ± 4	5 ± 1	76.6 ± 1.2	56.9 ± 0.2
ESNA1-LF2	92	8 ± 3	3 ± 1	5 ± 1	69.5 ± 1.1	48.0 ± 0.2

Table 6.4 also presents final COD and TOC rejection in the NF of BPA-ozone effluent at the end of the filtration. The COD and TOC rejections increased as the membrane fouling increased, thus NF90 is the membrane showing the best rejection but simultaneously the highest membrane fouling, too. The improvement of the rejection with membrane fouling could be explained by the formation of some sort of cake layer on the membrane surface by the foulant material, or as well by the blocking of the larger pores with small organic molecules, both of them preventing solute transport and resulting in enhanced rejection. As

already commented, the rejection of organic compounds can change because of the membrane fouling. As a result of this fouling, the solute-membrane interactions that determine organic compound rejection may be affected, and thus the rejection of the organic compounds become altered.

Taking into account the whole process, the initial solution containing 300 mg/L of BPA, 757 mg/L of COD and 237 mg/L of TOC was firstly ozonated and then filtrated to obtained a permeate with no detectable amount of BPA and with COD and TOC values below 90 and 65 mg/L, respectively, for all the studied membranes. This represents an overall rejection greater than 88% for COD and 73% for TOC. For NF90 membrane, which showed the highest rejections, the COD and TOC overall rejection were as large as 95 and 83%, respectively.

Regarding the normalised permeate flux of the NF of BPA-ozone effluent and those obtained in the NF of BPA-Fenton effluent (Figure 5.11 and 6.8) for the studied membranes, it can be noted that, in spite of having the similar organic content (TOC), the normalised permeate flux for BPA-ozone effluent are better in 39, 35, 28, 38 and 18% for NFD, NF90, NF270, CK and ESNA1-LF2, respectively. This is in agreement with the lower concentration polarisation and fouling underwent for these membranes in the NF of BPA-ozone effluent when compared to BPA-Fenton effluent behaviour.

6.4.2 Nanofiltration of ozonated tartrazine effluent

The observed fluxes as a function of time in the NF of the final solution after ozonation of tartrazine (TAR-ozone effluent) are shown in Figure 6.10 for the different membranes. The starting feed solution contained 104 ± 2 mg/L of COD, 74 ± 2 mg/L of TOC, at pH 2.68 ± 0.04 and with an absorbance of 0.0442 ± 0.0002 at 427 nm. This resulted from the ozonation of 300 mg/L of tartrazine using 11 mg/L of inlet ozone gas concentration, 100 NL/h of ozone-air flow rate, pH₀ 6 and 30 °C. Since the optimal condition in the ozonation of TAR reached relatively low values of COD and TOC abatement, the conditions to prepare the feed solution for the NF experiments were those where tartrazine was degraded with a minimal ozone consumption and lowest COD and TOC conversion.

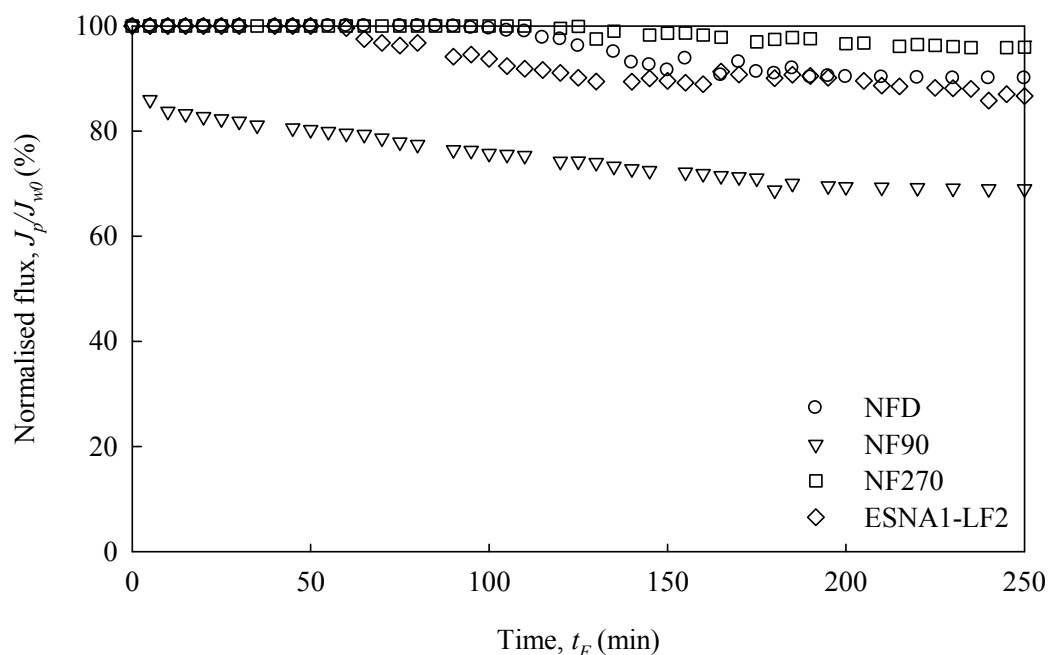


Figure 6.10. Nanofiltration of TAR-ozone effluent. Normalised permeate flux as a function of time for several membranes. Experimental filtration conditions: $TMP = 6$ bar, $v = 5.3$ cm/s, $pH_F \approx 3$ and $T_F = 30$ °C.

NF90 was the only membrane where the flux strongly dropped during the first period of filtration; the flux of NF90 was 86% of the original pure water flux after just 5 minutes of filtration. Afterwards, the NF90 flux declined more gradually until an apparently steady state value was obtained at approximately 200 min. Very slow flux decline is observed for NFD, NF270 and ESNA1-LF before 90, 120 and 60 min of operation, respectively. Figure 6.11, which shows the normalised permeate fluxes before, at the end, and after NF of TAR-ozone effluent, demonstrates that the flux declines observed for NFD and ESNA1-LF2 membrane were mainly due to concentration polarisation. For NF90 and NF270 was the fouling the predominant mechanism influencing the performance of these membranes.

Concentration polarisation seems to increase with the membrane isoelectric point (see Table 3.3). At the interfaces between the membrane surface and the feed solution, a discontinuity in the concentration may be present as a result of electrostatic effects. Depending on compound and membrane charge, the compound will be attracted to the membrane or repelled. Repulsion of molecules by the membrane surface may enhance concentration polarisation. At the pH of the feed solution, around 3, all the membranes are positively charged. The TAR-ozone effluent at this pH may contain compounds with caustic groups or with pKa lower than 3 that could be repelled by the membrane and increase the concentration polarisation.

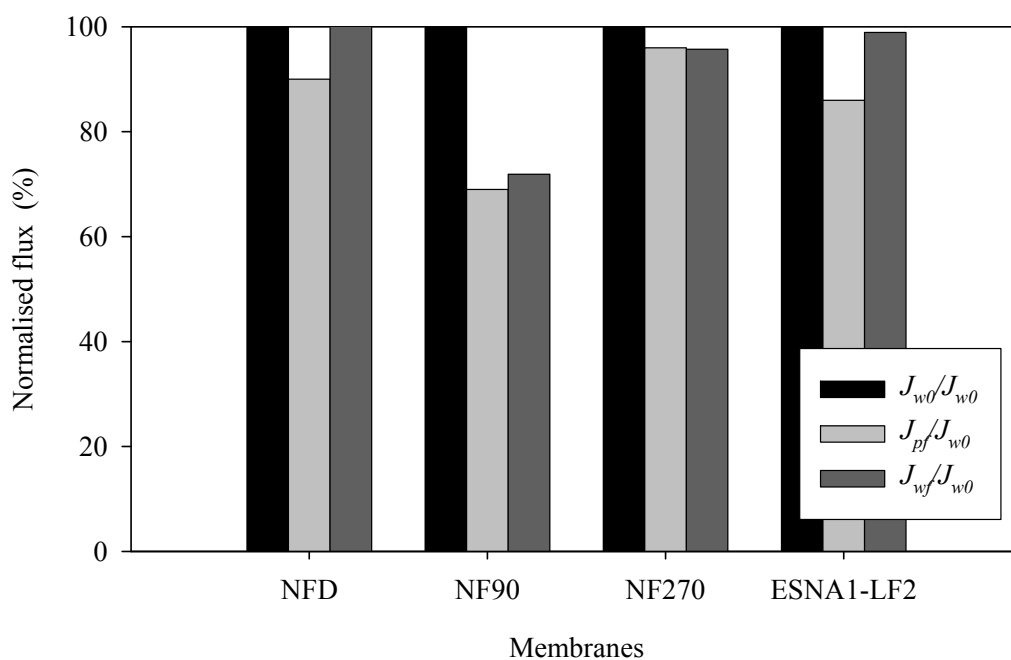


Figure 6.11. Nanofiltration of TAR-ozone effluent. Normalised permeate flux before, J_{w0}/J_{w0} , at the end, J_{pf}/J_{w0} , and after filtration, J_{wf}/J_{w0} for several membranes tested. Experimental filtration conditions: $TMP = 6$ bar, $v = 5.3$ cm/s, $pH_F \approx 3$ and $T_F = 30$ °C.

The final COD, TOC and colour rejections for the NF of TAR-ozone effluent by different membranes are summarized in Table 6.5. Differences observed in the rejections are probably due to the concentration polarisation and fouling underwent by the different membranes, which actually govern the interactions solute-surface. With the exception of the NF270 membrane, the rejections dropped when increasing the concentration polarisation. As usual, the rejection of organic compounds strongly deteriorates when increasing the solute concentration either close to the membrane or in the bulk solution. The enlarged concentration gradient between both sides of the membrane results in the increase of the solute transport.

In turn, the low rejection given by NF270 could be a consequence of its higher porosity and pore size. They can facilitate the pass of a large amount of compounds whose sizes were greater than the MWCO of the other three membranes tested, but not big enough to be rejected by NF270 membrane. The normalized fluxes at 200 min of operation time for all membranes in NF of TAR-ozone effluent were slightly higher than those obtained in the NF of TAR-Fenton effluent. The normalised flux declines were 14, 9, 17 and 4% higher in the NF of TAR-Fenton effluent for NFD, NF90, NF270 and ESNA1-LF2, respectively.

The ozonation coupled with NF to remove TAR reached overall rejections over 89 and 99% in COD and colour, respectively.

Table 6.5. Nanofiltration of TAR-ozone effluent. Flux decline, fouling and rejections for several membranes after 250 min of operation. Experimental filtration conditions: TMP = 6 bar, $v = 5.3$ cm/s, $pH_F \approx 3$ and $T_F = 30$ °C.

Membrane name	Final J_p/J_{w0} ($\pm 5\%$)	Flux decline (%)	CP (%)	fouling (%)	Rf_{COD} (%)	Rf_{TOC} (%)	Rf_{Colour} (%)
		$100 - J_p/J_{w0}$	$J_{wp}/J_{w0} - J_p/J_w$	$100 - J_{wp}/J_{w0}$			
NFD	90	9.5 ± 0.2	9.6 ± 0.4	0.0 ± 0.1	74.8 ± 1.6	54.2 ± 1.5	31.8 ± 1.0
NF90	70	30.5 ± 0.2	2.4 ± 0.4	28.1 ± 0.2	93.8 ± 1.6	85.8 ± 1.2	51.1 ± 1.4
NF270	96	4.1 ± 0.1	0.0 ± 0.2	4.2 ± 0.2	13.8 ± 0.8	2.7 ± 0.5	62.7 ± 1.4
ESNA1-LF2	87	13.4 ± 0.3	12.3 ± 0.5	1.1 ± 0.3	54.4 ± 1.3	34.7 ± 1.2	27.9 ± 1.3

6.5 Conclusions

Ozonation was very successful for BPA and tartrazine removal from aqueous solution. Under the optimal conditions (33 mg/L of inlet ozone gas concentration, 100 NL/h of ozone-air flow rate, pH_0 6 and 30 °C for a reaction time of 80 min), both model compounds (starting from initial solutions of 300 mg/L) could be efficiently decomposed by ozone oxidation, their removals reaching values close to 100%.

In general, ozonation is highly efficient in the decolourisation of the solutions, but considerably less efficient in terms of TOC abatement. At optimal conditions, TOC conversions were 33.1 and 68.0 % for the ozonation of BPA and tartrazine, respectively. For all the operation conditions tested, the degradation efficiency improves with the increase of the inlet ozone gas concentration and initial pH, and worsens with the increase of ozone-air flow rate and model compound initial concentration. Unexpectedly, no significant impact can be assigned to the reaction temperature. The results indicate that the reaction rate between BPA and O_3 is slower than the reaction between tartrazine and O_3 .

Coupling of ozonation and NF to deal with effluents allows complete BPA and TAR elimination. Moreover, ozonation indeed have a significant role to prevent membrane

fouling; the normalised permeate fluxes were considerable higher than for the NF of the model compounds (Chapter 4) as well as for the NF of Fenton-treated effluents (Chapter 6). Based on membrane-assisted ozonation process, the overall treatment efficiency gives over 83% TOC abatement for NF90, which was the best performing membrane, and nearly total elimination of the target compounds.

Chapter 7.

Removal of BPA by enzyme polymerization using nanofiltration membranes

7.1 Introduction

The removal of EDCs like BPA challenges the traditional water and wastewater treatment technologies. Due to its highly selective nature, researchers have been focusing on the study of enzymatic pre-treatment as a potential alternative to conventional methods. The catalytic action of enzymes is extremely efficient and selective compared to chemical catalysts due to higher reaction rates, unique substrate-specificity, capability to show activity in the presence of toxic substances, and under a wide range of environmental conditions (including temperature, pH, salinity, high and low concentrations of contaminants, etc.). Most research on enzymatic processes has concentrated on evaluating the application of oxidative enzymes, including polyphenols oxidases (e.g. laccases) or hydrogen peroxide oxidoreductases (e.g., peroxidases from horseradishes).

Laccases have multiple copper atoms at their active sites and utilize molecular oxygen as the oxidant for the degradation of a variety of phenols, including BPA, to the corresponding reactive quinones (Tanaka et al 2001). Peroxidases from horseradish (HRP) are typical oxidoreductases. HRP is a versatile enzyme applied in chemical, environmental, pharmaceutical and biotechnological industries (Jeng et al. 2006). It is able to catalyze different reactions using H_2O_2 . HRP has been used in the oxidative polymerization of a wide spectrum of phenols, biphenyls, anilines, benzidines and other aromatic compounds to generate polyaromatics as a clean alternative for detoxifying wastewater (Pirillo et al 2010).

Peroxidases and laccases comprise two important classes of enzymes able to catalyze the oxidative coupling reactions of phenolic substrates. Phenoxy radicals generated in these enzymatic processes couple with each other to form polymeric precipitates that can be then more readily removed from water (Uchida et al. 2001). In spite of the advantages of using enzyme catalysis for industrial applications, the major limitations are the susceptibility of the enzyme to inactivation, the high cost associated with isolation and purification of enzymes and the stability and activity of their structures after isolation (Modaressi et al. 2005).

The application of nanofiltration (NF) as promising membrane technology could be an alternative method either for removing and concentrating low molecular weight organic micropollutants or for removing polymeric precipitates after enzyme treatments. NF in combination with enzymes appears to be an attractive approach for the treatment of industrial wastewater, since removal by membrane filtration processes would benefit from polymerization of these phenolic compounds after HRP or laccase action. In wastewater treatment systems, polymerized phenolic compounds are assumed to be more easily removed by sedimentation and filtration (Borneman et al. 1997, Aktaş and Tanyolaç 2003). Nevertheless, studies regarding the possibility of recycling enzymes integrated with the use of membrane processes to separate both enzyme and polymerized phenolic compounds are still lacking. In this study, HRP and laccase are applied to polymerize BPA combined with a membrane process to enhance BPA removal. The investigation of operational conditions for the efficient treatment of BPA by laccase and HRP and the impact of enzyme polymerization on the membrane operation and membrane fouling are studied as well.

7.2 Enzymes

Enzymes are proteins which enhance the rate of a thermodynamically feasible reaction and are not permanently altered in the process. They are high molecular weight compounds, ranging from 10,000 to 2,000,000 g/mol, made up principally of chains of amino acids linked together by peptide bonds. Their catalytic efficiency is extremely high; one mole of a pure enzyme may catalyze the transformation of as many as 10^4 to 10^6 moles of substrate per minute. A very broad classification of enzymes would include hydrolytic enzymes (esterases, proteases), phosphorylases, oxidoreductive enzymes (dehydrogenases, oxidases, peroxidases), transferring enzymes, decarboxylases and others.

The existence of enzymes has been known for well over two century. Some of the earliest studies were performed in 1835 by the Swedish chemist Jon Jakob Berzelius who termed catalytic their chemical action. It was not until 1926, however, that the first enzyme was obtained in pure form, a feat accomplished by James B. Sumner of Cornell University. Sumner was able to isolate and crystallize the enzyme from the jack bean. His work was to earn him the 1947 Nobel Prize (Gurung et al. 2013).

Enzymatic activity is dependent upon several variables, such as enzyme and substrate concentrations, pH, salt concentration of the buffer milieu, temperature and light. The general formula describing the reactions of an enzyme with its substrate can be written as



where E represents the enzyme catalyzing the reaction, S the substrate, i.e., the substance being changed, ES is an enzyme-substrate complex and P the products of the reaction.

7.2.1 Horseradish Peroxidase (HRP)

HRP enzyme (molecular weight 40 kDa) is isolated from the root of the horseradish plant (*Cochlearia armoracia*). HRP has an iron-containing heme group (hematin) as its active site, and is coloured brown in solution. The hematin of HRP first forms a complex with hydrogen peroxide, and then causes it to decompose, resulting in water and atomic oxygen. Details of the reaction mechanism are reported by Nicell et al. (1993), Torres et al. (2003) and Hong-Mei and Nicell (2008). In earlier studies, it was demonstrated that HRP was able to catalyze the polymerization of phenols in non-aqueous media when used to produce phenolic resins (Klibanov 1997). Moreover, when used to treat BPA in aqueous phase, the use of HRP led to the elimination of its estrogenic activity (Sakuyama et al. 2003), which is a characteristic of growing concern associated with this chemical and related compounds (Staples et al. 1998).

7.2.2 Laccase

Laccases are metal-containing enzymes capable of oxidizing numerous phenolic substrates by one electron abstraction. Laccases (benzenediol: oxygen oxidoreductases) belong to the group of blue oxidases and represent the largest subgroup of multicopper oxidases. These enzymes have been studied since the nineteenth century due to their ability to oxidize phenolic compounds, and their applications in several industrial sectors (Giardina et al. 2010, Fernández-Fernández et al. 2012). Laccases are monomeric, dimeric or tetrameric glycoproteins with four copper atoms (belonging to three types: 1, 2 or 3) per monomer located at the catalytic site. Type 1 (T1) copper is responsible for the oxidation of the

substrate and imparts the blue colour to the enzyme (Kudanga et al. 2011, Majeau et al. 2010). Laccases use molecular oxygen to oxidize a variety of aromatic and non-aromatic hydrogen donors via a mechanism involving radicals.

Laccases have been isolated in higher plants (Yoshida 1883), prokaryotes (Claus 2003), insects (Kramer et al. 2001), and are widespread in fungi (Baldrian 2006). Stability of laccases is usually higher at acidic pH, but optimal temperature activity and temperature stability vary considerably among enzymes from different sources. Median values of isoelectric point, optimum pH, optimum temperature and molecular weight are 3.9, 3.0, 55 °C and 66 kDa, respectively. The effect of different potential inhibitors varied among laccases from different species. In most cases, Hg^{2+} caused irreversible inactivation. In addition to specific inhibitors, laccases are also sensitive to inhibitors of metallo-oxidases. Special attention should be paid to ionic copper and iron concentrations as they are common in wastewater and may interfere with laccase activity if they exceed a certain level.

7.2.3 Enzymatic membrane system

The enzymatic membrane system described here aims at coupling a membrane separation process with an enzymatic reaction. The main objective is to ensure the complete rejection of the enzyme in order to maintain the full activity inside the reacting volume. Because a lot of enzymes have a molecular weight between 10 and 80 kD, UF membranes are the most frequently used. Recent studies have reported the classification of the main free enzyme systems: dead-end or cross-flow filtration devices; continuous stirred tank or porous fibre plug flow reactors; enzymatic reactor with direct or indirect contact of enzyme and substrate; diffusion or convection reactor systems. The most important advantages and drawbacks of enzymatic membrane system with respect to the classical reactor configurations with enzymes immobilised on various solid supports are (Rios et al. 2004):

- Advantages: continuous mode (substrate feeding), free enzyme, retention and reuse of enzyme, reduction in substrate/product inhibition, free enzyme end-product, control of product properties by enzyme (specificity), and/or membrane (selectivity) choice, integrated process (single-step reaction/separation).

- Drawbacks: decrease of enzyme activity versus time (loss of catalytic functions, effect of shear stress, etc.), heterogeneity of reaction conditions between the core of solution and the membrane surface, polarisation layer and induced limitation, membrane fouling.

Membrane fouling and enzyme activity decay are responsible for strong limitation on performance of enzymatic membrane system. Membrane fouling has been examined in many works (Edwards et al. 2002, Ko and Chen 2008). Mechanisms have been analysed and various solutions such as membrane modifications, increased turbulence, back-flushing, etc., not always easy to implement or being energy consuming, have been suggested for classical separation processes. Enzyme activity decay has been far less investigated. It seems to be in tight connection with several phenomena such as enzyme leakage, but also enzyme denaturising under the effect of pH, temperature, shear stress or adsorption/deposition over the membrane.

7.3 Enzymatic BPA degradation

7.3.1 HRP enzymatic treatment

Experiments were carried out to find out the optimal H_2O_2 dose required to obtain the maximum conversion of BPA. Several assays were conducted varying the H_2O_2 initial concentration (0–40 mg/L) for two HRP concentrations (2.5 and 5% v/v). BPA concentration, temperature, T_R , and reaction time, t_R , were kept constant at 20 mg/L, 30 °C and 180 min, respectively. The results are presented in Figure 7.1. Hydrogen peroxide acts as a co-substrate to activate the enzymatic action of the peroxidase radical. It contributes to the catalytic cycle of peroxidase, oxidizing the native enzyme to form an enzymatic intermediate, which accepts the aromatic compound, then carrying out its oxidation to a free radical form. Thus, it is expected that the BPA conversion for a given amount of enzyme improves as initial H_2O_2 concentration increases. As it can be seen in Figure 7.1, for both enzyme doses, the XBPA rapidly increases with the H_2O_2 dose, but after peaking at around 10 mg/L, it smoothly drops. Therefore, the expected behaviour was only observed for concentrations below 10 mg/L, where the HRP seemed to be in excess and the H_2O_2 reagent limits the reaction.

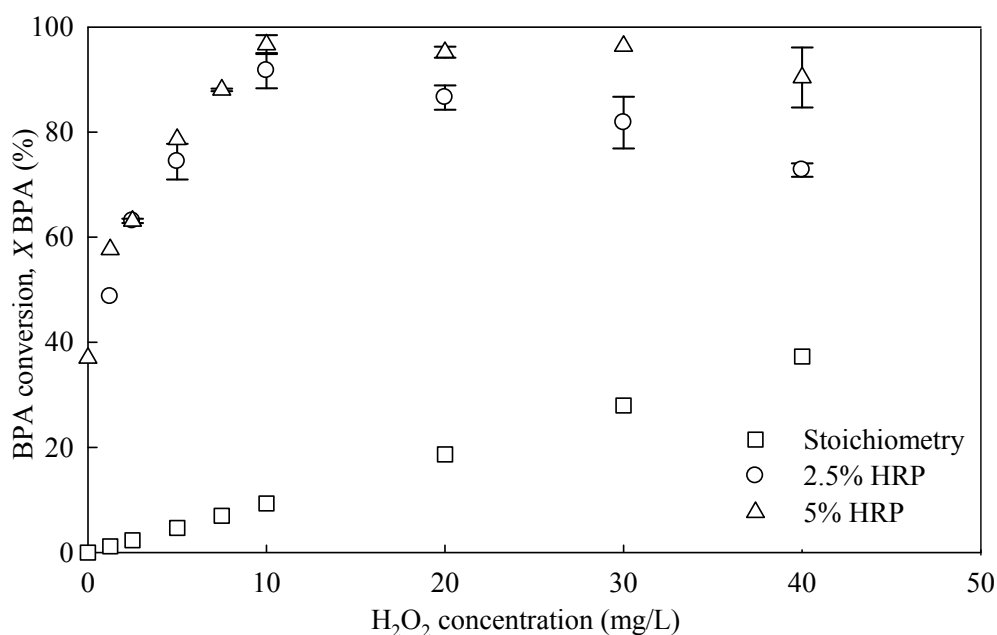


Figure 7.1. Effect of H₂O₂ concentration on HRP catalyzed BPA removal. Conditions: [BPA]₀ = 20 mg/L, T_R = 30 °C, pH₀ = 7, t_R = 180 min and [Na₂HPO₄] = 300 mg/L.

Above 10 mg/L, an increase in the H₂O₂ initial concentration resulted in a decrease in the BPA removal attained. This behaviour could be related to the excess of H₂O₂, which probably oxidizes the enzymatic intermediate to a different enzymatic intermediate that is catalytically less active (Hong-Mei and Nicell 2008). Nevertheless, its formation did not represent a terminal inactivation of HRP. This partial inactivation showed to be more relevant at lower enzyme dose. It must be noted that HRP showed activity in absence of H₂O₂, achieving a conversion of 37%. The stoichiometric conversion is also illustrated in Figure 7.1. Stoichiometric values were calculated using the BPA concentration corresponding to the theoretical stoichiometric concentration of BPA oxidized by H₂O₂ until complete mineralization, eq. 5.17. As it can be seen, for the same dose of H₂O₂, enzymatic treatment achieved higher BPA conversion than the calculated stoichiometrically.

The optimization of the enzyme amount was carried out aiming at a high efficiency of BPA degradation. As it can be seen in Figure 7.2, at HRP amounts below 3% v/v the enzyme dose was found to have significant influence on BPA oxidation reaction. The increase in the HRP dose resulted in an initially sharp increase, followed by a more gradual increase, in the BPA conversion for both studied H₂O₂ doses. Figure 7.2 also seems to

confirm enzyme deactivation at high H_2O_2 dose, since the BPA conversion was always lower for the highest H_2O_2 dose experiments. The concentration that showed the best enzyme performance for both H_2O_2 doses was 7.5% v/v (over 98% of BPA conversion). In the absence of HRP, degradation was also observed, indicating that H_2O_2 can directly react with BPA in absence of a catalyst. The effective removal of BPA using HRP observed is in good agreement with other researches (Hong-Mei and Nicell 2008, Huang and Weber 2005).

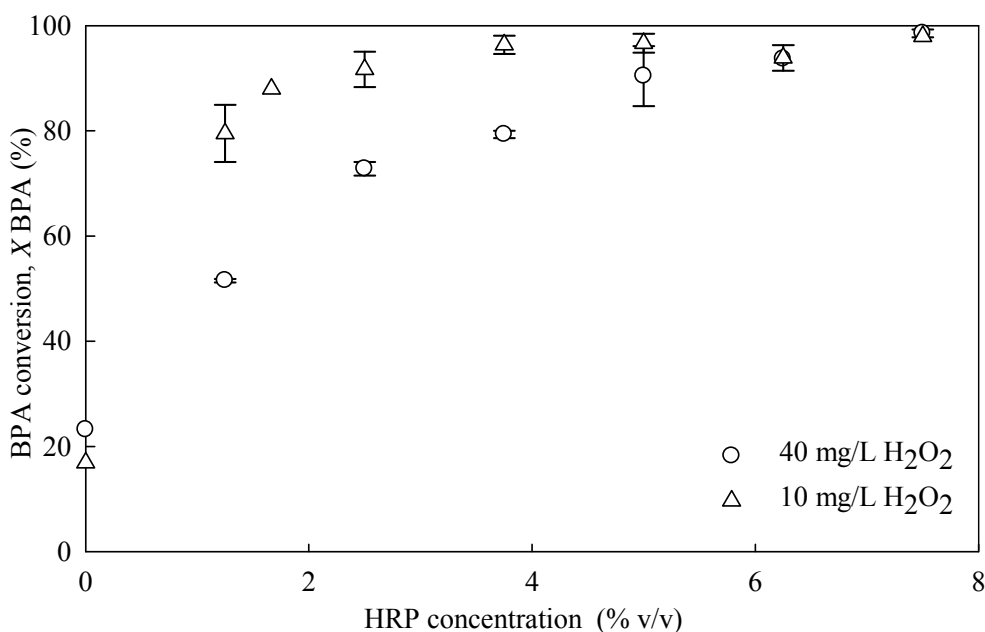


Figure 7.2. Effect of HRP initial concentration on HRP catalyzed BPA removal. Conditions: $[\text{BPA}]_0 = 20 \text{ mg/L}$, $T_R = 30 \text{ }^\circ\text{C}$, $\text{pH}_0 = 7$, $t_R = 180 \text{ min}$ and $[\text{Na}_2\text{HPO}_4] = 300 \text{ mg/L}$.

The effect of pH on the removal of BPA was examined in the range from 3 to 12 (Figure 7.3). Generally, all enzymes have an optimum pH at which their activity is maximal, but it is not necessarily identical to its normal intracellular surroundings (Venkata et al. 2005). The relation of the enzymatic activity with pH, for any enzyme, depends on the acidic-basic behaviour of the substrate, as well as other factors such as chemical structure of substrates, substrate concentration, buffer molarity, H_2O_2 concentration and temperature (de Souza et al. 2007). Depending on these factors, the ideal pH may vary for the same enzyme, highlighting the need to study the effect of pH at the chosen conditions. The results show that the enzyme was able to oxidize BPA over the full pH range studied, indicating that HRP is active over a broad pH range. Nevertheless, the optimal BPA conversion was achieved at pH 7. These results are in agreement with those

previously reported in the literature underlying that lower BPA conversions at non-optimal pH may be due to the increased instability of the enzyme and, consequently, the loss in activity, but also due to reduced interaction between the BPA and the enzyme (Tong et al. 1997, Kim and Nicell 2006).

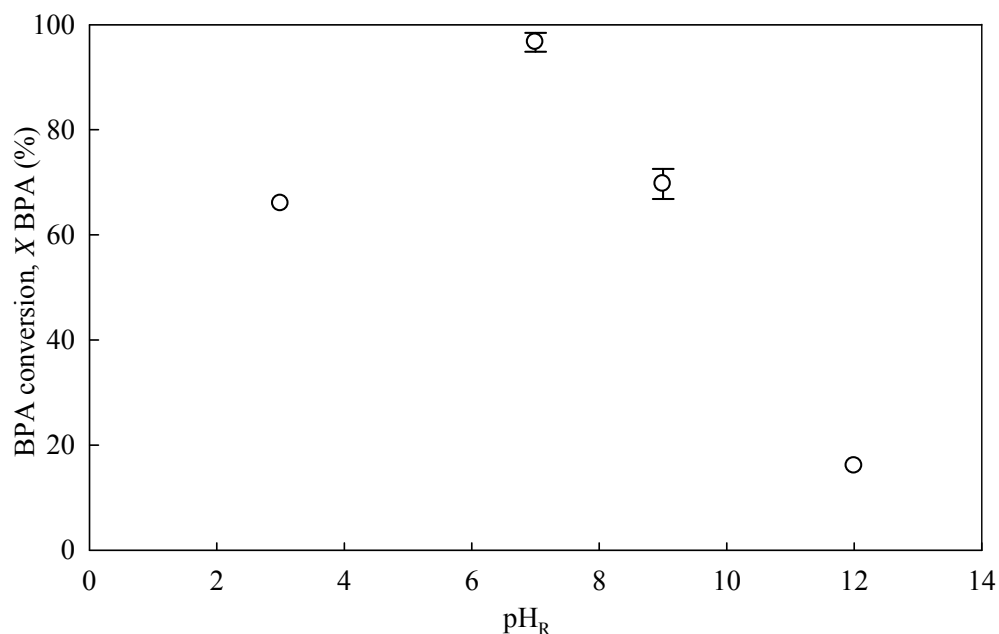


Figure 7.3. Effect of pH on HRP catalyzed BPA removal. Conditions: $[BPA]_0 = 20$ mg/L, $T_R = 30$ °C, $[HRP] = 5\%$ v/v, $[H_2O_2] = 10$ mg/L, $t_R = 180$ min and $[Na_2HPO_4] = 300$ mg/L.

7.3.2 Laccase enzymatic treatment

Data for BPA removal using laccase as catalyst are presented in Figure 7.4 after a treatment time of 180 min at different enzyme dosages and constant initial BPA concentration, 20 mg/L, and temperature, 30 °C. It is evident from the results that the BPA conversion achieved increases with increasing laccase concentration. The maximum was achieved at 0.2 U/mL; beyond this value the BPA conversion remains almost constant at very high values. Satisfactory BPA conversion of 95% can already be obtained at a laccase concentration of 0.12 U/mL. The removal of BPA by laccase was studied over a pH range from 3 to 11 at an initial BPA concentration of 20 mg/L, revealing the same behaviour shown by HRP. As evidenced in Figure 7.5, it can be concluded that the optimal pH for conversion of the BPA was approximately 6. This value is in good agreement with previously reported results (Kim and Nicell 2006).

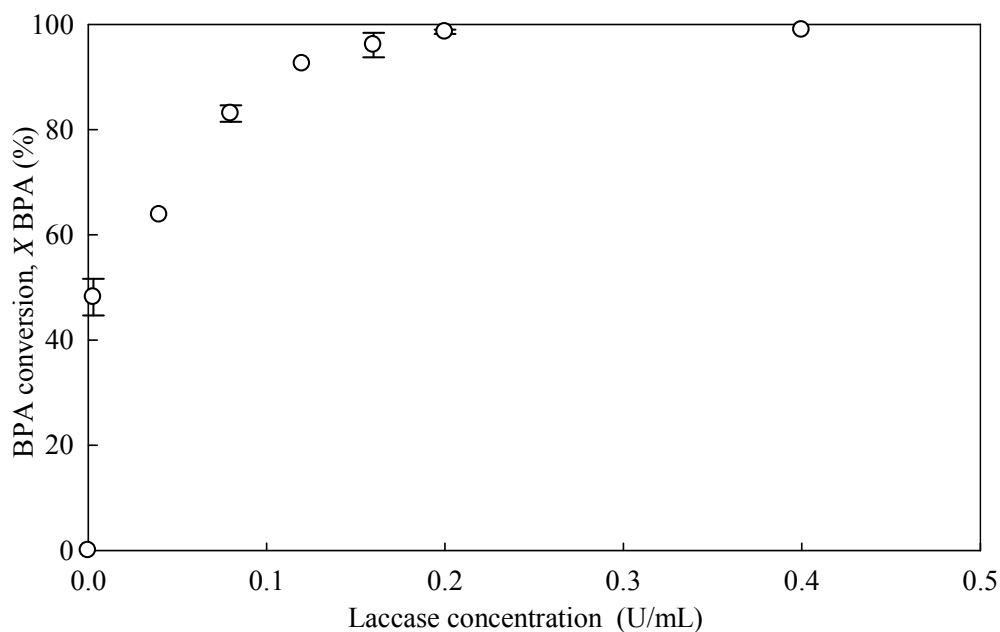


Figure 7.4. Effect of laccase dose on laccase catalyzed BPA removal. Conditions: $[BPA]_0 = 20$ mg/L, $T_R = 30$ °C, $pH_0 = 6$, $t_R = 180$ min and $[Na_2HPO_4] = 300$ mg/L.

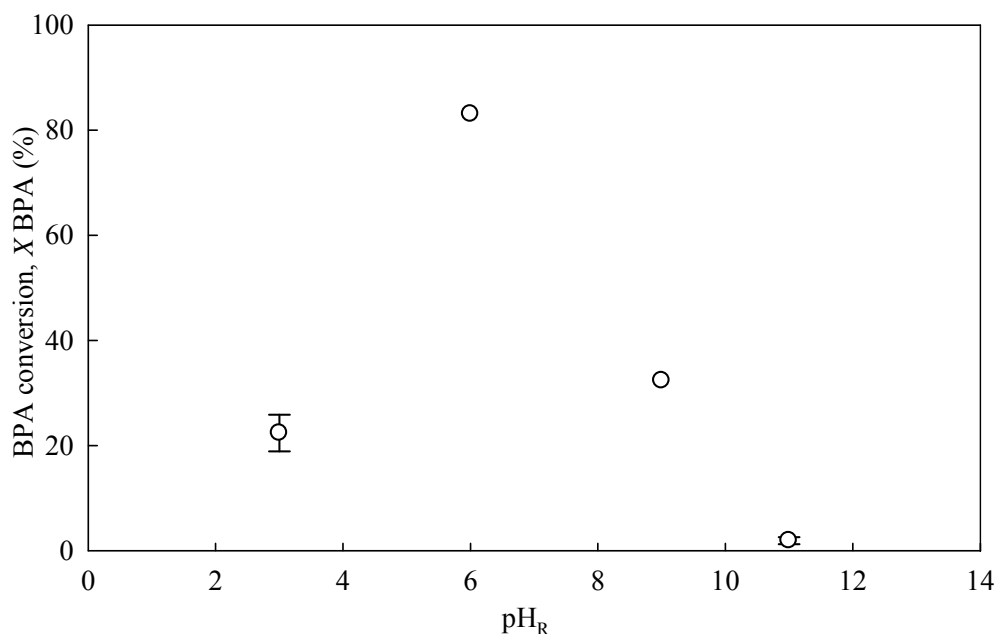


Figure 7.5. Effect of pH on laccase catalyzed BPA removal. Conditions: $[BPA]_0 = 20$ mg/L, $T_R = 30$ °C, $[Laccase] = 0.08$ U/mL, $t_R = 180$ min and $[Na_2HPO_4] = 300$ mg/L.

7.3.3 BPA removal using HRP and laccase in a membrane nanofiltration system

The integrated enzymatic degradation of BPA and NF of the exited effluent was investigated for the optimized conditions previously identified. A NF270 membrane was

used for this purpose. Experiments using HRP in the combined process were conducted at pH 7.0, room temperature, an initial BPA concentration of 20 mg/L, an initial H_2O_2 concentration of 10 mg/L and 50 mL of HRP in a 2 L reaction tank also performing as feed reservoir for the NF system. Experiments with laccase were conducted using the same operation parameters but without addition of H_2O_2 ; in this case, 10 mL of 24 U/mL enzyme solution were added to the reaction tank, achieving an initial enzyme concentration of 0.12 U/mL. Figure 7.6 shows the results for the combined membrane-enzyme BPA removal tests for laccase and HRP enzymes, again in form of normalised permeate flux. In the presence of enzyme, the normalised permeate flux additionally decreased around 17 and 29% for HRP and laccase cases, respectively, compared to the flux obtained for nanofiltration of pure BPA solutions using NF270 (full symbols in Figure 7.6). It must be noted that the progressive slight flux increase observed at the beginning in the NF of untreated BPA is due to the temperature rise in the system, from 22 to 27 °C, during the first hour approximately, i.e. until a nearly steady state is reached, as a result of the friction and the inability to control the system temperature.

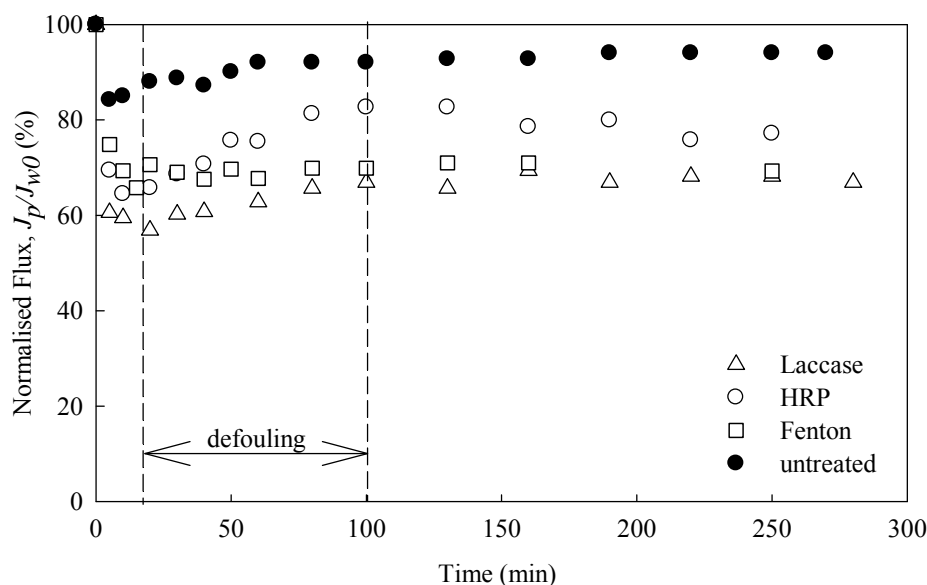


Figure 7.6. Nanofiltration of treated BPA effluent by laccase, HRP and Fenton at 6 bar, $Q_F = 70$ L/h, room temperature using a NF270 membrane. Full symbols represent normalised permeate flux in the NF of 20 mg/L BPA solution.

In both membrane-assisted enzymatic treatments, a decreasing flux is observed during the first 20 min of operation, which can be assigned to CP and fouling phenomena mainly due to the presence of enzymes in solution, but also to the polymeric products formed. Beyond

20 min, there is a recovery of the flux until 100 min, referred to as defouling period. Then, the flux mostly stabilizes although a slight progressive fall is again seen. Defouling is defined as the increase of the normalised permeate flux during operation owing to changes in CP and fouling. The fact that the feed solution is constantly changing due to the action of the enzyme could result in reducing the CP and fouling by the progressive decrease of the concentration reaching the membrane surface and changes in the feed solution properties through the generation of by-products.

This behaviour is much more evident for HRP treatment. These results suggest the formation of a reversible cake layer formed by the accumulation of polymeric by-product macromolecules at the membrane-solution interface. This cake layer was visually verified after NF test and then was characterised with ESEM-EDS, in contrast to the virgin NF270. Figure 7.7 shows the pictures of a non-used NF270 membrane and of membranes used for filtering the enzymatically treated BPA solutions. As it can be seen, morphology differences are clearly observed between the virgin and used membranes. The fouling layer on the membrane appears to be a cracked cake, especially for the laccase enzyme case. Table 7.1 shows the elemental analysis performed by EDS for the used NF270 membranes. EDS analysis provides a semi quantitative elemental composition of membrane surface, which has a depth of 4.5 μm . As it can be seen, the mass fraction of carbon (C) on the membrane surface increased around 1.51 and 11.06% due to the membrane use in HRP and laccase membrane enzyme treatment, respectively, which correlates well with its capacity to transform BPA in polymeric derivatives.

The differences in the membrane fouling trends for the two membrane-enzyme treatments could be related to present of different by-products resulting of the different oxidative mechanism. It is worth mentioning that laccase has demonstrated to possess a higher oxidation power than HRP, thus higher polymerization rate is expected and, consequently, higher fouling should follow. It must be noted that one of membrane-enzyme degradation experiments was conducted in triplicate and the deviation between experiments was less than 8%, which is a very satisfactory repeatability for filtration tests.

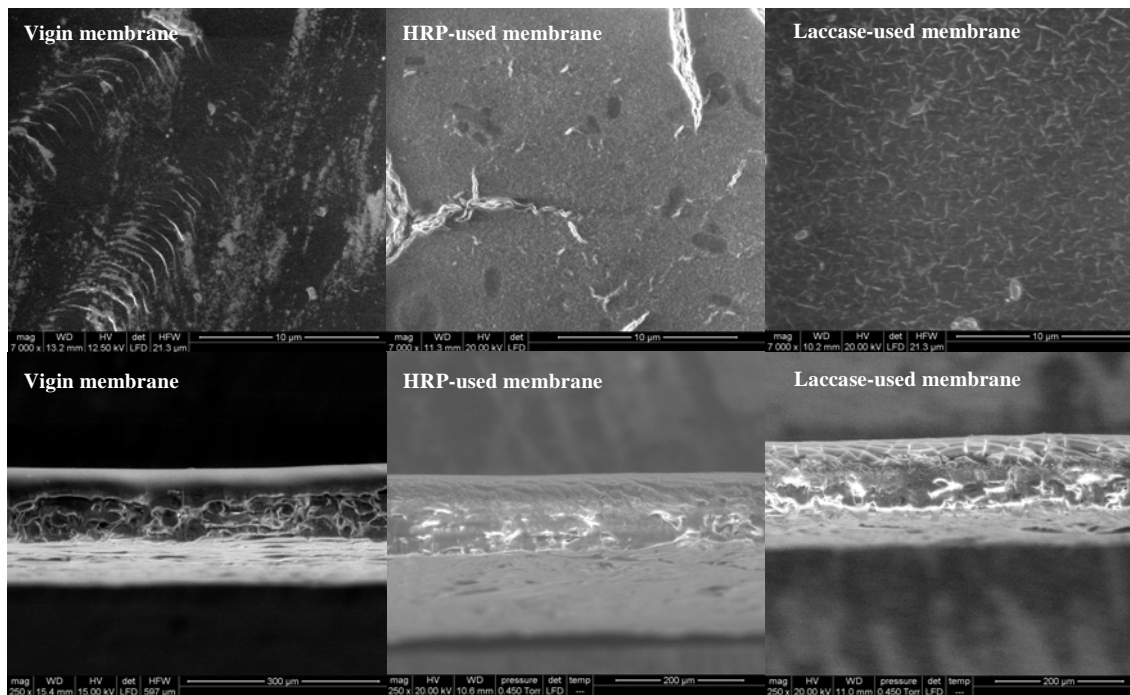


Figure 7.7. Micrographies of virgin and NF270 membranes applied for the enzymatic degradation of BPA using laccase and HRP.

Table 7.1. Elemental composition of virgin and used NF270 membranes after BPA NF experiments at 6 bar and room temperature for enzymatic degradation process.

Membrane	C (% wt)	O (% wt)	S (% wt)
Virgin	70.7 ± 1.1	18.9 ± 1.2	10.4 ± 1.3
NF270 Used-HRP	71.8 ± 0.7	23.4 ± 0.9	4.9 ± 0.3
Used-Laccase	78.5 ± 0.2	18.2 ± 0.1	3.4 ± 0.05

BPA concentration in the reactor tank (membrane feed) and permeate as a function of the time after filtration using the NF270 is shown in Figure 7.8. It must be noted that the BPA conversion, in connection to that obtained in the reactor alone, decreased in 4 and 13% for laccase and HRP, respectively, in comparison with the conversion achieved for the respective enzyme treatments without coupling to the NF system. This effect could be related to the presence of retained enzyme over the membrane as multiple layers could be formed by enzyme and polymeric by-products. The overall effect reduces the conversion by decreasing the actual enzyme concentration in the reactor, as well as reducing the permeate flux due to such additional barrier.

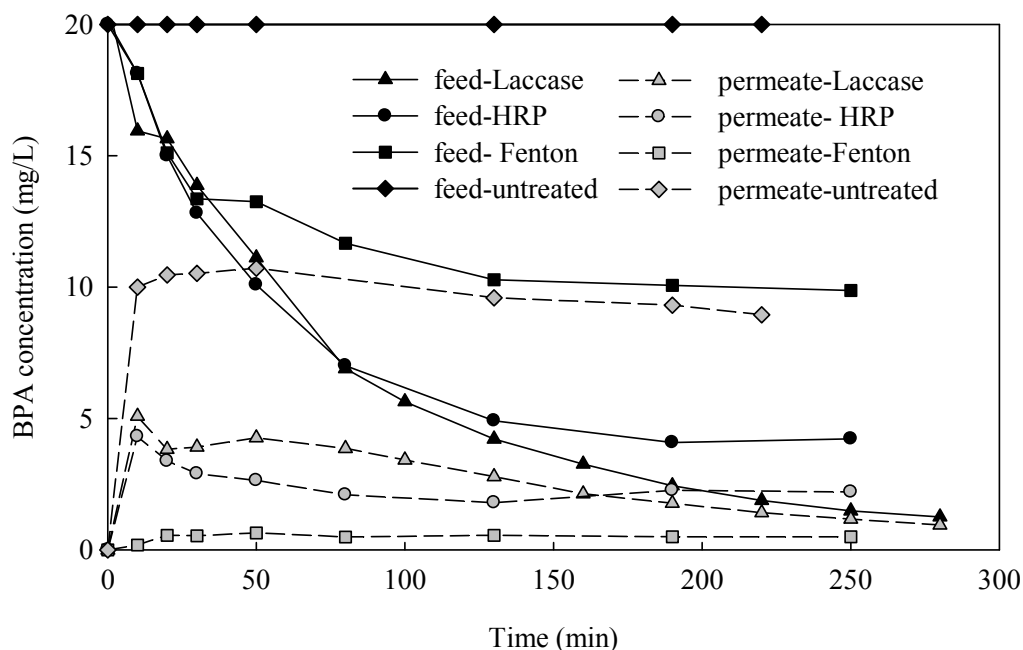


Figure 7.8. Permeate and feed concentration of BPA as a function of filtration time for different degradation process using NF270 membrane.

As Figure 7.8 also shows, BPA permeate concentration is initially around 5 mg/L for both membrane-enzyme processes, then gradually decreases to values between 1 and 3 mg/L as BPA concentration diminishes in the feed side. According to sorption-diffusion model transport (the most widely accepted), both water (solvent) and BPA can dissolve in the polymeric membrane and then diffuse through the membrane due to a chemical concentration gradient. Taking this model into account, the BPA rejection should increase when the feed BPA concentration decreases; however, this behaviour was not observed for the present membrane-assisted enzyme processes using NF270. The BPA rejection drops from 75 and 65% at 20 min up to 22 and 28% at 250 min for HRP and laccase membrane-enzyme processes, respectively. This suggests a much more complex transport model where adsorption-desorption phenomena and interaction with derived substances must play a key role.

In any case, the BPA permeate concentrations for both membrane-enzyme processes were initially well below the feed concentration, which indicates a relevant rejection due to steric repulsion or size exclusion mechanism. The later poor BPA rejection, i.e., relatively high BPA concentration in the permeate at large time, could be attributed to the formation of the cake layer which hindered the diffusion of BPA back to the bulk solution thus maintaining an elevated BPA concentration within the cake layer and close to the

membrane surface (Vogel et al. 2010). Consequently, this led to an increased concentration gradient of BPA across the membrane and, hence, a lower rejection. Similar behaviours have also been reported in previous studies (Nghiem et al. 2008). Salt rejection for both membrane-enzyme processes was also measured through permeate and feed conductivity using NF270 membrane. Membrane-assisted laccase treatment gave higher values in conductivity than HRP treatment, resulting in 99 and 96% of salt rejection, respectively. It is worth mentioning that BPA permeate concentrations using membrane-enzyme treated effluent were more than 50% lower than those observed for pure BPA solution nanofiltration using NF270 membrane (Figure 7.8). Thus, membrane-enzyme processes could be used as an enhanced method in the removal of BPA. Overall removal efficiencies of the coupled membrane-enzyme processes, calculated as percentage of BPA in the permeate, taken at 250 min, with respect to the initial BPA concentration in the reaction tank, were 89 and 94% for HRP and laccase, respectively.

Nanofiltration experiments were also done in the absence of BPA (without reaction) in order to study the potential recovery of laccase and HRP at reaction conditions (pH=7, buffer concentration=300 mg/L and H₂O₂=10 mg/L for HRP assays) using NF270 membrane. In this case, no cake layer was observed attached to the membrane surface, indicating that the fouling in reaction conditions mostly owns to the polymeric by-products. The normalised permeate flux rapidly reached a steady state value of 79%.

The performance of membrane-assisted BPA degradation using the classical Fenton process is added in Figures 7.6 and 7.8. The reaction conditions were set at 20, 10 and 0.4 mg/L for the initial BPA, H₂O₂ and Fe²⁺ concentration, respectively, whereas the pH was adjusted at 3. Fenton process showed to be less powerful than HRP treatment, since the BPA concentration in the reactor tank was almost one and a half times higher than that reached by HRP treatment at 250 min of reaction using the same amount of initial H₂O₂. Low values in the BPA permeate concentration for membrane-assisted Fenton degradation could be related to the occurrence of internal membrane fouling, either by pore blocking for the smaller by-products or by the solute membrane interactions taking place, which are expected to be stronger at low pH. Previous studies have shown that organic fouling was most severe at low pH (Hong and Elimelech 1997, Li and Elimelech 2004).

Flux recoveries after cleaning for the membrane-assisted treatments using NF270 membrane are listed in Table 7.2. The flux recovery for both treatments was lower than 100%, which indicates the occurrence of irreversible fouling. In particular, for Fenton process the formed layer was very stable and consolidated enough to be resistant against soft water rinsing. On the contrary, HRP treatment gives a satisfactory recovery, around 90%.

Table 7.2. Normalised permeate flux before, at the end and after of BPA nanofiltration at 6 bar and room temperature for several degradation processes using NF270 membrane.

Treatment	Normalised permeate flux		
	before, J_{w0}/J_{w0} (%)	At 250 min, J_{pf}/J_{w0} (%)	after, J_{wf}/J_{w0} (%)
Laccase	100	67	76
HRP	100	77	91
Fenton	100	71	69

A similar set of experiments was also conducted for membrane-assisted enzyme treatment using NF90. Figure 7.9 represents the normalised flux evolution for each enzyme process. As it can be observed, irrespective of the enzyme used, NF90 undergoes about 25% more loss of permeate flux than NF270 (Figure 7.6). Furthermore, normalised permeate flux was 62% lower for the enzyme treated effluent when compared to that given for nanofiltration of non-treated BPA solutions using the same membrane (Figure 7.6). Thus, both CP and fouling were probably substantially larger for the NF90 membrane in presence of enzyme. The defouling period is much less pronounced for the NF90 membrane. Thus, for membrane-assisted laccase treatment, almost no increase in the permeate flux was observed after the initial abrupt fall, while a slight increase around 7% in the period from 15 to 80 min can be observed for HRP. These results suggest the presence of severe fouling during the nanofiltration of the enzyme treated effluent using NF90 membrane. However, no cake layer formation was observed in these assays and, additionally, the mass fraction of carbon did not vary between a virgin NF90 and the used membrane, what therefore seems to indicate that internal fouling was the predominant fouling mechanism.

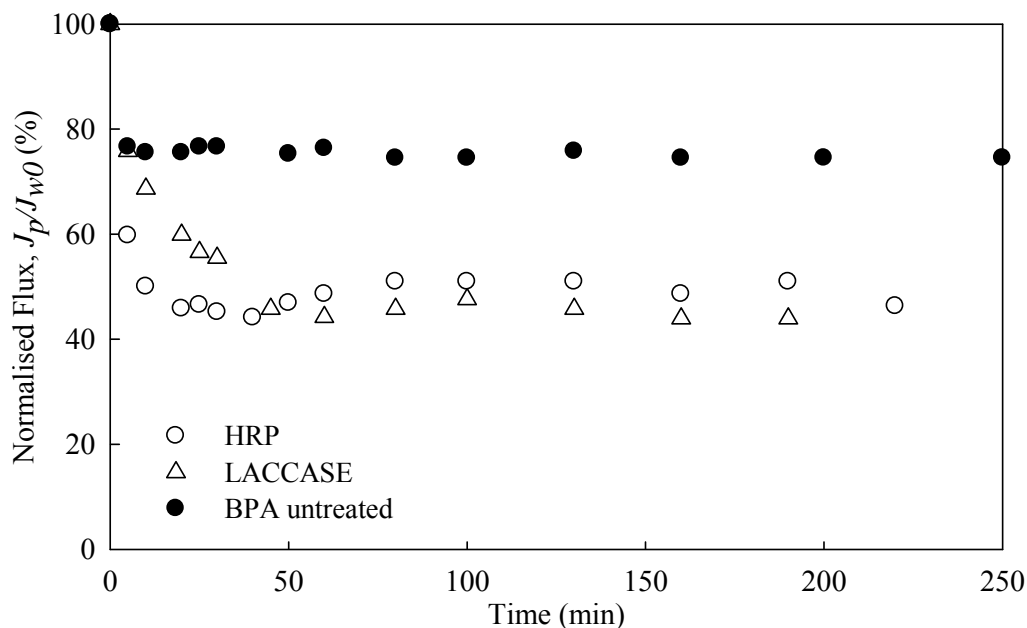


Figure 7.9. Nanofiltration of treated BPA effluent by laccase and HRP at 6 bar, room temperature, $Q_F = 70$ L/h and NF90 membrane. Full symbols represent normalised permeate flux in the NF of 20 mg/L BPA solution.

Furthermore, BPA concentration evolution in the feed side for NF90 (Figure 7.10) is very similar to that obtained using NF270 (Figure 7.8). Only slight differences were observed in the reaction rate for the HRP treatment, probably due to the successive decrease in enzyme activity with every reuse. BPA permeate concentrations were constant and equal for both treatments, although NF90 shows a better rejection as the BPA concentration of the permeate was always lower than that obtained using NF270. As previously mentioned, these differences could be mostly attributed to the lower pore size and slight higher hydrophobicity of NF90 that leads to higher BPA rejection by steric hindrance and adsorption. Table 7.3, which collects the normalised permeated fluxes of the virgin NF90 membrane, measured after 250 min filtration, and after soft rinsing with MilliQ water, corroborates that severe fouling occurred. Moreover, NF90 showed higher remaining fouling fraction (lowest normalised permeate flux after water rinsing) when compared to NF270, which again matches an internal fouling, much more difficult to clean.

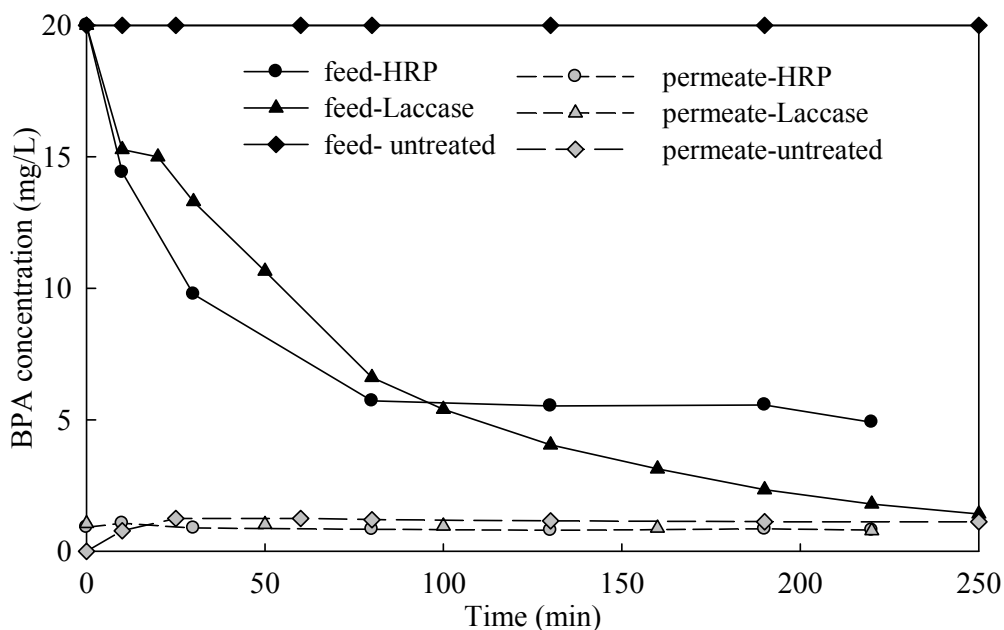


Figure 7.10. Permeate and feed concentration of BPA as a function of filtration time for the different enzyme process using NF90 membrane.

Table 7.3. Normalised permeate flux before, at the end and after of BPA nanofiltration at 6 bar and room temperature for several degradation processes using NF90 membrane.

Treatment	Normalised permeate flux		
	before $J_{w0}/J_{w0} (\pm 4\%)$	at 250 min, $J_{wf}/J_{w0} (\pm 4\%)$	after, $J_{wf}/J_{w0} (\pm 4\%)$
HRP	100	46	57
Laccase	100	44	55

7.4 Conclusions

BPA removal was conducted by means of enzymatic treatment using either HRP and hydrogen peroxide or laccase, which gives polymeric substances as main reaction products. The results reveal that the efficiency of the enzyme treatment for BPA degradation varies with enzyme dose and pH. Optimum levels have been identified. The wide pH range where the enzymes maintain their activity evidences the potential of this alternative as extreme fluctuations of pH can be expected for this kind of wastewater. Therefore, enzymatic membrane reactors are a promising technology for continuous degradation of wastewaters containing BPA.

Coupling of the reaction system with nanofiltration allows a further BPA removal by rejection and also the recycling and continuous use of the enzymes. With this membrane-

assisted enzyme treatment, using the NF270 membrane, over 89% removal of BPA was observed for the two enzyme treatments, which shows to be clearly superior to medium removal (55%) for classical Fenton treatment in similar conditions. In addition, acceptable flux decline is observed for this membrane. Nanofiltration of enzyme pre-treated BPA was also conducted using the NF90 membrane but this membrane undergoes a strong flux reduction without relevant improvement in BPA rejection.

The presence of the enzyme and the polymeric products reduced the permeability for around 50 min of filtration due to cake layer formation by polymerized BPA, pore blocking and adsorption. However, no additional flux decline was observed afterwards, reaching a quasi-steady state, which is acceptable for NF270 but too severe for NF90, regardless its higher BPA rejection.

Chapter 8

Conclusions and future work

8.1 Conclusions

The necessity of water reclamation is growing, which forces the mandatory improvement of current wastewater treatments. Numerous water reclamation schemes have been developed where nanofiltration (NF) is widely used. NF can produce high water quality, thus there is no doubt that NF will play an important role in the success of future water reclamation processes. This thesis deals with the design and application of NF membrane-assisted advanced oxidation processes. Fenton, ozonation and enzyme treatments in combination with NF have been studied to enhance Bisphenol A (BPA) and Tartrazine (TAR) removal. BPA and TAR were chosen as a model compounds since even traces of these contaminants in water sources is of concern for environmental health. This dissertation aims at contributing towards the promotion of both water reclamation and the use of NF membranes for the production of high water quality from wastewater.

Overall, the experimental data evidence that NF is a suitable technology for the treatment of solutions containing BPA or TAR. Experiments with commercial flat-sheet polymeric NF membranes showed that high BPA (>83%) or TAR (>98%) rejections can be obtained, which may be mainly attributed to size exclusion or sieving effect as well as adsorption whenever BPA is involved. While, as expected, pure water flux for these NF membranes linearly increased with pressure according to the solution-diffusion model and Darcy's law, polarisation concentration was the main responsible of flux decline during the NF of the models compounds, although fouling by adsorption and pore blockage also determined the final permeate fluxes underwent in the NF of BPA. Because the concentration polarisation governs the flux, feed concentration also had a significant effect on it, so fluxes decreased with growing feed concentration. NF90 and NF270, among other commercial membranes tested, were the elements that showed the best performance in BPA and TAR removal, respectively. These membranes showed relatively high BPA and TAR rejections and the lower permeate flux decays.

Fenton process has proved to be an effective method to treat solutions containing BPA or TAR since their complete degradation could be accomplished even with low doses of

hydrogen peroxide. Although an increase in the concentration of BPA or TAR in the initial solution resulted in a continuous decrease of their conversion, a maximum absolute amount of model compound has been simultaneously identified, which proves that is more favourable working at greater BPA or TAR concentrations in terms of overall disappearance rate and hydrogen peroxide use. Of course, higher amounts of hydrogen peroxide involved higher mineralization at the end of the reaction; however, its excess with respect to the organic compound (e.g., $H_2O_2/BPA > 1.12$) decreased the oxidation efficiency by favouring the radical scavenger effect of the hydrogen peroxide. An increase of the initial iron concentration always resulted in a faster reaction rate.

When comparing the results of the Fenton oxidation for treating BPA or TAR, it was found out that BPA was more easily degraded than TAR as a lower H_2O_2 to organic compound was needed to degrade BPA. Although both compounds were almost completely degraded, rather low total organic carbon (TOC) conversions were achieved. Thus, Fenton process was more beneficial for degradation of model compound rather than for mineralization. Concerning the NF of the exited effluents after Fenton treatment, it can be said that the high flux decrease in the NF of BPA-Fenton treated effluent was originated by membrane fouling. Meanwhile, concentration polarisation and membrane fouling showed to have a comparable contribution in the flux decay for NF of TAR-Fenton treated effluent. Anyway, high rejections were obtained in the NF of Fenton effluents allowing very high permeate quality.

The degradation of BPA or TAR by ozonation was also assessed. Ozonation showed to be an effective method for removal and decolourisation of both compounds. It was observed that the pH and the initial BPA and TAR concentrations had a significant role in the ozonation. Solutions with high pH and low BPA and TAR concentrations were degraded faster by ozone. Mineralization of BPA or TAR solutions was not as successful as their degradation for reaction times up to 80 min. At optimal conditions, practically all BPA or TAR content was degraded, while they were mineralized only around 33 and 68%, respectively. On the other hand, ozonation had a significant role to prevent membrane fouling, so the permeability during filtration of ozonized BPA and TAR solutions using NF90 membranes were consequently higher than the permeability measured for the untreated or Fenton treated effluents. Like NF of Fenton treated

effluents, high permeate quality was also obtained by NF of ozonized effluents, exhibiting high overall COD (>88%) and TOC (>73%) rejections, too.

Finally, the application of HRP or laccase treatment for the degradation of BPA was investigated. It has also showed that running enzymatic treatment in a membrane system allows the recycling of the enzyme and a simultaneous high BPA removal. The possibility of reusing the enzyme is important in order to promote its use in large-scale reactions. The lower permeate fluxes observed for the NF of enzyme pre-treated BPA effluents in comparison with the NF of untreated BPA solutions was mostly attributed to membrane fouling. The accumulation of polymeric by-products over the membrane surface was the main responsible of this membrane fouling for NF270 membrane. Meanwhile, internal fouling caused the loss of permeate flux when membrane assisted enzymatic treatment was conducted over a NF90 membrane. Therefore, NF270 membrane showed to be the best membrane to filter enzymatically treated effluents, since acceptable flux decline was observed (<33%).

8.2 Future work

As recommendations, in the first place, the scaling-up of these membrane-assisted advanced oxidation processes (bench, pilot or full scale) is strongly recommended. A change in the operating mode from batch to continuous mode, experimental demonstration using real wastewater effluents and changing of modules such as spiral wound and tubular should be tested in order to operate in pilot scale or industrial scale. Under these conditions, not only the efficiency of the processes in terms of organic load or pollutant degradation must be investigated, but also the actual economical aspects of the process. In this sense, the observed quality of NF permeate, as well as the results on the operation, performance and costs of the NF process could give reliable information about the performance of NF and the advantages of membrane-assisted advanced oxidation processes versus other wastewater treatment schemes.

Secondly, to better understand the impact of membrane fouling on rejection of oxidised effluents, more insight in the interactions between foulant material and the membrane surface is necessary. If more knowledge is available on the compounds formed after

oxidation and their interaction with membrane polymeric materials, it might be easier to predict their behaviour during filtration and thus on rejection, fouling or flux. For this purpose, a better characterisation of the used membrane surfaces and of the composition of the oxidised effluents is essential. It could help to determine which of these compounds mainly cause fouling and how the membrane surface properties could modify by the deposition or internal fouling of these compounds. As both fouling and cleaning alter the membrane characteristics, studies of long time membrane operation and application of different membrane cleaning protocols could also give reliable data that can be used for real application.

The use of membranes in combination with an oxidation treatment is attractive for wastewater treatment. However, it requires the use of oxidation agents such as H_2O_2 that might play an important role in membrane lifetime. It is well known that polyamide membranes, used in this work, can be degraded by oxidation agents. It could result from loss of functional membrane properties, till production that no longer meets the requirements in terms of volume or quality, or the sudden break down of the membrane, resulting in a shut down of the process for maintenance, which is expensive. Although no evidences of membrane deterioration have been seen in short-time tests, based on these considerations, the effect of hydrogen peroxide reagents on polymeric membrane materials needs to be investigated to allow selection of suitable membranes for the coupling between HRP enzyme and Fenton with nanofiltration in one compacted single unit. In addition, design and manufacture of oxidant-resistant membranes would allow performing the oxidizing processes in combination with separation by membranes in a safer manner.

References

- Abboah-Afari E. and B. Kiepper (2011). "The use of membrane filtration as an alternative pretreatment method for poultry processing wastewater." Proceedings of the 2011 Georgia Water Resources Conference, April 11-13, 2011, University of Georgia (USA).
- Abdelmalek, F., R. Torres, E. Combet, C. Petrier, C. Pulgarin and A. Addou (2006). "Gliding Arc Discharge (GAD) assisted catalytic degradation of bisphenol A in solution with ferrous ions." Separation and Purification Technology 63(1): 30-37.
- Agenson, K., J. Oh and T. Urase (2003). "Retention of a wide variety of organic pollutants by different nanofiltration/reverse osmosis membranes: controlling parameters of process." Journal of Membrane Science 225(1-2): 91-103.
- Ahn, K., H. Cha, I. Yeom and K. Song (1998). "Application of nanofiltration for recycling of paper regeneration wastewater and characterization of filtration resistance." Desalination 119(1-3): 169-176.
- Ahn, K., K. Song, H. Cha and I. Yeom (1999). "Removal of ions in nickel electroplating rinse water using low-pressure nanofiltration." Desalination 122(1): 77-84.
- Aktaş, N. and A. Tanyolaç (2003). "Kinetics of laccase-catalyzed oxidative polymerization of catechol." Journal of Molecular Catalysis B: Enzymatic 22(1-2): 61-69.
- American Water Association (Ed.) (1999). "Standard methods for the examination of water and wastewater." Washington American Public Health Association, Washington (USA).
- Amy, G., B. Alleman and C. Cluff (1990). "Removal of dissolved organic matter by nanofiltration." Journal of Environmental Engineering 116(1): 200-205.
- Andersen, H., H. Siegrist, H. Bent and T. Ternes (2003). "Fate of estrogens in a municipal sewage treatment plant." Environmental Science Technology 37(18): 4021-4026.
- Andreozzi, R. and R. Marotta (1999). "Ozonation of p-chlorophenol in aqueous solution." Journal of Hazardous Materials 69(3): 303-317.
- Andreozzi, R., V. Caprio, A. Insola and R. Marotta (1999). "Advanced oxidation processes (AOP) for water purification and recovery." Catalysis Today 53(1): 51-59.
- Anjaneyulu, A., N. Chary and D. Raj (2005). "Decolourization of industrial effluents-available methods and emerging technologies-a review." Reviews in Environmental Science and Biotechnology 4(4): 245-273.
- Al-Almoudi, A. and R. Lovitt (2007). "Fouling strategies and the cleaning system of NF membranes and factors affecting cleaning efficiency." Journal of Membrane Science 303(1-2): 4-28.
- Al-kdasi, A., A. Idris, K. Saed and C. Guan (2004). "Treatment of textile wastewater by advanced oxidation processes - a review." Global NEST: The International Journal 6(3): 222-230.
- Al-Sofi, M., A. Hassan, G. Mustafa, A. Dalvi, M. Kither (1998). "Nanofiltration as a means of achieving higher TBT of ≥ 120 degrees C in MSF." Desalination 118 (1-3): 123-129.
- Alcaina, M., S. Barredo, A. Bes, M. Iborra, A. Iborra and J. Mendoza (2009). "Nanofiltration as a final step towards textile wastewater reclamation." Desalination 240(1-3): 290-297.

- Alizadeh, M., F. Ota, K. Hosoi, M. Kato, T. Sakai and M. Satter (2006). "Altered allergic cytokine and antibody response in mice treated with Bisphenol A." *Journal of Investigative Medicine* 53(1/2):70-80.
- Alvares, A., C. Diaper, S. Parsons (2001). "Partial oxidation by ozone to remove recalcitrance from wastewaters - a review." *Environmental Technology* 22(4): 409-427.
- Alves, P., M. Brum, B. de Andrade and P. Netto (2008). "Determination of synthetic dyes in selected foodstuffs by high performance liquid chromatography with UV Alves DAD detection." *Food Chemistry* 107(1): 489-496.
- Arroyave, J., L. Garcés and J. Mejía (2009). "Empleo del reactivo de Fenton para la degradación del colorante Tartrazina." *Revista Lasallista de Investigación* 6(1): 27-34.
- Arslan, I., B. Hande and J. Schmidt (2008). Advanced oxidation of acid and reactive dyes: Effect of Fenton treatment on aerobic, anoxic and anaerobic processes. *Dyes and Pigments* 78(2): 117-130.
- Ashkenazi, P., C. Yarnitzky and M. Cais (1991). "Determination of synthetic food colours by means of a novel sample preparation system." *Analytica Chimica Acta* 248(1): 289-299.
- Aydiner, C., Y. Kaya, Z. Beril Gönder and I. Vergili (2010). "Evaluation of membrane fouling and flux decline related with mass transport in nanofiltration of tartrazine solution." *Journal of Chemical Technology and Biotechnology* 85(9): 1229-1240.
- Azbar, N., T. Yonar and K. Kestioglu (2004). "Comparison of various advanced oxidation processes and chemical treatment methods for COD and colour removal from a polyester and acetate fiber dyeing effluent." *Chemosphere* 55(1): 35-43.
- Balanec, B., M. Vourch, M. Rabiller-Baudry and B. Chaufe (2005). "Comparative study of different nanofiltration and reverse osmosis membranes for dairy effluent treatment by dead-end filtration." *Separation and Purification Technology* 42(2): 195-200.
- Baldrian, P. (2006). "Fungal laccases-occurrence and properties." *FEMS Microbiology Reviews* 30: 215-242.
- Banerjee, P., S. DasGupta and S. De (2007). "Removal of dye from aqueous solution using a combination of advanced oxidation process and nanofiltration." *Journal of Hazardous Materials* 140(1-2): 95-103.
- Bautista-Toledo, I., G. Ferro, U. Rivera, C. Moreno and F. Vegas (2005). "Bisphenol A removal from water carbon. Effects of carbon characteristics and solution chemistry." *Environmental Science and Technology* 39(16): 6246-6250.
- Bautista, P., A. Mohedano, M. Gilarranz, J. Casas and J. Rodríguez (2007). "Application of Fenton oxidation to cosmetic wastewaters treatment." *Journal of Hazardous Materials*. 143(1-2): 128-134.
- Beach, E., R. Malecky, R. Gil, C. Horwitz y and T Collins (2011). "Fe-TAML/hydrogen peroxide degradation of concentrated solutions of the commercial azo dye tartrazine." *Catalysis Science & Technology* 1(3): 437-443.
- Behnajady, M., N. Modirshahla and F. Ghanbary (2007). "A kinetic model for the decolorization of C.I. Acid Yellow 23 by Fenton process." *Journal of Hazardous Materials* 148(1-2): 98-102.

- Beltran, F., J. Garcia-Araya and B. Acedo (1994). "Advanced oxidation of atrazine in water. Part I: ozonation." *Water Research* 28(10): 2153-2164.
- Bellona C. and J. Drewes (2005). "The role of membrane surface charge and solute physico-chemical properties in the rejection of organic acids by NF membranes." *Journal of Membrane Science* 249(1-2): 227-234.
- Bellona, C., M. Marts and J. Drewes (2010). "The effect of organic membrane fouling on the properties and rejection characteristics of nanofiltration membranes." *Separation and Purification Technology* 74(1): 44-54.
- Benitez, F., J. Acero, F. Real, F. Rubio and A. Leal (2001). "The role of hydroxyl radicals for the decomposition of p-hydroxy phenylacetic acid in aqueous solutions." *Water Research* 35(5): 1338-1343.
- Benitez, F., J. Acero, F. Real and C. Garcia (2009). "Removal of phenyl-urea herbicides in ultrapure water by ultrafiltration and nanofiltration processes." *Water Research* 43(2): 267-276.
- Bergendahl, J. and J. O'Shaughnessy (2004) "Advanced Oxidation Processes for Wastewater Treatment." *Journal of the New England Water Environment Association* 38(2): 179-189.
- Bernat, X. (2010). "Treatment of biorefractory wastewater through membrane-assisted oxidation processes." Doctoral thesis. Universitat Rovira i Virgili. Tarragona (Spain).
- Bigda, R. (1996). "Fenton's chemistry: an effective advanced oxidation process." *Journal of Advanced Science and Engineering* 6(3): 34-39.
- Bing-zhi, D., W. Lin, G. Nai-yun (2008). "The removal of bisphenol A by ultrafiltration." *Desalination* 221(1-3): 312-317.
- Bing-zhi, D., C. Hua-qiang, W. Lin, X. Sheng-ji and G. Nai-yun (2010). "The removal of bisphenol A by hollow fiber microfiltration membrane." *Desalination* 250(2): 693-697.
- Borneman, Z., V. Gökmen and H. Nijhuis (1997). "Selective removal of polyphenols and brown colour in apple juices using PES/PVP membranes in a single-ultrafiltration process." *Journal of Membrane Science* 134(2): 191-197.
- Bowen, W., A. Mohammad and N. Hilal (1997). "Characterisation of nanofiltration membranes for predictive purposes - use of salts, uncharged solutes and atomic force microscopy." *Journal of Membrane Science* 126(1): 91-105.
- Braeken, L. (2005). "Influence of fouling by dissolved organic compounds in aqueous solution on the performance of nanofiltration." PhD thesis. Katholieke Universiteit Leuven. Leuven (Belgium).
- Brandhuber, P. and G. Amy (1998). "Alternative methods for membrane filtration of arsenic from drinking water." *Desalination* 117(1-3): 1-10.
- Brindle, K. and T. Stephenson (1996). "The application of membrane biological reactors for the treatment of wastewaters." *Biotechnology and Bioengineering* 49(6): 601-610.
- Brown D (1987). "Effects of colorants in the aquatic environment." *Ecotoxicology and Environmental Safety* 13: 139-147.

- Buxton, G., C. Greenstock, W. Helman and A. Ross (1988). "Critical review of rate constants for reactions of hydrated electrons, hydrogen atoms and hydroxyl radicals ($\bullet\text{OH}/\bullet\text{O}^-$) in aqueous solution." *Journal of Physical and Chemical Reference Data* 17(2): 513-886.
- Capar, G., L. Yilmaz, U. Yetis (2006). "Reclamation of acid dye bath wastewater: effect of pH on nanofiltration performance." *Journal of Membrane Science* 281(1-2): 560-569.
- Chakrabarty, B., A. Ghoshal and M. Purkait (2008). "Effect of molecular weight of PEG on membrane morphology and transport properties." *Journal of membrane Science* 309(1-2): 209-221.
- Chang, H., K. Choo, B. Lee and S. Choi (2009a). "The methods of identification, analysis, and removal of endocrine disrupting compounds (EDCs) in water." *Journal of Hazardous Materials* 172(1): 1-12.
- Chang, I., S. Lee and E. Choe (2009b). "Digital textile printing (DTP) wastewater treatment using ozone and membrane filtration." *Desalination* 235(1-3): 110-121.
- Chaturapruerk, A. (2003). "Ozonation combined with membrane bio-reactor for landfill leachate treatment." Master thesis. Asian Institute of Technology School of Environment, Resources and Development. Pathumthani (Thailand).
- Chen, R. and J. Pignatello (1997). "Role of quinone intermediates as electron shuttles in Fenton and photoassisted Fenton oxidations of aromatic compounds." *Environmental Science and Technology* 31(8): 2399-2406.
- Cheryan, M. and N. Rajagopalan (1998). Membrane processing of oily streams. Wastewater treatment and waste reduction." *Journal of Membrane Science* 151(1): 13-28.
- Cheryan, M. (1998). "Ultrafiltration and Microfiltration Handbook." Technomic Publishing Co. Inc., Lancaster (UK).
- Choi, K., S. Kim, C. Kim, K. Park (2006). "Removal efficiencies of endocrine disrupting chemicals by coagulation/flocculation, ozonation, powdered/ granular activated carbon adsorption, and chlorination." *Korean Journal of Chemical Engineering* 23(3): 399-408.
- Chung, K. (1983). "The significance of azo-reduction in mutagenesis and carcinogenesis of azo dyes." *Mutation Research/Reviews in Genetic Toxicology* 114(3): 269-281
- Claus, H. (2003). "Laccases and their occurrence in prokaryotes." *Archives of Microbiology* 179(3): 145-150.
- Clesceri, L., A. Greenberg, R. Trusel and M. Franson (1989). "Standard methods for the examination of water and wastewater." 17th Ed. American Public Health Association and American Water Works Association, Washington (USA).
- Cluff, C. (1992). "Slow sand/nanofiltration treatment for secondary treated wastewater." *Desalination* 88(1-3): 53-67.
- Comerton, A., R. Andrews, D. Bagley and C. Hao (2008). "The rejection of endocrine disrupting and pharmaceutically active compounds by NF and RO membranes as a function of compound and water matrix properties." *Journal of Membrane Science* 313(1-2): 323-335.
- Commission of the European Communities (CEC), "On the implementation of the Community strategy for endocrine disrupters-a range of substances suspected of interfering with the

hormone systems of humans and wildlife". Communication from the Commission to the Council and the European Parliament, Brussels, COM (2001) 262 final (2001).

- Conlon, W. (1985). "Pilot field test data for prototype ultra low pressure reverse osmosis elements." *Desalination* 56: 203-226.
- Connell, D. (1990). "Bioaccumulation of Xenobiotic compounds." CRC, Press, Boca Raton (USA).
- Cornelissen, E. (1997). "Membrane fouling in waste water filtration. Causes, consequences and prevention." PhD thesis. Twente University. Enschede (The Netherlands).
- Côté, P., M. Masini and D. Mourato (2004). "Comparison of membrane options for water reuse and reclamation." *Desalination* 167: 1-11.
- Davidson, G. and W. Deen (1988). "Hydrodynamic theory for the hindered transport of flexible macromolecules in porous membranes." *Journal of Membrane Science* 35(2): 167-192.
- de Souza, S., E. Forgiarini and A. de Souza (2007). "Toxicity of textile dyes and their degradation by the enzyme horseradish peroxidase (HRP)." *Journal of Hazardous Materials* 147(3): 1073-1078.
- Deborde, M., S. Rabouan, P. Mazellier, J. Duguet and B. Legube (2008). "Oxidation of bisphenol A by ozone in aqueous solution." *Water Research* 42(16): 4299-4308.
- Devlin, J. and T. David (1992). "Tartrazine in atopic eczema." *Archives of Disease in Childhood* 67(6): 709-711.
- Donnan, F. (1911). "Theory of membrane equilibria and membrane potentials in the presence of non-dialysing electrolytes. A contribution to physical-chemical physiology, *Zeitschrift für chemie* 17(10): 572-581.
- EC (European Commission), 2008. Commission Directive 2008/128/EC of 22 December 2008 laying down specific purity criteria concerning colours for use in foodstuffs.
- EC (European Community), 1994. European Parliament and Council Directive 94/36/EC of 30 June 1994 on colours for use in foodstuffs.
- Edwards, W., W. Leukes, J. Bezuidenhout (2002). "Ultrafiltration of petrochemical industrial wastewater using immobilised manganese peroxidase and laccase: application in the defouling of polysulphone membranes." *Desalination* 149(1-3): 275-278.
- Ellouze, E., N. Tahri and R. Amar (2012). "Enhancement of textile wastewater treatment process using Nanofiltration." *Desalination* 286: 16-23.
- Élysée-Collen, B. and R. Lencki (1997). "Protein ultrafiltration concentration polarization layer flux resistance I. Importance of protein layer morphology on flux decline with gelatine." *Journal of Membrane Science* 129(1): 101-113.
- Erickson, B. (2008). "Bisphenol A under scrutiny." *Chemical & Engineering News* 86(22): 36-39.
- Eriksson, P. (1988). "Nanofiltration extends the range of membrane filtration." *Environmental Progress* 7(1): 58-62.
- Erjavec, B., R. Kaplan, P. Djinović and A. Pintar (2013). "Catalytic wet air oxidation of bisphenol A model solution in a trickle-bed reactor over titanate nanotube-based catalysts." *Applied Catalysis B: Environmental* 132-133: 342-352.

- Esplugas, S., D. Bila, L. Krause and M. Dezotti (2007). "Ozonation and advanced oxidation technologies to remove endocrine disrupting chemicals (EDCs) and pharmaceuticals and personal care products (PPCPs) in water effluents." *Journal of Hazardous Materials* 149(3): 631-642.
- Fenton, H. (1894). "Oxidation of tartaric acid in presence of iron." *Journal of the Chemical Society, Transactions* 65: 899-910.
- Fernández-Fernández, M., M. Sanromán, D. Moldes (2012). "Recent developments and applications of immobilized laccase." *Biotechnology Advances* 31(8): 1808-1825.
- Fersi, C., L. Gzara and M. Dhahbi (2005). "Treatment of textile effluents by membrane technologies." *Desalination* 185(1-3): 399-409.
- Flemming, H. (1995). "Biofouling bei Membranprozessen." German, Springer- Verlag, Berlin - Heidelberg (Germany).
- Forgacs, E., T. Cserháti and G. Oros (2004). Removal of synthetic dyes from wastewaters: a review." *Environment International* 30(7): 953-971.
- Fragoso, C., R. Battisti, C. Miranda and P. De Jesus (2009). "Kinetic of the degradation of C.I. Food Yellow 3 and C.I. Food Yellow 4 azo dyes by the oxidation with hydrogen peroxide." *Journal of Molecular Catalysis A: Chemical* 301(1-2): 93-97.
- Fukahori, S., H. Ichiura, T. Kitaoka and H. Tanaka (2003). "Capturing of bisphenol A photodecomposition intermediates by composite TiO₂-zeolite sheets." *Applied Catalysis B: Environmental* 46(3): 453-462.
- García, V., S. Lyko, S. Esplugas, Th. Wintgens and Th. Melin (2006). "Ultrafiltration of aqueous solutions containing organic polymers." *Desalination* 189(1-3): 110-118.
- Garoma, T. and S. Matsumoto (2009). "Ozonation of aqueous solution containing bisphenol A: Effect of operational parameters." *Journal of Hazardous Materials* 167(1-3): 1185-1191.
- Garoma, T., S. Matsumoto, Y. Wu and R. Klinger (2010). "Removal of bisphenol A and its reaction-intermediates from aqueous solution by ozonation. Ozone: Science and Engineering 32(5): 338-343.
- Ghisari M and E. Bonfeld-Jorgensen (2005). "Impact of environmental chemicals on the thyroid hormone function in pituitary rat GH3 cells." *Molecular and Cellular Endocrinology* 244(1/2): 31-41.
- Giardina, P., V. Faraco, C. Pezzella, A. Piscitelli, S. Vanhulle and G.Sannia (2010). "Laccases: a never-ending story." *Cellular and Molecular Life Science* 67(3): 369-85.
- Glaze, W., J. Kang and D. Chapin (1987). "The chemistry of water treatment processes involving ozone, hydrogen peroxide, and ultraviolet radiation." *Ozone Science and Engineering* 9(4): 335-352.
- Gogate, P. and A. Pandit (2004). "A review of imperative technologies for wastewater treatment I: oxidation technologies at ambient conditions." *Advances in Environmental Research* 8(3-4): 501-551.
- Gomes, A., I. Gonçalves and M. de Pinho (2005). "The role of adsorption on nanofiltration of azo dyes." *Journal of Membrane Science* 255(1-2): 157-165.

- Gómez, M., G. Garralón, F. Plaza, R. Vilchez, E. Hontoria and M. Gómez (2007). "Rejection of endocrine disrupting compounds (bisphenol A, bisphenol F and triethyleneglycol dimethacrylate) by membrane technologies." *Desalination* 212(1-3): 79-91.
- Gould, J. and K. Groff (1987). "The kinetics of ozonolysis of synthetic dyes." *Ozone Science Engineering* 9(2): 153-164.
- Guedes, A., L. Madeira, R. Boaventura and C. Costa (2003). "Fenton oxidation of cork cooking wastewater-overall kinetic analysis." *Water Research* 37(13): 3061-3069.
- Guifang, L., M. Jun, L. Xuchun and Q. Qingdong (2009). "Adsorption of bisphenol A from aqueous solution onto activated carbons with different modification treatments." *Journal of Hazardous Materials* 164(2-3): 1275-1280.
- Gül, Ş. And Ö. Özcan-Yildirim (2009). "Degradation of reactive red 194 and reactive yellow 145 azo dyes by O₃ and H₂O₂/UV processes." *Chemical Engineering Journal* 155(3): 684-690.
- Guo, Z. and R. Feng (2009). "Ultrasonic irradiation-induced degradation of low-concentration bisphenol A in aqueous solution." *Journal of Hazardous Materials* 163(2-3): 855-860.
- Gupta, V., R. Jain, A. Nayak, S. Agarwal and M. Shrivastova (2011). "Removal of the hazardous dye-Tartrazine by photodegradation on titanium dioxide surface." *Materials Science and Engineering: C* 31(5): 1062-1067.
- Gurung, N., S. Ray, S. Bose and V. Rai (2013). "A Broader View: Microbial Enzymes and Their Relevance in Industries, Medicine, and Beyond." *BioMed Research International* 2013: 1-18.
- Hao, O., H. Kim, and P. Chiang (2000). "Decolorization of wastewater." *Environmental Science and Technology* 30(4): 449-502.
- Hassan, A., M. Al-Sofi, A. Al-Amoudi, A. Jamaluddin, A. Farooque, A. Rowaili, A. Dalvi, N. Kither, G. Mustafa and I. Al-Tisan (1998). "A new approach to thermal seawater desalination processes using nanofiltration membranes (Part 1)." *Desalination* 118 (1-3): 35-51.
- Hassan, A., A. Farooque, A. Jamaluddin, A. Al-Amoudi, M. Al-Sofi, A. Al-Rubaian, N. Kither, I. Al-Tisan, A. Rowaili (2000). "A demonstration plant based on the new NF SWRO process." *Desalination* 131 (1-3): 157--171.
- He, P., Z. Zheng, H. Zhang, L. Shao and Q. Tang (2009). "PAEs and BPA removal in landfill leachate with Fenton process and its relationship with leachate DOM composition." *Science of the Total Environment* 407(17): 4928-4933.
- Heng, S., K. Yeung, M. Djafer and J. Schrotter (2007). "A novel membrane reactor for ozone water treatment." *Journal of Membrane Science* 289(1-2): 67--75.
- Her, N., G. Amy, A. Plottu-Pecheux and Y. Yoon (2007). "Identification of nanofiltration membrane foulants." *Water Research* 41(17): 3936--3947.
- Ho, H., W. Chan, A. Blondy, K. Yeung and J. Schrotter (2012). "Experiment and modeling of advanced ozone membrane reactor for treatment of organic endocrine disrupting pollutants in water." *Catalysis Today* 193(1): 120-127.
- Hoigné, J. and H. Bader (1976). "Role of Hydroxyl Radical Reactions in Ozonation Processes in Aqueous Solutions." *Water Research* 10(5): 377-386.

- Hoigné, J. and H. Bader (1983). "Rate constants of reaction of ozone with organic and inorganic compounds in water. Part II. Dissociating organic compounds." *Water Research* 17(2): 185-194.
- Hong, S. and M. Elimelech (1997). "Chemical and physical aspects of natural organic matter (NOM) fouling of nanofiltration membranes." *Journal of Membrane Science* 132(2): 159-181.
- Hong-Mei, L. and J. Nicell (2008). "Biocatalytic oxidation of bisphenol A in a reverse micelle system using horseradish peroxidase." *Bioresource Technology* 99(10): 4428-4437.
- Huang, C., C. Dong and Z. Tang (1993). "Advanced chemical oxidation: Its present role and potential future in hazardous waste treatment." *Waste Management* 13(5-7): 361-377.
- Huang, Q. and W. J. Weber (2005) "Transformation and Removal of Bisphenol A from Aqueous Phase via Peroxidase-Mediated Oxidative Coupling Reactions: Efficacy, Products, and Pathways." *Environmental Science and Technology* 39(16): 6029-6036.
- Hunger, K. (2003). "Industrial Dyes: Chemistry, Properties, and Applications." Wiley-VCH, Weinheim; Cambridge (UK).
- Hunsberger, J. (1977). "Standard reduction potentials", in: R.C. Weast (Ed.), *Handbook of Chemistry and Physics*, 58th Ed. CRC Press, Ohio (USA).
- Inoue, M., Y. Masuda, F. Okada, A. Sakurai, I. Takahashi and M. Sakakibara (2008). "Degradation of bisphenol A using sonochemical reactions." *Water Research* 42(6-7): 1379-1386.
- Ioan, I., S. Wilson, E. Lundanes and A. Neculai (2007). "Comparison of Fenton and sono-Fenton bisphenol A degradation." *Journal of Hazardous Materials* 142(1-2): 559-563.
- Irmak, S., O. Erbatur and A. Akgerman (2005). "Degradation of 17-estradiol and bisphenol A in aqueous medium by using ozone and ozone/UV techniques." *Journal of Hazardous Materials* 126(1-3): 54-62.
- Ishido M., Y. Masuo, M. Kunimoto, S. Oka and M. Morita (2004). "Bisphenol A causes hyperactivity in the rat concomitantly with impairment of tyrosine hydroxylase immunoreactivity." *Journal of Neuroscience Research* 76(3):423--433.
- Ispas, C., M. Ravalli, A. Steere and S. Andreescu (2010). "Multifunctional biomagnetic capsules for easy removal of phenol and bisphenol A." *Water Research* 44(6):1961-1969.
- Janknecht, P., P. Wilderer, C. Picard and A. Labort (2001). "Ozone water contacting by ceramic membranes." *Separation and Purification Technology* 25(1-3): 341-346.
- Jasen, R. (2005). "Ozonation of humic substances in a membrane contactor. Mass transfer, product characterization and biodegradability." PhD Thesis. University of Twente. Enschede (The Netherlands).
- Jarusutthirak, C., S. Mattaraj and R. Jiratananon (2007). Factors affecting nanofiltration performances in natural organic matter rejection and flux decline." *Separation and Purification Technology* 58(1): 68-75.
- Jeng, F.-Y. and S.-C. Lin (2006). "Characterization and application of PEGylated horseradish peroxidase for the synthesis of poly(2-naphthol)." *Process Biochemistry* 41(7): 1566-1573.

- Jiang, J., Q. Yin, J. Zhou and P. Pearce (2005). "Occurrence and treatment trials of endocrine disrupting chemicals (EDCs) in wastewaters." *Chemosphere* 61(4): 544-50.
- Kabdash I, T. Olmez and O. Tunay (2002). "Factors affecting color removal from reactive dye bath by ozonation." *Water Science and Technology* 45(12): 261-270.
- Kamel, M and H. El-Iethy (2011). "The potential health hazard of tartrazine and levels of hyperactivity, anxiety-like symptoms, depression and anti-social behaviour in Rats." *Journal of American Science* 7(6): 1211-1218.
- Kang, Y., M. Cho and K. Hwang (1999). "Correction of hydrogen peroxide interference on standard chemical oxygen demand test." *Water Research* 33(5): 1247-1251.
- Kang, J. and F. Kondo (2002). "Bisphenol a degradation by bacteria isolated from river water." *Archives of Environmental Contamination Toxicology* 43: 265--269.
- Kang, N., D. Lee and J. Yoon (2002). "Kinetic modeling of Fenton oxidation of phenol and monochlorophenols." *Chemosphere* 47(9): 915-924.
- Kang, J., F. Kondo and Y. Katayama (2006). Human exposure to bisphenol A. *Toxicology* 226(2-3): 79-89.
- Karnik, B., S. Davies, K. Chen, D. Jaglowski, M. Baumann and S. Masten (2005). "Effects of ozonation on the permeate flux of nanocrystalline ceramic membranes." *Water Research* 39(4): 728--734.
- Karthikeyan, S., A. Titus, A. Gnanamani, A. Mandal and G. Sekaran (2011). "Treatment of textile wastewater by homogeneous and heterogeneous Fenton oxidation processes." *Desalination* 281: 438-445.
- Katsumata, H., S. Kawabe, S. Kaneco, T. Suzuki and O. Kiyohisa (2004). "Degradation of bisphenol A in water by the photo-Fenton reaction." *Journal of Photochemistry and Photobiology A: Chemistry* 162(2-3): 297--305.
- Kavitha, V. and K. Palanivelu (2005). "Destruction of cresols by Fenton oxidation process." *Water Research* 39(13): 3062-3072.
- Kaya, Y., H. Barlas and S. Arayici (2009). "Nanofiltration of Cleaning-in-Place (CIP) wastewater in a detergent plant: Effects of pH, temperature and transmembrane pressure on flux behaviour." *Separation and Purification Technology* 65(2): 117-129.
- Kim, Y. and J. Nicell (2006). "Impact of reaction conditions on the laccase-catalyzed conversion of bisphenol A." *Bioresource Technology* 97(12): 1431-1442.
- Kim, J., P. Park, C. Lee, H. Kwon, S. Lee (2008). "A novel hybrid system for the removal of endocrine disrupting chemicals: Nanofiltration and homogeneous catalytic oxidation." *Journal of Membrane Science* 312(1-2): 66-75.
- Kimura, K., G. Amy, J. Drewes, T. Heberer, T. Kim, Y. Watanabe (2003). "Rejection of organic micropollutants (disinfection by-products, endocrine disrupting chemicals and pharmaceutically active compounds) by NF/RO membranes." *Journal of Membrane Science* 227(1-2): 113-121.
- Kimura, K., S. Toshima, G. Amy and Y. Watanabe (2004). Rejection of neutral endocrine disrupting compounds (EDCs) and pharmaceutical active compounds (PhACs) by RO membranes." *Journal of Membrane Science* 245(1-2): 71-78.

- Kinman, R. (1975). "Water and Wastewater Disinfection with Ozone: A Critical Review." *Critical Reviews in Environmental Control* 5: 141-152.
- Kiso, Y., T. Kitao, K. Jinno and M. Miyagi (1992). "The effects of molecular width on permeation of organic solute through cellulose-acetate reverse-osmosis membranes. *Journal of Membrane Science* 74(1-2): 95-103.
- Kiso, Y., Y. Nishimura, T. Kitao and K. Nishimura (2000). "Rejection properties of non-phenylic pesticides with nanofiltration membranes." *Journal of Membrane Science* 171(2): 229-237.
- Kiso, Y., T. Kon, T. Kitao and K. Nishimura (2001a). "Rejection properties of alkyl phthalates with nanofiltration membranes." *Journal of Membrane Science* 182(1-2): 205-214.
- Kiso, Y., Y. Sugiura, T. Kitao and K. Nishimura (2001b). "Effects of hydrophobicity and molecular size on rejection of aromatic pesticides with nanofiltration membranes." *Journal of Membrane Science* 192(1-2): 1-10.
- Klibanov, A. (1997). "Why are enzymes less active in organic solvents than in water?." *Trends in Biotechnology* 15(3): 97--101.
- Ko C. and S. Chen (2008). "Enhanced removal of three phenols by laccase polymerization with MF/UF membranes." *Bioresource Technology* 99(7): 2293-2298.
- Kolpin, D., E. Furlong, M. Meyer, E. Thurman, S. Zaugg, L. Barber and H. Buxton (2002). "Pharmaceuticals, hormones, and other organic wastewater contaminants in U.S. streams, 1999–2000: a national reconnaissance." *Environmental Science and Technology* 36(6): 1202-1211.
- Koops, G. (1995). "Nomenclature and symbols in membrane science and technology." 1st Ed. CIP-data Koninklijke bibliotheek, Den Haag (The Netherlands).
- Korshin, G., J. Kim and L. Gan (2006). "Comparative study of reactions of endocrine disruptors bisphenol A and diethylstilbestrol in electrochemical treatment and chlorination." *Water Research* 40(5): 1070--1078.
- Kosutic, K., L. Furac, L. Sipos and B. Kunst (2005). "Removal of arsenic and pesticides from drinkingwater by nanofiltration membranes." *Separation and Purification Technology* 42(2): 137--144.
- Koutsoqeorqopoulou, L., C. Maravelias, G. Methenitou and A. Koutselinis (1998). "Immunological aspects of the common food colorants, Amaranth and Tartrazine." *Veterinary and Human Toxicology* 40(1): 1-4.
- Kramer, K., M. Kanost, T. Hopkins, H. Jiang, Y. Zhu, R. Xu, J. Kerwin and F. Turecek (2001). "Oxidative conjugation of catechols with proteins in insect skeletal systems." *Tetrahedron* 57(2): 385--392.
- Krishnan, A., P. Stathis, S. Permuth, L. Tokes and D. Feldman (1993). "Bisphenol-A: an estrogenic substance is released from polycarbonate flasks during autoclaving" *Endocrinology* 132(6): 2279-2286.
- Kudanga, T., G. Nyanhongo, G. Guebitz, S. Burton (2011). "Potential applications of laccase-mediated coupling and grafting reactions: A review." *Enzyme and Microbial Technology* 48(3): 195-208.

- Kuo W. (1992). "Decolorizing dye wastewater with Fenton's reagent." *Water Research* 26(7): 881-886.
- Kuramitz, H., M. Matsushita and S. Tanaka (2004). "Electrochemical removal of bisphenol A based on the anodic polymerization using a column type carbon fiber electrode." *Water Research* 38(9): 2331-2338.
- Kwon, B., D. Lee, N. Kang and J. Yoon (1999). "Characteristics of P-Chlorophenol Oxidation by Fenton's Reagent." *Water Research* 33(9): 2110-2118.
- Labbez, C., P. Fievet, A. Szymczyk, A. Vidonne, A. Foissy and J. Pagetti (2003). "Retention of mineral salts by a polyamide nanofiltration membrane." *Separation and Purification Technology* 30(1): 47--55.
- Langlais, B., D. Reckhow and D. Brink (Eds). (1991). "Ozone in drinking water treatment: Application and Engineering." AWWARF and Lewis Publishers, Boca Raton (USA).
- Latorre, A., S. Lacorte and D. Barceló (2002). "Presence of nonylphenol, octylphenol and bisphenol a in two aquifers close to agricultural, industrial and urban areas." *Chromatography* 57(2): 111--116.
- Ledakowicz, S., R. Maciejewska, J. Perkowski and A. Bin, (2001). "Ozonation of reactive blue 81 in the bubble column." *Water Science and Technology* 44(5): 47-52.
- Lee, J., H. Park and J. Yoon (2003). "Ozonation characteristics of bisphenol A in water." *Environmental Technology* 24(2): 241--248.
- Legrini, O., E. Oliveros and A. Braun (1993). "Photochemical processes for water treatment." *Chemical Reviews* 93 (2): 671-698.
- Legube, B., S. Guyon, H. Sugimitsu and M. Dore (1983). "Ozonation of some aromatic compounds in aqueous-solution-styrene, benzaldehyde, naphthalene, diethylphthalate, ethyl and chloro benzenes." *Ozone Science Engineering* 5(3): 151-170.
- Li, Q. and M. Elimelech (2004). "Organic fouling and chemical cleaning of nanofiltration membranes: measurements and mechanisms." *Environmental Science and Technology* 38(17): 4683--4693.
- Liikanen, R. (2006). Nanofiltration as a refining phase in surface water treatment. PhD Thesis. Helsinki University of Technology. Helsinki (Finland).
- Lin, S. and C. Peng (1995). "Treatment of textile wastewater by Fenton's reagent." *Journal of Environmental Science and Health Part: A* 30(1): 89--101.
- Lin, S. and C. Lo (1997). "Fenton process for treatment of desizing wastewater." *Water Research* 31(8): 2050-2056.
- Liu, G., J. Ma, X. Li and Q. Qin (2009a). "Adsorption of bisphenol A from aqueous solution onto activated carbons with different modification treatments." *Journal of Hazardous Materials* 164(2-3): 1275-1280.
- Liu, Z., Y. Kanjo and S. Mizutani (2009b). "Removal mechanisms for endocrine disrupting compounds (EDCs) in wastewater treatment - physical means, biodegradation, and chemical advanced oxidation: A review." *Science of The Total Environment* 407(2): 731-748.

- Lockey, S. (1977). "Hypersensitivity to Tartrazine (FD & C yellow No.5) and other dyes and additives present in foods and pharmaceutical products." *Annals of Allergy*, 38(3): 206-210.
- Lonsdale, H., U. Merten and R. Riley (1965). "Transport properties of cellulose acetate osmotic membranes." *Journal of Applied Polymer Science* 9(4): 1341-1362.
- Lopez, A., M. Pagano, A. Volpe and A. Di Pinto (2004). "Fenton's pre-treatment of mature landfill leachate." *Chemosphere* 54(7): 1005--1010.
- López, C., A. Valade, B. Combourieu, I. Mielgo, B. Bouchon and J. Lema (2004). "Mechanism of enzymatic degradation of the azo dye Orange II determined by ex situ 1H nuclear magnetic resonance and electrospray ionization-ion trap mass spectrometry." *Analytical Biochemistry* 335(1): 135--149.
- Lu, N., Y. Lu, F. Liu, K. Zhao, X. Yuan, Y. Zhao, Y. Li, H. Qin and J. Zhu (2013). " $\text{H}_3\text{PW}_{12}\text{O}_{40}/\text{TiO}_2$ catalyst-induced photodegradation of bisphenol A (BPA): Kinetics, toxicity and degradation pathways." *Chemosphere* 91(9): 1266-1272.
- Luis P., M. Saquib, C. Vinckier, and B. Van der Bruggen (2011). "Effect of membrane filtration on ozonation efficiency for removal of atrazine from surface water." *Industrial & Engineering Chemistry Research* 50(14): 8686--8692.
- Ma, Y., S. Huang and J. Lin (2000). "Degradation of p-nitrophenol using the Fenton process." *Water Science and Technology* 42(1-2): 155-160.
- Majeau, J., S. Brar and R. Tyagi (2010). "Laccases for removal of recalcitrant and emerging pollutants." *Bioresource Technology* 101(7): 2331-2350.
- Malato, S., J. Blanco, A. Vidal and C. Richter (2002). "Photocatalysis with solar energy at a pilot-plant scale: an overview." *Applied Catalysis B: Environmental* 37(1): 1-15.
- Mallevalle, J., P. Odendall, and M. Wiesner (1996). "Water treatment membrane processes." McGraw-Hill, New York (USA).
- Marmagne, O. and C. Coste (1996). "Color removal from textile plant effluents." *American Dyestuff Reports* 85(4): 5-21.
- Martínez, L., G. Hodaifa, S. Rodríguez, J. Giménez and J. Ochando (2011). "Degradation of organic matter in olive-oil mill wastewater through homogeneous Fenton-like reaction" *Chemical Engineering Journal* 173(2): 503-510.
- Masciola, D. (1999). "Effects of feed oil content, transmembrane pressure and membrane rotational speed on permeate water quality in high-shear rotary ultrafiltration." Master thesis. West Virginia University. Virginia (EEUU).
- Matsui, Y., D. Knappe and R. Takagi (2002). "Pesticide adsorption by granular activated carbon adsorbers. Effect of natural organic matter preloading on removal rates and model simplification." *Environmental Science Technology* 36(15): 3426-3431.
- Meijers, R., E. Oderwald-Muller, P. Nuhn., J. Kruithof (1995). "Degradation of pesticides by ozonation and advanced oxidation." *Ozone: Science and Engineering* 17 (6): 673.
- Metcalf and Eddy. (2003). "Wastewater engineering. Treatment and Reuse." 4th Ed. Mc Graw Hill. New York (USA). p. 1-23.
- Mijangos, F., F. Varona and N. Villota (2006). Changes in solution color during phenol oxidation by Fenton reagent." *Environmental Science and Technology* 40(17): 5538-5543.

- Mittal, A., L. Kurup and J. Mittal (2007). "Freundlich and Langmuir adsorption isotherms and kinetics for the removal of Tartrazine from aqueous solutions using hen feathers." *Journal of Hazardous Materials* 146(1-2): 243-248.
- Ministry of Health, Labour and Welfare of Japan (Eds.) (2000). "Exposure and behaviour researches of endocrine disrupting chemicals in tap water." Japan.
- Modaressi, K., K. Taylor, J. Bewtra and N. Biswas (2005). "Laccase-catalyzed removal of bisphenol-A from water: Protective effect of PEG on enzyme activity." *Water Research* 39(18): 4309-4316.
- Mulder, M. (1997). "Basic Principles of Membrane Technology." 2nd Ed. Kluwer Academic Publishers (The Netherlands).
- Muthukumar, M., D. Sargunamani, N. Selvakumar and J. Venkata Rao (2004). "Optimisation of ozone treatment for colour and COD removal of acid dye effluent using central composite design experiment." *Dyes and Pigments* 63(2): 127--134.
- Nakada, N., H. Shinohara, A. Murata, K. Kiri, S. Managaki, N. Sato and H. Takada (2007). "Removal of selected pharmaceuticals and personal care products (PPCPs) and endocrine-disrupting chemicals (EDCs) during sand filtration and ozonation at a municipal sewage treatment plant." *Water Research* 41(19): 4373--4382.
- Negaresh, E., A. Antony, M. Bassandeh, D. Richardson and G. Leslie (2012). "Selective separation of contaminants from paper mill effluent using nanofiltration." *Chemical Engineering Research and Design* 90(4): 576--583.
- Nesheiwat, F. and A. Swanson (2000). "Clean contaminated sites using Fenton's reagent." *Chemical Engineering Progress* 96(4): 61-66.
- Neyens, E. and J. Baeyens (2003). "A review of classic Fenton's peroxidation as an advanced oxidation technique." *Journal of Hazardous Materials* 98(1-3): 33-50.
- Nghiem L. and A. Schäfer (2002). "Adsorption and transport of trace contaminant estrone in NF/RO membranes." *Environmental Engineering Science* 19 (6): 441-451.
- Nghiem, L., A. Schafer and M. Elimelech (2004). "Removal of natural hormones by nanofiltration membranes: measurement, modeling, and mechanisms." *Environmental Science and Technology* 38(6): 1888--1896.
- Nghiem, L. (2005). "Removal of emerging trace organic contaminants by nanofiltration and reverse osmosis." PhD thesis. University of Wollongong. Wollongong (Australia).
- Nghiem, L., A. Schäfer and M. Elimelech (2006). "Role of electrostatic interactions in the retention of pharmaceutically active contaminants by a loose nanofiltration membrane." *Journal of Membrane Science* 286(1-2): 52-59.
- Nghiem, L. and S. Hawkes (2007). "Effects of membrane fouling on the nanofiltration of pharmaceutically active compounds (PhACs): Mechanisms and role of membrane pore size." *Separation and Purification Technology* 57(1): 176-184.
- Nghiem, L., D. Vogel and S. Kha (2008). "Characterising humic acid fouling of nanofiltration membranes using bisphenol A as a molecular indicator." *Water Research* 42(15): 4049-4058.

- Nicell, J., J. Bewtra, N. Biswas and E. Taylor (1993). "Reactor development for peroxidase catalyzed polymerization and precipitation of phenols from wastewater." *Water Research* 27(11): 1629-1639.
- Núñez, L., J. García-Hortal and F. Torrades. (2007) "Study of kinetic parameters related to the decolourization and mineralization of reactive dyes from textile dyeing using Fenton and photo-Fenton processes." *Dyes and Pigments* 75(3): 647-652.
- Nuortila-Jokinen, J., A. Kuparinen and M. Nystrom (1998). "Tailoring an economical membrane process for internal purification in the paper industry." *Desalination* 119(1-3): 11--19.
- Oancea, P. and V. Meltzer (2013). "Photo-Fenton process for the degradation of Tartrazine (E102) in aqueous medium." *Journal of the Taiwan Institute of Chemical Engineers* 44(6): 990-994.
- Ozaki, H. and H. Li (2002). "Rejection of organic compounds by ultra-low pressure reverse osmosis membrane." *Water Research* 36(1): 123-130.
- Park, Y. (2002). "Effect of ozonation for reducing membrane-fouling in the UF membrane." *Desalination* 147(1-3): 43-48.
- Parsons, J. (Ed.) (2004). *Advanced Oxidation Processes for Water and Wastewater Treatment*, IWA Publishing, London (UK).
- Patel, R. And S. Suresh (2006). "Decolourization of azo dyes using magnesium--palladium system." *Journal of Hazardous Materials* 137(3): 1729-1741.
- Peeters, J. (1997). *Characterization of nanofiltration membranes*. PhD. thesis. Twente University. Enschede (The Netherlands).
- Perry, R. and D. Green (1997). "Perry's Chemical Engineering Handbook." 7th Ed. McGraw-Hill, New York (USA).
- Phattaranawik, J., T. Leiknes and W. Pronk (2005). "Mass transfer studies in flat-sheet membrane contactor with ozonation." *Journal of Membrane Science* 247(1-2): 153-167.
- Pignatello, J., E. Oliveros and A. MacKay (2006). "Advanced Oxidation Processes for organic contaminant destruction based on the Fenton reaction and related chemistry." *Critical Reviews in Environmental Science and Technology* 36(1): 1-84.
- Pirillo, S., F. García, M. Ferreira and E. Rueda (2010). "Eriochrome Blue Black R and Fluorescein degradation by hydrogen peroxide oxidation with horseradish peroxidase and hematin as biocatalysts." *Journal of Molecular Catalysis B: Enzymatic* 66(1-2): 63-71.
- Poerschmann, J., U. Trommler and T. Góreck (2010). "Aromatic intermediate formation during oxidative degradation of Bisphenol A by homogeneous sub-stoichiometric Fenton reaction." *Chemosphere* 79(10): 975-986.
- Pohl, R., R. Balon, R. Berchou, V. Yeragani (1987). "Allergy to tartrazine in antidepressants." *The American Journal of Psychiatry* 144(2): 237-238.
- Pontes, R., J. Moraes, J. Machulek and J. Pinto (2010). "A mechanistic kinetic model for phenol degradation by the Fenton process." *Journal of Hazardous Materials* 176(1-3): 402-413.
- Ramakrishnan, S., B. Lakshmi and P. Surya (2011). "Estimation of synthetic colorant tartrazine in food stuff and formulations and effect of colorant on the protein binding of drugs." *The International Journal of Pharmacy & Industrial Research* 1(2): 141-152.

- Rautenbach, R. and R. Mellis (1995). "Hybrid processes involving membranes for the treatment of highly organic--inorganic contaminated wastewater." *Desalination* 101(2): 105--113.
- Reed, B., W. Lin, R. Viadero and J. Young (1997). "Treatment of oily wastes using high-shear rotary ultrafiltration." *Journal of Environmental Engineering* 123(12): 1234--1242.
- Reutergårdh, L. and M. Iangphasuk (1997). "Photocatalytic decolourization of reactive azo dye: A comparison between TiO_2 and us photocatalysis." *Chemosphere* 35(3): 585-596.
- Rigg, T., W. Taylor and J. Weiss (1954). "The rate constant of the reaction between hydrogen peroxide and ferrous ions." *Journal Chemical Physics* 22(4): 575-577.
- Rigol, A., A. Latorre, S. Lacorte and D. Barceló (2002). "Determination of toxic compounds in paper recycling process waters by gas chromatography--mass spectrometry and liquid chromatography--mass spectrometry." *Journal of Chromatography A* 963(1-2): 265-275.
- Rios, G., M. Belleville, D. Paolucci and J. Sanchez (2004). "Progress in enzymatic membrane reactors-a review." *Journal of Membrane Science* 242(1-2): 189-196.
- Rivas, F.; F. Beltran, J. Frades and P. Buxeda (2001). "Oxidation of p-hydroxybenzoic acid by Fenton's reagent." *Water Research* 35(2): 387-396.
- Rongchang, W., R. Dianjun, X. Siqing, Z. Yalei and Z. Jianfu (2009). "Photocatalytic degradation of Bisphenol A (BPA) using immobilized TiO_2 and UV illumination in a horizontal circulating bed photocatalytic reactor (HCBPR)." *Journal of Hazardous Materials* 169(1-3): 926-932.
- Rosenfeldt, E. and K. Linden (2004). "Degradation of endocrine disrupting chemicals BPA, ethinyl estradiol, and estradiol during UV photolysis and AOP." *Environmental Science and Technology* 38(20): 5476-5483.
- Roy P., H. Salminen, P. Koskimies, J. Simola, A. Smeds, P. Saukko and I. Huhtaniemi (2004). "Screening of some anti-androgenic endocrine disruptors using a recombinant cell-based in vitro bioassay." *The Journal of Steroid Biochemistry and Molecular Biology* 88(2): 157-166.
- Ruppert G., R. Bauer and G. Heisle (1994). "UV- O_3 , UV- H_2O_2 , UV- TiO_2 and the photo-Fenton reaction - comparison of advanced oxidation processes for wastewater treatment." *Chemosphere* 28(8): 1447-1454.
- Sajiki, J. and J. Yonekubo (2004). "Inhibition of seawater on bisphenol A (BPA) degradation by Fenton reagents." *Environment International* 30(2): 145-150.
- Sakuyama, H., Y. Endo, K Fujimoto and Y. Hatano (2003). "Oxidative degradation of alkylphenols by horseradish peroxidase." *Journal of Bioscience and Bioengineering* 96 (3): 227-231.
- Salem, M. and A. Gemeay (2000). "Kinetics of the oxidation of Tartrazine with peroxydisulfate in the presence and absence of catalysts." *Monatshefte für Chemie/ Chemical Monthly* 131(2): 117-129.
- Samuelsen, M., C. Olsen and J. Holme (2001). "Estrogen-like properties of brominated analogs of bisphenol-A in the MCF-7 human breast cancer cell line, *Cell Biol.*" *Toxicology* 17(3): 139-151.

- Sancar, B. and O. Balci (2013). "Decolorization of different reactive dye wastewaters by O₃ and O₃/ultrasound alternatives depending on different working parameters." *Textile Research Journal* 83(6): 574-590.
- Sanchez, J. and T. Tsotsis (2002). "Catalytic Membranes and Membrane Reactors." Wiley-VCH, Weinheim (Germany).
- Sangster, J. (1997). "Octanol-water partition coefficients: Fundamentals and physical chemistry." John Wiley & Sons, Chichester (UK).
- Santos, A., P. Yustos, A. Quintanilla, S. Rodríguez and F. García-Ochoa (2002). "Route of the catalytic oxidation of phenol in aqueous phase." *Applied Catalysis B: Environmental*, 39(2): 97-113.
- Sarasa, J., M. Roche, M. Ormad, E. Gimeno, A. Puig and J. Ovellerio (1998). "Treatment of a wastewater resulting from dyes manufacturing with ozone and chemical coagulation." *Water Research* 32(9): 2721-2727.
- Sarayu, K., K. Swaminathan and S. Sandhya (2007). "Assessment of degradation of eight commercial reactive azo dyes individually and in mixture in aqueous solution by ozonation." *Dyes and Pigments* 75(2): 362-368.
- Schaep, J., B. Van der Bruggen, C. Vandecasteele and D. Wilms (1998). "Influence of ion size and charge in nanofiltration." *Separation and Purification Technology* 14(1-3): 155-162.
- Schaep, J. (1999). "Nanofiltration for the removal of ionic compounds from water." PhD thesis. Katholieke Universiteit Leuven. Leuven (Belgium).
- Schaep, J., C. Vandecasteele, A. Wahab Mohammad and W. Bowen (2001). "Modelling the retention of ionic components for different nanofiltration membranes." *Separation and Purification Technology* 22-23: 169-179.
- Schäfer, A., N. Andritsos, A. Karabelas, E. Hoek, R. Schneider and M. Nyström (2004). "Fouling in Nanofiltration, in: Nanofiltration -Principles and Applications." Schäfer A.I., Waite T.D., Fane A.G. (Eds). Elsevier (The Netherlands) Chapter 20, p. 169-239.
- Schäfer, A., L. Nghiem, N. Oschmann (2006). "Bisphenol A retention in the direct ultrafiltration of greywater." *Journal of Membrane Science* 283(1-2): 233-243.
- Schlichter, B., V. Mavrov and H. Chmiel (2004). "Study of a hybrid process combining ozonation and microfiltration/ultrafiltration from drinking water production from surface water." *Desalination* 168: 307-317.
- Schummer, J. (1997). "Scientometric studies on chemistry I: The exponential growth of chemical substances, 1800-1995." *Scientometrics* 39(1): 107-123.
- Seidel, A. and M. Elimelech (2002). "Coupling between chemical and physical interactions in natural organic matter (NOM) fouling of nanofiltration membranes: implications for fouling control." *Journal of Membrane Science* 203(1-2): 245-255.
- Shaw, D. (1992). "Introduction to colloidal and surface chemistry." 4th Ed. Butterworth Heinemann, Oxford (UK).
- Sherwood, T., P. Brian, R. Fisher and L. Dresner (1965). "Salt concentration at phase boundaries in desalination by reverse osmosis." *Industrial and Engineering Chemistry Fundamentals* 4(2): 113-118.

- Shih, M.C. (2005). "An overview of arsenic removal by pressure-driven membrane processes." *Desalination* 172(1): 85-97.
- Shu, H. and C. Huang (1995). "Degradation of commercial azo dyes in water using ozonation and UV enhanced ozonation process" *Chemosphere* 31(8): 3813-3825.
- Shyh-Fang, K., L. Chih-Hsaing and C. Mon-Chun (2002). "Pre-Oxidation and Coagulation of Textile Wastewater by the Fenton Process." *Chemosphere* 46(6): 923-928.
- Sirtori, C., A. Zapata, I. Oller, W. Gernjak, A. Agüera and S. Malato (2009): "Decontamination industrial pharmaceutical wastewater by combining solar photo-Fenton and biological treatment" *Water Research* 43(3): 661-668.
- Soares, O., J. Órfão, D. Portela, A. Vieira and M. Pereira (2006). "Ozonation of textile effluents and dye solutions under continuous operation: Influence of operating parameters." *Journal of Hazardous Materials* 137(3): 1664-1673.
- Song, W., V. Ravindran, B. Koel and Massoud Pirbazar (2004). "Nanofiltration of natural organic matter with H₂O₂/UV pretreatment: fouling mitigation and membrane surface characterization." *Journal of Membrane Science* 241(1): 143-160.
- Sourirajan, S. (1970). "Reverse Osmosis." Academic Press, New York (USA).
- Staples, C., P. Dorn, G. Klecka, S. O'Block and L. Harris (1998). "A review of the environmental fate, effects, and exposures of bisphenol A." *Chemosphere* 36(10): 2149-2173.
- Strickland, A. and W. Perkins (1995). "Decoloration of continuous dyeing wastewater by ozonation." *Textile chemist and colorist* 27(5): 11-15.
- Stüber, J., U. Mieke, R. Stein, M. Köhler, and B. Lesjean (2013). "Combining ozonation and ceramic membrane filtration for tertiary treatment." *Chemie Ingenieur Technik* 85(8): 1-7.
- Su, C., M. Pukdee-Asa, C. Ratanatamskul and M. Lu (2011). Effect of operating parameters on decolorization and COD removal of three reactive dyes by Fenton's reagent using fluidized-bed reactor." *Desalination* 278: 211-218
- Su-Hua, W., D. Bing-zhi and H. Yu (2010). "Adsorption of bisphenol A by polysulphone membrane." *Desalination* 253(1-3): 22-29.
- Sun, J., S. Sun, M. Fan, H. Guo, L. Qiao, and R. Sun (2007). "A kinetic study on the degradation of p-nitroaniline by Fenton oxidation process." *Journal of Hazardous Materials* 148(1-2): 172-177.
- Tanaka, K., K. Padernpole and T. Hisanaga (2000). "Photocatalytic degradation of commercial azo dyes." *Water Research* 34(1): 327-333.
- Tanaka, T., T. Tonosaki, M. Nose, N. Tomidokoro, N. Kadomura, T. Fujii and M. Taniguchi (2001). "Treatment of model soils contaminated with phenolic endocrine-disrupting chemicals with laccase from *Trametes* sp. in a rotating reactor." *Journal of Bioscience and Bioengineering* 92(4): 312-316.
- Tang, W. and C. Huang (1997). "Stoichiometry of Fenton's reagent in the oxidation of chlorinated organic pollutants." *Environmental Science and Technology* 18(1): 13-23.

- Tang, W. and S. Tassos (1997). "Oxidation kinetics and mechanisms of trihalomethanes by fentones reagent." *Water Research* 31: 1117-1125.
- Tanninen, J., M. Mänttari and M. Nyström (2006). "Effect of salt mixture concentration on fractionation with NF membranes." *Journal of Membrane Science* 283(1-2): 57-64.
- Tekin, H., O. Bilkay, S. Ataberk, T. Balta, I. Ceribasi, F. Sanin, F. Dilek and U. Yetis. (2006). "Use of Fenton oxidation to improve the biodegradability of a pharmaceutical wastewater." *Journal of Hazardous Materials* 136(2): 258-265.
- Thorsen, T. (1999). "Membrane filtration of humic substances – state of the art." *Water Science and Technology* 40(9): 105-112.
- Tong, Z., Z. Qingxiang, H. Hui, L. Qin and Z. Yi (1997). "Removal of toxic phenol and 4-chlorophenol from waste water by horseradish peroxidase." *Chemosphere* 34(4): 893-903.
- Torres, E., I. Bustos-Jaimes and S. Le Borgne (2003). "Potential use of oxidative enzymes for the detoxification of organic pollutants." *Applied Catalysis B: Environmental* 46(1): 1-15.
- Torres, R., F. Abdelmalek, E. Combet, C. Pétrier and C. Pulgarin (2007). "A comparative study of ultrasonic cavitation and Fenton's reagent for bisphenol A degradation in deionised and natural waters." *Journal of Hazardous Materials* 46(3): 546-551.
- Turhan, K. and Z. Turgut (2009a) "Treatment and Degradability of Direct Dyes in Textile Wastewater by Ozonation: A Laboratory Investigation." *Desalination Water Treatment* 11: 184-191.
- Turhan K. and Z. Turgut (2009b). "Decolorization of direct dye in textile wastewater by ozonation in a semi-batch bubble column reactor." *Desalination* 242(1-3): 256-263.
- Uchida, H., T. Fukuda, H. Miyamoto, T. Kawabata, M. Suzuki and T. Uwajima (2001). "Polymerization of Bisphenol A by Purified Laccase from *Trametes villosa*." *Biochemical and Biophysical Research Communications* 287(2): 355-358.
- Umar, M., F. Roddick, L. Fan and H. Aziz (2013). "Application of ozone for the removal of bisphenol A from water and wastewater-a review." *Chemosphere* 90(8):2197-2207.
- Van der Bruggen, B., J. Schaep, W. Maes, D. Wilms and C. Vandecasteele (1998). "Nanofiltration as a treatment method for the removal of pesticides from ground waters." *Desalination* 117(1-3): 139-147.
- Van der Bruggen, B., J. Schaep, D. Wilms and C. Vandecasteele (1999). "Influence of molecular size, polarity and charge on the retention of organic molecules by nanofiltration." *Journal of Membrane Science* 156(1): 29-41.
- Van der bruggen, B., J. Schaep, D. Wilms and C. Vandecasteele (2000). "A comparison of models to describe the maximal retention of organic molecules in Nanofiltration." *Separation Science and technology* 35(2): 169-182.
- Van der Bruggen B. and C. Vandecasteele (2001). "Flux decline during nanofiltration of organic components in aqueous solution." *Environmental Science and Technology* 35(17): 3535-3540.
- Van der Bruggen, B. and C. Vandecasteele (2003). "Removal of pollutants from surface water and groundwater by nanofiltration: overview of possible applications in the drinking water industry." *Environmental Pollution* 122(3): 435-445.

- Van Geluwe, S., C. Vinckier, E. Bobu, C. Trandafir, J. Vanelslander, L. Braekena and B. Van der Bruggen (2010). "Eightfold increased membrane flux of NF 270 by O₃ oxidation of natural humic acids without deteriorated permeate quality." *Journal of Chemical Technology and Biotechnology* 85(11): 1480-1488.
- Vandenberg, L., R. Hauser, M. Marcus, N. Olea and W. Welshons (2007). "Human exposure to bisphenol A (BPA)." *Reproductive Toxicology* 24(2): 139-177.
- Venkata, S., K. Krishna, N. Chandrasekhara and P. Sarma (2005). "Acid azo dye degradation by free and immobilized horseradish peroxidase (HRP) catalyzed process." *Chemosphere* 58(8): 1097-1105.
- Venkatadri, R., and R. Peters (1993). "Chemical Oxidation Technologies: Ultraviolet Light/Hydrogen Peroxide, Fenton's Reagent, and Titanium Dioxide-Assisted Photocatalysis." *Hazardous Waste and Hazardous Materials* 10(2): 107-149.
- Vezzani, D. and S. Bandini (2002). "Donnan equilibrium and dielectric exclusion for characterization of nanofiltration membranes." *Desalination* 149(1-3): 477-483.
- Vogel, D., A. Simon, A. Alturki, B. Bilitewski, W. Price and L. Nghiem (2010). "Effects of fouling and scaling on the retention of trace organic contaminants by a nanofiltration membrane: The role of cake-enhanced concentration polarization." *Separation and Purification Technology* 73(2): 256-263.
- Voordeckers, J., Fennell D., Jones K., Häggblom M. James, W., E. Donna and J. Kristi (2002). "Anaerobic Biotransformation of Tetrabromobisphenol A, Tetrachlorobisphenol A, and Bisphenol A in Estuarine Sediments." *Environmental Science and Technology* 36(4): 696-701.
- Walling, C. and S. Kato (1971). "Oxidation of alcohols by Fenton's reagent. Effect of copper ion." *Journal of the American Chemical Society* 93(17): 4275-4281.
- Walling, C. (1975). "Fenton's reagent revisited." *Accounts of Chemical Research* 8(4): 125-131.
- Walton, K, R. Walker, J. van de Sandt, J. Castell, A. Knapp, G. Kozianowski, M. Roberfroei and B. Schilter (1999). "The application of in vitro data in the derivation of the acceptable daily intake of food additives." *Food and Chemical Toxicology* 37(12): 1175-1197.
- Wang, R., D. Ren, S. Xia, Y. Zhang and J. Zhao (2009). "Photocatalytic degradation of BPA using immobilized TiO₂ and UV illumination in a horizontal circulating bed photocatalytic reactor." *Journal of Hazardous Materials* 169(1-3): 926-932.
- Weinberg, H. and W. Glaze (1997). "A unified approach to the analysis of polar organic by-products of oxidation in aqueous matrices." *Water Research* 31(7): 1555-1572.
- Westerhoff, P., Y. Yoon, S. Snyder and E. Wert (2005). "Fate of endocrine-disruptor, pharmaceutical, and personal care product chemicals during simulated drinking water treatment processes." *Environmental Science and Technology* 39(17): 6649-6663.
- Wetherill, Y., C. Petra, K. Monk, A. Puga and K. Knudsen (2002). "The xenoestrogen BPA induces inappropriate androgen receptor activation and mitogenesis in prostate adenocarcinoma cells." *Molecular Cancer Therapeutics* 1(7): 515-524.

- Wetherill, Y., B. Akingbemi, J. Kanno, J. McLachlan, A. Nadal, C. Sonnenschein, C. Watson, R. Thomas Zoeller and S. Belcher (2007). "In vitro molecular mechanisms of bisphenol A action." *Reproductive Toxicology* 24(2): 178-198.
- Wintgens, T, M. Gallenkemper and T. Melin (2002). "Endocrine disrupter removal from wastewater using membrane bioreactor and nanofiltration technology." *Desalination* 146(1-3): 387-391.
- Wintgens, T., T. Melin, A. Schiller, S. Khan, M. Muston, D. Bixio and C. Thoeye. (2005). "The role of membrane processes in municipal wastewater reclamation and reuse." *Desalination* 178(1-3): 1-11.
- Wu, J., M. Eiteman and S. Law (1998). "Evaluation of membrane filtration and ozonation processes for treatment of reactive-dye wastewater." *Journal of Environmental Engineering* 124(3): 272-277.
- Wu, J., K. Rudy and J. Spark (2000). "Oxidation of aqueous phenol by ozone and peroxidase." *Advances in Environmental Research* 4(4): 339-346.
- Wu, J. and T. Wang (2001). "Ozonation of aqueous azo dye in a semi-batch reactor." *Water Research* 35(4): 1093-1099.
- Wu, C. and H. Ng (2008). "Degradation of C.I. Reactive Red 2 (RR2) using ozone-based systems: Comparisons of decolorization efficiency and power consumption." *Journal of Hazardous Materials* 152(1): 120-127.
- Wuthrich B (1993). "Adverse reactions to food additives." *Annals of Allergy, Asthma and Immunology* 71: 379-384.
- Xu, P., J. Drewes, C. Bellona, G. Amy, T. Kim, M. Adam and T. Heberer (2005). "Rejection of emerging organic micropollutants in nanofiltration-reverse osmosis membrane applications." *Water Environmental Research* 77(1): 40-48.
- Xu, B., N. Gao, M. Rui, H. Wang and H. Wu (2007). "Degradation of endocrine disruptor bisphenol A in drinking water by ozone oxidation." *Frontiers of Environmental Science and Engineering in China* 1(3): 350-356.
- Xuan, Y., Y. Endo and K. Fujimoto (2002). "Oxidative degradation of bisphenol a by crude enzyme prepared from potato." *Journal of Agricultural and Food Chemistry* 50(22): 6575-6578.
- Yamamoto, T., A. Yasuhara, H. Shiraishi and O. Nakasugi (2001). "Bisphenol A in hazardous waste landfill leachates." *Chemosphere* 42(4): 415-418.
- Ying, G., S. Kookana and P. Dillon (2003). "Sorption and degradation of selected five endocrine disrupting chemicals in aquifer material." *Water Research* 37(15): 3785-3791.
- Yoon, Y., P. Westerhoff, S. Snyder and E. Wert (2006). "Nanofiltration and ultrafiltration of endocrine disrupting compounds, pharmaceuticals and personal care products." *Journal of Membrane Science* 270(1-2): 88-100.
- Yoon, Y., P. Westerhoff, S. Snyder, E. Wert and J. Yoon (2007). "Removal of endocrine disrupting compounds and pharmaceuticals by nanofiltration and ultrafiltration membranes." *Desalination* 202(1-3): 16-23.

- Yoshida, H (1883). "Chemistry of Lacquer (Urishi) part 1." *Journal of Chemical Society* 43: 472-486.
- Young, T., M. Geng, L. Lin, and S. Mededovic (2013). "Oxidative Degradation of Bisphenol A: A Comparison between Fenton Reagent, UV, UV/H₂O₂ and Ultrasound." *Journal of Advanced Oxidation Technologies* 16(1): 89-101.
- Yüksel, S., N. Kabay and M. Yüksel (2013). "Removal of bisphenol A (BPA) from water by various nanofiltration (NF) and reverse osmosis (RO) membranes." *Journal of Hazardous Materials* 263(part 2): 307-310.
- Zazo, J., J. Casas, A. Mohedano, M. Gilarranz and J. Rodriguez (2005). "Chemical Pathway and Kinetics of Phenol Oxidation by Fenton's Reagent." *Environmental Science and Technology* 39(23): 9295-9302.
- Zhang, Y., C. Causserand, P. Aimar and J. Cravedi (2006). "Removal of bisphenol A by a nanofiltration membrane in view of drinking water production." *Water Research* 40(20): 3793-3799.
- Zhang, Y., C. Maa, F. Yeb, Y. Konga and H. Lia (2009). "The treatment of wastewater of paper mill with integrated membrane process." *Desalination* 236(1-3): 349-356.
- Zhao, M., Y. Li and W. Chang (2003). "The analysis of phenolic environmental estrogens." *Chinese Journal of Analytical Chemistry* 31: 103-109.
- Zhao, L., J. Ma, Z. Sun and X. Zhai (2009). "Mechanism of heterogeneous catalytic ozonation of nitrobenzene in aqueous solution with modified ceramic honeycomb." *Applied Catalysis B-Environmental* 89(3-4): 326-334.
- Zhou H. and D. Smith (2002). "Advanced technologies in water and wastewater treatment." *Journal of Environmental Engineering and Science* 1: 247-264.
- Zhou, D., F. Wu, N. Deng and W. Xiang (2004). "Photooxidation of bisphenol A (BPA) in water in the presence of ferric and carboxylate salts." *Water research* 38(19): 4107-4116.
- Zhou, M. and J. He (2007). "Degradation of azo dye by three clean advanced oxidation processes: Wet oxidation, electrochemical oxidation and wet electrochemical oxidation—A comparative study." *Electrochimica Acta* 53(4): 1902-1910.
- Zorpas, A. and N. Costa (2010). "Combination of Fenton oxidation and composting for the treatment of the olive solid residue and the olive mill wastewater from the olive oil industry in Cyprus." *Bioresource Technology* 101(20): 7984-7987.

About the Author

Ivonne Escalona was born on the 15th of January, 1981 in Maracay, Venezuela. She obtained her Bachelor of Science degree in Chemical Engineering in May 2004 at Simón Bolívar University in Caracas, Venezuela. Upon graduation, she was employed as a graduate assistant at the Department of Thermodynamics and Transport Phenomena of Simón Bolívar University. In March 2009 she obtained her Master of Science degree in Chemical Engineering from the Simón Bolívar University. Related to her studies, she performed a 13 months internship on fundamental requirements for the convective drying of carbon xerogels at the Department of Applied Chemistry of University of Liège, in Liège, Belgium. From April 2009 to November 2014 she joined the Chemical Reaction Engineering & Process Intensification group (CREPI) at the Rovira I Virgili University in Tarragona, Spain, as a PhD student, focusing on the research topic presented in this dissertation: membrane-assisted advanced oxidation processes for wastewater treatment. She also did a three months research stay at the Membrane Technology Group at the University of Twente in Enschede, The Netherlands, where she did the removal of BPA by enzyme polymerization using nanofiltration membranes.

Journal Publications

Escalona, I., de Groot J.; Font, J.; Nijmeijer, K. (2014). Removal of BPA by enzyme polymerization using NF membranes. *Journal of Membrane Science*, 468, 192–201.
DOI: 10.1016/j.memsci.2014.06.011

Escalona, I.; Fortuny, A.; Stüber, F.; Bengoa, C.; Fabregat, A.; Font, J.(2014). Fenton coupled with nanofiltration for elimination of Bisphenol A. *Desalination* 345, 77–84.
DOI: 10.1016/j.desal.2014.04.024

Escalona, I.; Jomaa, W.; Olivera-Fuentes, C.; Crine, M.; Léonard, A. (2010). Convective drying of gels: comparison between simulated and experimental moisture profiles obtained by X-ray microtomography. *Drying Technology*, 28(5), 644-650.
DOI: 10.1080/07373931003788734

Escalona, I.; Gommaes, C.; Job, N.; Blacher, S.; Olivera-Fuentes, C.; Pirard, J.; Léonard, A. (2009). Water desorption from resorcinol-formaldehyde hydrogels and adsorption in the resulting xerogels. *Microporous and Mesoporous Materials*, 117(1-2), 61-66.
DOI: 10.1016/j.micromeso.2008.06.007

Participations in Congresses and Meetings

I. Escalona, F. Stüber, A. Fortuny, C. Bengoa, A. Fabregat, J. Font (2013). Fenton Coupled with Nanofiltration for Elimination of Tartrazine. Poster, 10th Doctoral Day and Poster Exhibition, Rovira I Virgili University, Tarragona, SPAIN.

I. Escalona, A. Fortuna, F. Stüber, C. Bengoa, A. Fabregat, J. Font (2012). Fenton coupled with nanofiltration for elimination of BPA. Poster, 14th Aachener Membrane Kolloquium, Aachen, GERMANY.

I. Escalona, F. Stüber, A. Fortuny, C. Bengoa, A. Fabregat, J. Font (2012). Fenton Coupled with Nanofiltration for Elimination of Tartrazine. Poster, Euromembrane 2012, London, UNITED KINGDOM.

I. Escalona.(2012). XXIX E.M.S Summer school on Membranes “Dense polymeric membranes fundamentals & applications: packaging, barriers & industrial separations”, Nancy, FRANCE.

I. Escalona; X. Bernat; F. Stüber; A. Fortuny; C. Bengoa; A. Fabregat; J. Font (2011). Removal of commercial dyes from aqueous solution by nanofiltration. Poster, Water & Industry. IWA Specialist Conference Chemical Industries, Valladolid, SPAIN.

I. Escalona; J. Font (2011). Membrane-assisted advanced oxidation processes for wastewater treatment. Poster, 9th Doctoral Day and Poster Exhibition, Rovira I Virgili University, Tarragona, SPAIN.

Escalona, I.; Bernat, X.; Mezohegyi, G.; Stüber, F.; Bengoa, C.; Fabregat, A.; Font, J. (2010). Treatment of aqueous solutions of synthetic dyes by nanofiltration membranas. Oral presentation, Reunión de la Mesa Española de Tratamiento de Aguas, META, Bilbao, SPAIN.

Ivonne Escalona (2010). Removal of dyes by nanofiltration. Oral presentation, The 12th Network Young Membrains, Lappeenranta, FINLAND.

I. Escalona, X. Bernat, G. Mezohegyi, D. Nabarlatz, F. Stüber, C. Bengoa, A. Fabregat, J. Font (2009). Removal of commercial dyes from aqueous solution by nanofiltration. Poster, IMeTI Workshop on Membrane applications in Agrofood, Cetraro, ITALY

Escalona, I.; Jomaa, W.; Olivera-Fuentes, C.; Crine, M.; Léonard, A. (2008). Convective drying of gels: comparison between simulated and experimental moisture profiles obtained by x-ray microtomography. Oral presentation, 16th International Drying Symposium, Ramoji Film City, Hyderabad, INDIA

Escalona, I.; Léonard, A.; Job, N.; Olivera-Fuentes, C.G.; Pirard, J.P.; Crine, M.; Blacher, S. (2007). Moisture profiles determination during convective drying and water isotherms of resorcinol-formaldehyde hydrogels. Oral presentation, Lignocarb Final Meeting, Nancy, FRANCE.

Léonard, A.; Escalona, I.G.; Job, N.; Olivera-Fuentes, C.G.; Pirard, J.P.; Crine, M.; Blacher, S. (2007). Water isotherms of resorcinol-formaldehyde hydrogels, xerogels and carbon xerogels. Oral presentation, CARBON 2007 Conference, Seattle, WA, UNITED STATES.

Stays abroad in Research Centers

2012. Removal of BPA by enzyme polymerization using nanofiltration membranes. University of Twente. Membrane Technology Group. Enschede, The Netherlands.

2007-2008. Convective drying of carbon xerogels. University of Liège. Department of applied Chemistry. Liège, BELGIUM.

Awards

Pre-doctoral fellowship. Departament d'Innovació, Universitats i Empresa, Generalitat de Catalunya. FIB - Ajuts per contractar a personal investigador novell. Ref. 2010FI_B 00876. 01/05/2010 - 30/04/2013.